

Control of underactuated mechanical systems

Citation for published version (APA):

Aneke, N. P. I. (2003). *Control of underactuated mechanical systems*. [Phd Thesis 1 (Research TU/e / Graduation TU/e), Mechanical Engineering]. Technische Universiteit Eindhoven.
<https://doi.org/10.6100/IR559509>

DOI:

[10.6100/IR559509](https://doi.org/10.6100/IR559509)

Document status and date:

Published: 01/01/2003

Document Version:

Publisher's PDF, also known as Version of Record (includes final page, issue and volume numbers)

Please check the document version of this publication:

- A submitted manuscript is the version of the article upon submission and before peer-review. There can be important differences between the submitted version and the official published version of record. People interested in the research are advised to contact the author for the final version of the publication, or visit the DOI to the publisher's website.
- The final author version and the galley proof are versions of the publication after peer review.
- The final published version features the final layout of the paper including the volume, issue and page numbers.

[Link to publication](#)

General rights

Copyright and moral rights for the publications made accessible in the public portal are retained by the authors and/or other copyright owners and it is a condition of accessing publications that users recognise and abide by the legal requirements associated with these rights.

- Users may download and print one copy of any publication from the public portal for the purpose of private study or research.
- You may not further distribute the material or use it for any profit-making activity or commercial gain
- You may freely distribute the URL identifying the publication in the public portal.

If the publication is distributed under the terms of Article 25fa of the Dutch Copyright Act, indicated by the "Taverne" license above, please follow below link for the End User Agreement:

www.tue.nl/taverne

Take down policy

If you believe that this document breaches copyright please contact us at:

openaccess@tue.nl

providing details and we will investigate your claim.

CONTROL OF UNDERACTUATED MECHANICAL SYSTEMS



CIP-DATA LIBRARY TECHNISCHE UNIVERSITEIT EINDHOVEN

Aneke, N.P.I.

Control of underactuated mechanical systems / by N.P.I. Aneke. - Eindhoven :

Technische Universiteit Eindhoven, 2003.

Proefschrift. - ISBN 90-386-2684-3

NUR 929

Trefwoorden: mechanische systemen; niet-lineaire regeltechniek / ondergeactueerde mechanische systemen / robotica; niet-holonome systemen

Subject headings: mechanical systems; non-linear control / underactuated mechanical systems / robotics; non-holonomic systems

© 2002 by N.P.I. Aneke

All rights reserved. This publication may not be translated or copied, in whole or in part, or used in connection with any form of information storage and retrieval, electronic adaptation, electronic or mechanical recording, including photocopying, or by any similar or dissimilar methodology now known or developed hereafter, without the permission of the copyright holder.

This dissertation has been prepared with the $\text{\LaTeX} 2_{\epsilon}$ documentation system.

Printed by University Press Facilities, Eindhoven, The Netherlands.

The research reported in this thesis is part of the research program of the Dutch Institute of Systems and Control (DISC).

CONTROL OF UNDERACTUATED MECHANICAL SYSTEMS

PROEFSCHRIFT

ter verkrijging van de graad van doctor
aan de Technische Universiteit Eindhoven
op gezag van de Rector Magnificus, prof.dr. R.A. van Santen,
voor een commissie aangewezen door het College voor Promoties
in het openbaar te verdedigen op
15 april 2003 om 16.00 uur

door

Nnaedozie Pauling Ikegwonu Aneke

geboren te Delft

Dit proefschrift is goedgekeurd door de promotoren:

prof.dr. H. Nijmeijer

en

prof.dr.ir. M. Steinbuch

Copromotor:

dr.ir. A.G. de Jager

Contents

| | | |
|----------|---|-----------|
| 1 | Introduction | 9 |
| 1.1 | First-order nonholonomic constraints | 11 |
| 1.2 | Second-order nonholonomic constraints | 12 |
| 1.3 | Contributions of this thesis | 14 |
| 1.4 | Outline of the thesis | 15 |
| 2 | Problem formulation | 17 |
| 2.1 | Second-order chained form transformations | 17 |
| 2.1.1 | The first-order chained form system | 17 |
| 2.1.2 | The second-order chained form system | 18 |
| 2.2 | The feedback stabilization problem | 20 |
| 2.3 | The tracking control problem | 21 |
| 2.4 | Robustness considerations | 22 |
| 2.5 | Summary | 22 |
| 3 | Preliminaries | 25 |
| 3.1 | Mathematical preliminaries | 25 |
| 3.2 | Lyapunov stability | 25 |
| 3.3 | Converse theorems | 28 |
| 3.4 | Linear time-varying systems | 29 |
| 3.5 | Perturbation theory | 29 |
| 3.5.1 | Vanishing perturbations | 30 |
| 3.5.2 | Non-vanishing perturbations | 30 |
| 3.6 | Cascaded systems | 32 |
| 3.7 | Homogeneous systems | 35 |
| 3.8 | Summary | 37 |
| 4 | Trajectory generation | 39 |
| 4.1 | Problem formulation | 41 |
| 4.2 | Controllability and stabilizability | 41 |
| 4.3 | Constructive proof of controllability | 43 |
| 4.4 | The flatness property | 44 |
| 4.5 | The point to point steering problem | 45 |
| 4.6 | A variational method | 48 |
| 4.6.1 | The SQP algorithm | 49 |
| 4.7 | A sub-optimal method | 50 |

| | | |
|----------|--|------------|
| 4.7.1 | The Finite Differences Method | 52 |
| 4.8 | Summary | 53 |
| 5 | Tracking control | 55 |
| 5.1 | Cascaded backstepping control | 55 |
| 5.1.1 | Stabilization of the (Δ_1, Δ_2) subsystem | 56 |
| 5.2 | Stability of the tracking-error dynamics | 61 |
| 5.3 | Robustness considerations | 63 |
| 5.4 | Summary | 65 |
| 6 | Point stabilization | 67 |
| 6.1 | Homogeneous feedback stabilization | 68 |
| 6.1.1 | Stabilizing the Δ_1 subsystem | 69 |
| 6.1.2 | Stabilizing the (Δ_1, Δ_2) subsystem | 70 |
| 6.2 | Robust stabilizers for the second-order chained form | 71 |
| 6.2.1 | Preliminaries and definition of the problem | 71 |
| 6.2.2 | Design of the periodically updated feedback law | 73 |
| 6.2.3 | Notational conventions | 74 |
| 6.2.4 | Stability and robustness analysis | 74 |
| 6.3 | Summary | 76 |
| 7 | Computer simulations | 77 |
| 7.1 | The dynamic model | 78 |
| 7.2 | The second-order chained form transformation | 80 |
| 7.2.1 | The influence of friction | 82 |
| 7.3 | Friction Compensation | 84 |
| 7.4 | Tracking Control | 86 |
| 7.4.1 | Simulation without friction in the rotational link | 89 |
| 7.4.2 | Simulation with friction in the rotational link | 89 |
| 7.5 | Feedback Stabilization | 92 |
| 7.5.1 | Simulation without friction in the rotational link | 95 |
| 7.5.2 | Simulation with friction in the rotational link | 96 |
| 7.6 | Conclusions | 99 |
| 8 | Experimental results | 103 |
| 8.1 | Parameter identification | 105 |
| 8.1.1 | The location of the Center of Percussion | 106 |
| 8.1.2 | Linear least-squares identification | 106 |
| 8.2 | Experiment with the Tracking Controller | 109 |
| 8.3 | Experiment with the Homogeneous Stabilizing Controller | 114 |
| 8.4 | A heuristic modification of the stabilizing controller | 116 |
| 8.5 | Extension to practical point-to-point control | 119 |
| 8.6 | Conclusions | 123 |

| | | |
|----------|--|------------|
| 9 | Conclusions and Recommendations | 127 |
| 9.1 | Conclusions | 128 |
| 9.1.1 | The control design approach | 128 |
| 9.1.2 | The simulations and experiments | 129 |
| 9.1.3 | Robustness issues | 130 |
| 9.2 | Recommendations | 130 |
| 9.2.1 | The second-order chained form | 130 |
| 9.2.2 | Robust control design | 131 |
| 9.2.3 | Improving the experimental set-up | 132 |
| A | A stability result for cascaded systems | 135 |
| A.1 | A global \mathcal{H} -exponential stability result for non-autonomous cascaded systems | 135 |
| B | Tracking control of the higher-dimensional chained form | 139 |
| B.1 | Cascaded backstepping control | 139 |
| B.1.1 | Stabilization of the (Δ_1, Δ_2) subsystem | 140 |
| B.1.2 | Stability of the tracking-error dynamics | 144 |
| B.2 | Robustness considerations | 147 |
| C | The underactuated H-Drive manipulator | 153 |
| C.1 | Dynamic model of the underactuated H-Drive Manipulator | 153 |
| C.2 | The servo controllers | 155 |
| C.3 | Motion Planning | 157 |
| | Bibliography | 163 |
| | Summary | 169 |
| | Samenvatting | 171 |
| | Acknowledgements | 173 |
| | Curriculum Vitae | 175 |

Introduction

The last decades have shown an increasing interest in the control of underactuated mechanical systems. These systems are characterized by the fact that there are more degrees of freedom than actuators, *i.e.*, one or more degrees of freedom are unactuated. This class of mechanical systems are abundant in real life; examples of such systems include, but are not limited to, surface vessels, spacecraft, underwater vehicles, helicopters, road vehicles, mobile robots, space robots and underactuated manipulators. Underactuated mechanical systems generate interesting control problems which require fundamental nonlinear approaches. The linear approximation around equilibrium points may, in general, not be controllable and the feedback stabilization problem, in general, can not be transformed into a linear control problem. Therefore linear control methods can not be used to solve the feedback stabilization problem, not even locally. Also, the tracking control problem can not be transformed into a linear control problem. However, it turns out that, under certain conditions, the tracking control problem can be solved by linear time-varying control.

Many underactuated mechanical systems are subject to nonholonomic constraints. In classical mechanics, nonholonomic constraints are defined as linear constraints of the type $\Phi(q)\dot{q} = 0$ which are non-integrable, where the generalized coordinates are denoted by q . The constraint is called non-integrable if it can not be written as the time-derivative of some function of the generalized coordinates, *i.e.*, $\phi(q) = 0$, and thus can not be solved by integration. Contrary to classical mechanics, a more general characterization of nonholonomic constraints will be adopted in this thesis. The nonholonomic constraints are divided into two classes, the first-order nonholonomic constraints and the second-order nonholonomic constraints. The first-order nonholonomic constraints are defined as constraints on the generalized coordinates and velocities of the form $\Phi(q, \dot{q}) = 0$ that are non-integrable, *i.e.*, can not be written as the time-derivative of some function of the generalized coordinates, *i.e.*, $\phi(q) = 0$. These constraints include nonholonomic constraints arising in classical mechanics and nonholonomic constraints arising from kinematics. The second-order constraints are defined as constraints on the generalized coordinates, velocities and accelerations of the form $\Phi(q, \dot{q}, \ddot{q}) = 0$ which are non-integrable, *i.e.*, can not be written as the time-derivative of some function of the generalized coordinates and velocities, *i.e.*, $\phi(q, \dot{q}) = 0$.

These first-order nonholonomic or second-order nonholonomic constraints most commonly arise in mechanical systems where constraints are imposed on the motion, for example, underactuated vehicles and underactuated robot manipulators. These constraints are non-integrable, *i.e.*, can not be solved by integration, and are therefore an essential part of the dynamics. The first-order nonholonomic constraints, or velocity constraints, most commonly occur in, for example, wheeled mobile robots and wheeled vehicles, including tractor with trailer systems. The second-order nonholonomic constraints, or acceleration constraints, most commonly occur in, for example, surface vessels, under-

water vehicles, spacecraft, space robots and underactuated manipulators.

In addition to classical formulations, nonholonomic constraints can arise in other ways. If the motion of a mechanical system exhibits certain symmetry properties, there exist conserved quantities. If these conserved quantities, for example the angular momentum, are non-integrable, this may be interpreted as a nonholonomic constraint. It should be noted that, in classical mechanics, conserved quantities are not regarded as constraints on a system. In the control community, however, it has been commonly accepted to regard these conserved quantities as constraints that are imposed on the system. Examples of such systems include multi-body spacecraft and underactuated symmetric rigid spacecraft. Nonholonomic constraints also arise as a result of imposing design constraints on the allowable motions of the mechanical system. Examples of such systems include the case of kinematically redundant manipulators and underactuated manipulators. The general connection between underactuated systems and nonholonomic systems is not completely understood. An introduction to nonholonomic control systems is given in (Murray et al., 1994), and the formulation of nonholonomic systems is considered in (Neimark and Fufaev, 1972). An overview of developments in nonholonomic control problems can be found in (Kolmanovsky and McClamroch, 1995).

This thesis addresses the tracking and stabilization problem for underactuated mechanical systems with second-order nonholonomic constraints. Most publications on underactuated systems with nonholonomic constraints have dealt with systems that exhibit first-order nonholonomic constraints. For these systems an extensive amount of literature is available on the feedback stabilization problem and research in this field is still continuing. In the last decade underactuated systems with second-order nonholonomic constraints have received more interest, but so far the interest was focused on the feedback stabilization problem and the tracking problem has received less attention.

The interest in underactuated mechanical systems with second-order nonholonomic constraints can be motivated by the fact that, in general, these systems have a structural obstruction to the existence of smooth (or even continuous) time-invariant stabilizing feedback laws; they do not meet Brockett's well-known condition for smooth time-invariant feedback stabilization (Brockett, 1983). Typically, a first indication of this obstruction follows from the fact that the linearization around any equilibrium point is uncontrollable. Furthermore, it follows that the tracking control problem can only be solved by smooth feedback when additional requirements are imposed on the trajectory to be tracked, see (Jiang and Nijmeijer, 1999). These underactuated mechanical systems, not satisfying Brockett's condition, also satisfy certain nonlinear controllability properties, but these properties are not sufficient to prove complete controllability of the mechanical system. In short, the control of underactuated systems with second-order nonholonomic constraints is a challenging control problem for which many open problems still exist. For instance, it is not clear whether the tracking control problem can be solved by time-invariant feedback, as in the case of underactuated mechanical systems with first-order nonholonomic constraints. It is also not clear whether the feedback stabilization problem can be solved by smooth time-varying feedback.

The interest in underactuated mechanical systems with second-order nonholonomic constraints is also motivated from a more practical point of view. Underactuated mechanical systems are abundant in real life and many of these systems exhibit nonholonomic constraints. Therefore control methodologies are needed that can be applied in practice. This means that the control methodologies should satisfy some robustness properties, *i.e.*, they should be able to deal with parameter uncertainties and un-modelled dynamics. Therefore, the control methodologies should be tested in real-life experiments.

1.1 First-order nonholonomic constraints

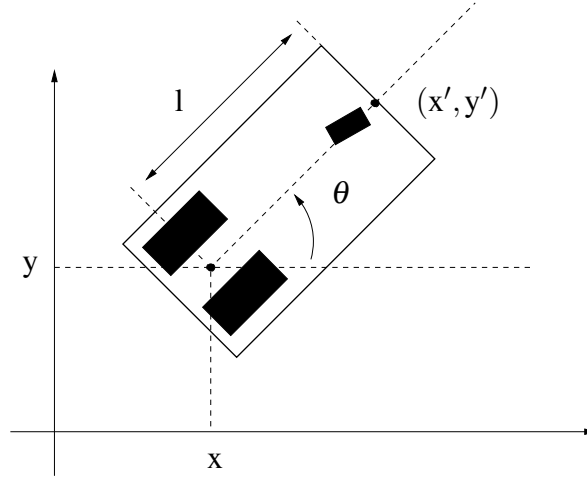


Figure 1.1: A wheeled mobile robot (unicycle type)

For mechanical systems, first-order nonholonomic constraints are velocity constraints that are non-integrable. In order to clarify what the non-integrability condition means, consider a wheeled mobile robot of unicycle type, shown in Figure 1.1. Assume that the forward velocity u and angular velocity ω are inputs that can be controlled independently. It is assumed that the front castor wheel and the rear wheels roll without slipping. When (x, y) denotes the coordinates of the center of mass and θ the angle between the heading direction and the x -axis, the kinematic model of this mobile robot is given by

$$\begin{aligned}\dot{x} &= \cos(\theta)v \\ \dot{y} &= \sin(\theta)v \\ \dot{\theta} &= \omega\end{aligned}\tag{1.1}$$

Consider a point (x', y') located at a distance l along the centerline of the mobile robot. The velocity orthogonal to the centerline of the robot should be equal to the angular velocity at the point (x', y') . The velocity (\dot{x}', \dot{y}') , orthogonal to the centerline, at the point (x', y') thus satisfies the constraint

$$\dot{x}' \sin(\theta) - \dot{y}' \cos(\theta) = -l\dot{\theta}.\tag{1.2}$$

The roll-without-slip condition of the rear-wheels, located on the axis through the point (x, y) and perpendicular to the centerline, requires that the velocity orthogonal to the center line is equal to zero. Thus equation (1.2) with $l = 0$ gives the constraint

$$\dot{x} \sin(\theta) - \dot{y} \cos(\theta) = 0\tag{1.3}$$

Consider the constraint (1.2). Using constraint (1.3), it follows that (1.2) is satisfied by

$$\begin{aligned}\dot{x}' &= \dot{x} - l \sin(\theta)\dot{\theta} \\ \dot{y}' &= \dot{y} + l \cos(\theta)\dot{\theta}.\end{aligned}\tag{1.4}$$

Integration of (1.4) leads to the relationship between the positions of the points (x, y) and (x', y') given by

$$\begin{aligned}x' &= x + l \cos(\theta) \\y' &= y + l \sin(\theta)\end{aligned}\tag{1.5}$$

This means that constraint (1.4), which is equivalent to (1.2), can be integrated to obtain (1.5). Therefore (1.2) defines a holonomic constraint. Unlike constraint (1.2), constraint (1.3) can not be integrated, *i.e.*, it can not be written as the time-derivative of some function of the state (x, y, θ) . It is an essential part of the dynamics of the system. The constraint (1.3) is therefore called a nonholonomic constraint. As a result, the stabilization of the system (1.1) is far from trivial. In fact, it can be shown that, in general, first-order nonholonomic systems can not be stabilized by any smooth time-invariant static state-feedback.

To illustrate why the underactuated system (1.1) can not be stabilized by any smooth time-invariant static state-feedback, consider the problem of stabilizing the system (1.1) to the origin. Suppose that a time-invariant static state feedback exists that stabilizes the system to the origin by smooth functions $v(x, y, \theta)$ and $\omega(x, y, \theta)$ with $v(0, 0, 0) = 0$, $\omega(0, 0, 0) = 0$. The equilibria of the closed-loop system are given by solutions of $v(x, y, \theta) = 0$ together with $\omega(x, y, \theta) = 0$. Because we have three unknowns in two equations, there exists (locally) a one-dimensional manifold of equilibria which passes through the origin. Thus the origin of the system can not be stabilized by smooth static time-invariant state-feedback. Only a manifold of dimension one can be stabilized by a smooth static time-invariant state-feedback. A formal generalization of this observation is given by Brockett's necessary condition. It is a necessary condition for feedback stabilization by continuous time-invariant feedback. It was presented in (Brockett, 1983) for \mathcal{C}^1 time-invariant feedback laws and was shown in (Zabczyk, 1989) to hold also for continuous time-invariant feedback laws.

1.2 Second-order nonholonomic constraints

As mentioned earlier, underactuated mechanical systems, *i.e.*, systems with more degrees of freedom than inputs, can give rise to second-order nonholonomic constraints. Consider an underactuated mechanical system and let $q = (q_1, \dots, q_n)$ denote the set of generalized coordinates. Partition the set of generalized coordinates as $q = (q_a, q_b)$, where $q_a \in \mathbb{R}^m$ denotes the directly actuated part and $q_b \in \mathbb{R}^{n-m}$ denotes the unactuated part. With $u \in \mathbb{R}^m$ denoting the vector of control variables, the equations of motion of the underactuated mechanical system become:

$$M_{11}(q)\ddot{q}_a + M_{12}(q)\ddot{q}_b + F_1(q, \dot{q}) = B(q)u\tag{1.6}$$

$$M_{21}(q)\ddot{q}_a + M_{22}(q)\ddot{q}_b + F_2(q, \dot{q}) = 0\tag{1.7}$$

The equations (1.7) define $n - m$ relations involving the generalized coordinates as well as their first-order and second-order derivatives. If there exists no non-trivial integral, *i.e.*, a smooth function $\sigma(t, q, \dot{q})$ such that $d\sigma/dt = 0$ along all solutions of (1.7), then these $n - m$ relations can be interpreted as nonholonomic constraints. In (Reyhanoglu et al., 1996) a class of underactuated mechanical systems was identified that exhibit second-order nonholonomic constraints. Examples of systems belonging to this class are given by underactuated robot manipulators (Oriolo and Nakamura, 1991), autonomous underwater vehicles (Egeland et al., 1994; Pettersen, 1996), underactuated surface vessels (Pettersen and Nijmeijer, 1998), the Acrobot system (Spong, 1995) and the planar vertical/short take-off and landing aircraft (V/STOL) (Hauser et al., 1992).

In this thesis only underactuated mechanical systems which exhibit second-order nonholonomic constraints are considered. In contrast to systems with first-order nonholonomic constraints, the second-order nonholonomic constraints include drift-terms that make control of these systems more difficult. Similar to the case of first-order nonholonomic systems, in certain cases second-order nonholonomic systems also have a structural obstruction to the existence of smooth (or even continuous) time-invariant stabilizing static state-feedbacks; they do not meet Brockett's necessary condition for feedback stabilization (Brockett, 1983). However, there do exist second-order nonholonomic systems that are smoothly (or even linearly) stabilizable. These systems are, in general, directly influenced by gravity and therefore the linearization around equilibrium points is controllable. The Acrobot, a two link underactuated robot (Spong, 1995), and the planar vertical/short take off and landing aircraft (V/STOL) are examples of such systems. As an example of second-order nonholonomic systems,

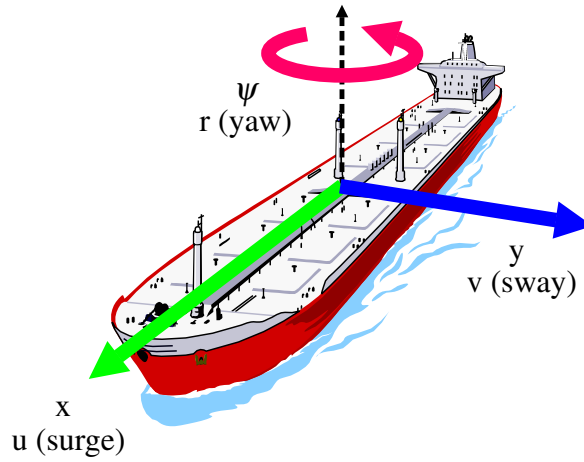


Figure 1.2: An underactuated surface vessel

consider underactuated vehicles described by the following model:

$$M\dot{v} + C(v)v + D(v)v + g(v) = \begin{bmatrix} \tau \\ 0 \end{bmatrix} \quad (1.8)$$

$$\dot{\eta} = J(\eta)v \quad (1.9)$$

where $\eta \in \mathbb{R}^n$, $v \in \mathbb{R}^m$, $n > m$ and $\tau \in \mathbb{R}^k$, $k < m$. The inertia matrix M is nonsingular and constant, *i.e.*, $\dot{M} = 0$, and the matrix $J(\eta)$ has full rank, *i.e.*, $\text{rank}(J(\eta)) = m$, $\forall \eta$. Underactuated vehicles described by (1.8,1.9) are underactuated surface vessels, underwater vehicles and spacecraft. The vector $v = [u, v, r]^T$ denotes the linear and angular velocities of the vehicle decomposed in the body-fixed frame, see Figure 1.2, $\eta = [x, y, \psi]^T$ denotes the position and orientation decomposed in the earth-fixed frame, and τ denotes the control forces and torques decomposed in the body-fixed frame. M is the inertia matrix including added mass, $C(v)$ is the Coriolis and centripetal matrix, also including added mass, $D(v)$ is the damping matrix and $g(v)$ is the vector of gravitational and buoyant forces and torques. The matrices $C(v)$ and $D(v)$ depend on the vector of linear and angular velocities v . Equation (1.9) represents the kinematics of the vehicle.

Let $M_u, C_u(v), D_u(v)$ and $g_u(v)$ denote the last $m - k$ rows of the matrices $M, C(v), D(v)$ and the vector $g(v)$, respectively. Then the constraint imposed by the unactuated dynamics can be written as

$$M_u\dot{v} + C_u(v)v + D_u(v)v + g_u(v) = 0 \quad (1.10)$$

The gravitation and buoyancy vector $g(v)$ is important for the stabilizability properties of underactuated vehicles. If the vector $g_u(v)$ corresponding to the unactuated dynamics contains a zero function, then the constraint (1.10) is a second-order nonholonomic constraint. By using Brockett's condition, it can be shown that there exists no continuous time-invariant feedback law such that the equilibrium $(0,0)$ is asymptotically stable (Pettersen, 1996).

1.3 Contributions of this thesis

In this thesis the tracking and stabilization problems for underactuated mechanical systems with second-order nonholonomic constraints are considered. A special class of underactuated mechanical systems with second-order nonholonomic constraints is considered, namely the class of underactuated mechanical systems that can be transformed, by a suitable coordinate and feedback transformation, into a special canonical form. This special canonical form, *i.e.*, the so-called second-order chained form, considerably simplifies the dynamical equations of the system and is therefore more suitable for control design than the original dynamical equations. Moreover, the transformation bringing the system into the second-order chained form, in most cases, has a clear physical interpretation. To date, studies concerning the control of nonholonomic systems have primarily been limited to tracking and stabilization problems for first-order nonholonomic systems. When second-order nonholonomic systems have been considered, the interest has been focused on the stabilization problem and the tracking control problem has received less attention. Although the dynamics of second-order nonholonomic systems are quite well understood, the tracking and control problems for these systems still remain a challenging task. For instance, it is not clear whether the tracking control problem can be solved by time-invariant feedback, like in the case of underactuated mechanical systems with first-order nonholonomic constraints. It is also not clear whether the feedback stabilization problem can be solved by smooth (or even continuous) time-varying feedback.

To our knowledge, only a few results are available that have successfully solved the tracking problem for second-order nonholonomic systems. In (Walsh et al., 1994) a result for tracking of first-order nonholonomic systems has been given that may be extended to second-order nonholonomic systems. The feedback stabilization problem has received more attention. In (Laiou and Astolfi, 1999) a discontinuous controller has been developed for the high-order chained-form system with two inputs. The discontinuous controller does not stabilize the system, but only achieves exponential convergence towards the point to be stabilized. This means that the trajectories of the closed-loop system converge exponentially towards the point to be stabilized. However, since the controller and therefore the closed-loop system is discontinuous at the point to be stabilized, no stability property in the sense of Lyapunov can be shown to hold.

The contribution of this thesis to the control of second-order nonholonomic systems is as follows. In this thesis the tracking control problem and the feedback stabilization problem for second-order nonholonomic systems is considered. In the tracking control problem only smooth state-feedback are considered and it is shown that the tracking control problem for the second-order chained form can be solved by a linear time-varying feedback. In addition, the control design approach is extended to the case of higher-dimensional chained form systems. The tracking controller has been first presented in (Aneke et al., 2000) and has been published in (Aneke et al., 2003).

The feedback stabilization problem for second-order nonholonomic systems is shown to be solvable by using continuous feedback, namely a homogeneous time-varying feedback controller that exponentially stabilizes the system with respect to a homogeneous norm. This continuous time-varying homogeneous controller has been first presented in (Aneke et al., 2002b). To date and to our knowl-

edge, this homogeneous controller is the only one capable of ensuring Lyapunov stability as well as exponential convergence, *i.e.*, ρ -exponential stability. It is well-known that homogeneous controllers are not robust with respect to parameter uncertainties and, therefore, a robust version of the homogeneous stabilizing controller is presented. The periodically updated homogeneous controller is designed by using a hybrid open-loop/feedback approach, in which the states of the system are periodically updated at discrete time instants. This approach results in a feedback stabilizer that is shown to be robust with respect to a class of additive perturbations that includes perturbations resulting from parameter uncertainties, but excludes non-smooth effects, such as friction, or measurement noise. To our knowledge, this robust controller or feedback stabilizer, presented in (Lizárraga et al., 2003), is one of the first capable of achieving robust stabilization of the second-order chained form system.

For both the tracking and stabilizing controllers, the robustness properties are investigated and bounds for a specific class of perturbations of the second-order chained form system are given that ensure robustness of the controllers. In addition, the proposed control methods are not only validated by simulation but also through experiments. The experimental results show the validity of the control approaches, but also reveal the need for controllers which are robust with respect to perturbations resulting from non-smooth effects and non-vanishing disturbances.

1.4 Outline of the thesis

This thesis deals with the tracking and feedback stabilization problems for underactuated mechanical systems with second-order nonholonomic constraints. In Chapter 2 the tracking problem and the feedback stabilization problem are formulated. In Chapter 3 some preliminaries are presented that will be used throughout this thesis. In Chapter 4 the controllability properties of the second-order chained form system are investigated and motion planning methodologies are presented for generating state-to-state trajectories. In Chapter 5 the tracking control problem is considered and a cascaded backstepping approach is proposed to stabilize the tracking-error dynamics. In Chapter 6 the feedback stabilization problem is solved by using homogeneous time-varying feedback. In Chapter 7 the proposed control methods are illustrated by computer simulations. The proposed control methods are tested on an experimental set-up of an underactuated H-Drive manipulator in Chapter 8. In Chapter 9 conclusions are drawn and recommendations for further research are given. In Appendix A a stability result is presented for cascaded systems. In Appendix B the methodology for tracking control in Chapter 5 is extended to the case of higher-dimensional chained form systems, *i.e.*, second-chained form systems with dimension $n > 3$. Finally, in Appendix C, the dynamic model of the underactuated H-Drive manipulator is presented.

Problem formulation

In this chapter, the tracking and feedback stabilization problems are formulated for a class of underactuated mechanical systems. This class consists of underactuated mechanical systems that can be transformed, by a suitable coordinate and feedback transformation, into the second-order chained form.

2.1 Second-order chained form transformations

When designing controllers for underactuated systems with nonholonomic constraints, a commonly used approach is to transform the system into some canonical form for which the control design can be carried out more easily. The most important canonical forms are the transformations into the chained form (Murray and Sastry, 1991) and the power form (McCloskey and Murray, 1993). These canonical forms are equivalent; meaning that the chained form can be transformed into the power form and vice versa. Transformations into chained or power form have mainly been used when designing controllers for underactuated systems with first-order nonholonomic constraints, such as mobile robots and car-trailer systems (Lefeber, 2000). The second-order chained form can be used to design controllers for certain systems with second-order nonholonomic constraints, such as underactuated robot manipulators and underactuated vehicles.

2.1.1 The first-order chained form system

First-order nonholonomic mechanical systems can be modeled using kinematic models or dynamic models. A general form of a nonholonomic mechanical control system, expressed in kinematic form, is given by a drift-less nonlinear control system of the form

$$\dot{x} = g_1(x)u_1 + \cdots + g_m(x)u_m, \quad (2.1)$$

where $2 \leq m < n$, $x = (x_1, \dots, x_n)$ is the state-vector and $u_i, i \in (1, \dots, m)$, are the control variables. The system is supposed to satisfy some first-order nonholonomic constraints given as $h(x) = 0$. An essential assumption is that the system (2.1) is completely controllable; it satisfies the controllability Lie algebra rank condition. This assumption guarantees, see (Kolmanovsky and McClamroch, 1995), that there exists no non-trivial integral to the nonholonomic constraint $\Phi(x) = 0$, *i.e.*, when denoting the state as $x = [q, \dot{q}]^T$ with q the generalized coordinates, there does not exist a smooth function $\phi(q)$ such that $d\phi/dt = 0$ along all solutions of (2.1).

A general form of the dynamics of a first-order nonholonomic mechanical control system is given by a nonlinear control system of the form

$$\begin{aligned}\dot{x} &= g_1(x)y_1 + \cdots + g_m(x)y_m, \\ \dot{y}_i &= u_i, \quad i = 1, \dots, m,\end{aligned}\tag{2.2}$$

where $2 \leq m < n$, $x = (x_1, \dots, x_n)$ and $u_i, i \in (1, \dots, m)$, are the control variables. This drift-less dynamic extension of the kinematic model (2.1) also includes the d'Alembert-Lagrange formulation, which under a reasonable set of assumptions can be transformed into (2.2). Further generalization of the kinematic system (2.1) and the dynamic system (2.2) are possible, but most research is restricted to this class of first-order nonholonomic systems.

In many applications, nonholonomic control systems are transformed into the chained-form system given by

$$\begin{aligned}\dot{\xi}_1 &= u_1 \\ \dot{\xi}_2 &= u_2 \\ \dot{\xi}_3 &= \xi_2 u_1.\end{aligned}\tag{2.3}$$

Many mechanical systems with first-order nonholonomic constraints can be locally or globally transformed into the chained-form (2.3), or higher dimensional variants thereof, by a coordinate and feedback transformation. In fact, in (Murray and Sastry, 1993) it was shown that any kinematic model of a first-order nonholonomic system with three states and two inputs can be converted into the chained-form (2.3). The chained-form system can be used to facilitate control design because its structure is simpler, or at least looks simpler, than that of the original system. Furthermore, it facilitates the systematic construction of controllers for a wide range of nonholonomic mechanical systems.

For example, consider the system of a wheeled mobile robot illustrated in Figure 1.1:

$$\begin{aligned}\dot{x} &= \cos(\theta)v \\ \dot{y} &= \sin(\theta)v \\ \dot{\theta} &= \omega\end{aligned}\tag{2.4}$$

The kinematic model (2.4) of the wheeled mobile robot can be transformed into the chained-form (2.3) by the coordinate and feedback transformation given by

$$\begin{aligned}\xi_1 &= \theta & u_1 &= \omega \\ \xi_2 &= x \cos(\theta) + y \sin(\theta) & u_2 &= v - \omega x_3 \\ \xi_3 &= x \sin(\theta) - y \cos(\theta).\end{aligned}\tag{2.5}$$

2.1.2 The second-order chained form system

A special canonical form called the general n -dimensional second-order chained form system is given by

$$\begin{aligned}\ddot{\xi}_1 &= u_1 \\ \ddot{\xi}_2 &= u_2 \\ \ddot{\xi}_3 &= \xi_2 u_1 \\ &\vdots \\ \ddot{\xi}_n &= \xi_{n-1} u_1\end{aligned}\tag{2.6}$$

It plays the same role for second-order nonholonomic systems as the chained form system for first-order nonholonomic systems. In this thesis the dimension n of the second-order chained is defined as the number of equations. The number of degrees of freedom (DOF) of the mechanical system is defined as the number of generalized coordinates. It has been shown that certain 2-input and 3-DOF systems with second-order nonholonomic constraints can be transformed into the 3-dimensional second-order chained form given by

$$\begin{aligned}\ddot{\xi}_1 &= u_1 \\ \ddot{\xi}_2 &= u_2 \\ \ddot{\xi}_3 &= \xi_2 u_1.\end{aligned}\tag{2.7}$$

To our knowledge, so far, no underactuated mechanical systems have been found that are transformable into a second-order chained form system of dimension higher than 3. Therefore, the results in this thesis will focus on the 3-dimensional second-order chained form. Contrary to the first-order chained form system which contained first-order derivatives, the second-order chained form contains second-order derivatives. The resulting drift vector-field $f(\xi, \dot{\xi}) = (\dot{\xi}_1, 0, \dot{\xi}_2, 0, \dot{\xi}_3, 0)^T$ makes the second-order chained form system more difficult to control than the first-order chained form system. Systems that can be transformed into the second-order chained form, or systems with a similar structure, include, but are not limited to, an underactuated planar horizontal three-link serial-drive PPR manipulator (Arai et al., 1998a) (where PPR denotes a manipulator with two prismatic and one unactuated or passive revolute joint), an underactuated planar horizontal PPR manipulator with a spring-coupled third link (Reyhanoglu et al., 1999), an underactuated planar horizontal three-link serial-drive RR manipulator (Yoshikawa et al., 2000), an underactuated planar horizontal parallel-drive RRR manipulator with any two joints unactuated, a manipulator driven by end-effector forces (Luca et al., 1998), a planar rigid body with an unactuated degree of freedom (Reyhanoglu et al., 1998), an underactuated surface vessel (Reyhanoglu et al., 1999), a simplified underactuated underwater vehicle (Egeland and Berglund, 1994; Rathinam and Murray, 1998) and the planar V/STOL (vertical/short take-off and landing) aircraft in the absence of gravity (Aneke et al., 2002a). Additional examples are given by a planar rigid body with two thrusters moving on a flat horizontal plane (McClamroch and Morin, 1998), the planar motion of a rigid body with an internal degree of freedom (McClamroch et al., 1998) and a hovercraft type vehicle (Tanaka et al., 2000). It should be noted that all the transformations involved in these examples allow one to map an arbitrary equilibrium point to the origin of the second-order chained form. Thereby, the stabilization of arbitrary configurations can be reduced to the stabilization of the origin of the second-order chained form.

In fact, there may be other systems that can be transformed into the second-order chained form, or into a system that has a similar structure. For example, in (Reyhanoglu et al., 1996) the underactuated surface vessel with two independent thrusters was shown to be feedback equivalent to the second-order chained form, up to an additional term, *i.e.*,

$$\begin{aligned}\ddot{z}_1 &= v_1 \\ \ddot{z}_2 &= v_2 \\ \ddot{z}_3 &= z_2 v_1 + c_y/m(\dot{z}_1 z_2 - \dot{z}_3),\end{aligned}\tag{2.8}$$

where c_y is a positive constant representing the hydro-dynamic damping coefficient and m is the mass of the vessel. In (Egeland and Berglund, 1994) an idealized underactuated underwater vehicle was

shown to be transformable into the system given by

$$\begin{aligned}\ddot{z}_1 &= u_1 \\ \ddot{z}_2 &= u_2 & \ddot{z}_4 &= u_3 \\ \ddot{z}_3 &= z_2 u_1 & \ddot{z}_5 &= z_4 u_1 \\ \ddot{z}_6 &= u_4.\end{aligned}\tag{2.9}$$

This system consists of two interconnected second-order chained-form systems in conjunction with the dynamics $\ddot{z}_6 = u_4$.

2.2 The feedback stabilization problem

Consider the general second-order chained form (2.7), with $n = 3$ variables, in state-space form:

$$\begin{aligned}\dot{x}_1 &= x_2 & \dot{x}_2 &= u_1 \\ \dot{x}_3 &= x_4 & \dot{x}_4 &= u_2 \\ \dot{x}_5 &= x_6 & \dot{x}_6 &= x_3 u_1\end{aligned}\tag{2.10}$$

where $x_{2i-1} = \xi_i$, $x_{2i} = \dot{\xi}_i$, $i = 1, 2, 3$. Define the state vector by $x = [x_1, \dots, x_6]^T$. The feedback stabilization problem can be formulated as follows.

Problem 2.2.1 (Point stabilization problem). Design appropriate continuous or discontinuous time-varying state feedback controllers of the form

$$u_1 = u_1(t, x), \quad u_2 = u_2(t, x)\tag{2.11}$$

such that the equilibrium $x = 0$ of the closed-loop system (2.10,2.11) is globally asymptotically stable.

In (Brockett, 1983) a necessary condition for stabilizability by continuous time-invariant feedback was presented. It is often referred to as Brockett's condition. It was shown to hold for \mathcal{C}^1 time-invariant state feedback, and shown to also hold for continuous time-invariant state feedback by (Zabczyk, 1989). It can be formulated as follows

Theorem 2.2.1. *Assume that there exists a continuous time-invariant state feedback $u : \mathbb{R}^n \rightarrow \mathbb{R}^m$, that renders the origin of $\dot{x} = f(x, u)$, with $x \in \mathbb{R}^n$ and $u \in \mathbb{R}^m$, asymptotically stable. Then the function $f : \mathbb{R}^n \times \mathbb{R}^m \rightarrow \mathbb{R}^n$ is locally surjective, i.e., the function f maps an arbitrary neighborhood of $(0, 0) \in \mathbb{R}^n \times \mathbb{R}^m$ onto a neighborhood of 0 in \mathbb{R}^n .*

Since the image of the mapping $(x, u) \mapsto f(x, u) = (x_4, x_5, x_6, u_1, u_2, x_3 u_1)$ of the second-order chained form does not contain any point $(0, 0, 0, 0, 0, \varepsilon)$ for $\varepsilon \neq 0$, the system does not satisfy Brockett's condition. Therefore, the system can not be asymptotically stabilized by continuous time-invariant feedback. In fact, it can not even be stabilized by discontinuous time-invariant feedback when the Filippov solutions of the closed-loop system are considered (Coron and Rosier, 1994).

To our knowledge the asymptotic feedback stabilization problem for the second-order chained form system (2.7) has not been solved yet. The second-order chained form system is a generalization of the drift-less chained form (Murray and Sastry, 1993), in the sense that it does contain a drift vector field. The stabilization problem for the drift-less chained form system has received a lot of attention in control literature, however, the stabilization problem for the second-order chained form system has received less attention. In fact, it is well-known that the existence of a drift-term makes

the stabilization of the second-order chained form more difficult. Nevertheless, several results for the stabilization of the second-order chained form have been obtained, such as the references (Astolfi, 1996), (Laiou and Astolfi, 1999) and (Imura et al., 1996) in which discontinuous controllers were presented that achieve exponential convergence towards the origin. However, due to the fact that these controllers are discontinuous at the origin they are no feedback stabilizers as they do not achieve stability of the origin in a Lyapunov sense. In the reference (Laiou and Astolfi, 1999) this result was extended to obtain a weakened Lyapunov stability result called quasi-smooth exponential stability.

To our knowledge, one of the few feedback stabilizers was given in (Sørdalen and Egeland, 1993). It consists of a hybrid feedback controller that \mathcal{H} -exponentially stabilizes the three-dimensional ($n=3$) second-order chained form. However, the closed-loop system is not stable in a Lyapunov sense. It is not yet clear whether the second-order chained form system can be stabilized by means of smooth time-varying feedback. It is, however, clear that exponential stability of the origin can not be achieved by smooth feedback, since the linearization around any equilibrium point is uncontrollable. In this thesis, it is investigated whether the second-order chained form system can be ρ -exponentially stabilized by continuous periodic time-varying feedback. The notion of ρ -exponentially is weaker than exponential stability and stronger than asymptotic stability in the sense that a system is ρ -exponentially if it is asymptotically stable with exponential convergence.

2.3 The tracking control problem

Consider the second-order chained form (2.10). Suppose that we want the system to follow a predefined realizable trajectory, i.e. we want the state $x = [x_1, \dots, x_6]^T$ to follow a prescribed path $x_d = [x_{1d}, \dots, x_{6d}]^T$. This reference trajectory x_d thus satisfies

$$\begin{aligned}\dot{x}_{1d} &= x_{2d} & \dot{x}_{2d} &= u_{1d} \\ \dot{x}_{3d} &= x_{4d} & \dot{x}_{4d} &= u_{2d} \\ \dot{x}_{5d} &= x_{6d} & \dot{x}_{6d} &= x_{3d}u_{1d}\end{aligned}\tag{2.12}$$

The tracking-error $x_e = [x_{1e}, x_{2e}, \dots, x_{6e}]^T$ is given by

$$x_{ie} = x_i - x_{id}, \quad i = 1, 2, \dots, 6.\tag{2.13}$$

The tracking-error dynamics in state-space form are derived from (2.10,2.12) and are given by

$$\begin{aligned}\dot{x}_{1e} &= x_{2e} & \dot{x}_{2e} &= u_1 - u_{1d} \\ \dot{x}_{3e} &= x_{4e} & \dot{x}_{4e} &= u_2 - u_{2d} \\ \dot{x}_{5e} &= x_{6e} & \dot{x}_{6e} &= x_{3e}u_{1d} + x_3(u_1 - u_{1d})\end{aligned}\tag{2.14}$$

Problem 2.3.1 (State feedback tracking control problem). The tracking control problem is solvable if we can design appropriate continuous or discontinuous time-varying state feedback controllers of the form

$$u_1 = u_1(t, x_e, \bar{u}_d), \quad u_2 = u_2(t, x_e, \bar{u}_d)\tag{2.15}$$

such that the closed-loop system (2.14,2.15) is globally uniformly asymptotically stable. The vector \bar{u}_d contains $u_d = [u_{1d}, u_{2d}]$ and higher order derivatives up to some order k , i.e $\bar{u}_d = [u_d, \dot{u}_d, \dots, u_d^{(k)}]$.

In this thesis, it will be investigated whether the tracking-error dynamics can be asymptotically or even exponentially stabilized. It follows that for smooth feedback tracking, additional constraints on

the desired trajectory are required (Jiang and Nijmeijer, 1999). In (Lefeber, 2000) cascade type controllers have successfully been applied to solve the trajectory tracking problem for an underactuated surface vessel. However, this result was not based on a transformation into the second-order chained form. There are very few results that have addressed the tracking problem for the second-order chained form. One of these results is given in (Kobayashi, 1999), where a discontinuous and flatness-based tracking controller could be derived for a class of trajectories of the second-order chained-form system. In (Walsh et al., 1994) a result for tracking of first-order nonholonomic systems has been given that may be extended to second-order nonholonomic systems. It consists of linearizing the chained form system around the reference trajectory and designing a linear time-varying feedback that stabilizes the resulting linear time-varying system. The reference trajectory should be chosen such that the resulting time-varying system is uniformly completely controllable (Rugh, 1996) over intervals of length δ . This approach means that one should also face the problem of finding feasible trajectories. Moreover, the controller depends explicitly on the trajectory to be tracked, and should be re-computed for different trajectories.

2.4 Robustness considerations

Consider the perturbed system

$$\dot{x} = f(t, x) + g(t, x) \quad (2.16)$$

The unknown perturbation term $g(t, x)$ can result from modeling errors, wear/aging, parameter uncertainties, and disturbances. The system (3.13) can be thought of as a perturbation of the nominal system

$$\dot{x} = f(t, x), \quad (2.17)$$

where $f(t, x)$ represents either the closed-loop system (2.10,2.11) in the case of the feedback stabilization problem or the closed-loop tracking-error dynamics (2.14,2.15) in the case of the tracking control problem. The perturbation to the system may result from unmodelled dynamics and parameter uncertainties. We can distinguish between vanishing perturbations, *i.e.*, $g(t, 0) = 0 \forall t > t_0$, and non-vanishing perturbations, *i.e.*, $\exists t > t_0 : g(t, 0) \neq 0$. Suppose that the nominal system (3.14) has a uniformly exponentially stable equilibrium at the origin. If the perturbation $g(t, x)$ is vanishing at the origin, the point $x = 0$ is also an equilibrium of the perturbed system. In that case, we would like to know whether the perturbed system (3.13) remains exponentially stable. On the other hand, if the perturbation is non-vanishing, the origin $x = 0$ may not be an equilibrium point of the perturbed system (3.13). It is then no longer possible to investigate the stability properties of the origin as an equilibrium point, nor should one expect the solution of the perturbed system to approach the origin as $t \rightarrow \infty$. The best we can hope for is that if the perturbation $g(t, x)$ is small in some sense, then the solution $x(t)$ approaches the origin for sufficiently large t . In the ideal case, the state $x(t)$ remains bounded while the bound depends on the magnitude of the perturbation $g(t, x)$.

2.5 Summary

In this section we formulated the tracking control and the feedback stabilization problems. In the tracking control problem the system should follow a pre-defined and realizable reference trajectory. In the feedback stabilization problem the system should be stabilized to a certain equilibrium point. In general, the tracking problem for underactuated mechanical systems has not received much attention, but most researches focused on the feedback stabilization problem. Nevertheless, the tracking problem

is more important, because, in general, one not only wants the system to move towards a certain equilibrium point, but one also wants the system to move along a specified path. It is well-known that the feedback stabilization problem can not be solved by any continuous time-invariant feedback. The tracking control problem, however, can be solved by smooth feedback when additional constraints are imposed on the trajectory to be tracked. In Chapter 4 some methodologies for motion planning of nonholonomic mechanical systems will be presented.

Preliminaries

This chapter starts with recalling some basic definitions and results that will be used throughout this thesis. First some fundamental definitions are given and the concept of Lyapunov stability is introduced. Most of the definitions can be found in (Khalil, 1996). Also some robustness results are presented for the stability of perturbed systems. In addition, a result for asymptotic stability of time-varying cascaded systems is presented. This result was given in (Lefeber et al., 2000) and will be used in conjunction with a backstepping approach to solve the tracking control problem. Finally, the theory of homogeneous systems, used to solve the feedback stabilization problem, is introduced.

3.1 Mathematical preliminaries

The class of n times continuously differentiable functions will be denoted by \mathcal{C}^n and the class of smooth function by \mathcal{C}^∞ .

Definition 3.1.1. A continuous function $\alpha : [0, a) \rightarrow [0, \infty)$ is said to belong to class \mathcal{K} (i.e., $\alpha \in \mathcal{K}$) if it is strictly increasing and $\alpha(0) = 0$. It is said to belong to class \mathcal{K}_∞ ($\alpha \in \mathcal{K}_\infty$) if $a = \infty$ and $\alpha(r) \rightarrow \infty$ as $r \rightarrow \infty$.

Definition 3.1.2. A continuous function $\beta : [0, a) \times [0, \infty) \rightarrow [0, \infty)$ is said to belong to class \mathcal{KL} ($\beta \in \mathcal{KL}$) if, for each fixed s , the mapping $\beta(r, s)$ belongs to class \mathcal{K} with respect to r and, for each r , the mapping $\beta(r, s)$ is decreasing with respect to s and $\beta(r, s) \rightarrow 0$ as $s \rightarrow \infty$.

Definition 3.1.3. An open ball of radius r around a point x_0 will be denoted by $B_r(x_0)$, i.e.,

$$B_r(x_0) = \{x \in \mathbb{R}^n \mid \|x - x_0\| < r\}$$

If $x_0 = 0$ then the open ball is denoted by B_r .

3.2 Lyapunov stability

Consider a non-autonomous system described by

$$\dot{x} = f(t, x) \tag{3.1}$$

where $f : \mathbb{R}_+ \times D \rightarrow \mathbb{R}^n$ is piecewise continuous on $\mathbb{R}_+ \times D$ and locally Lipschitz in x on $\mathbb{R}_+ \times D$, and $D \subset \mathbb{R}^n$ is a domain that contains the origin $x = 0$. Assume that the origin $x = 0$ is an equilibrium point of the system, i.e., $f(t, 0) = 0, \forall t \geq 0$. The assumption that $f(t, x)$ is piecewise continuous in t , allows one to include the case in which $f(t, x)$ depends on a time-varying input that may experience step changes in time. In that case, the solutions $x(t)$ of (3.1) are piecewise continuously differentiable.

Definition 3.2.1. The equilibrium $x = 0$ of (3.1) is said to be

- **(locally) stable** if a constant $r > 0$ exists such that for all $t_0 \in \mathbb{R}_+$ a class \mathcal{K} function $\alpha(\cdot)$ exists such that

$$\|x(t)\| \leq \alpha(\|x(t_0)\|), \quad \forall t \geq t_0, \forall x(t_0) \in B_r;$$

- **(locally) asymptotically stable** if a constant $r > 0$ exists such that for all $t_0 \in \mathbb{R}_+$ a class \mathcal{KL} function $\beta(\cdot, \cdot)$ exists such that

$$\|x(t)\| \leq \beta(\|x(t_0)\|, t - t_0), \quad \forall t \geq t_0, \forall x(t_0) \in B_r;$$

- **(locally) exponentially stable** if it is locally asymptotically stable and a constant $r > 0$ exists such that for all $t_0 \in \mathbb{R}_+$ there exists constants $K > 0$ and $\gamma > 0$ such that

$$\|x(t)\| \leq K\|x(t_0)\| \exp(-\gamma(t - t_0)), \quad \forall t \geq t_0, \forall x(t_0) \in B_r;$$

If the above definitions are valid for any initial state $x(t_0) \in D$, then the equilibrium $x = 0$ of (3.1) is said to be globally stable, globally asymptotically stable and globally exponentially stable, respectively.

In the above definitions the solutions of the non-autonomous system may depend on both t and t_0 . Therefore, the stability behavior of the equilibrium point $x = 0$, in general, may depend on the initial time t_0 . In fact, the constants r , K , γ , the class \mathcal{K} function $\alpha(\cdot)$ and the class \mathcal{KL} function $\beta(\cdot, \cdot)$ may be dependent on the initial time t_0 . Of course, the fact that such constants and functions exist for every t_0 , does not guarantee that there exists one pair of constants and functions such that the conditions are fulfilled. In order to distinguish between the dependency on the initial time t_0 , we introduce the notion of uniformity.

Definition 3.2.2. The equilibrium $x = 0$ of (3.1) is said to be

- **(locally) uniformly stable** if a constant $r > 0$ and a class \mathcal{K} function $\alpha(\cdot)$ exists, both independent on t_0 , such that

$$\|x(t)\| \leq \alpha(\|x(t_0)\|), \quad \forall t \geq t_0, \forall x(t_0) \in B_r;$$

- **(locally) uniformly asymptotically stable** if a constant $r > 0$ and a class \mathcal{KL} function $\beta(\cdot, \cdot)$ exists, both independent on t_0 , such that

$$\|x(t)\| \leq \beta(\|x(t_0)\|, t - t_0), \quad \forall t \geq t_0, \forall x(t_0) \in B_r;$$

- **(locally) uniformly exponentially stable** if it is locally asymptotically stable and a constant $r > 0$ and constants $K > 0$ and $\gamma > 0$ such that

$$\|x(t)\| \leq K\|x(t_0)\| \exp(-\gamma(t - t_0)), \quad \forall t \geq t_0, \forall x(t_0) \in B_r;$$

If the above definitions are valid for any initial state $x(t_0) \in D$, then the equilibrium $x = 0$ of (3.1) is said to be globally uniformly stable, globally uniformly asymptotically stable and globally uniformly exponentially stable, respectively. Unfortunately, uniform exponential stability can not always be achieved. A notion that is stronger than global uniform asymptotic stability, but weaker than uniform exponential stability is \mathcal{K} -exponential stability as defined in (Sørdalen and Egeland, 1995).

Definition 3.2.3. (Sørdalen and Egeland 1995, Definition 2) The equilibrium $x = 0$ of (3.1) is said to be globally \mathcal{K} -**exponentially stable** if a class \mathcal{K} function $\kappa : \mathbb{R} \rightarrow \mathbb{R}$ and a constant $\gamma > 0$ exists such that for all $(t_0, x(t_0)) \in \mathbb{R}_+ \times \mathbb{R}^n$ it holds that

$$\|x(t)\| \leq \kappa(\|x(t_0)\|) \exp(-\gamma(t-t_0)), \quad \forall t \geq t_0 \geq 0. \quad (3.2)$$

In some cases, stability in the sense of Lyapunov, as shown above, can not be achieved. This commonly arises when discontinuous controllers are used to control the system. By using discontinuous control, it may be possible to achieve exponential convergence towards the origin. However, these discontinuous controllers only guarantee exponential convergence for all initial conditions in an open and dense set $\Omega \subset D$ of the state space. Most commonly, see for example (Astolfi, 1996), the closed-loop system exponentially converges towards the origin for all initial conditions in the set $\Omega = \{x \in D | x_1 \neq 0\}$, and is not defined or may grow unbounded outside the set Ω .

Definition 3.2.4. The system (3.1) is said to **converge exponentially towards** $x = 0$ if there exists an open and dense set $\Omega \subset D$ and a constant $\gamma > 0$ such that for all $(t_0, x(t_0)) \in \mathbb{R}_+ \times \Omega$ it holds that

$$\|x(t)\| \leq \|x(t_0)\| \exp(-\gamma(t-t_0)), \quad \forall t \geq t_0 \geq 0. \quad (3.3)$$

The notions of uniform asymptotic and uniform exponential stability can be characterized in terms of the existence of a so-called Lyapunov function. This is stated in the following theorem.

Theorem 3.2.1. (Khalil 1996, Theorem 3.8) Let $x = 0$ be an equilibrium point for (3.1) and $E \subset D \subset \mathbb{R}^n$ be a domain containing $x = 0$. If $V : \mathbb{R}_+ \times E \rightarrow \mathbb{R}$ is a continuously differentiable function such that

$$\begin{aligned} W_1(x) &\leq V(t, x) \leq W_2(x) \\ \frac{\partial V(t, x)}{\partial t} + \frac{\partial V(t, x)}{\partial x} f(t, x) &\leq -W_3(x) \end{aligned} \quad (3.4)$$

$\forall t \geq t_0, \forall x \in E$ and where $W_1(x)$, $W_2(x)$ and $W_3(x)$ are continuous positive definite functions on E . Then $x = 0$ is locally uniformly asymptotically stable. Moreover, if

$$W_1(x) \geq c_1 \|x\|^c, \quad W_2(x) \leq c_2 \|x\|^c, \quad W_3(x) \geq c_3 \|x\|^c, \quad (3.5)$$

for some positive constants c_1, c_2, c_3 and c , then $x = 0$ is locally uniformly exponentially stable.

A function $V(t, x)$ satisfying conditions (3.4) is said to be a Lyapunov function for the system (3.1). Suppose that all conditions hold globally, i.e., $\forall x \in D$, then the equilibrium $x = 0$ is globally uniformly asymptotically stable. If additionally (3.5) holds, then $x = 0$ is globally uniformly exponentially stable. Similar to autonomous systems, (uniform) exponential stability of the linearization of a non-autonomous system is a necessary and sufficient condition for local (uniform) exponential stability of the origin.

Theorem 3.2.2. (Khalil 1996, Theorem 3.13) Suppose that $x = 0$ is an equilibrium point for the nonlinear system

$$\dot{x} = f(t, x),$$

where $f : \mathbb{R}_+ \times D \rightarrow \mathbb{R}^n$ is continuously differentiable, $D = \{x \in \mathbb{R}^n | \|x\| < r\}$, and the Jacobian matrix $[\partial f / \partial x]$ is bounded and Lipschitz on D , uniformly in t . Let

$$A(t) = \left. \frac{\partial f}{\partial x}(t, x) \right|_{x=0}.$$

Then the origin is a locally exponentially stable equilibrium point for the nonlinear system if and only if it is an exponentially stable equilibrium point for the linear system

$$\dot{x} = A(t)x.$$

3.3 Converse theorems

We start by stating some converse theorems that prove the existence of a suitable Lyapunov function when the system is (locally) uniformly asymptotically or (locally) uniformly exponentially stable, respectively. These converse theorems will be used to prove stability of the controlled systems in Chapter 5.

Theorem 3.3.1. (Khalil 1996, Theorem 3.14) *Suppose $x = 0$ is an equilibrium point of the nonlinear system $\dot{x} = f(t, x)$, where $f : \mathbb{R}_+ \times D \rightarrow \mathbb{R}^n$ is continuously differentiable, $D = \{x \in \mathbb{R}^n \mid \|x\| < r\}$, and the Jacobian matrix $[\partial f / \partial x]$ is bounded on D , uniformly in t . Let k , γ and r_0 be positive constants with $r_0 < r/k$ and $D_0 = \{x \in \mathbb{R}^n \mid \|x\| < r_0\}$. Assume that the trajectories of the system satisfy*

$$\|x(t)\| \leq \beta(\|x(t_0)\|, t - t_0), \quad \forall x(t_0) \in D_0, \forall t \geq t_0.$$

Then there exists a \mathcal{C}^1 function $V : \mathbb{R}_+ \times D_0 \rightarrow \mathbb{R}$ that satisfies the inequalities

$$\begin{aligned} \bullet \quad & \alpha_1(\|x\|) \leq V(t, x) \leq \alpha_2(\|x\|), \\ \bullet \quad & \dot{V}(t, x) \leq -\alpha_3(\|x\|), \\ \bullet \quad & \left\| \frac{\partial V(t, x)}{\partial x} \right\| \leq \alpha_4(\|x\|), \end{aligned} \tag{3.6}$$

for all $t \geq t_0$ and all $x \in D$ and where $\alpha_1(\cdot)$, $\alpha_2(\cdot)$, $\alpha_3(\cdot)$ and $\alpha_4(\cdot)$ are class \mathcal{K} functions defined on $[0, r_0]$. Moreover, if $r = \infty$ and the origin is globally exponentially stable, then $V(t, x)$ is defined on $\mathbb{R}_+ \times \mathbb{R}^n$ and the above inequalities are valid for all $x \in \mathbb{R}^n$.

If the system is uniformly exponentially stable, the existence of a Lyapunov function is given by the following theorem.

Theorem 3.3.2. (Khalil 1996, Theorem 3.12) *Suppose $x = 0$ is an equilibrium point of the nonlinear system $\dot{x} = f(t, x)$, where $f : \mathbb{R}_+ \times D \rightarrow \mathbb{R}^n$ is continuously differentiable, $D = \{x \in \mathbb{R}^n \mid \|x\| < r\}$, and the Jacobian matrix $[\partial f / \partial x]$ is bounded on D , uniformly in t . Let k , γ and r_0 be positive constants with $r_0 < r/k$ and $D_0 = \{x \in \mathbb{R}^n \mid \|x\| < r_0\}$. Assume that the trajectories of the system satisfy*

$$\|x(t)\| \leq k\|x(t_0)\| \exp(-\gamma(t - t_0)), \quad \forall x(t_0) \in D_0, \forall t \geq t_0 \geq 0.$$

Then there exists a \mathcal{C}^1 function $V : \mathbb{R}_+ \times D_0 \rightarrow \mathbb{R}$ that satisfies the inequalities

$$\begin{aligned} \bullet \quad & c_1\|x\|^2 \leq V(t, x) \leq c_2\|x\|^2, \\ \bullet \quad & \dot{V}(t, x) \leq -c_3\|x\|^2, \\ \bullet \quad & \left\| \frac{\partial V(t, x)}{\partial x} \right\| \leq c_4\|x\|, \end{aligned} \tag{3.7}$$

for all $t \geq t_0$ and all $x \in D$ and where c_1, c_2, c_3 and c_4 are some positive constants. Moreover, if $r = \infty$ and the origin is globally exponentially stable, then $V(t, x)$ is defined on \mathbb{R}^n and the above inequalities are defined on \mathbb{R}^n .

3.4 Linear time-varying systems

Consider the linear time-varying system given by

$$\dot{x} = A(t)x \quad (3.8)$$

with $x \in \mathbb{R}^n$ and $A(t)$ continuous for all $t \geq t_0$. From linear system theory (Rugh, 1996), the solution of the system (3.8) is given by $x(t) = \phi(t, t_0)x(t_0)$, where $\phi(t, t_0)$ is the state transition matrix of (3.8). For linear time-varying systems, in general, uniform asymptotic stability can not be characterized by the location of the eigenvalues of the matrix $A(t)$. In fact, for a linear system to be uniformly asymptotically stable, the following should hold for some $k > 0$ and $\gamma > 0$

$$\|\phi(t, t_0)\| \leq k \exp(-\gamma(t - t_0)), \quad \forall t \geq t_0 \geq 0. \quad (3.9)$$

This shows that for linear systems uniform asymptotic stability (GUAS) and uniform exponential stability (GUES) are equivalent. Similar to non-autonomous systems, uniform exponential stability can be characterized in terms of the existence of a Lyapunov function $V(t, x)$. The following converse theorem states that when the origin is uniformly exponentially stable, there exists a Lyapunov function for the system.

Theorem 3.4.1. (Khalil 1996, Theorem 7.4) *Suppose that the equilibrium $x = 0$ of the system (3.8) is uniformly exponentially stable. Let $Q(t)$ be a continuous, bounded, positive definite, symmetric matrix $Q(t)$, i.e., $0 < q_3 I \leq Q(t) \leq q_4 I, \forall t \geq t_0$. Then there exists a continuously differentiable, bounded, positive definite, symmetric matrix $P(t)$, i.e., $0 < c_1 I \leq P(t) \leq c_2 I, \forall t \geq t_0$, such that*

$$\dot{P}(t) + P(t)A(t) + A(t)^T P(t) = -Q(t) \quad (3.10)$$

Therefore $V(t, x) = x^T P(t)x$ is a Lyapunov function for the system as it satisfies $\dot{V}(t, x) = -x^T Q(t)x$.

Remark 3.4.1. When the transition matrix $\phi(t, t_0)$ of the linear system is known, it can be shown that the matrix given by

$$P(t) = \int_t^{\infty} \phi^T(\tau, t) Q(\tau) \phi(\tau, t) d\tau \quad (3.11)$$

is a solution of (3.10), see Theorem 3.10 in (Khalil, 1996). When the matrix $A(t)$ is uniformly bounded, i.e., $\|A(t)\| \leq L, \forall t \geq t_0$, then the matrix $P(t)$ satisfies all conditions (3.5) (3.7) with

$$c_1 = \frac{q_3}{2L}, \quad c_2 = \frac{q_4 k^2}{2\gamma}, \quad c_3 = q_3, \quad c_4 = \frac{q_4 k^2}{\gamma}. \quad (3.12)$$

with q_3 and q_4 arbitrary positive constants satisfying $q_3 I \leq Q(t) \leq q_4 I$. The constants k and γ are given by (3.9).

3.5 Perturbation theory

Consider the perturbed system

$$\dot{x} = f(t, x) + g(t, x) \quad (3.13)$$

where $f : \mathbb{R}_+ \times D \rightarrow \mathbb{R}^n$ and $g : \mathbb{R}_+ \times D \rightarrow \mathbb{R}^n$ are piecewise continuous in t and locally Lipschitz in x on $\mathbb{R}_+ \times D$ and $D \subset \mathbb{R}^n$ is a domain that contains the origin $x = 0$. Moreover, assume that

$f: \mathbb{R}_+ \times D \rightarrow \mathbb{R}^n$ is continuously differentiable, and the Jacobian $[\partial f / \partial x]$ is bounded on D , uniformly in t . The system (3.13) can be thought of as a perturbation of the nominal system

$$\dot{x} = f(t, x). \quad (3.14)$$

Suppose that the nominal system (3.14) has a uniformly exponentially stable equilibrium at the origin, then we would like to know what the stability behavior of the perturbed system (3.13) is. Since the equilibrium $x = 0$ is an exponentially stable equilibrium point of the nominal system, Theorem 3.3.2 states that a Lyapunov function exists for the nominal system. A commonly used approach to investigate the stability behavior of the perturbed system is to use a Lyapunov function candidate for the perturbed system. Then one distinguishes between vanishing perturbations, *i.e.*, $g(t, 0) = 0 \forall t > 0$, and non-vanishing perturbations, *i.e.*, $\exists t > t_0 : g(t, 0) \neq 0$.

3.5.1 Vanishing perturbations

If the perturbation term is vanishing at the origin, the origin $x = 0$ is still a equilibrium point of the perturbed system. In the case that $x = 0$ is a uniformly exponentially stable equilibrium point of the nominal system, Theorem 3.3.2 guarantees the existence of a Lyapunov $V(t, x)$ for the nominal system. By directly calculating the derivative of the Lyapunov function along solutions of the perturbed system, we obtain the following result that can be used to investigate the stability properties of the perturbed system.

Theorem 3.5.1. (*Khalil 1996, Lemma 5.1*) *Suppose that $x = 0$ is an uniformly exponentially stable equilibrium of the nominal system (3.14). Let $V(t, x)$ be a Lyapunov function of the nominal system that satisfies (3.7) in $\mathbb{R}_+ \times D$. Suppose that the perturbation term $g(t, x)$ satisfies a linear growth bound*

$$\|g(t, x)\| \leq \gamma \|x\|, \quad \forall t \geq t_0, \forall x \in D. \quad (3.15)$$

Then the origin is a uniformly exponentially stable equilibrium point of the perturbed system (3.13) if

$$\gamma < \frac{c_3}{c_4}. \quad (3.16)$$

Moreover, if all assumptions hold globally, then the origin is globally exponentially stable.

This theorem shows that uniform exponential stability of the origin is robust with respect to a class of perturbation that satisfy a linear growth condition (3.15)-(3.16). If a Lyapunov function $V(t, x)$ is known explicitly, then the bound (3.16) can be calculated. If a Lyapunov function $V(t, x)$ is not known explicitly, then the robustness conclusion becomes a qualitative one where one says that the origin is uniformly exponentially stable for all perturbation satisfying (3.15) with sufficiently small γ . It should be noted that the bound (3.15) could be conservative for a given perturbation $g(t, x)$. This conservatism results from the worst-case analysis performed in the analysis of the derivative of the Lyapunov function for the nominal system along solutions of the perturbed system. If the bound is required for all $g(t, x)$ satisfying (3.15), including dynamic mappings, then this bound is not conservative.

3.5.2 Non-vanishing perturbations

If the perturbation is non-vanishing at the origin, the origin $x = 0$ may not be an equilibrium point of the perturbed system (3.13) anymore. It is then no longer possible to investigate the stability properties

of the origin as an equilibrium point, nor should one expect the solution of the perturbed system to approach the origin as $t \rightarrow \infty$. The best we can hope for is that if the perturbation $g(t, x)$ is small in some sense, then the solution $x(t)$ becomes ultimately bounded by a small bound; in other words, $\|x(t)\|$ becomes small for sufficiently large t .

Definition 3.5.1. The solutions of $\dot{x} = f(t, x)$ are said to be uniformly ultimately bounded if there exist positive constants b and c , and for every $\alpha \in (0, c)$ there exists a positive constant $T = T(\alpha)$ such that

$$\|x(t_0)\| < \alpha \implies \|x(t)\| \leq b, \quad \forall t \geq t_0 + T, \forall t_0 > 0. \quad (3.17)$$

The solutions of the system are said to be globally uniformly ultimately bounded if (3.17) holds for arbitrary large α .

Uniform ultimate boundedness of the solutions is usually referred to as practical stability. The constant b in (3.17) is known as the ultimate bound. If the equilibrium $x = 0$ of the nominal system is uniformly exponentially stable, the analysis of the perturbed system can be performed with the following theorem.

Theorem 3.5.2. (Khalil 1996, Lemma 5.2) Suppose that $x = 0$ is a uniformly exponentially stable equilibrium point of the nominal system (3.14). Let $V(t, x)$ be a Lyapunov function that satisfies (3.7) on $\mathbb{R}_+ \times D$, where $D = \{x \in \mathbb{R}^n \mid \|x\| < r\}$. Suppose that the perturbation term $g(t, x)$ satisfies

$$\|g(t, x)\| \leq \delta < \frac{c_3}{c_4} \sqrt{\frac{c_1}{c_2}} \theta r, \quad \forall t \geq t_0, \forall x \in D \quad (3.18)$$

for some positive constant $\theta < 1$. Then for all initial conditions $\|x(t_0)\| \leq \sqrt{c_1} c_2 r$, the solution $x(t)$ of the perturbed system (3.13) satisfies

$$\|x(t)\| \leq k \|x(t_0)\| \exp(-\gamma(t - t_0)), \quad \forall t_0 \leq t \leq t_1,$$

and

$$\|x(t)\| \leq b, \quad \forall t \geq t_1,$$

for some finite time t_1 , where

$$k = \sqrt{\frac{c_2}{c_1}}, \quad \gamma = \frac{(1 - \theta)c_3}{2c_2}, \quad b = \frac{c_4 \delta}{c_3 \theta} \sqrt{\frac{c_2}{c_1}}.$$

Furthermore, we can allow for arbitrary large δ by choosing r large enough.

The previous result states that when the nominal system is globally uniformly exponentially stable, the solution of the perturbed system will be uniformly bounded for any uniformly bounded perturbation. If the system is only uniformly asymptotically stable, then a bounded perturbation could drive the solutions of the perturbed system to infinity. This explains why uniform exponential stability is a desirable property. It should be noted that exponential stability by itself is not sufficient to achieve the robustness result in Theorem 3.5.2; one needs uniformity. In this thesis we will aim for uniform exponential stability, or K-exponential stability, if possible.

3.6 Cascaded systems

In (Lefeber et al., 1999, 2000) a result on exponential stability of cascaded systems was given that is based on (Panteley and Loría, 1998). Consider the cascaded system with equilibrium $(z_1, z_2) = (0, 0)$ given by

$$\begin{aligned}\dot{z}_1 &= f_1(t, z_1) + g(t, z_1, z_2)z_2, \\ \dot{z}_2 &= f_2(t, z_2),\end{aligned}\tag{3.19}$$

where $z_1 \in \mathbb{R}^n$, $z_2 \in \mathbb{R}^m$; $f_1(t, z_1)$ is continuously differentiable in (t, z_1) and $f_2(t, z_2), g(t, z_1, z_2)$ are continuous in their arguments and locally Lipschitz in z_2 and (z_1, z_2) respectively. The total system (3.19) is a system Σ_1 with state z_1 that is perturbed by the state z_2 of the system Σ_2 , where

$$\Sigma_1 : \dot{z}_1 = f_1(t, z_1) \quad \Sigma_2 : \dot{z}_2 = f_2(t, z_2),\tag{3.20}$$

and the perturbation term is given by $g(t, z_1, z_2)z_2$. If Σ_2 is asymptotically stable, z_2 tends to zero and the dynamics of z_1 reduces to Σ_1 . If Σ_1 is also asymptotically stable we may investigate whether this implies asymptotic stability of the cascaded system (3.19). We state the following result from (Lefeber et al., 2000).

Theorem 3.6.1. *(Lefeber et al., 2000) The cascaded system (3.19) is globally uniformly asymptotically stable (GUAS) if the following three assumptions hold:*

- (1) Σ_1 subsystem: *The subsystem $\dot{z}_1 = f_1(t, z_1)$ is GUAS and there exists a continuously differentiable function $V(t, z_1) : \mathbb{R}_+ \times \mathbb{R}^n \rightarrow \mathbb{R}$ and positive definite functions $W_1(z_1)$ and $W_2(z_1)$ such that*

$$\begin{aligned}\text{(i)} \quad & W_1(z_1) \leq V(t, z_1) \leq W_2(z_1) \quad \forall t \geq t_0, \forall z_1 \in \mathbb{R}^n, \\ \text{(ii)} \quad & \frac{\partial V(t, z_1)}{\partial t} + \frac{\partial V(t, z_1)}{\partial z_1} f_1(t, z_1) \leq 0, \quad \forall \|z_1\| \geq \eta, \\ \text{(iii)} \quad & \left\| \frac{\partial V}{\partial z_1} \right\| \|z_1\| \leq \zeta V(t, z_1), \quad \forall \|z_1\| \geq \eta,\end{aligned}\tag{3.21}$$

where $\zeta > 0$ and $\eta > 0$ are constants.

- (2) interconnection: *The function $g(t, z_1, z_2)$ satisfies*

$$\|g(t, z_1, z_2)\| \leq \kappa_1(\|z_2\|) + \kappa_2(\|z_2\|)\|z_1\|, \quad \forall t \geq t_0,\tag{3.22}$$

where $\kappa_1, \kappa_2 : \mathbb{R}_+ \rightarrow \mathbb{R}_+$ are continuous functions.

- (3) Σ_2 subsystem: *The subsystem $\dot{z}_2 = f_2(t, z_2)$ is GUAS and satisfies*

$$\int_{t_0}^{\infty} \|z_2(t_0, t, z_2(t_0))\| dt \leq \beta(\|z_2(t_0)\|), \quad \forall t_0 \geq 0,\tag{3.23}$$

where the function $\beta(\cdot)$ is a class \mathcal{K} function.

In (Panteley et al., 1998) the authors claimed that when both subsystems Σ_1 and Σ_2 are globally \mathcal{K} -exponentially stable, the cascaded system (3.19) is also \mathcal{K} -exponentially stable. To our knowledge, the proof given in (Panteley et al., 1998) is incorrect. The claim that global \mathcal{K} -exponential stability, as defined in (Sørdalen and Egeland, 1995), is equivalent to having global uniform asymptotic stability (GUAS) and local uniform exponential stability (LUES) is not valid. Therefore, the fact that both subsystems Σ_1 and Σ_2 are \mathcal{K} -exponentially stable does not imply that the cascaded system (3.19) is also \mathcal{K} -exponentially stable. It is only valid when both subsystems are globally uniformly asymptotically stable (GUAS) and locally uniformly exponentially stable (LUES).

A stronger result for the stability of the cascaded system can be obtained when both subsystems are globally exponentially stable. The result, stated in the following lemma, is based on the result in (Panteley et al., 1998) and the proof is a slight modification of the proof therein, adapted to the case when both subsystems Σ_1 and Σ_2 are exponentially stable.

Lemma 3.6.2. *If in addition to the assumptions in Theorem 3.6.1 both Σ_1 and Σ_2 are globally exponentially stable, then the cascaded system (3.19) is globally \mathcal{K} -exponentially stable.*

Proof. Since the Σ_2 subsystem is globally exponentially stable, it is also globally \mathcal{K} -exponentially stable and the bound (3.2) is satisfied for $z_2(t)$. Therefore it suffices to show the result for $z_1(t)$. Since all conditions of Theorem 3.6.1 are satisfied, the system 3.19 is GUAS and $z = [z_1, z_2]^T$ satisfies

$$\|z(t)\| \leq \beta(\|z(t_0)\|, t - t_0), \quad \forall t \geq t_0 \geq 0,$$

where $\beta(\cdot)$ is a class \mathcal{KL} function. For all initial conditions $\|z(t_0)\| \leq r$, with $z = [z_1, z_2]^T$, the function $g(t, z_1, z_2)$ can be upper-bounded as $\|g(t, z_1, z_2)\| \leq c_g$, where $c_g = c_g(r) > 0$ is a constant. Consider the subsystem

$$\dot{z}_1 = f_1(t, z_1) + g(t, z_1, z_2)z_2 \quad (3.24)$$

By assumption, the systems $\dot{z}_1 = f_1(t, z_1)$ and $\dot{z}_2 = f_2(t, z_2)$ are globally exponentially stable. Using converse Lyapunov theory, *i.e.*, Theorem 3.3.2, there exists Lyapunov functions $V_1(t, x)$ and $V_2(t, x)$ such that

$$\alpha_1 \|z_1\|^2 \leq V_1(t, z_1) \leq \alpha_2 \|z_1\|^2, \quad \dot{V}_1(t, z_1) \leq -\alpha_3 \|z_1\|^2, \quad \left\| \frac{\partial V_1(t, z_1)}{\partial x} \right\| \leq \alpha_4 \|z_1\|, \quad (3.25)$$

and

$$\beta_1 \|z_2\|^2 \leq V_2(t, z_2) \leq \beta_2 \|z_2\|^2, \quad \dot{V}_2(t, z_2) \leq -\beta_3 \|z_2\|^2, \quad \left\| \frac{\partial V_2(t, z_2)}{\partial x} \right\| \leq \beta_4 \|z_2\|. \quad (3.26)$$

Taking the derivative of $V_1(t, x)$ with respect to (3.24) we obtain

$$\begin{aligned} \dot{V}_1(t, x) &\leq -\alpha_3 \|z_1\|^2 + \alpha_4 \|g(t, z_1, z_2)\| \|z_1\| \|z_2\| \leq -\alpha_3 \|z_1\|^2 + \alpha_4 c_g(r) \|z_1\| \|z_2\| \\ &\leq -\frac{\alpha_3}{2} \|z_1\|^2 + \frac{\alpha_4^2 c_g(r)^2}{2\alpha_3} \|z_2\|^2 \end{aligned}$$

Define $\delta_g(r) = \frac{\alpha_4^2 c_g(r)^2}{2\alpha_3}$ and consider the candidate Lyapunov function

$$V(t, z_1, z_2) = V_1(t, z_1) + \Gamma V_2(t, z_2), \quad (3.27)$$

where $\Gamma > 0$ is a constant which will be defined later. The derivative of $V(t, z_1, z_2)$ along the solutions of (3.19) satisfies

$$\dot{V}(t, z_1, z_2) \leq -\frac{\alpha_3}{2} \|z_1\|^2 + (\delta_g(r) - \beta_3 \Gamma) \|z_2\|^2 \quad (3.28)$$

There is still some choice of freedom for the parameter Γ . In order to modify the upper-bound of (3.28), we select Γ as

$$\Gamma = \frac{2\delta_g(r)}{2\beta_3 - \bar{\beta}_3} \delta_g(r),$$

with $0 < \bar{\beta}_3 < 2\beta_3$. Then equation (3.28) becomes

$$\dot{V} \leq -\frac{\alpha_3}{2\alpha_2} V_1(t, z_1) - \frac{\bar{\beta}_3}{2\beta_2} \Gamma V_2(t, z_2) \leq -\gamma V, \quad (3.29)$$

where

$$\gamma = \frac{1}{2} \min\left(\frac{\alpha_3}{\alpha_2}, \frac{\bar{\beta}_3}{\beta_2}\right).$$

Therefore, using the bound $\|z_1\|^2 \leq \frac{V(t, z_1, z_2)}{\alpha_1}$, we obtain

$$\begin{aligned} \|z_1(t, t_0, z_{10}, z_{20})\|^2 &\leq \frac{V(t_0, z_{10}, z_{20})}{\alpha_1} \exp(-\gamma(t - t_0)) \\ &\leq \frac{\alpha_2 \|z_{10}\|^2 + \Gamma \beta_2 \|z_{20}\|^2}{\alpha_1} \exp(-\gamma(t - t_0)) \\ &\leq 2 \frac{\max(\alpha_2, \Gamma \beta_2)}{\alpha_1} \|z_0\|^2 \exp(-\gamma(t - t_0)), \end{aligned}$$

where z_0 denotes the vector $z_0 = [z_{1(0)}, z_{20}]$. Thus the solutions $z_1(t, t_0, z_{10}, z_{20})$ satisfy

$$\|z_1(t, t_0, z_{10}, z_{20})\| \leq k(r) \|z_0\| \exp\left(-\frac{\gamma}{2}(t - t_0)\right), \quad (3.30)$$

with the continuous function $k(r)$ given by

$$k(r) = \sqrt{2 \frac{\max(\alpha_2, \delta_g(r) \beta_2)}{\alpha_1}}. \quad (3.31)$$

The bound (3.2) is satisfied and we conclude that the system (3.19) is globally \mathcal{K} -exponentially stable. \square

Remark 3.6.1. Note that a stronger result than Lemma (3.6.2) is not feasible. If both subsystems Σ_1 and Σ_2 are globally exponentially stable, the cascaded system (3.19) is not necessarily globally exponentially stable. A counter example is the system given by,

$$\begin{aligned} \dot{x}_1 &= -x_1 + x_1 x_2 \\ \dot{x}_2 &= -x_2. \end{aligned}$$

When both subsystems are globally \mathcal{K} -exponentially stable, and not globally exponentially stable, additional assumptions are needed to conclude global \mathcal{K} -exponential stability of the cascaded system (3.19). In fact, if both systems are globally \mathcal{K} -exponentially stable and admit Lyapunov functions $V_1(t, z_1)$ and $V_2(t, z_2)$ that satisfy (3.21) with quadratic functions $W_i = c_i \|z_i\|^2$, and additionally

$$\left\| \frac{\partial V_1}{\partial x} \right\| \leq \alpha_4 \|z_1\|, \quad \alpha_4 > 0,$$

then the cascaded system (3.19) is also globally \mathcal{K} -exponentially stable. This is shown in Proposition A.1.2 of the appendix.

3.7 Homogeneous systems

In this section, homogeneous systems will be introduced. It is well-known that the stability analysis of nonlinear time-varying systems can be quite involved and, in general, is very hard to solve. In these situations, the theory of homogeneous systems may be used to investigate the stability properties of a non-linear time-varying system. We use the elements of $C^0(\mathbb{R} \times \mathbb{R}^n; \mathbb{R}^n)$, the set of continuous mappings from $\mathbb{R} \times \mathbb{R}^n$ to \mathbb{R}^n , to represent continuous (time-varying) vector fields on \mathbb{R}^n . We start by recalling some definitions and properties related to homogeneous systems.

Given a weight vector $r = (r_1, \dots, r_n)$ of real parameters $r_i > 0$ ($i = 1, \dots, n$) and a real number $\lambda > 0$, the mapping $\delta_\lambda^r : \mathbb{R}^n \rightarrow \mathbb{R}^n$ defined by

$$\delta_\lambda^r(x) = (\lambda^{r_1}x_1, \dots, \lambda^{r_n}x_n)$$

is called a dilation of weight r . A continuous function $f : \mathbb{R} \times \mathbb{R}^n \rightarrow \mathbb{R}$ is said to be homogeneous of degree τ with respect to the dilation δ_λ^r if

$$f(\delta_{\lambda}^r(x)) = \lambda^\tau f(t, x)$$

for every couple $(t, x) \in \mathbb{R} \times \mathbb{R}^n$.

A homogeneous norm associated with a dilation δ_λ^r is a continuous positive-definite function $\rho : \mathbb{R}^n \rightarrow \mathbb{R}$ which is homogeneous of degree one with respect to δ_λ^r . For example, a homogeneous norm associated with the dilation δ_λ^r is given by

$$\rho_p^r(x) = \left(\sum_{j=1}^n |x_j|^{p/r_j} \right)^{1/p}, \quad p > 0.$$

Definition 3.7.1. A (time-varying) vector field $f : \mathbb{R} \times \mathbb{R}^n \rightarrow \mathbb{R}^n$ given by $f(t, x) = \sum_{i=1}^n f_i(t, x) \partial / \partial x_i$, is said to be homogeneous of degree $\tau \geq 0$ with respect to δ_λ^r if, for each $i = 1, \dots, n$, the i -th component f_i is a homogeneous function of degree $\tau + r_i$ with respect to δ_λ^r . More precisely, for $i = 1, \dots, n$,

$$f_i(t, \delta_\lambda^r(x)) = \lambda^{\tau+r_i} f_i(t, x)$$

for all $\lambda > 0$ and every couple $(t, x) \in \mathbb{R} \times \mathbb{R}^n$.

Definition 3.7.2. Consider a homogeneous norm $\rho : \mathbb{R}^n \rightarrow \mathbb{R}$ associated with a dilation δ_λ^r . The origin of the system $\dot{x} = f(t, x)$ with $f(t, 0) = 0, \forall t$, is said to be locally ρ -exponentially stable (with respect to a dilation δ_λ^r) if there exist strictly positive constants δ, K and γ such that for any $t_0 \in \mathbb{R}$ and any solution $x(t)$, with $x(t_0) = x_0$,

$$\rho(x_0) < \delta \implies \rho(x(t)) \leq K \rho(x_0) e^{\gamma(t-t_0)}.$$

Note that (local) ρ -exponential stability implies (local) \mathcal{H} -exponential stability as defined in Section 3.2. Let us recall a result that will be used to deduce ρ -exponential stability of the controlled system.

Proposition 3.7.1. (Pomet and Samson, 1994) Let δ_λ^r be a dilation and assume that the vector fields $f, h \in C^0(\mathbb{R} \times \mathbb{R}^n; \mathbb{R}^n)$ are T -periodic in their first argument, f is homogeneous of degree zero with respect to δ_λ^r , and h can be written as a (possibly infinite) sum of homogeneous vector fields, of strictly positive degree, with respect to δ_λ^r . If the origin $x = 0$ is a locally asymptotically stable equilibrium point for

$$\dot{x} = f(t, x)$$

then

(i) the origin $x = 0$ is also globally ρ -exponentially stable

(ii) the origin $x = 0$ of the ‘perturbed’ system

$$\dot{x} = f(t, x) + h(t, x)$$

is locally ρ -exponentially stable with respect to δ_λ^r .

The previous result states that for homogeneous systems local asymptotic stability and global ρ -exponential stability are equivalent properties. The following averaging result for (fast) time-varying homogeneous systems will be used in the stability analysis of the controlled system in Chapter 6.

Proposition 3.7.2. (M’Closkey and Murray, 1993) Consider the system

$$\dot{x} = f(t/\varepsilon, x), \quad (3.32)$$

with $f : \mathbb{R} \times \mathbb{R}^n \rightarrow \mathbb{R}^n$ a continuous T -periodic vector field ($f(t+T, x) = f(t, x)$) and $f(t, 0) = 0, \forall t$. Assume that (3.32) is homogeneous of degree zero with respect to a dilation $\delta_\lambda^r(x)$ and that the origin $y = 0$ of the ‘averaged system’

$$\dot{y} = \bar{f}(y), \quad \bar{f}(y) = 1/T \int_0^T f(t, y) dt, \quad (3.33)$$

is a locally asymptotically stable equilibrium point. Then there exists $\varepsilon_0 > 0$ such that, for any $\varepsilon \in (0, \varepsilon_0)$, the origin $x = 0$ of (3.32) is exponentially stable with respect to the dilation $\delta_\lambda^r(x)$.

The main result that will be used to prove ρ -exponential stability of the controlled system is a result for cascaded high-gain control of a class of homogeneous systems, given in (Morin and Samson, 1997). It concerns the classical problem of integrator backstepping for homogeneous time-varying systems, and is given by the following proposition:

Proposition 3.7.3. (Morin and Samson, 1997) Consider the following system:

$$\dot{x} = f(t, x, v(t, x^1)) \quad (3.34)$$

with $f : \mathbb{R} \times \mathbb{R}^n \times \mathbb{R} \rightarrow \mathbb{R}^n$ a continuous T -periodic function in its first argument, $x^1 = (x_1, \dots, x_m)$, $m \leq n$ and $v : \mathbb{R} \times \mathbb{R}^m \rightarrow \mathbb{R}$ a continuous T -periodic function in its first argument, differentiable with respect to t , of class \mathcal{C}^1 on $\mathbb{R} \times (\mathbb{R}^m \setminus \{0\})$, homogeneous of degree q with respect to the dilation $\delta_\lambda^r(x)$.

Assume that (3.34) is homogeneous of degree zero with respect to the dilation $\delta_\lambda^r(x)$ and that the origin $x = 0$ is an asymptotically stable equilibrium point. Then for k positive and large enough, the origin $(x = 0, y = 0)$ is an asymptotically stable equilibrium point of the system

$$\begin{aligned} \dot{x} &= f(t, x, y) \\ \dot{y} &= -k(y - v(t, x^1)). \end{aligned} \quad (3.35)$$

Remark 3.7.1. Proposition 3.7.3 can be applied recursively to the asymptotic stabilization of the system

$$\begin{aligned} \dot{x} &= f(t, x, y_1) \\ \dot{y}_1 &= y_2 \\ &\vdots \\ \dot{y}_n &= u. \end{aligned} \quad (3.36)$$

Suppose that the feedback $y_1 = v_1(t, x^1)$, $x^1 = (x_1, \dots, x_m)$, $m \leq n$, asymptotically stabilizes the x -subsystem, *i.e.*, the first equation in (3.36). Then by recursive application of Proposition 3.7.3 it follows that the feedback

$$u = -k_n(y_n - v_{n-1}(t, x^1, y_1, \dots, y_{n-1})), \quad (3.37)$$

where $v_i = -k_i(y_i - v_{i-1}(t, x^1, y_1, \dots, y_{i-1}))$ for $i = 2, \dots, n-1$, asymptotically stabilizes the origin.

Remark 3.7.2. Note that if the system (3.36) is homogeneous of degree zero with respect to some dilation δ_λ^r , then Proposition (3.7.1) implies that the closed-loop system (3.36,3.37) is *globally* ρ -exponentially stable.

3.8 Summary

In this chapter, some preliminaries were presented that will be used through the sequel of this thesis. We presented some basic definitions of Lyapunov stability in Section 3.2. Besides the definitions of asymptotic, exponential and ρ -exponential stability, also a weaker result called exponential convergence was treated. Some references have presented controllers that achieve exponential convergence towards the desired equilibrium point, however, these approaches do not guarantee asymptotic stability in a Lyapunov sense.

Furthermore, in Section 3.3 some converse theorems have been presented that can be used to prove the existence of a suitable Lyapunov function of a system. In Section 3.4 a similar result was shown to hold in the case of linear time-varying systems. In Section 3.5 robustness properties of uniformly exponentially stable systems were presented. It turns out that uniform exponential stability is a desirable property, because it implies that solutions of the perturbed system remain uniformly bounded for any uniformly bounded perturbation. In fact, if the perturbation vanishes at the origin, specific bounds can be given for which the system remains exponentially stable, see Theorem 3.5.1.

In Section 3.6 we consider cascaded nonlinear systems. It is shown that under some additional conditions, the stability of a cascaded system can be completely characterized in terms of the stability of the two subsystems. This result will be used in Chapter 5 where a solution to the tracking control problem is given. In Section 3.7 the theory of homogeneous systems has been introduced. In this section an averaging result and a backstepping or high-gain feedback result was presented for the class of homogeneous systems, and will be used to solve the feedback stabilization problem in Chapter 6. In the following chapter we will present some methodologies for generating state-to-state trajectories that can be used in the tracking control problem.

Trajectory generation

In recent years, so-called nonholonomic motion planning problems have received increasing interest. In these nonholonomic motion planning problems one tries to find open loop controls that steer a nonholonomic system from an initial state to a final state over a given finite time interval. These open-loop controls generate a feasible trajectory that connects the initial state and the final state. This feasible trajectory can then be used in a trajectory tracking problem, where one wants the system to follow this specified trajectory. To understand why nonholonomic motion planning is more involved, it is useful to compare it with holonomic motion planning. In holonomic motion planning, an arbitrary motion, satisfying some continuity property, in the space of independent generalized coordinates is possible. For example, a disk that rolls with slip can perform an arbitrary holonomic motion by transferring the disk from a motion without slip to a motion with slip. In contrast, in nonholonomic motion planning the trajectories of the system have to satisfy the nonholonomic constraint at each time-instant. This is the case when the disk is constrained to roll without slip, resulting in a nonholonomic constraint that relates the velocity of the center of mass to the angular velocity of the disk. Therefore, only motions are possible that satisfy the nonholonomic constraint. Nevertheless, depending on the controllability properties of the system, feasible motions do exist that connect an arbitrary initial state and an arbitrary final state of the nonholonomic system.

A variety of motion planning techniques have been described in (Li and Canny, 1993) while an introduction to motion planning for nonholonomic robots can be found in (Murray et al., 1994). The motion planning methodologies can be classified into differential-geometric and differential-algebraic methods, geometric phase (holonomy) methods and control parameterization methods, see (Kolmanovsky and McClamroch, 1995). However, many of these approaches are only applicable to kinematic models of nonholonomic control systems, such as, for example, wheeled mobile robots and trailer systems. Since systems with second-order nonholonomic constraints, can only be described by dynamic models, these techniques can not be applied to second-order nonholonomic systems, considered in this thesis. In fact, no general theory for planning trajectories for systems with second-order nonholonomic constraints is yet available and most successful approaches have been tailored to specific cases. Nevertheless, some of the techniques for motion planning of systems with first-order constraints may also be applicable to motion planning for systems with second-order constraints.

In differential-geometric and differential-algebraic approaches net motions are generated in the direction of the iterated Lie-brackets of the systems input vectorfields g_i , $i = 1, \dots, m$. The majority of these approaches consider only the motion planning problem for kinematic models, *i.e.*, without drift. The fact that the system satisfies a Lie algebra rank condition (LARC) then guarantees that any initial state can be steered to an arbitrary final state. These techniques also include averaging techniques, flatness-based approaches and techniques in which one steers the system by using piece-

wise continuous inputs.

In the geometric phase methods, a special class of nonholonomic control systems are those of the kinematic Chaplygin type given by

$$\begin{aligned}\dot{z} &= g_1(y)\dot{y}_1 + g_2(y)\dot{y}_2 + \cdots + g_m(y)\dot{y}_m \\ \dot{y}_i &= u_i, \quad i = 1, \dots, m.\end{aligned}$$

When the base vector y undergoes a cyclic motion, the resulting change in the fiber vector z can be written as a line integral along the path γ of the base vector:

$$z(t) - z(0) = \oint_{\gamma} g(y)dy$$

The value of the line integral is independent of any specific parameterization and only depends on the geometry of the path. Thus for Chaplygin systems the motion planning problem reduces to finding an appropriate base path γ which produces the desired change in the fiber vector z , also referred to as the geometric phase. For details and references to geometric phase methods, the reader is referred to Kolmanovsky and McClamroch (1995).

The most elementary method for motion planning is based on parameterization of the inputs within a given finite dimensional set of functions. Suppose that the input $u(t)$ is parameterized by a parameter $\alpha \in \mathbb{R}^k$. This parameterization reduces the problem of finding inputs $u(t)$ in a infinite dimensional function space, to finding a finite number, *i.e.*, k , of decision variables α . This simple idea has appeared in many publications and has been very successful in solving a wide range of nonholonomic motion planning problems. Because the control parameterization approach is suitable for both kinematic and dynamic models, it can also be used to solve motion planning problems for systems with second-order nonholonomic constraints.

As mentioned earlier, no general theory is available for motion planning of second-order nonholonomic systems. Some results tackle the motion planning problem in specific cases. For example, in (Arai et al., 1998b) a numerical motion planner was proposed for a planar underactuated 2R manipulator with an unactuated base joint. The case of a planar horizontal underactuated three-link manipulator has been considered in (Arai et al., 1998a). In that reference, rest-to-rest motions could be generated by using a sequence of elementary maneuvers, *i.e.*, maneuvers consisting of either a pure translation of the third link or a pure rotation of the third link around its center of percussion. In (Lynch et al., 1998) a motion planner is developed that can also generate collision-free paths amongst obstacles. In (Luca and Oriolo, 2000), the motion planning problem for the planar horizontal underactuated three-link manipulator has been solved by applying dynamic feedback linearization. The flatness property of the system can then be used to generate state-to-state paths, provided that these paths do not cross singularities of the inverse transformation induced by the flat outputs. In (Iwamura et al., 2000) a near-optimal motion planning scheme is obtained by formulating the motion planning problem as an optimal control problem. This optimal control problem is too difficult to solve, in general, and it is converted into a bidirectional fixed-domain optimal control problem by using a different time-variable. Then a numerical algorithm, based on the gradient method, is used to solve this bidirectional optimal control problem.

In this chapter, some trajectory generation methods will be presented for the second-order chained form system (2.10). The goal of these methods is to generate inputs u_1 and u_2 that steer the states of system (2.10) from an initial state x_A to a final state x_B . These inputs together with the corresponding trajectory $x(t)$ can be used as a desired trajectory, *e.g.* (2.12), in the trajectory tracking problem. The proposed methods consist of a control parameterization approach and a combined optimal control

and control parameterization approach. The reader is referred to (Verhoeven, 2002) for details on the proposed methods.

4.1 Problem formulation

The general goal of the motion planning strategies in this chapter is to derive trajectories of motion for the second-order chained form system that connect two arbitrarily chosen points A and B . Consider the second-order chained form system given by

$$\begin{aligned}\dot{x}_1 &= x_2 & \dot{x}_2 &= u_1 \\ \dot{x}_3 &= x_5 & \dot{x}_4 &= u_2 \\ \dot{x}_5 &= x_6 & \dot{x}_6 &= x_3 u_1,\end{aligned}\tag{4.1}$$

with state vector $x \in \mathbb{R}^6$ given by $x = [x_1, x_2, \dots, x_6]^T$. The goal in this chapter is to develop a motion planner that generates open-loop input functions $u_1(t)$ and $u_2(t)$ which drive the state $x(t)$ of the system from some initial state x_A to an arbitrary state x_B , at some pre-specified time $t = T$. This state-to-state motion planning problem can be formulated as follows

Problem 4.1.1. Given a final time $T > t_0$ and two states $x_A \in \mathbb{R}^6$ and $x_B \in \mathbb{R}^6$, find input functions $u_1(t)$ and $u_2(t)$ such that the resulting state trajectory $x(t)$ satisfies $x(t_0) = x_A$ and $x(T) = x_B$.

An algorithm that generates the input functions $u_1(t)$, $u_2(t)$ and the corresponding feasible trajectory $x(t)$, given arbitrary initial and final states x_A and x_B , respectively, will be referred to as a motion planner.

4.2 Controllability and stabilizability

In order to be able to generate inputs and corresponding feasible trajectories that connect an arbitrary initial and arbitrary final state, the system must satisfy some controllability property. This section investigates certain controllability properties of the second-order chained form system. The controllability concepts used have been developed in (Nijmeijer and van der Schaft, 1990) and (Sussmann, 1987). In fact, by using a Lie algebra approach, the *local accessibility* and small-time local controllability (STLC) properties will be investigated.

Consider the second-order chained form system written as

$$\dot{x} = f(x) + g_1(x)u_1 + g_2(x)u_2,\tag{4.2}$$

with $x \in \mathbb{R}^6$ and $u_1, u_2 \in \mathbb{R}$ and

$$f(x) = [x_2, 0, x_4, 0, x_6, 0]^T, g_1(x) = [0, 1, 0, 0, 0, x_3]^T, g_2(x) = [0, 0, 0, 1, 0, 0]^T\tag{4.3}$$

The reachable set from x_0 , given a neighborhood V of x_0 , is defined as

$$R_T^V(x_0) = \bigcup_{\tau \leq T} R^V(x_0, \tau)$$

where the reachable set $R^V(x_0, T)$ from x_0 at time $T > 0$ is given by

$$R^V(x_0, T) = \{x \in \mathbb{R}^6 \mid \text{there exists an admissible input } u : [0, T] \rightarrow \mathbb{R}^2 \text{ such that the evolution of (4.2) for } x(0) = x_0 \text{ satisfies } x(t) \in V, 0 \leq t \leq T \text{ and } x(T) = x\}$$

Definition 4.2.1. The system (4.2) is locally strongly accessible from x_0 if for any neighborhood V of x_0 the set $R^V(x_0, T)$ contains a non-empty open set for any $T > 0$ sufficiently small. If this holds for any $x_0 \in \mathbb{R}^6$ then the system is called locally strongly accessible.

Proposition 4.2.1. *The system (4.2) is locally strongly accessible.*

Proof. This claim can be verified by the strong accessibility rank condition. Consider the following set of repeated Lie brackets $\tilde{\mathcal{C}}_0 = \{g_1, g_2, [f, g_1], [f, g_2], [g_1, [f, g_2]], [f, [g_2, [f, g_1]]\}$ given by

$$\tilde{\mathcal{C}}_0 = \left\{ \begin{array}{l} \begin{bmatrix} 0 \\ 1 \\ 0 \\ 0 \\ 0 \\ x_3 \end{bmatrix}, \begin{bmatrix} 0 \\ 0 \\ 0 \\ 1 \\ 0 \\ 0 \end{bmatrix}, \begin{bmatrix} -1 \\ 0 \\ 0 \\ 0 \\ -x_3 \\ x_4 \end{bmatrix}, \begin{bmatrix} 0 \\ 0 \\ -1 \\ 0 \\ 0 \\ 0 \end{bmatrix}, \begin{bmatrix} 0 \\ 0 \\ 0 \\ 0 \\ 0 \\ 1 \end{bmatrix}, \begin{bmatrix} 0 \\ 0 \\ 0 \\ 0 \\ -1 \\ 0 \end{bmatrix} \right\}$$

Then $\dim(\text{span}(\tilde{\mathcal{C}}_0)) = 6$ for all $x \in \mathbb{R}^6$ and we conclude that the system (4.2) is locally strongly accessible, see Theorem 3.21 in (Nijmeijer and van der Schaft, 1990). \square

The fact that the system is locally strongly accessible means that, given any neighborhood V of $x_0 \in \mathbb{R}^6$, the reachable set $R^V(x_0, T)$ from x_0 at time T contains a non-empty open set for any $T > 0$ sufficiently small. Obviously, this is far from showing controllability of the system. A stronger result that states that the reachable set $R^V(x_0, T)$ from x_0 at time T contains a non-empty open set for all $T > 0$ is the following.

Definition 4.2.2. The system (4.2) is small-time locally controllable (STLC) from x_0 if for any neighborhood V of x_0 the set $R^V(x_0, T)$ contains a non-empty open set for any $T > 0$. If this holds for any $x_0 \in \mathbb{R}^6$ then the system is called small-time locally controllable.

In (Sussmann, 1987) a sufficient condition was given for small-time local controllability (STLC) of nonlinear systems with drift. Consider a system $\dot{x} = f(x) + \sum_{i=1}^m g_i(x)u_i$, where $x \in D \subset \mathbb{R}^n$ and $u_i \in \mathbb{R}$, together with a point $p \in D$ such that $f(p) = 0$. Let $X = [f, g_1, \dots, g_m]$ and denote the set of all possible iterated Lie brackets involving f, g_1, \dots, g_m by $Br(X)$. Let the degree of a Lie bracket $B \in Br(x)$, denoted by $\delta(B)$, be the sum

$$\delta(B) = \delta^0(B) + \sum_{i=1}^m \delta^i(B),$$

where δ^0 is the number of times that f occurs in B and δ^i , $i = 1, 2, \dots, m$, the number of times that g_i occurs in B . A Lie bracket B is said to be “bad” if $\delta^0(B)$ is odd and $\delta^1(B), \delta^2(B), \dots, \delta^m(B)$ are even. The main lines of the sufficient condition for STLC can be formulated as follows. A nonlinear system with drift is STLC if (1) the system is locally accessible, *i.e.*, satisfies the Lie algebra rank condition and (2) all “bad” brackets can be written as linear combinations of “good” brackets of lower degree. The reader is referred to (Sussmann, 1987) for the complete result.

Theorem 4.2.2. (Sussmann 1987, Corollary 7.2) *Consider a system $\dot{x} = f(x) + \sum_{i=1}^m g_i(x)u_i$, where $x \in D$ and $u_i \in \mathbb{R}$, and a point $p \in D$ such that $f(p) = 0$. Assume that the system is locally accessible, *i.e.*, satisfies the Lie algebra rank condition. If whenever B is a “bad” bracket, there exist brackets C_1, \dots, C_k with $\delta(C_i) < \delta(B)$ such that*

$$B = \sum_{i=1}^k a_i C_i \tag{4.4}$$

for some $a_1, \dots, a_k \in \mathbb{R}$, then the system is STLC from p .

Proposition 4.2.3. *The second-order chained form system (4.2) is small-time locally controllable from any equilibrium.*

Proof. The system is locally strongly accessible, and thus satisfies the Lie algebra rank condition (LARC). Since the highest degree of a bracket is 4 this means that all brackets of order higher than 4 can be written as a linear combination of lower order brackets. The “bad” brackets of degree lower than 4 are the brackets f , $[g_1, [f, g_1]]$ and $[g_2, [f, g_2]]$. The bracket f vanishes at any equilibrium points and the brackets $[g_1, [f, g_1]]$ and $[g_2, [f, g_2]]$ are identical zero vectorfields. Therefore the system satisfies Sussmann’s sufficient condition, see Theorem 4.2.2, at any equilibrium. Thus the system (4.2) is STLC from any equilibrium. \square

Since the system is real analytic, the above proposition implies the existence of piecewise analytic feedback laws (Sussmann, 1979) which asymptotically stabilize the closed-loop system to an equilibrium point. In (Astolfi, 1996; Laiou and Astolfi, 1999) time-invariant discontinuous controllers have been presented that guarantee exponential convergence towards an equilibrium point. However, these controllers do not asymptotically stabilize the equilibrium point in a Lyapunov sense. The STLC property of the system can be linked to a stabilizability property. In (Coron, 1995) it is shown that analytic systems can be locally stabilized by time-varying feedback. In fact, it is shown that STLC systems are locally stabilizable in small time by means of almost smooth periodic time-varying feedback. In this thesis, we will focus on the feedback stabilization problem by continuous periodic time-varying feedback.

4.3 Constructive proof of controllability

The STLC property can be used to show local controllability of general nonlinear systems, but does not imply complete controllability of the system. For the specific second-order chained form system, however, complete controllability can be shown by a constructive procedure in which inputs and trajectories are generated that steer the system from an initial state $x_A = [x_{1A}, x_{2A}, \dots, x_{6A}]^T$ to a desired final state $x_B = [x_{1B}, x_{2B}, \dots, x_{6B}]^T$. This constructive procedure shows great resemblance with the constructive procedure in (Arai et al., 1998a), where controllability of a planar horizontal underactuated 3-DOF manipulator was shown. This underactuated manipulator is equivalent to the second-order chained form by a suitable state and feedback transformation. The constructive procedure shown in this section, will be based on the second-order chained-form.

Consider a partitioning $t_0 < t_1 < t_2 < t_3 < t_4 < T$ of the time interval $[t_0, T]$, where T is a finite time instant at which the final state x_B should be reached. First it should be noted that a double integrator system

$$\dot{y}_1 = y_2, \quad \dot{y}_2 = u$$

can be steered from an arbitrary initial state $[y_{1A}, y_{2A}]$ at time t_A to an arbitrary state $[y_{1B}, y_{2B}]$ at time t_B by the input u given by

$$\begin{aligned} u(t) &= a(t - t_A) + b, \quad t_A \leq t \leq t_B, \\ a &= 6 \frac{y_{2B} + y_{2A}}{(t_B - t_A)^2} - 12 \frac{y_{1B} - y_{1A}}{(t_B - t_A)^3} \\ b &= 6 \frac{y_{1B} - y_{1A}}{(t_B - t_A)^2} - 2 \frac{y_{2B} + 2y_{2A}}{t_B - t_A} \end{aligned}$$

with suitable coefficients a and b . Note that this is not the only way to steer a double integrator, many other solutions exist. The constructive procedure that generates a feasible trajectory for the system

(4.2) connecting the states x_A at $t = t_0$ and x_B at $t = T$ generates five trajectory segments. During these trajectory segments, the states that are not excited by a control input can change due to drift of the system. The trajectory segments of the system (4.2) can be described as follows:

1. $t_0 \leq t < t_1$: **control of $(\mathbf{x}_3, \mathbf{x}_4)$** . During this segment $u_1 = 0$ and the states (x_1, x_2, x_5, x_6) are not excited. The input u_2 is used to steer the state (x_3, x_4) from their initial values (x_{3A}, x_{4A}) at t_0 to the final values $(1, 0)$ at time t_1 .
2. $t_1 \leq t < t_2$: **control of $(\mathbf{x}_5, \mathbf{x}_6)$** . During this segment $u_2 = 0$ and the states (x_3, x_4) are unchanged. The input u_1 is used to steer the states (x_5, x_6) from their initial values $(x_{5A} + x_{6A}(t_1 - t_0), x_{6A})$ at time t_1 to $(x_{5B} - x_{6B}(T - t_2), x_{6B})$ at time t_2 . Note that during this trajectory segment the dynamics of x_5 behave as a double integrator since $x_3(t) = 1, t_1 \leq t < t_2$.
3. $t_2 \leq t < t_3$: **control of $(\mathbf{x}_3, \mathbf{x}_4)$** . During this segment $u_1 = 0$ and the states (x_1, x_2, x_5, x_6) are not excited. The input u_2 is used to steer the states (x_3, x_4) from their initial values $(1, 0)$ at time $t = t_2$ to the final values $(0, 0)$ at time $t = t_3$.
4. $t_3 \leq t < t_4$: **control of $(\mathbf{x}_1, \mathbf{x}_2)$** . During this segment $u_2 = 0, x_3 = 0$ and the states (x_3, x_4, x_5, x_6) are not excited. The input u_1 is used to steer the states (x_1, x_2) from their initial values at time $t = t_3$ to the final values $(x_{1B} - x_{2B}(T - t_4), x_{2B})$ at time $t = t_4$.
5. $t_4 \leq t < T$: **control of $(\mathbf{x}_3, \mathbf{x}_4)$** . During this segment $u_1 = 0$ and the states (x_1, x_2, x_5, x_6) are not excited. The input u_2 is used to steer the states (x_3, x_4) from their initial values $(0, 0)$ at time $t = t_4$ to the final values (x_{3B}, x_{4B}) at time $t = T$. At time $t = T$ the states (x_1, x_2) have drifted from their initial values at time $t = t_4$ to their desired values (x_{1B}, x_{2B}) and the states (x_5, x_6) have drifted from their initial values $(x_{5B} - x_{6B}(T - t_2), x_{6B})$ at time $t = t_2$ to their desired values (x_{5B}, x_{6B}) .

This procedure generates inputs $u(t)$ and trajectories $x(t)$ that steer the second-order chained form system from an arbitrary initial state x_A to an arbitrary final state x_B . The second-order chained form system is thus controllable. In the following sections we will investigate more sophisticated motion planners.

4.4 The flatness property

In (Fliess et al., 1994) it has been shown that certain nonlinear systems can be converted to linear systems at the cost of extending their dimensionality. For these systems, so-called flat outputs $y(t)$ can be assigned for which all state variables $x(t)$ and inputs $u(t)$ can be expressed in terms of the flat outputs and a finite number of their time-derivatives.

Definition 4.4.1. A system $\dot{x} = f(x, u)$ with state $x \in \mathbb{R}^n$ and inputs $u \in \mathbb{R}^m$ is said to be differentially flat if there exist outputs $y \in \mathbb{R}^m$ of the form $y = y(x, u, \dot{u}, \dots, u^{(k)})$ such that $x = x(y, \dot{y}, \dots, y^{(k)})$ and $u = u(y, \dot{y}, \dots, y^{(k)})$.

Since the behavior of the flat system is completely determined by the flat outputs, trajectories of the system can be obtained in terms of the flat outputs and these flat outputs can then be mapped to the required inputs. The flatness property is closely related to dynamic feedback linearization in the sense that the flat outputs define a so-called endogenous transformation and a dynamic feedback that brings the system into a linear controllable system that consists of m independent chains of integrators, with

m being the number of inputs to the system. A drawback of flatness-based motion planning methodologies is the fact that the flat outputs are not given a priori and cannot be computed systematically. In fact, it is not even clear which systems are flat and which systems are non-flat. Also, there exists no test to check whether a system is flat. Moreover, the endogenous transformation induced by the flat outputs is not always a diffeomorphism, but may contain singularities. This means that the trajectories to be planned must avoid these singular points. For example, possible flat outputs for the second-order chained form system are

$$y = \begin{bmatrix} y_1 \\ y_2 \end{bmatrix} = \begin{bmatrix} x_1 \\ x_5 \end{bmatrix}.$$

The state x and the inputs u can be expressed in terms of the flat outputs by

$$x(y, \dot{y}, \ddot{y}, y^{(3)}) = \begin{bmatrix} y_1 \\ \dot{y}_1 \\ \ddot{y}_2 \\ \frac{\ddot{y}_1 \dot{y}_2^{(3)} - \ddot{y}_2 \dot{y}_1^{(3)}}{(\dot{y}_1)^2} \\ y_2 \\ \dot{y}_2 \end{bmatrix},$$

$$u(y, \dot{y}, \dots, y^{(4)}) = \begin{bmatrix} \frac{\dot{y}_1}{(\dot{y}_1)^2 (\ddot{y}_1 \dot{y}_2^{(4)} - \ddot{y}_2 \dot{y}_1^{(4)}) - 2(\ddot{y}_1 \dot{y}_2^{(3)} - \ddot{y}_2 \dot{y}_1^{(3)}) \dot{y}_1 \dot{y}_1^{(3)}} \end{bmatrix}$$

However, these equations are undefined for $\dot{y}_1 = 0$. This restriction has severe consequences for motion planning using the flatness property. Thus singularities occur at $\dot{y}_1 = 0$, which implies that the input $u_1(t)$ is not allowed to be identically zero. Therefore the only way to avoid these singularities in a state-to-state motion planning problem is to use a discontinuous or piece-wise continuous input function $u_1(t)$. For this reason, the flatness property will not be considered here, but instead we will use alternative methods that do not suffer from singularities. It should be noted that, in certain cases, it is possible to avoid the singularities in the flatness-based approach by using time-scaling. For example in the case of the car with n -trailers, singularities in the endogenous transformation have been avoided by time-scaling with respect to the arc-length of the trajectory of the mobile robot (Fliess et al., 1995).

4.5 The point to point steering problem

The main objective in this section is to generate input functions $u_1(t)$ and $u_2(t)$ that steer the state trajectories of the second-order chained form system from an initial state x_A to a final state x_B . A common approach is to parameterize the inputs of the system. This parameterization reduces the problem of finding two inputs in an infinite dimensional function space to finding a finite number of decision variables and basis functions.

Consider the second-order chained form system $\dot{x} = f(x, u_1, u_2)$, with state $x = [x_1, x_2, \dots, x_5, x_6]^T$, given by

$$f(x, u) = [x_2, u_1, x_4, u_2, x_6, x_3 u_1]^T. \quad (4.5)$$

Suppose that the input functions $u_1(t)$ and $u_2(t)$ can be written as a finite sum of basis functions:

$$u_1(t) = \sum_{i=1}^q a_{1i} h_i(t) = \bar{a}_1 h(t), \quad u_2(t) = \sum_{i=1}^q a_{2i} h_i(t) = \bar{a}_2 h(t), \quad (4.6)$$

where $h(t)$ is a q dimensional vector of basis functions. For example, the basis functions can be chosen such that the inputs $u_1(t)$ and $u_2(t)$ are a finite sum of harmonic functions, *i.e.*, a Fourier series with fundamental pulsation ω , by selecting

$$h(t) = [1 \quad \sin(\omega t) \quad \cos(\omega t) \quad \dots \quad \sin((p-1)\omega t) \quad \cos((p-1)\omega t)]^T, \quad q = 2p - 1. \quad (4.7)$$

This parametrization has reduced the problem of finding two input functions $u_1(t)$ and $u_2(t)$ to finding a set of $2q$ parameters \bar{a}_1 and \bar{a}_2 . Suppose that we want to steer the system from an initial state x_A at time $t = 0$ to a final state x_B at time $t = T$, where $T > 0$. In order to be able to find a set of parameters that solve the motion planning problem, the set of basis functions has to be rich enough. This means that for the set of basis functions, there should exist parameters \bar{a}_1 and \bar{a}_2 such that $x(T) = x_B$. This is however not possible for every combination of a set of basis functions $h(t)$, an initial state x_A and a final state x_B . Some necessary regularity conditions will be given for the set of basis functions such that a solution to the motion planning problem exists.

By integration, it is easily seen that the solution of the open-loop system (4.5,4.6) at time $t = T$ satisfies

$$x(T) = \begin{bmatrix} \bar{a}_1^T m_1 + x_{20}T + x_{10} \\ \bar{a}_1^T m_2 + x_{20} \\ \bar{a}_2^T m_1 + x_{40}T + x_{30} \\ \bar{a}_2^T m_2 + x_{40} \\ \bar{a}_1^T M_1 \bar{a}_2 + \bar{a}_1^T m_3 + x_{60}T + x_{50} \\ \bar{a}_1^T M_2 \bar{a}_2 + \bar{a}_1^T m_4 + x_{60} \end{bmatrix} \quad (4.8)$$

where

$$\begin{aligned} m_1 &= \int_0^T \int_0^t h(\sigma) d\sigma dt, & m_2 &= \int_0^T h(\sigma) dt, \\ m_3 &= \int_0^T \int_0^t (\sigma x_{40} + x_{30}) h(\sigma) d\sigma dt, & m_4 &= \int_0^T (t x_{40} + x_{30}) h(t) dt \\ M_1 &= \int_0^T \int_0^t \left(h(\sigma) \int_0^\sigma \int_0^\tau h^T(s) ds d\tau \right) d\sigma dt, & M_2 &= \int_0^T \left(h(t) \int_0^t \int_0^\sigma h^T(s) ds d\tau \right) dt \end{aligned} \quad (4.9)$$

where $x_A = [x_{10}, x_{20}, x_{30}, x_{40}, x_{50}, x_{60}]^T$ represents the initial state. Because the six-dimensional state x has to be steered from its initial value x_A to an arbitrary final value $x_B = [x_{1T}, x_{2T}, x_{3T}, x_{4T}, x_{5T}, x_{6T}]^T$, at least 6 coefficients are needed. Therefore we need at least three basis functions and the first regularity condition is $q \geq 3$. Looking at the first four equations of (4.8), it is clear that in order for a solution to exist the $2 \times q$ matrix B_1 given by

$$B_1 = \begin{bmatrix} m_1^T \\ m_2^T \end{bmatrix}, \quad (4.10)$$

should have full row rank. This is the case when the vectors m_1 and m_2 are linearly independent and clearly the parameterization results in solving a system of nonlinear equations. This set of nonlinear equations can be solved by using nonlinear optimization techniques. Under appropriate conditions,

these nonlinear equations can be reduced to a linear set of equations. To that end, consider the equations (4.8) written in a partially linear form as

$$\begin{aligned} \begin{bmatrix} m_1^T \\ m_2^T \end{bmatrix} \bar{a}_1 &= \begin{bmatrix} x_{1T} - x_{20}T - x_{10} \\ x_{2T} - x_{20} \end{bmatrix} \\ \begin{bmatrix} m_1^T \\ m_2^T \end{bmatrix} \bar{a}_2 &= \begin{bmatrix} x_{2T} - x_{40}T - x_{30} \\ x_{4T} - x_{40} \end{bmatrix} \\ \begin{bmatrix} m_3^T \\ m_4^T \end{bmatrix} \bar{a}_1 + \begin{bmatrix} \bar{a}_1^T M_1 \bar{a}_2 \\ \bar{a}_1^T M_2 \bar{a}_2 \end{bmatrix} &= \begin{bmatrix} x_{5T} - x_{60}T - x_{50} \\ x_{6T} - x_{60} \end{bmatrix} \end{aligned} \quad (4.11)$$

Suppose that m_1 and m_2 are linearly independent. Suppose that we select a solution to the first two linear equations in (4.11) as

$$\begin{aligned} \bar{a}_1 &= B_1^T (B_1 B_1^T)^{-1} \begin{bmatrix} x_{1T} - x_{20}T - x_{10} \\ x_{2T} - x_{20} \end{bmatrix} = \bar{a}_{10} \\ \bar{a}_2 &= B_1^T (B_1 B_1^T)^{-1} \begin{bmatrix} x_{3T} - x_{40}T - x_{30} \\ x_{4T} - x_{40} \end{bmatrix} + A_1 y_1 = \bar{a}_{20} + A_1 y_1 \end{aligned} \quad (4.12)$$

where the columns of the $q \times (q-2)$ matrix A_1 form a basis for the nullspace of B_1 , and y_1 is an arbitrary $(q-2) \times 1$ column vector. Then substitution of (4.12) into the last equation of (4.11), results in a linear set of equations given by

$$\begin{bmatrix} \bar{a}_{10}^T M_1 A_1 \\ \bar{a}_{10}^T M_2 A_1 \end{bmatrix} y_1 + \begin{bmatrix} m_3^T \bar{a}_{10} + \bar{a}_{10}^T M_1 \bar{a}_{20} \\ m_4^T \bar{a}_{10} + \bar{a}_{10}^T M_2 \bar{a}_{20} \end{bmatrix} = \begin{bmatrix} x_{5T} - x_{60}T - x_{50} \\ x_{6T} - x_{60} \end{bmatrix} \quad (4.13)$$

This linear set of equations can be solved for all right hand sides of (4.13) when the matrix B_2 given by

$$B_2 = \begin{bmatrix} \bar{a}_{10}^T M_1 A_1 \\ \bar{a}_{10}^T M_2 A_1 \end{bmatrix} \quad (4.14)$$

has full row rank. This condition is met if and only if the matrices M_1 and M_2 are linearly independent, *i.e.*, there exists no $\alpha \in \mathbb{R}$ such that $M_1 = \alpha M_2$, and additionally $\bar{a}_{10} \neq 0$. The latter condition is met if either $x_{1T} - x_{20}T - x_{10} \neq 0$ or $x_{2T} - x_{20} \neq 0$. These inequalities imply that the desired final state (x_{1T}, x_{2T}) can not be reached by drift, *i.e.*, for $u_1 = 0$ and $u_2 = 0$ the initial velocities x_{20} can not be used to transfer the states x_1 from x_{10} to x_{1T} while $x_{2T} = x_{20}$. In other words, the (x_1, x_2) dynamics should be excited. Note that $\bar{a}_{10} = 0$ implies $u_1(t) = 0, \forall t$, while the second-order chained form is not controllable for $u_1 = 0$. A solution to (4.13) is given by

$$y_1 = B_2^T (B_2 B_2^T)^{-1} \begin{bmatrix} x_{5T} - x_{60}T - x_{50} - m_3^T \bar{a}_{10} - \bar{a}_{10}^T M_1 \bar{a}_{20} \\ x_{6T} - x_{60} - m_4^T \bar{a}_{10} - \bar{a}_{10}^T M_2 \bar{a}_{20} \end{bmatrix} + A_2 y_2 = y_{10} + A_2 y_2 \quad (4.15)$$

where the columns of the $q \times (q-2)$ matrix A_2 form a basis for the nullspace of B_2 , and y_2 is an arbitrary $(q-2) \times 1$ column vector. A class of solutions to the motion planning problem is thus given by

$$\begin{aligned} \bar{a}_1 &= B_1^T (B_1 B_1^T)^{-1} \begin{bmatrix} x_{1T} - x_{20}T - x_{10} \\ x_{2T} - x_{20} \end{bmatrix} \\ \bar{a}_2 &= A_1 A_2 y_2 + A_1 y_{10} + B_1^T (B_1 B_1^T)^{-1} \begin{bmatrix} x_{3T} - x_{40}T - x_{30} \\ x_{4T} - x_{40} \end{bmatrix} \end{aligned} \quad (4.16)$$

where y_{10} is given in (4.15). In this section we have also found regularity conditions under which there exists a solution, given by (4.16), of the motion planning problem. These conditions can be summarized as follows.

- R1** The number of basis functions should be at least 3, *i.e.*, $q \geq 3$.
- R2** The matrices B_1 and B_2 should have rank 2, *i.e.*, the vectors m_1 and m_2 as well as the vectors m_3 and m_4 should be linearly independent.
- R3** The desired final states (x_{1T}, x_{2T}) can not be reached by drift, *i.e.*, either $x_{1T} - x_{20}T - x_{10} \neq 0$ or $x_{2T} - x_{20} \neq 0$.

In the next section, the set of nonlinear equations (4.11) will be used to formulate a constrained optimization problem, and numerical optimization algorithms will be used to solve the problem. The solutions given by (4.16), or randomly computed vectors \bar{a}_1 and \bar{a}_2 , can then be used as initial conditions to the optimization problem.

4.6 A variational method

In this section calculus of variations will be used to solve the nonlinear set of equations that were given in the previous section. First we will define a cost criterion $J(\bar{a})$. For simplicity, we select the following cost criterion:

$$J = \int_0^T (u_1(t)^2 + u_2(t)^2) dt = \bar{a}_1^T \left(\int_0^T h(t)h(t)^T dt \right) \bar{a}_1 + \bar{a}_2^T \left(\int_0^T h(t)h(t)^T dt \right) \bar{a}_2 \quad (4.17)$$

The motion planning problem can then be formulated as the following constrained optimization problem.

$$\begin{aligned} & \underset{\bar{a} \in \mathbb{R}^{2q}}{\text{minimize}} && J(\bar{a}) \\ & \text{subject to} && r(\bar{a}) \triangleq x(T) - x_B = 0 \end{aligned} \quad (4.18)$$

where $\bar{a} = [\bar{a}_1, \bar{a}_2]^T$ and $x(T)$ is given by

$$x(T) = \begin{bmatrix} \bar{a}_1^T m_1 + x_{20}T + x_{10} \\ \bar{a}_1^T m_2 + x_{20} \\ \bar{a}_2^T m_1 + x_{40}T + x_{30} \\ \bar{a}_2^T m_2 + x_{40} \\ \bar{a}_1^T M_1 \bar{a}_2 + \bar{a}_1^T m_3 + x_{60}T + x_{50} \\ \bar{a}_1^T M_2 \bar{a}_2 + \bar{a}_1^T m_4 + x_{60} \end{bmatrix}$$

In the previous section the motion planning problem could be reduced to the problem of solving a set of linear equations, at the expense of reducing the parameterization. In this section, the motion planning problem is formulated as a constrained optimization problem in which the parametrization of the inputs is used to find a solution that is optimal with respect to the cost criterion (4.17). The advantage of formulating the problem as a constrained optimization problem is the fact that it can be solved using optimization algorithms. Of course, we assume that the basis functions are chosen such that a solution exists. At the cost of some computational load, in general, these methods can find local extrema of the optimization problem.

The numerical optimization algorithm that will be used is an SQP-type algorithm 'fmincon', available through the optimization toolbox of MATLAB . The 'fmincon' algorithm is a Sequential Quadratic Programming (SQP) method. SQP methods resemble Newton's methods for constrained optimization; at each iteration step the Hessian of a Lagrangian function is approximated by using a quasi-Newton updating method. This approximation of the Hessian is then used to formulate a Quadratic-Programming problem that is based on the quadratic approximation of the Lagrangian and the linearized constraints. An overview of SQP methods can be found in (Fletcher, 1980; Gill et al., 1981).

4.6.1 The SQP algorithm

Consider the constrained optimization problem given by (4.18). The Lagrangian associated with the constrained optimization problem is given by

$$L(\bar{a}, \lambda) = J(\bar{a}) + \lambda^T r(\bar{a})$$

where λ is a 1×6 column vector of Lagrange multipliers. The Lagrangian allows us to replace the constrained optimization problem by an unconstrained optimization problem given by

$$\underset{\bar{a} \in \mathbb{R}^{2q}}{\text{minimize}} \quad L(\bar{a}, \lambda)$$

A necessary condition for an optimal value \bar{a} is:

$$\nabla_{\bar{a}} L(\bar{a}, \lambda) = 0$$

This condition can be written as the well-known Karush-Kuhn-Tucker equations given by

$$\begin{aligned} \nabla_{\bar{a}} J(\bar{a}) + \lambda \nabla_{\bar{a}} r(\bar{a}) &= 0 \\ r(\bar{a}) &= 0 \end{aligned} \tag{4.19}$$

The Karush-Kuhn-Tucker (KKT) equations are necessary conditions for optimality of the constrained optimization problem. They are referred to as the first-order conditions for optimality. The sufficient conditions, also known as the second-order conditions, are given by

$$y^T \nabla_{\bar{a}}^2 L(\bar{a}, \lambda) y > 0, \quad \forall y \in \mathbb{R}^n / \{0\} \text{ such that } y^T \nabla_{\bar{a}} L(\bar{a}, \lambda) = 0 \tag{4.20}$$

where $\nabla_{\bar{a}}^2 L(\bar{a}, \lambda)$ denotes the Hessian of the Lagrangian. If the second-order conditions (4.20) are satisfied, then the point \bar{a} is a global minimizer of the cost function $J(\bar{a})$. If the constrained optimization problem is convex, *i.e.*, $J(\bar{a})$ and $r(\bar{a})$ are convex functions, and the equalities $r(\bar{a}) = 0$ are linear then the KKT equations (4.19) are both necessary and sufficient conditions.

In order to find a solution to the KKT equations, the equations (4.19) can be transformed into an easier subproblem that can be solved and used as a basis of an iterative process. By using a quadratic approximation of the Lagrangian and by linearizing the constraints, we can formulate the following Quadratic Programming problem

$$\begin{aligned} \underset{d \in \mathbb{R}^{2q}}{\text{minimize}} \quad & d^T H_k d + \nabla_{\bar{a}} J(\bar{a})^T d \\ \text{subject to} \quad & (\nabla_{\bar{a}} r(\bar{a})^T)^T d + r(\bar{a}) = 0 \end{aligned} \tag{4.21}$$

where H_k is a positive definite approximation of the Hessian of the Lagrangian: $\nabla_{\bar{a}}^2 L(\bar{a}, \lambda)$ at iteration k . The Hessian H_k can be updated by any of the quasi-Newton methods, although the BFGS method (Bertsekas, 1995) appears to be the most successful. If the initial solution \bar{a}_0 is sufficiently close to a solution point, then the BFGS method has been shown to lead to super-linear convergence towards a solution point. The resulting QP problem (4.21) can be solved using any QP algorithm, see for example (Bertsekas, 1995). The solution is used to form a new iteration $\bar{a}_{k+1} = \bar{a}_k + \alpha d$ where the step length α is determined by an appropriate line search procedure.

The 'fmincon' procedure is computationally quite intensive in the sense that many functions have to be evaluated at each iteration. Moreover, this SQP method does not guarantee that a solution is found; in some cases the method does not converge to a solution. If a solution exists, one has to change the initial 'guess' \bar{a}_0 , otherwise one needs to increase the number of basis functions so that a solution exists. If a solution can be found using the method in Section 4.5 then this solution may be used as a feasible initial 'guess'. The 'fmincon' procedure can be replaced by more efficient and robust SQP implementations.

4.7 A sub-optimal method

In the previous section the motion planning problem could be transformed into a constrained optimization problem by parameterizing the inputs $u_1(t)$ and $u_2(t)$ with respect to a set of basis functions. In this approach the parameterization parameters act as the decision variables and are used to minimize a certain cost criterion. The optimal solution to the constrained optimization problem and the resulting value of the cost criterion are, however, completely dependent on the parametrization. In this section, the inputs will not be parameterized but, instead, the motion planning problem is treated as an optimal control problem, see (Lewis and Syrmos, 1995).

Consider a system $\dot{x} = f(x, u)$ with $f : \mathbb{R}^n \times \mathbb{R}^m \rightarrow \mathbb{R}^n$. Again we consider a pre-defined time $T > 0$ and consider a cost criterion

$$J(x, u) = \int_0^T j(x, u) dt$$

where $x = [x_1, x_2, \dots, x_n]^T$ and $u = [u_1, u_2, \dots, u_m]^T$. Then formulate the following optimal control problem:

$$\begin{aligned} & \underset{u}{\text{minimize}} && J(x, u) \\ & \text{subject to} && \dot{x} = f(x, u) \\ & && x(0) = x_A \\ & && x(T) = x_B, \end{aligned}$$

where $u : \mathbb{R} \rightarrow \mathbb{R}^m$. Associated with this system we consider the Hamiltonian function

$$H(x, p, u) = j(x, u) + p^T f(x, u)$$

where the co-state vector $p(t) = [p_1(t), \dots, p_n(t)]^T$ is given by, to be defined, functions $p_i(t)$, $i = 1, 2, \dots, n$. The minimum principle states that an optimal solution $[x_{opt}(t), u_{opt}(t), p_{opt}(t)]$ satisfies

$$\begin{aligned} \dot{x}_{opt} &= f(x_{opt}, u_{opt}) \\ \dot{p}_{opt} &= -\frac{\partial H}{\partial x}(p_{opt}, x_{opt}, u_{opt}) \\ x(0) &= x_A \\ x(T) &= x_B \end{aligned} \tag{4.22}$$

and for almost any $t \in [0, T]$

$$H(p_{opt}(t), x_{opt}(t), u_{opt}(t)) = \min_v H(p_{opt}(t), x_{opt}(t), v), \quad (4.23)$$

where $v : \mathbb{R} \rightarrow \mathbb{R}^m$. The equations (4.22,4.23) are necessary conditions for $[x_{opt}(t), u_{opt}(t)]$ to be an optimal solution. In (Lee and Markus, 1967) a set of conditions which, in addition to (4.22,4.23), are sufficient conditions for $[x_{opt}(t), u_{opt}(t)]$ to be a locally optimal solution are

A The $(n+m) \times (n+m)$ matrix

$$D = \begin{bmatrix} \frac{\partial^2 j(x, u)}{\partial x^2} & \frac{\partial^2 j(x, u)}{\partial x \partial u} \\ \frac{\partial^2 j(x, u)}{\partial u \partial x} & \frac{\partial^2 j(x, u)}{\partial u^2} \end{bmatrix} \quad (4.24)$$

is positive definite along the trajectory $[x_{opt}(t), u_{opt}(t)]$.

B Along the trajectory $[x_{opt}(t), u_{opt}(t)]$ either $\frac{\partial^2 f(x, u)}{\partial x^2} = \frac{\partial^2 f(x, u)}{\partial x \partial u} = \frac{\partial^2 f(x, u)}{\partial u^2} = 0$ or $\frac{\partial j(x, u)}{\partial x} = 0$.

Condition (4.23) implies that

$$\frac{\partial H}{\partial u}(p_{opt}(t), x_{opt}(t), u_{opt}(t)) = 0 \quad (4.25)$$

Condition (4.25) only guarantees that the Hamiltonian is stationary for the optimal input $u_{opt}(t)$. In order to guarantee that the input $u_{opt}(t)$ is a global minimizer of the Hamiltonian $H(p_{opt}(t), x_{opt}(t), \cdot)$, $H(p, x, u)$ should be a convex function with respect to its argument u . Therefore condition (4.23) is equivalent to (4.25), when $H(p, x, u)$ is convex in its argument u .

In this thesis, the cost-criterion $j(x, u)$ is selected as $j(x, u) = u_1^2 + u_2^2$. The Hamiltonian is then given by

$$H(x, p, u) = p_1 x_4 + p_2 x_5 + p_3 x_6 + p_4 u_1 + p_5 u_2 + p_6 x_2 u_1 + u_1^2 + u_2^2$$

The equations (4.22,4.23) form a boundary value problem in which one has to find an optimal input $u_{opt}(t)$. As the second-order chained form has been shown to be controllable, a solution is known to exist. Since $H(x, p, u)$ is convex with respect to its argument u , we can use equation (4.25) to eliminate $u_{opt}(t)$ from these equations. Evaluating (4.25) gives

$$\frac{\partial H}{\partial u} = \begin{bmatrix} p_4 + p_6 x_2 + 2u_1 \\ p_5 + 2u_2 \end{bmatrix} = \begin{bmatrix} 0 \\ 0 \end{bmatrix}$$

This implies that the optimal inputs u_1^{opt} and u_2^{opt} are given by

$$\begin{aligned} u_1^{opt} &= -\frac{p_4^{opt} + p_6^{opt} x_2^{opt}}{2} \\ u_2^{opt} &= -\frac{p_5^{opt}}{2} \end{aligned} \quad (4.26)$$

Since the matrix in (4.24) is given by

$$D = \begin{bmatrix} O_{55} & O_{52} \\ O_{25} & 2I_2 \end{bmatrix}$$

where O_{nm} denotes a $n \times m$ matrix with zeros and I_n denotes a $n \times n$ identity matrix, it is positive semi-definite. We conclude that condition A is not satisfied and a solution $u_{opt}(t)$ is not guaranteed to be a local optimum. Note that if we choose $j(x, u)$ to be given by $j(x, u) = x_1(t)^2 + \dots + x_6(t)^2 + u_1(t)^2 + u_2(t)^2$, then condition A is satisfied, but condition B isn't. In order to check whether the solution $u_{opt}(t)$ is a local optimum, it is necessary to check a higher-order condition. Here, we will be satisfied with finding one of these candidate solutions, *i.e.*, we want to generate a candidate trajectory $[x_{opt}(t), u_{opt}(t)]$ that may or may not be a local optimum. This can be motivated by the fact that we just want to find a trajectory that connects the states x_A and x_B and we do not care if the candidate trajectory minimizes the cost function. Substituting (4.26) into the equations (4.22) and defining the augmented state $s(t)$ with

$$s = \begin{bmatrix} s_a \\ s_b \end{bmatrix} = \begin{bmatrix} p_{opt} \\ x_{opt} \end{bmatrix}$$

we obtain the system, with boundary conditions, given by

$$\dot{s} = b(s), \quad s_b(0) = x_A, \quad s_b(T) = x_B \quad (4.27)$$

where

$$b(s) = \begin{bmatrix} 0 \\ (s_4 + s_6 s_8) s_6 / 2 \\ 0 \\ -s_1 \\ -s_2 \\ -s_3 \\ s_{10} \\ s_{11} \\ s_{12} \\ -(s_4 + s_6 s_8) s_6 / 2 \\ -s_5 / 2 \\ -(s_4 + s_6 s_8) s_8 / 2 \end{bmatrix} \quad (4.28)$$

If we can find a solution to the system (4.27), then a candidate optimal solution $[x_c(t), u_c(t)]$ has been found. This solution provides a trajectory $[x_c(t), u_c(t)]$ from the initial state x_A to the final state x_B . Finding a solution means solving the boundary value problem (BVP) (4.27). It is very hard to solve equations (4.27) analytically and we propose a numerical method in order to find an approximate solution. The numerical method that will be used to find an approximate solution is the Finite Differences Method (Ascher et al., 1988).

4.7.1 The Finite Differences Method

The Finite Differences Method consists of the following three steps (Ascher et al., 1988):

1. On the time interval $0 \leq t \leq T$ a uniform mesh π of $N + 1$ points is defined, *i.e.*,

$$\pi : t_i = \Delta(i - 1), \quad \forall i \in 1, 2, \dots, N + 1$$

where $\Delta = T/N$. The approximate solution of $s(t)$ at time $t = t_i$ is denoted by $s_i = [s_{a,i}^T, s_{b,i}^T]^T$. The approximate solution $s_\pi = [s_1^T, s_2^T, \dots, s_{N+1}^T]^T$ is a $12 \times (N + 1)$ matrix.

2. A set of algebraic equations is formed by replacing the derivative in (4.27) by a trapezoidal approximation scheme:

$$\frac{s_{i+1} - s_i}{\Delta} = \frac{b(s_{i+1}) + b(s_i)}{2}, \quad 1 \leq i \leq N \quad (4.29)$$

$$s_{b,1} = x_A, \quad s_{b,N+1} = x_B$$

Equations (4.29) constitute of $12(N+1)$ equations.

3. The equations (4.29) can be written in vector notation as

$$F(s_\pi) = 0 \quad (4.30)$$

where

$$F(s_\pi) = \begin{bmatrix} \frac{s_2 - s_1}{\Delta} - \frac{b(s_2) + b(s_1)}{2} \\ \frac{s_3 - s_2}{\Delta} - \frac{b(s_3) + b(s_2)}{2} \\ \vdots \\ \frac{s_{N+1} - s_N}{\Delta} - \frac{b(s_{N+1}) + b(s_N)}{2} \\ s_{b,1} - x_A \\ s_{b,N+1} - x_B \end{bmatrix} \quad (4.31)$$

An approximate solution of these equation is sought by using a damped Newton algorithm. This Newton algorithm is an iterative root finding procedure for the linear approximation of the (nonlinear) equation (4.30). The procedure is as follows:

- Select an initial solution s_π^0 . This choice is a guess because no information about the solution is available.
- Find updates of the solution using the damped Newton procedure:

$$s_\pi^{i+1} = s_\pi^i - \gamma \left[\frac{\partial F(s_\pi^i)}{\partial s_\pi^i} \right]^{-1} F(s_\pi^i)$$

where γ is the damping factor, which is determined empirically. The iterative solution is stopped when some convergence criterion is satisfied. For example, the iterative procedure can be stopped when $F(s_\pi^i)^T F(s_\pi^i) < \varepsilon$, with ε a small parameter.

The obtained approximate solution s_π , defined on a uniform mesh π of $N+1$ points, can be interpolated to construct $s(t)$ at every time-instant $t \in [0, T]$. The resulting candidate solution is then given by $[x_c(t), u_c(t)] = [s_b^\pi(t), \bar{u}_c(t)]$ where $\bar{u}_c(t)$ is obtained by substitution of s_a^π in (4.26). The term 'candidate solution' implies that there is possibly more than one solution to the boundary value problem and the solution may or may not be a local optimum of the optimal control problem. In addition, 'shooting' techniques may be much more effective in finding these candidate solution.

4.8 Summary

In this chapter, two methods to solve the motion planning problem were presented. These methods can be used to compute feasible trajectories, connecting two arbitrary states, which are optimal in

some sense. In the variational method, the motion planning problem is formulated as a constrained optimization problem in which the norm of the inputs is minimized. By parameterizing the inputs over a set of basis functions, a numerical optimization algorithm can be used to compute a feasible state-trajectory that connects two arbitrary states. If the numerical optimization algorithm converges, the solution of the constrained optimization is a local minimizer of the optimization problem. The variational method can be extended to incorporate obstacle avoidance. Then a feasible trajectory connecting two arbitrary states is to be found amongst obstacles. See (Verhoeven, 2002) for details.

In the sub-optimal method, the motion planning problem is formulated as an optimal control problem in which the norm of the inputs is minimized. The solution to the optimal control problem can be found by solving a boundary value problem. Because the boundary value problem is hard to solve, an approximate solution is sought by using the Finite Differences Method. The Finite Differences Method (FDM) finds an approximate solution to the boundary value problem by discretizing the boundary value problem. The solution of the FDM is sub-optimal in the sense that it is an approximation of the optimal solution. The presented sub-optimal methods may be extended to deal with time-optimal control problems in which the end time T is also optimized. However, the extensions of both methods to obstacle avoidance and time-optimal control problems falls outside the scope of this thesis and will not be considered here.

Tracking control

As mentioned in the introduction, only a few results are known that have addressed the tracking control problem for the second-order chained form, defined in Section 2.3. In (Kobayashi, 1999), a discontinuous and flatness-based tracking controller has been given for a class of trajectories of the extended chained-form system. These trajectories are not allowed to pass through singular points of the controller. Moreover, the error-dynamics are not stable in a Lyapunov sense, but only converge exponentially to the origin. In (Walsh et al., 1994), linear time-varying controllers were given that stabilize the system to a class of trajectories. The trajectories should be chosen such that the time-varying system, resulting from linearizing the system along the trajectory, is uniformly completely controllable (Rugh, 1996) over intervals of length δ . This approach means that one should also face the problem of finding feasible trajectories. Moreover, the error-dynamics are only locally asymptotically stable.

In this chapter, a linear time-varying controller will be developed that globally asymptotically stabilizes the second-order chained form system to a reference trajectory. These reference trajectories can not be chosen arbitrarily, but have to satisfy a so-called 'persistence of excitation' condition. In fact, under this persistence of excitation condition, the system is \mathcal{H} -exponentially stabilized towards the reference trajectory. The control design approach has been published in (Aneke et al., 2000, 2003).

5.1 Cascaded backstepping control

In this section we apply a cascade design to stabilize the equilibrium $x = 0$ of the error dynamics (2.14). We start by rewriting the tracking dynamics into a more convenient form given by

$$\begin{aligned} \Delta_1 \begin{cases} \dot{x}_{31} &= x_{32} \\ \dot{x}_{32} &= x_{21}u_{1d} + (x_{21} + \xi_{2d})(u_1 - u_{1d}) \end{cases} & \quad \Delta_2 \begin{cases} \dot{x}_{21} &= x_{22} \\ \dot{x}_{22} &= u_2 - u_{2d} \end{cases} \\ \Delta_3 \begin{cases} \dot{x}_{11} &= x_{12} \\ \dot{x}_{12} &= u_1 - u_{1d} \end{cases} \end{aligned} \quad (5.1)$$

where ξ_{2d} denotes the reference trajectory of the state ξ_2 in (2.7). Suppose that the subsystem Δ_3 has been stabilized to the origin $(x_{11}, x_{12}) = (0, 0)$ by a controller $u_1(u_{1d}, x_{11}, x_{12})$. Then since $x_{12} \equiv 0$ it also holds that $u_1 - u_{1d} \equiv 0$. We design the remaining input u_2 such that the remaining subsystem (Δ_1, Δ_2) is stabilized for $u_1 - u_{1d} \equiv 0$.

Remark 5.1.1. The perturbation or interconnection term $g(t, z_1, z_2)z_2$ of (5.1), as defined in Theorem 3.6.1, is given by $(x_{21} + \xi_{2d})(u_1 - u_{1d})$. The perturbation term thus depends on the, to be designed, feedback $u_1(t, x)$. When considering (Δ_1, Δ_2) as the perturbed subsystem Σ_1 and Δ_3 as the

unperturbed subsystem Σ_2 , the resulting perturbation matrix $g(t, z_1, z_2)$ has to be linear with respect to the variable $z_1 = (x_{21}, x_{22}, x_{31}, x_{32})$ in order to satisfy condition (2) in Theorem 3.6.1. This is the case when choosing the feedback $u_1 = u_{1d} + k(x_{11}, x_{12})$ with $k : \mathbb{R}^2 \rightarrow \mathbb{R}$ a linear function in (x_{11}, x_{12}) .

5.1.1 Stabilization of the (Δ_1, Δ_2) subsystem

Suppose that the Δ_3 subsystem has been stabilized by choosing

$$u_1 = u_{1d} - k_1 x_{11} - k_2 x_{12}, \quad k_1 > 0, k_2 > 0, \quad (5.2)$$

where the polynomial $p(\lambda) = \lambda^2 + k_1 \lambda + k_2$ is Hurwitz. The time-varying subsystem Δ_1 with $u_1 - u_{1d} \equiv 0$ can be written as

$$\begin{aligned} \dot{x}_{31} &= x_{32} \\ \dot{x}_{32} &= x_{21} u_{1d} \end{aligned} \quad (5.3)$$

We aim at designing a stabilizing feedback x_{21} for the subsystem (5.3). This stabilizing feedback is designed using a backstepping procedure in which x_{21} is a virtual input. First we need to make some assumptions on the reference input signal u_{1d} .

Assumption 5.1.1. Assume that the function $u_{1d} : \mathbb{R}_+ \rightarrow \mathbb{R}$ is uniformly bounded in t and continuously differentiable. Moreover, assume that $u_{1d}(t)$ is persistently exciting, *i.e.*, for all $r \geq 0$ and for all $\delta > 0$ there exists $\varepsilon_1 > 0$ and $\varepsilon_2 > 0$ such that

$$\varepsilon_1 \leq \int_t^{t+\delta} u_{1d}^{2r+2}(\tau) d\tau \leq \varepsilon_2, \quad \forall t \geq 0. \quad (5.4)$$

Consider the first equation $\dot{x}_{31} = x_{32}$ of the subsystem (5.3) and assume that x_{32} is the virtual input. A stabilizing function $x_{32} = \alpha_1(x_{31})$ for the x_{31} -subsystem is

$$\alpha_1(u_{1d}(t), x_{31}) = -c_1 u_{1d}^{2d_1+2} x_{31},$$

where $c_1 > 0$ and $d_1 \geq 0$. This choice of the stabilizing function $\alpha_1(x_{31})$ guarantees that the (Δ_1, Δ_2) subsystem can be stabilized by a backstepping procedure in which no divisions by $u_{1d}(t)$ occur. Define $\bar{x}_{32} = x_{32} - \alpha_1(x_{31}) = x_{32} + c_1 u_{1d}^{2d_1+2} x_{31}$ and consider the \bar{x}_{32} -subsystem

$$\dot{\bar{x}}_{32} = x_{21} u_{1d} + c_1 u_{1d}^{2d_1+2} x_{32} + c_1 (2d_1 + 2) u_{1d}^{2d_1+1} \dot{u}_{1d} x_{31}.$$

Suppose that x_{21} is the virtual input and let \bar{u}_d denote the vector $\bar{u}_d = (u_{1d}, \dot{u}_{1d}, \dots, u_{1d}^{(3)})$. A stabilizing function $x_{21} = \alpha_2(\bar{u}_d, x_{31}, x_{32})$ for the \bar{x}_{32} -subsystem is then given by

$$\begin{aligned} \alpha_2(\bar{u}_d, x_{31}, x_{32}) &= -c_1 u_{1d}^{2d_1+1} x_{32} - c_1 (2d_1 + 2) u_{1d}^{2d_1} \dot{u}_{1d} x_{31} - c_2 u_{1d}^{2d_2+1} \bar{x}_{32} \\ &= -\left(c_1 c_2 u_{1d}^{2d_1+2d_2+3} + c_1 (2d_1 + 2) u_{1d}^{2d_1} \dot{u}_{1d} \right) x_{31} - \left(c_1 u_{1d}^{2d_1+1} + c_2 u_{1d}^{2d_2+1} \right) x_{32}, \end{aligned} \quad (5.5)$$

where $c_2 > 0$, $d_2 \geq 0$ and the relation $\bar{x}_{32} = x_{32} + c_1 u_{1d}^{2d_1+2} x_{31}$ has been substituted. Define $\bar{x}_{31} = x_{31}$ and $\bar{x}_{21} = x_{21} - \alpha_2(\bar{u}_d, x_{31}, x_{32})$. The closed-loop $(\bar{x}_{31}, \bar{x}_{32})$ subsystem is given by

$$\begin{aligned} \dot{\bar{x}}_{31} &= -c_1 u_{1d}^{2d_1+2} \bar{x}_{31} + \bar{x}_{32} \\ \dot{\bar{x}}_{32} &= -c_2 u_{1d}^{2d_2+2} \bar{x}_{32} + \bar{x}_{21} u_{1d}. \end{aligned} \quad (5.6)$$

Consider the \bar{x}_{21} -subsystem

$$\dot{\bar{x}}_{21} = x_{22} - \frac{d}{dt} [\alpha_2(\bar{u}_{1d}, x_{31}, x_{32})],$$

where x_{22} denotes a new virtual input. For clarity of the derivations, the time-derivative of α_2 along the trajectories of the system is written as $d/dt [\alpha_2(\bar{u}_{1d}, x_{31}, x_{32})]$ and will not be expanded. We define a new variable $\bar{x}_{22} = x_{22} - \alpha_3(\bar{u}_{1d}, \bar{x}_{21}, x_{31}, x_{32})$ where the stabilizing function $\alpha_3(\bar{u}_{1d}, \bar{x}_{21}, x_{31}, x_{32})$ is given by

$$\alpha_3(\bar{u}_{1d}, \bar{x}_{21}, x_{31}, x_{32}) = -c_3 \bar{x}_{21} + \frac{d}{dt} [\alpha_2(\bar{u}_{1d}, x_{31}, x_{32})].$$

The \bar{x}_{21} -subsystem is then given by $\dot{\bar{x}}_{21} = -c_3 \bar{x}_{21} + \bar{x}_{22}$. Consider the \bar{x}_{22} -subsystem

$$\dot{\bar{x}}_{22} = (u_2 - u_{2d}) - \frac{d}{dt} [\alpha_3(\bar{u}_{1d}, \bar{x}_{21}, x_{31}, x_{32})].$$

This subsystem can be stabilized by choosing the input u_2 as

$$\begin{aligned} u_2 - u_{2d} &= -c_4 \bar{x}_{22} + \frac{d}{dt} [\alpha_3(\bar{u}_{1d}, \bar{x}_{21}, x_{31}, x_{32})] \\ &= -c_3 c_4 x_{21} - (c_3 + c_4) x_{22} + c_3 c_4 \alpha_2(\bar{u}_{1d}, x_{31}, x_{32}) + (c_3 + c_4) \frac{d}{dt} [\alpha_2(\bar{u}_{1d}, x_{31}, x_{32})] \\ &\quad + \frac{d^2}{dt^2} [\alpha_2(\bar{u}_{1d}, x_{31}, x_{32})] \end{aligned} \quad (5.7)$$

The closed-loop (Δ_1, Δ_2) subsystem, after the coordinate change defined implicitly in the previous equations, then becomes

$$\begin{aligned} \dot{\bar{x}}_{31} &= -c_1 u_{1d}^{2d_1+2} \bar{x}_{31} + \bar{x}_{32} \\ \dot{\bar{x}}_{32} &= -c_2 u_{1d}^{2d_2+2} \bar{x}_{32} + \bar{x}_{21} u_{1d} \\ \dot{\bar{x}}_{21} &= -c_3 \bar{x}_{21} + \bar{x}_{22} \\ \dot{\bar{x}}_{22} &= -c_4 \bar{x}_{22} \end{aligned} \quad (5.8)$$

Under Assumption 5.1.1 we can prove that the closed-loop system given by

$$\begin{aligned} \dot{\bar{x}}_{31} &= -c_1 u_{1d}^{2d_1+2} \bar{x}_{31} + \bar{x}_{32} \\ \dot{\bar{x}}_{32} &= -c_2 u_{1d}^{2d_2+2} \bar{x}_{32} \end{aligned} \quad (5.9)$$

is globally exponentially stable (GES). This is shown in Proposition 5.1.2, by applying the following lemma and some basic theory for linear time-varying systems (Rugh, 1996). The influence of the term $\bar{x}_{21} u_{1d}$ on the stability of the system (5.6) will be considered in Section 5.2.

Lemma 5.1.1. *Suppose that Assumption 5.1.1 holds, i.e., for all $r > 0$ there exist $\delta > 0$ and $\varepsilon_1, \varepsilon_2 > 0$ such that (5.4) is satisfied. Then it holds that for all $r > 0$ and for all $t_0 \geq 0$*

$$\frac{t-t_0}{\delta} \varepsilon_1 - \varepsilon_1 \leq \int_{t_0}^t u_{1d}^{2r+2}(\tau) d\tau \leq \frac{t-t_0}{\delta} \varepsilon_2 + \varepsilon_2, \quad \forall t \geq t_0. \quad (5.10)$$

Proof. For $t = t_0$ the result is trivial. Suppose that $t > t_0$. Given any $\delta \leq (t - t_0)$, define N to be the largest integer smaller than the real number $(t - t_0)/\delta$, i.e.

$$N = \left\lfloor \frac{t - t_0}{\delta} \right\rfloor, \quad \mu_1 = \frac{(t - t_0)}{\delta} - N.$$

Divide the interval $[t_0, t]$ into N equal subintervals of length δ and a subinterval of length $0 \leq \mu_1 < \delta$. where $0 \leq \mu_1 < \delta$. This division into N subintervals $[t_0 + i\delta, t_0 + (i + 1)\delta]$, $i = 0 \dots N - 1$ with length δ and one interval $[t_0 + N\delta, t]$ of length $\mu_1\delta$ yields

$$\int_{t_0}^t u_{1d}^{2r+2}(\tau) d\tau = \sum_{i=0}^{N-1} \left(\int_{t_0+i\delta}^{t_0+(i+1)\delta} u_{1d}^{2r+2}(\tau) d\tau \right) + \int_{t_0+N\delta}^t u_{1d}^{2r+2}(\tau) d\tau. \quad (5.11)$$

The difference between the integral over $[t_0, t]$ and the integral over $[t_0, t_0 + N\delta]$ satisfies

$$0 \leq \int_{t_0+N\delta}^t u_{1d}^{2r+2}(\tau) d\tau < \varepsilon_2.$$

Substitution of (5.4) into (5.11) then gives

$$\begin{aligned} \sum_{i=0}^{N-1} \varepsilon_1 &\leq \int_{t_0}^t u_{1d}^{2r+2}(\tau) d\tau \leq \sum_{i=0}^{N-1} \varepsilon_2 + \varepsilon_2 \\ N\varepsilon_1 &\leq \int_{t_0}^t u_{1d}^{2r+2}(\tau) d\tau \leq N\varepsilon_2 + \varepsilon_2 \end{aligned}$$

By substitution of $N = (t - t_0)\delta^{-1} - \mu_1$ we obtain

$$\frac{t - t_0}{\delta} \varepsilon_1 - \mu_1 \varepsilon_1 \leq \int_{t_0}^t u_{1d}^{2r+2}(\tau) d\tau \leq \frac{t - t_0}{\delta} \varepsilon_2 + \varepsilon_2 - \mu_1 \varepsilon_2.$$

Since $0 \leq \mu_1 < 1$ we finally obtain the desired result (5.10):

$$\frac{t - t_0}{\delta} \varepsilon_1 - \varepsilon_1 \leq \int_{t_0}^t u_{1d}^{2r+2}(\tau) d\tau \leq \frac{t - t_0}{\delta} \varepsilon_2 + \varepsilon_2.$$

□

Remark 5.1.2. Equation (5.10) gives upper- and lower-bounds for the integral of u_{1d}^{2r+2} ; there exist two straight lines of the form $y_1 = \varepsilon_1/\lambda(t - t_0) - \varepsilon_1$, $y_2 = \varepsilon_2/\lambda(t - t_0) + \varepsilon_1$, with $\delta \in \mathbb{R}$ and $\varepsilon_i \in \mathbb{R}$, $i = 1, 2$ that upper- and lower-bound the integral. Note that the inequality is conservative when $t - t_0 < \delta$, in the sense that the lower-bound is negative while the integral is always positive.

Proposition 5.1.2. Consider the system

$$\begin{aligned} \dot{\bar{x}}_1 &= -c_1 u_{1,d}(t)^{2d_1+2} \bar{x}_1 + \bar{x}_2 \\ \dot{\bar{x}}_2 &= -c_2 u_{1,d}(t)^{2d_2+2} \bar{x}_2 \end{aligned} \quad (5.12)$$

Suppose that the reference input $u_{1d}(t)$ satisfies the persistence of excitation condition (5.4) for some $r \geq 0$. Suppose that $\min(d_1, d_2) \geq r$ holds. Then the equilibrium $x = 0$ is globally exponentially stable (GES).

Proof. One can easily verify that the general solution of the linear time-varying system (5.12) with initial condition $\bar{x}(t_0) = [\bar{x}_1(t_0), \bar{x}_2(t_0)]$ is given by

$$\begin{aligned}\bar{x}_1(t) &= \bar{x}_1(t_0) \exp\left(-c_1 \int_{t_0}^t u_{1d}^{2d_1+2}(\tau) d\tau\right) + G(t), \\ \bar{x}_2(t) &= \bar{x}_2(t_0) \exp\left(-c_2 \int_{t_0}^t u_{1d}^{2d_2+2}(\tau) d\tau\right),\end{aligned}\tag{5.13}$$

where the additional term $G(t)$ is given as

$$G(t) = \int_{t_0}^t \bar{x}_2(t_0) \exp\left(-c_1 \int_{\sigma}^t u_{1d}^{2d_1+2}(\tau) d\tau - c_2 \int_{t_0}^{\sigma} u_{1d}^{2d_2+2}(\tau) d\tau\right) d\sigma\tag{5.14}$$

We will use Lemma 5.1.1 to prove the exponential stability of the solution (\bar{x}_1, \bar{x}_2) . By Lemma 5.1.1, see (5.10), there exists positive constants ε_1 and ε_2 , dependent on d_1 and d_2 respectively, such that

$$\begin{aligned}\frac{t-t_0}{\delta} \varepsilon_1 - \varepsilon_1 &\leq \int_{t_0}^t u_{1d}^{2d_1+2}(\tau) d\tau \\ \frac{t-t_0}{\delta} \varepsilon_2 - \varepsilon_2 &\leq \int_{t_0}^t u_{1d}^{2d_2+2}(\tau) d\tau\end{aligned}$$

Therefore the solution (5.13) satisfies

$$\begin{aligned}|\bar{x}_1(t)| &\leq |\bar{x}_1(t_0)| \varphi_1 \exp(-\gamma_1(t-t_0)) + |G(t)|, \\ |\bar{x}_2(t)| &\leq |\bar{x}_2(t_0)| \varphi_2 \exp(-\gamma_2(t-t_0)),\end{aligned}$$

where we defined the coefficients $\gamma_1 = \frac{c_1 \varepsilon_1}{\delta}$, $\gamma_2 = \frac{c_2 \varepsilon_2}{\delta}$ and $\varphi_1 = \exp(-c_1 \varepsilon_1)$, $\varphi_2 = \exp(-c_2 \varepsilon_2)$. Similarly, using (5.10) in (5.14) gives

$$|G(t)| \leq \varphi_1 \varphi_2 |\bar{x}_2(t_0)| \exp(-(\gamma_1 t - \gamma_2 t_0)) \int_{t_0}^t \exp(-(\gamma_2 - \gamma_1)\sigma) d\sigma, \quad \forall t \geq t_0$$

We distinguish two cases; $\gamma_1 = \gamma_2$ and $\gamma_1 \neq \gamma_2$.

(I) In the case $\gamma_1 = \gamma_2$ the perturbation term $G(t)$ satisfies

$$|G(t)| \leq \varphi_1 \varphi_2 |\bar{x}_2(t_0)| (t-t_0) \exp(-\gamma_1(t-t_0)), \quad \forall t \geq t_0.$$

The term $(t-t_0) \exp(-\gamma_1(t-t_0))$ can be shown to be upper bounded, *i.e.*, for an arbitrarily chosen constant $0 < \gamma_3 < \gamma_1$ it holds that

$$(t-t_0) \exp(-\gamma_1(t-t_0)) \leq \frac{1}{\gamma_1 - \gamma_3} (\exp(-\gamma_3(t-t_0)) - \exp(-\gamma_1(t-t_0))), \quad \forall t \geq t_0.$$

This yields

$$\begin{aligned} |G(t)| &\leq \frac{\varphi_1 \varphi_2 |\bar{x}_2(t_0)|}{\gamma_1 - \gamma_3} (\exp(-\gamma_3(t-t_0)) - \exp(-\gamma_1(t-t_0))) \\ &\leq \frac{\varphi_1 \varphi_2 |\bar{x}_2(t_0)|}{\gamma_1 - \gamma_3} \exp(-\gamma_3(t-t_0)) \end{aligned}$$

The general solution $\bar{x} = (\bar{x}_1, \bar{x}_2)$ then satisfies the inequality

$$\begin{aligned} |\bar{x}_1(t)| &\leq \zeta_1 \exp(-\gamma_1(t-t_0)) + \zeta_2 \exp(-\gamma_3(t-t_0)), \\ |\bar{x}_2(t)| &\leq \zeta_3 \exp(-\gamma_1(t-t_0)), \end{aligned}$$

where we defined

$$\zeta_1 = \varphi_1 |\bar{x}_1(t_0)|, \quad \zeta_2 = \varphi_1 \varphi_2 \frac{|\bar{x}_2(t_0)|}{\gamma_1 - \gamma_3}, \quad \zeta_3 = \varphi_2 |\bar{x}_2(t_0)|.$$

The equilibrium $x = 0$ is thus globally uniformly exponentially stable (GUES), *i.e.*,

$$\|x(t)\| \leq k \|x(t_0)\| \exp(-\gamma_3(t-t_0)), \quad k = \left\| \begin{bmatrix} \varphi_1 & \frac{\varphi_1 \varphi_2}{\gamma_1 - \gamma_3} \\ 0 & \varphi_2 \end{bmatrix} \right\|.$$

(2) In the case $\gamma_1 \neq \gamma_2$ the perturbation term $G(t)$ satisfies

$$|G(t)| \leq \frac{\varphi_1 \varphi_2 |x_{32}(t_0)|}{\gamma_1 - \gamma_2} (\exp(-\gamma_2(t-t_0)) - \exp(-\gamma_1(t-t_0))).$$

The right-hand term can be shown to be upper bounded, *i.e.*,

$$\frac{1}{\gamma_1 - \gamma_2} (\exp(-\gamma_2(t-t_0)) - \exp(-\gamma_1(t-t_0))) \leq (t-t_0) \exp(-\min(\gamma_1, \gamma_2)(t-t_0)) \quad \forall t \geq t_0,$$

The perturbation term $G(t)$ then satisfies

$$|G(t)| \leq \varphi_1 \varphi_2 |\bar{x}_2(t_0)| \exp(-\bar{\gamma}(t-t_0))(t-t_0)$$

where $\gamma = \min(\gamma_1, \gamma_2)$. The term $(t-t_0) \exp(-\min(\gamma_1, \gamma_2)(t-t_0))$ can be upper bounded, *i.e.*, for an arbitrarily chosen $\gamma_3 < \gamma$, it holds that

$$(t-t_0) \exp(-\min(\gamma)(t-t_0)) \leq \frac{1}{\gamma - \gamma_3} (\exp(-\gamma_3(t-t_0)) - \exp(-\gamma(t-t_0))), \quad \forall t \geq t_0.$$

The perturbation term $G(t)$ then satisfies

$$\begin{aligned} |G(t)| &\leq \frac{\varphi_1 \varphi_2 |\bar{x}_2(t_0)|}{\gamma - \gamma_3} (\exp(-\gamma_3(t-t_0)) - \exp(-\gamma(t-t_0))) \\ &\leq \frac{\varphi_1 \varphi_2 |\bar{x}_2(t_0)|}{\gamma - \gamma_3} \exp(-\gamma_3(t-t_0)). \end{aligned}$$

The general solution $\bar{x} = (\bar{x}_1, \bar{x}_2)$ then satisfies the inequality

$$\begin{aligned} |\bar{x}_1(t)| &\leq \zeta_1 \exp(-\gamma_1(t-t_0)) + \zeta_2 \exp(-\gamma_3(t-t_0)), \\ |\bar{x}_2(t)| &\leq \zeta_3 \exp(-\gamma_2(t-t_0)), \end{aligned}$$

where we defined

$$\zeta_1 = \varphi_1 |\bar{x}_1(t_0)|, \quad \zeta_2 = \varphi_1 \varphi_2 \frac{|\bar{x}_2(t_0)|}{\gamma - \gamma_3}, \quad \zeta_3 = \varphi_2 |\bar{x}_2(t_0)|.$$

The equilibrium $x = 0$ is thus globally exponentially stable, *i.e.*,

$$\|x(t)\| \leq k \|x(t_0)\| \exp(-\gamma(t - t_0)), \quad k = \left\| \begin{bmatrix} \varphi_1 & \frac{\varphi_1 \varphi_2}{\gamma - \gamma_3} \\ 0 & \varphi_2 \end{bmatrix} \right\|$$

with $\gamma = \min\{\gamma_1, \gamma_2\}$, as defined before, and $\gamma_3 \leq \gamma$. Concluding, we have shown that the linear time-varying system is exponentially stable in both the cases $\gamma_1 = \gamma_2$ and $\gamma_1 \neq \gamma_2$. By defining $\gamma_3 = \gamma - \varepsilon$, it can be shown that all solutions of the system satisfy

$$\forall \varepsilon > 0, \quad \|x(t)\| \leq \bar{k} \|x(t_0)\| \exp(-(\gamma - \varepsilon)(t - t_0)), \quad \forall t \geq t_0,$$

with $\gamma = \min(\gamma_1, \gamma_2) = \min(\frac{c_1 \varepsilon_1}{\delta}, \frac{c_2 \varepsilon_2}{\delta})$ for a small number $\varepsilon > 0$ and k given by

$$k = \left\| \begin{bmatrix} \varphi_1 & \frac{\varphi_1 \varphi_2}{\varepsilon} \\ 0 & \varphi_2 \end{bmatrix} \right\| = \left\| \begin{bmatrix} \exp(-c_1 \varepsilon_1) & \frac{\exp(-c_1 \varepsilon_1 - c_2 \varepsilon_2)}{\varepsilon} \\ 0 & \exp(-c_2 \varepsilon_2) \end{bmatrix} \right\|$$

This concludes the proof. \square

Concluding, Proposition 5.1.2 states that the subsystem (5.12) is GUES. This result will be used in the following section to prove global uniform asymptotic stability of the complete closed-loop system.

5.2 Stability of the tracking-error dynamics

In this section we show that the complete tracking dynamics are globally exponentially stable. In the previous sections we have stabilized the (Δ_1, Δ_2) -subsystem when $u_1 = u_{1d}$ and the Δ_3 subsystem in (5.1). The influence of the term $\bar{x}_{21} u_{1d}$ was, however, not included. In this section Theorem 3.6.1 will be used to investigate the stability properties of the complete system. The result is stated in the following proposition.

Proposition 5.2.1. *Consider the system (5.1) and the controller u_1 given by*

$$u_1 = u_{1d} - k_1 x_{11} - k_2 x_{12}, \quad p(s) = s^2 + k_2 s + k_1 \text{ is Hurwitz}, \quad (5.15)$$

and the controller u_2 given by (5.7). Suppose that the reference input $u_{1d}(t)$ satisfies Assumption 5.1.1. If the reference trajectory $\xi_{2d}(t)$ and the derivative $\dot{u}_{1d}(t)$ in (2.12) are uniformly bounded in t , then the closed-loop system is globally \mathcal{K} -exponentially stable.

Proof. The closed-loop system ((5.1),(5.15),(5.7)), using (5.6) and (5.8), is given by

$$\begin{aligned} \dot{\bar{x}}_{31} &= -c_1 u_{1d}^{2d_1+2} \bar{x}_{31} &+ \bar{x}_{32} \\ \dot{\bar{x}}_{32} &= -c_2 u_{1d}^{2d_2+2} \bar{x}_{32} &+ \bar{x}_{21} u_{1d} - \xi_2(k_1 x_{11} + k_2 x_{12}) \\ \dot{\bar{x}}_{21} &= -c_3 \bar{x}_{21} &+ \bar{x}_{22} \\ \dot{\bar{x}}_{22} &= -c_4 \bar{x}_{22} \\ \dot{x}_{11} &= x_{12} \\ \dot{x}_{12} &= -k_1 x_{11} - k_2 x_{12} \end{aligned}$$

The closed-loop system can be written in the form (3.19) with

$$f_1(t, z_1) = A_1(t)z_1, \quad f_2(t, z_2) = A_2z_2, \quad (5.16)$$

where $z_1 = [\bar{x}_{31}, \bar{x}_{32}]^T$, $z_2 = [\bar{x}_{21}, \bar{x}_{22}, x_{11}, x_{12}]^T$ and the matrices $A_1(t), A_2$ are given by

$$A_1(t) = \begin{bmatrix} -c_1 u_{1d}^{2d_1+2}(t) & 1 \\ 0 & -c_2 u_{1d}^{2d_2+2}(t) \end{bmatrix}, \quad A_2 = \begin{bmatrix} -c_3 & 1 & 0 & 0 \\ 0 & -c_4 & 0 & 0 \\ 0 & 0 & 0 & 1 \\ 0 & 0 & -k_1 & -k_2 \end{bmatrix}.$$

The perturbation matrix $g(t, z_1, z_2)$ is given by

$$g(t, z_1, z_2) = -(x_{21} + \xi_{2d}) \begin{bmatrix} 0 & 0 & 0 & 0 \\ 0 & 0 & k_1 & k_2 \end{bmatrix} + \begin{bmatrix} 0 & 0 & 0 & 0 \\ u_{1d}(t) & 0 & 0 & 0 \end{bmatrix} \quad (5.17)$$

In order to apply Theorem 3.6.1 and Lemma 3.6.2 we verify the three assumptions.

- (1) Due to Assumption 5.1.1 and Proposition 5.1.2 the Σ_1 subsystem (5.9) is globally exponentially stable (GES). By converse Lyapunov theory, *i.e.*, Theorem 3.3.2 in Section 3.3, the existence of a suitable Lyapunov function $V(t, z_1)$ is guaranteed when the matrix $A_1(t)$ is uniformly bounded in t . Since $r = \infty$ and the system is globally exponentially stable, the Lyapunov function $V(t, z_1)$ is defined on $\mathbb{R}_+ \times \mathbb{R}^n$ and not only on $\mathbb{R}_+ \times D_0$ with $D_0 \subset \mathbb{R}^n$ a compact subset of the state-space. By assumption the reference input u_{1d} is uniformly bounded and therefore also the matrix $A_1(t)$, which gives the desired result.
- (2) By assumption the signals u_{1d}, \dot{u}_{1d} and ξ_{2d} are bounded, *i.e.*, $|u_{1d}(t)| \leq M_1$, $|\dot{u}_{1d}(t)| \leq M_2$, and $|\xi_{2d}(t)| \leq M_3 \forall t \geq 0$. Therefore we have

$$\|g(t, z_1, z_2)\| \leq \|k\| (|x_{21}| + |\xi_{2d}(t)|) + |u_{1d}(t)| \leq \|k\| (|x_{21}| + M_3) + M_1.$$

where $k = [k_1, k_2]$. Furthermore, using the states $\bar{x}_{21} = x_{21} - \alpha_2(u_{1d}, x_{31}, x_{32})$, $\bar{x}_{31} = x_{31}$ and $\bar{x}_{32} = x_{32} + c_1 u_{1d}^{2d_1+2} x_{31}$ from the backstepping procedure in sections 5.1.1 yields

$$|x_{21}| = \left| \bar{x}_{21} - \left(c_1^2 u_{1d}^{4d_1+3} - c_1(2d_1+2)u_{1d}^{2d_1}\dot{u}_{1d} \right) \bar{x}_{31} - \left(c_1 u_{1d}^{2d_1+1} + c_2 u_{1d}^{2d_2+1} \right) \bar{x}_{32} \right|$$

Using the boundedness of $u_{1d}(t)$ and $\dot{u}_{1d}(t)$ yields the inequality

$$\begin{aligned} |x_{21}| &\leq |\bar{x}_{21}| + \left(c_1^2 M_1^{4d_1+3} + c_1(2d_1+2)M_1^{2d_1}M_2 \right) |\bar{x}_{31}| + \left(c_1 M_1^{2d_1+1} + c_2 M_1^{2d_2+1} \right) |\bar{x}_{32}| \\ &\leq \|z_2\| + \left(c_1^2 M_1^{4d_1+3} + c_1(2d_1+2)M_1^{2d_1}M_2 + c_1 M_1^{2d_1+1} + c_2 M_1^{2d_2+1} \right) \|z_1\| \end{aligned}$$

Introducing the continuous function $\kappa_1(\|z_2\|) = \|k\| (\|z_2\| + M_3) + M_1$ and the parameter κ_2 given by

$$\kappa_2 = \|k\| \left(1 + c_1^2 M_1^{4d_1+3} + c_1(2d_1+2)M_1^{2d_1}M_{1d} + c_1 M_1^{2d_1+1} + c_2 M_1^{2d_2+1} \right)$$

this finally gives the desired result

$$\|g(t, z_1, z_2)\| \leq \kappa_1(\|z_2\|) + \kappa_2\|z_1\|,$$

- (3) The characteristic polynomial of the Σ_2 subsystem is given by $\chi(s) = (s + c_1)(s + c_2)p(s)$ where $p(s)$ is given in (5.15). Because the polynomial $p(s)$ is Hurwitz and the c_i 's are positive, the Σ_2 subsystem is GES. The existence of a class \mathcal{K} function $\zeta(\cdot)$ satisfying condition (3.23) follows directly from the GES of the Σ_2 subsystem.

By Theorem 3.6.1 and Lemma 3.6.2 we conclude \mathcal{K} -exponentially stability of the complete closed loop system. \square

Summarizing, we have exponentially stabilized the (Δ_1, Δ_2) and Δ_3 subsystems separately. We then concluded by Theorem 3.6.1 and Lemma 3.6.2 that the combined system is \mathcal{K} -exponentially stable when the reference input u_{1d} satisfies Assumption 5.1.1 and its derivative \dot{u}_{1d} is uniformly bounded over t .

5.3 Robustness considerations

In this section we investigate the robustness properties of the closed-loop system. In the previous section, we saw that the closed-loop system can be written in cascade form (3.19) with a Σ_1 subsystem $\dot{z}_1 = A_1(t)z_1$ and a Σ_2 subsystem $\dot{x}_2 = A_2z_2$. It was also shown that these closed-loop subsystems Σ_1 and Σ_2 are uniformly exponentially stable. Uniform exponential stability is a desirable property, because it implies exponential stability with respect to bounded vanishing perturbations and uniformly bounded solutions with respect to bounded non-vanishing perturbations.

In this section we will determine (conservative) bounds on the perturbation, for which the closed-loop systems Σ_1 and Σ_2 are robust in some sense. This generally means that one has to find a Lyapunov function for the system. Because the Σ_1 subsystem is time-varying and depends on the reference input $u_{1d}(t)$ and the to be defined parameters d_i , $i = 1, 2$, finding a Lyapunov function is quite difficult. However, by using Proposition 5.1.2 in conjunction with the converse theorem Theorem 3.4.1, we can find these bounds without explicitly calculating the Lyapunov function.

Consider the closed-loop subsystem Σ_1 , $\dot{z}_1 = A_1(t)z_1$, given by

$$\begin{aligned}\dot{\bar{x}}_{31} &= -c_1 u_{1,d}(t)^{2d_1+2} \bar{x}_{31} + \bar{x}_{32} \\ \dot{\bar{x}}_{32} &= -c_2 u_{1,d}(t)^{2d_2+2} \bar{x}_{32}\end{aligned}\quad (5.18)$$

By Proposition 5.1.2, the $(\bar{x}_{31}, \bar{x}_{32})$ subsystem is exponentially stable, *i.e.*, with $z_1(t) = [\bar{x}_{31}, \bar{x}_{32}]^T$ it holds that

$$\|z_1(t)\| \leq \|D\| \|z_1(t_0)\| \exp(-\lambda(t - t_0)),$$

where $\lambda = \min(\gamma_1, \gamma_2) - \varepsilon_1$ and the matrix D is given by

$$D = \begin{bmatrix} \varphi_1 & \frac{\varphi_1 \varphi_2}{\varepsilon} \\ 0 & \varphi_2 \end{bmatrix}$$

with ε a small parameter. Therefore, see Remark 3.4.1, a Lyapunov function for the Σ_1 subsystem is given by (3.11), *i.e.*, $V_1(t, z_1) = z_1^T P(t) z_1$ with

$$P(t) = \int_t^\infty \phi^T(\tau, t) \phi(\tau, t) d\tau \quad (5.19)$$

Along solutions of the Σ_1 subsystem the Lyapunov function $V_1(t, z_1)$ satisfies

$$(i) \quad \frac{1}{2L} \|z_1\|^2 \leq V_1(t, z_1) \leq \frac{\|D\|^2}{2\lambda} \|z_1\|^2, \quad (ii) \quad \dot{V}_1(t, z_1) \leq -\|z_1\|^2, \quad (iii) \quad \frac{\partial V_1(t, z_1)}{\partial z_1} \leq \frac{\|D\|^2}{\lambda} \|z_1\|$$

where $\|A_1(t)\| \leq L$, *i.e.*, the parameter L is an upper-bound for the norm of the time-varying matrix $A_1(t)$ that depends on the reference input $u_{1d}(t)$. The closed-loop (Σ_2) subsystem is given by

$$\dot{z}_2 = \begin{bmatrix} -c_3 & 1 & 0 & 0 \\ 0 & -c_4 & 0 & 0 \\ 0 & 0 & 0 & 1 \\ 0 & 0 & -k_1 & -k_2 \end{bmatrix} z_2. \quad (5.20)$$

By solving (3.10) for $Q(t) = I$ and $\dot{P}(t) = 0$ we obtain the time-invariant Lyapunov function $V_2(z_2) = z_2^T P z_2$ with

$$P = 1/2 \begin{bmatrix} \frac{1}{c_3} & \frac{1}{c_3(c_4 + c_3)} & 0 & 0 \\ \frac{1}{c_3(c_4 + c_3)} & \frac{c_3(c_4 + c_3) + 1}{c_3 c_4 (c_4 + c_3)} & 0 & 0 \\ 0 & 0 & \frac{k_2^2 + k_1^2 + k_1}{k_1 k_2} & \frac{1}{k_1} \\ 0 & 0 & \frac{1}{k_1} & \frac{k_1 + 1}{k_1 k_2} \end{bmatrix}.$$

The time-invariant Lyapunov function $V_2(z_2)$ satisfies

$$(i) \quad \lambda_{\min}(P) \|z_2\|^2 \leq V_2(z_2) \leq \lambda_{\max}(P) \|z_2\|^2 \\ (ii) \quad \dot{V}_2(z_2) \leq -\|z_2\|^2 \\ (iii) \quad \frac{\partial V_2(z_2)}{\partial z_2} \leq 2\lambda_{\max}(P) \|z_2\| \quad (5.21)$$

where $\lambda_{\min}(\cdot)$ and $\lambda_{\max}(\cdot)$ denote the smallest and largest eigenvalue, respectively. Now define $z = [z_1, z_2]$ and consider the Lyapunov function $V(t, z) = V_1(t, z_1) + V_2(z_2)$. Then the Lyapunov function $V(t, z)$ satisfies

$$(i) \quad \min\left(\frac{1}{2L}, \lambda_{\min}(P)\right) \|z\|^2 \leq V(t, z) \leq \max\left(\frac{\|D\|^2}{2\lambda}, \lambda_{\max}(P)\right) \|z\|^2 \\ (ii) \quad \dot{V}(t, z) \leq -\|z\|^2 \\ (iii) \quad \frac{\partial V(t, z)}{\partial z} \leq \max\left(\frac{\|D\|^2}{\lambda}, 2\lambda_{\max}(P)\right) \|z\| \quad (5.22)$$

By Theorem 3.5.1 we conclude that the closed-loop system (Σ_1, Σ_2) is robust with respect to vanishing perturbations, *i.e.*, $\delta(t, z) = 0$ for $z = 0$, satisfying

$$\|\delta(t, z)\| < \frac{1}{\max\left(\frac{\|D\|^2}{\lambda}, 2\lambda_{\max}(P)\right)}, \quad \forall z \in \mathbb{R}^n \quad (5.23)$$

By Theorem 3.5.2 we conclude that solutions of the system are globally ultimately bounded for non-vanishing perturbations, *i.e.*, $\delta(t, z) \neq 0$ for $z = 0$, satisfying

$$\|\delta(t, z)\| < \frac{1}{\max\left(\frac{\|D\|^2}{\lambda}, 2\lambda_{\max}(P)\right)} \sqrt{\frac{\min\left(\frac{1}{2L}, \lambda_{\min}(P)\right)}{\max\left(\frac{\|D\|^2}{2\lambda}, \lambda_{\max}(P)\right)}} \theta r, \quad \forall \|z\| < r, z \in \mathbb{R}^n. \quad (5.24)$$

5.4 Summary

In this section we have presented a linear time-varying controller for trajectory tracking of the second-order chained form system. The controller was designed by using a cascaded backstepping technique in which the tracking error dynamics are treated as two separate subsystems. Using a result for nonlinear cascade system in (Lefeber et al., 2000), exponential stability of the two separate subsystems implies \mathcal{K} -exponential stability of the complete system. The linear time-varying controller stabilizes the system to a desired reference trajectory with exponential convergence if the reference trajectory satisfies a so-called persistence of excitation condition. This persistence of excitation condition implies that the reference trajectory is not allowed to converge to a point. The tracking controllers may be used to steer the system towards a certain equilibrium point, however, no stability can be guaranteed. This means that tracking controllers can not be used to solve the stabilization problem, as in the case of linear systems. Instead, the stabilization problem has to be treated differently. Additionally, conditions were given under which the closed-loop system is robust with respect to perturbations. These conditions are given as uniform bounds on the perturbations. These perturbations can be caused by parameter uncertainties, disturbances or unmodelled dynamics. A generalization of the proposed control design method to the case of high-order chained form systems (2.6) can be found in Appendix B.

The proposed design approach can be used to explicitly design a tracking controller as a function of the reference input $u_{1d}(t)$. This tracking controller globally \mathcal{K} -exponentially stabilizes the closed-loop system to a reference trajectory, whereas the tracking controller presented in (Walsh et al., 1994) only achieves local asymptotic stability of the error-dynamics. In contrast to the tracking controller of (Walsh et al., 1994), the tracking controller presented in this thesis is given in closed form and does not have to be re-computed when the reference trajectory changes.

The discontinuous and flatness-based tracking controller from (Kobayashi, 1999) can be used to stabilize the system to trajectories that do not pass through points where $u_1(t) = 0$. In these singular points the system is not controllable and these singular points coincide with the singular points of the endogenous transformation induced by the flat outputs, see Section 4.4. Moreover, the closed-loop error dynamics are not stable in a Lyapunov sense and only converge exponentially towards the trajectory to be stabilized. The tracking controller presented in this thesis can be used to stabilize the system to reference trajectories passing through these singular points and, in addition, achieves Lyapunov stability of the closed-loop error dynamics. The stabilization problem will be treated in the following chapter.

Point stabilization

In this section we consider the feedback stabilization problem for the second-order chained form system. It is well-known that the second-order chained form system can not be stabilized by any continuous time-varying feedback. From Theorem 3.2.2 it is known that an equilibrium of a continuously differentiable system is only exponentially stable if and only if its linearization around the equilibrium point is also an exponentially stable system. This implies that an unstable system can only be exponentially stabilized by smooth feedback when its linearization around the equilibrium is stabilizable. Since the linearization of the second-order chained form system around any equilibrium is not controllable, we conclude that it cannot be exponentially stabilized by any smooth time-varying feedback. The best we can hope for is a weaker notion of exponential stability, called ρ -exponential stability.

In order to stabilize the system, discontinuous controllers or time-varying controllers are needed. In references (Astolfi, 1996; Imura et al., 1996), discontinuous controllers that achieve exponential convergence towards the origin, as defined in Definition 3.2.4, were developed. However, these discontinuous controllers are no feedback stabilizers in the sense that they only guarantee exponential convergence on an open and dense set of the state-space. In (Laiou and Astolfi, 1999) this result was extended to obtain a weakened Lyapunov stability result called quasi-smooth exponential stability. Moreover, due to Brockett's condition, the system can not be stabilized by any continuous time-invariant feedback.

In (M'Closkey and Morin, 1998) a homogeneous time-varying feedback was designed that ρ -exponentially stabilized the system of a planar body, with two thrusters, sliding on a flat surface. The planar body with two thrusters is equivalent to the second-order chained form system after a suitable coordinate and feedback transformation. The continuous periodic time-varying feedback was designed in three steps. In the first step, one derived a homogeneous approximation of the system. In the second step, a continuous homogeneous controller is derived that asymptotically stabilizes a four-dimensional subsystem of the homogeneous approximation. In the third and last step, the continuous asymptotic stabilizer is scaled to an exponential stabilizer and a backstepping or high gain feedback approach is applied to stabilize the complete system.

In this section we consider the feedback stabilization problem by continuous periodic time-varying feedback. We try to derive continuous periodic time-varying feedbacks that \mathcal{K} -exponentially stabilize the second-order chained form (2.7). The idea is to use a homogeneous feedback, to stabilize a subsystem of the second-order chained form, and use a backstepping or high gain approach to stabilize the complete system. This approach has been presented in (Aneke et al., 2002a,b) and follows that of (Morin and Samson, 1997).

6.1 Homogeneous feedback stabilization

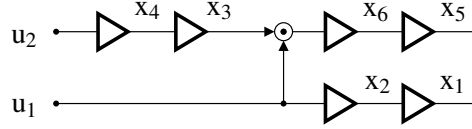


Figure 6.1: The second-order chained form system (SCF) in strict-feedback form

Consider the three-dimensional, *i.e.*, 6-state, second-order chained form system

$$\begin{aligned}\ddot{\xi}_1 &= u_1 \\ \ddot{\xi}_2 &= u_2 \\ \ddot{\xi}_3 &= \xi_2 u_1.\end{aligned}\tag{6.1}$$

The dynamics in state-space form are given by:

$$\begin{aligned}\dot{x}_1 &= x_2 & \dot{x}_2 &= u_1 \\ \dot{x}_3 &= x_4 & \dot{x}_4 &= u_2 \\ \dot{x}_5 &= x_6 & \dot{x}_6 &= x_3 u_1,\end{aligned}\tag{6.2}$$

with state-vector $x = [x_1, x_2, \dots, x_6]^T$ given by $x_i = \xi_i$, $x_{i+1} = \dot{\xi}_i$, $i = 1, 3, 5$. The system does not satisfy Brockett's condition (Brockett, 1983) as the image of the mapping $(x, u) \mapsto (x_2, x_4, x_6, u_1, u_2, x_3 u_1)$ does not contain any point $(0, 0, 0, 0, 0, \varepsilon)$ for $\varepsilon \neq 0$. Therefore no continuous time-invariant state feedback exists that asymptotically stabilizes the system to the origin.

Consider the equilibrium $x = 0$ of (6.2). The dynamics of the (x_5, x_6, x_3, x_4) -part are in strict feedback form as illustrated in Figure 6.1. Therefore we can apply a backstepping approach, using the input u_2 , in order to stabilize the dynamics of (x_5, x_6, x_3, x_4) .

The idea of using a combined homogeneous and backstepping approach has already been proposed in (Morin and Samson, 1997). In the following sections this result will be extended to the case of the second-order chained form system. First we rewrite the system into

$$\Delta_1 \begin{cases} \dot{x}_5 = x_6 \\ \dot{x}_6 = x_3 u_1 \\ \dot{x}_1 = x_2 \\ \dot{x}_2 = u_1 \end{cases} \quad \Delta_2 \begin{cases} \dot{x}_3 = x_4 \\ \dot{x}_4 = u_2. \end{cases}\tag{6.3}$$

In the first part of the approach we consider the state x_3 as a “virtual input” and use it, along with the input u_1 to stabilize the origin of the Δ_1 subsystem. The second part of the approach consists of using a backstepping technique to stabilize the origin of the complete system (Δ_1, Δ_2) . This approach is described in the following two sections.

6.1.1 Stabilizing the Δ_1 subsystem

The subsystem Δ_1 with $v = x_3$ as a virtual input is given by

$$\Delta_1 \begin{cases} \dot{x}_5 &= x_6 \\ \dot{x}_6 &= vu_1 \\ \dot{x}_1 &= x_2 \\ \dot{x}_2 &= u_1 \end{cases} \quad (6.4)$$

Notice that the vector field $x \mapsto f(x, (u_1, v))$, which defines the Δ_1 subsystem, is not affine in the control variables (u_1, v) . Nevertheless, if we define a dilation $\bar{\delta}_\lambda^r$ with weight $r = (2, 2, 1, 1)$ and apply feedback functions $u_1 = \alpha_1(t, x)$ and $v = \alpha_2(t, x)$, with $(\alpha_1, \alpha_2) \in C^0(\mathbb{R} \times \mathbb{R}^4; \mathbb{R}^1)$ r -homogeneous of degree one, then the closed-loop vector field $(t, x) \mapsto f(x, \alpha_1(t, x), \alpha_2(t, x))$ becomes r -homogeneous of degree zero.

Define $x^1 = (x_1, x_2, x_5, x_6)$. Consider the feedback laws $(u_1, v) \in C^0(\mathbb{R} \times \mathbb{R}^4; \mathbb{R}^1)$ given by

$$\begin{aligned} u_1 &= -k_1x_1 - k_2x_2 + h(x^1)g(t/\varepsilon) \\ v &= -\frac{k_5x_5 + k_6x_6}{\sigma h(x^1)}g(t/\varepsilon) \end{aligned} \quad (6.5)$$

with $k_i > 0$, $i \in \{1, 2, 5, 6\}$ and $g : \mathbb{R} \rightarrow \mathbb{R}$ a T -periodic function satisfying $\int_0^T g(\tau) d\tau = 0$ and $\sigma = \frac{1}{T} \int_0^T g^2(\tau) d\tau > 0$. The continuous function $h : \mathbb{R}^4 \rightarrow \mathbb{R}$ is positive-definite and homogeneous of degree one with respect to $\bar{\delta}_\lambda^r$. As any homogeneous norm associated with a dilation is homogeneous of degree one with respect to that dilation, an example of such a function is given by $h(x^1) = \bar{\rho}(x)$, where $\bar{\rho}(x)$ denoted the homogeneous norm associated with the dilation $\bar{\delta}_\lambda^r$ given by

$$\bar{\delta}_\lambda^r(x^1) = (\lambda^2x_5, \lambda^2x_6, \lambda x_1, \lambda x_2). \quad (6.6)$$

Proposition 6.1.1. *Consider the closed-loop system (6.4,6.5) with $g : \mathbb{R} \rightarrow \mathbb{R}$ a continuous T -periodic function satisfying $\int_0^T g(\tau) d\tau = 0$ and $\sigma = \frac{1}{T} \int_0^T g^2(\tau) d\tau > 0$. Assume that the continuous function $h : \mathbb{R}^n \rightarrow \mathbb{R}$ is homogeneous of degree one with respect to the dilation $\bar{\delta}_\lambda^r(x^1, t)$. Then there exists $\varepsilon_0 > 0$ such that, for all $\varepsilon \in (0, \varepsilon_0)$, the origin of the closed-loop system (6.4,6.5) is $\bar{\rho}$ -exponentially stable.*

Proof. The closed-loop system is given by

$$\begin{aligned} \dot{x}_5 &= x_6 \\ \dot{x}_6 &= -\frac{(k_5x_5 + k_6x_6)}{\sigma h(x^1)} \left(-(k_1x_1 + k_2x_2)g(t/\varepsilon) + h(x^1)g(t/\varepsilon)^2 \right) \\ \dot{x}_1 &= x_2 \\ \dot{x}_2 &= -k_1x_1 - k_2x_2 + h(x^1)g(t/\varepsilon) \end{aligned}$$

This system is homogeneous of order zero with respect to the dilation $\bar{\delta}_\lambda^r$ and can be written as $\dot{x} = f(x, t)$ where $f(x, t)$ is T -periodic in t . By assumption $h(x^1)$ is homogeneous of degree one with respect to $\bar{\delta}_\lambda^r$. Therefore the closed-loop system is homogeneous of degree zero with respect to $\bar{\delta}_\lambda^r$. The ‘‘averaged system’’, see (3.33), is given by

$$\begin{aligned} \dot{x}_5 &= x_6 \\ \dot{x}_6 &= -k_5x_5 - k_6x_6 \\ \dot{x}_1 &= x_2 \\ \dot{x}_2 &= -k_1x_1 - k_2x_2 \end{aligned} \quad (6.7)$$

which is globally exponentially stable. The conclusion follows by application of Proposition 3.7.2. \square

Remark 6.1.1. The input $v(t, x^1)$ in (6.5) is not defined for $x^1 = 0$, i.e., $h(x^1) = 0$. However, any function $g(t, x)$ that is homogeneous of degree $\tau > 0$ with respect to a dilation $\bar{\delta}_\lambda^r(x)$ and continuous for all $x \neq 0$, can be extended by continuity to be continuous at $x = 0$. Therefore $v(t, x^1)$ becomes continuous and bounded at $x^1 = 0$ by defining $v(t, x^1) = \lim_{x^1 \rightarrow 0} v(t, x^1) = 0$ for $x^1 = 0$.

6.1.2 Stabilizing the (Δ_1, Δ_2) subsystem

We now consider the Δ_2 subsystem. In the previous section we designed a feedback $u_1 = \alpha_1(t, x)$ and a virtual feedback $v = \alpha_2(t, x)$ that exponentially stabilized the Δ_1 subsystem w.r.t. the dilation $\bar{\delta}_\lambda^r(x)$. The input u_2 can be obtained by using the backstepping approach given in Proposition 3.7.3.

By Proposition 6.1.1 the Δ_1 subsystem is asymptotically stabilized by $x_3 := v(t, x^1)$, with v given by (6.5). The (Δ_1, Δ_2) system can be written as

$$\begin{aligned}\dot{x}^1 &= f(t, x^1, x_3) \\ \dot{x}_3 &= x_4 \\ \dot{x}_4 &= u_2.\end{aligned}$$

By recursive application of Proposition 3.7.3, see Remark 3.7.1, we conclude that the equilibrium point $x = 0$ can be asymptotically stabilized by the feedback $u_2 = -k_4(x_4 + k_3(x_3 - v(t, x^1)))$. By substitution of (6.5) we obtain the continuous periodic time-varying feedback

$$u_2 = -k_4(x_4 + k_3(x_3 + \frac{(k_5x_5 + k_6x_6)}{\sigma h(x^1)}g(t/\varepsilon))),$$

with $k_i > 0$, $i \in 1, 2, \dots, 6$. By rewriting the last equation, we conclude that the continuous periodic time-varying feedbacks that ρ -exponentially stabilize the system are given by

$$\begin{aligned}u_1 &= -k_1x_1 - k_2x_2 + h(x^1)g(t/\varepsilon) \\ u_2 &= -k_3k_4x_3 - k_4x_4 - k_3k_4\frac{(k_5x_5 + k_6x_6)}{\sigma h(x^1)}g(t/\varepsilon),\end{aligned}\tag{6.8}$$

The stability result is formulated in the following corollary.

Corollary 6.1.2. Consider the closed-loop system (6.2, 6.8) where $g: \mathbb{R} \rightarrow \mathbb{R}$ a continuous T -periodic function satisfying $\int_0^T g(\tau) d\tau = 0$ and $\sigma = \frac{1}{T} \int_0^T g^2(\tau) d\tau > 0$ and the continuous function $h: \mathbb{R}^n \rightarrow \mathbb{R}$ is homogeneous of degree one with respect to the dilation $\bar{\delta}_\lambda^r(x^1, t)$ given by (6.6). Then there exists $\varepsilon_0 > 0$ such that, for all $\varepsilon \in (0, \varepsilon_0)$, the origin $x = 0$ is globally exponentially stable with respect to the dilation δ_λ^r given by

$$\delta_\lambda^r(x) = (\lambda x_1, \lambda x_2, \lambda x_3, \lambda x_4, \lambda^2 x_5, \lambda^2 x_6).\tag{6.9}$$

Proof. The weight vector is $r = (1, 1, 1, 1, 2, 2)$. The vector field $f(x) = (x_2, 0, x_4, 0, x_6, 0)^T$ and the input vector fields $g_1(x) = (0, 1, 0, 0, 0, x_3)^T$ and $g_2(x) = (0, 0, 0, 1, 0, 0)^T$ of (6.2) are of degree 0, -1 and -1 respectively with respect to the dilation δ_λ^r . The control laws u_1 and u_2 given in (6.8) are of degree one with respect to $\delta_\lambda^r(x)$. The closed-loop system is therefore of degree zero with respect to δ_λ^r . By application of Proposition 3.7.1 we conclude that the origin of the closed-loop system is globally ρ -exponentially stable with respect to the dilation $\delta_\lambda^r(x^1)$. \square

6.2 Robust stabilizers for the second-order chained form

In (Lizárraga et al., 1999) it was shown that continuous homogeneous ρ -exponential stabilizers are not robust with respect to modelling errors. In this section a hybrid/open-loop feedback controller will be developed that not only exponentially stabilizes the system in a discrete sense, but is also robust with respect to a class of additive perturbations that represent modelling errors. In the previous section we derived homogeneous feedbacks that ρ -exponentially stabilize the second-order chained form. In this section we will present a modification of the controllers (6.8) that is robust with respect to certain modelling errors. By periodically updating the states in (6.8) the closed-loop system can be given certain robustness properties. We start with a problem formulation in which we define the problem of designing a periodically updated homogeneous feedbacks of the form (6.8) that is robust with respect to a certain class of perturbations for the system (6.1). Then, we design the periodically updated homogeneous feedbacks. Finally a stability and robustness analysis is performed in order to show that the designed feedback laws solve the problem. The presented results will appear in (Lizárraga et al., 2003).

6.2.1 Preliminaries and definition of the problem

Prior to stating the problem, we start by defining the notions of stability and robustness used in this context. Although the results presented here only apply to the second-order chained form, it is convenient to define these notions in terms of the more general class of analytic control-affine systems. To this end, consider the second-order chained form (6.1), regarded as the *nominal system*, written as

$$\dot{x} = b_0(x) + u_1 b_1(x) + u_2 b_2(x), \quad (6.10)$$

with

$$b_0(x) = [x_2, 0, x_4, 0, x_6, 0]^T, \quad b_1(x) = [0, 1, 0, 0, 0, x_3]^T, \quad b_2(x) = [0, 0, 0, 1, 0, 0]^T \quad (6.11)$$

As a result of model errors, such as parameter uncertainties, disturbance vector fields may be present in the system, and one way to model this is by considering the *perturbed system* given by

$$\dot{x} = b_0(x) + h_0(x, \varepsilon) + \sum_{i=1}^2 u_i (b_i(x) + h_i(x, \varepsilon)), \quad (6.12)$$

where $h = (h_0, h_1, h_2)$ is a 3-tuple of real-analytic mappings $h_i : U \times E \rightarrow \mathbb{R}^n$, and $E \subset \mathbb{R}$ is an interval containing 0. The 3-tuple h , referred to in the sequel as a disturbance, is assumed to satisfy $h_0(0, \varepsilon) = 0$ for every $\varepsilon \in E$, so that $(x, u) = (0, 0)$ is an equilibrium point for the perturbed system. In other words, the perturbation or disturbance $h_0(x, \varepsilon)$ is a vanishing perturbation. The interpretation of ε is that of an additional parameter that represents the magnitude of the perturbation (*cf.* also Remark 6.2.2(i) after Proposition 6.2.1). For ease of reference we denote by \mathcal{D}^3 the set of all disturbances $\mathbf{h} = (h_0, h_1, h_2)$, each defined on a set $U \times E$ (E may thus depend on the choice of \mathbf{h}). In the sequel we also write $h_i^\varepsilon(x) = h_i(x, \varepsilon)$.

It is clear that not all disturbances can be modelled by additive vector fields as in (6.12). In fact, phenomena such as neglected modes, non-smooth effects (e.g. friction) or measurement noise would require different representations. Therefore, the notion of robustness one can aim at by considering such disturbances is limited.

Suppose that a continuous, time-varying (T -periodic) feedback law $\alpha : U \times \mathbb{R} \rightarrow \mathbb{R}^2$ is given. As mentioned earlier, we intend to control the perturbed system (6.12) by periodically iterating this

control law. When the initial time $t_0 \in \mathbb{R}$ is a multiple of the update period T (i.e. $t_0 \bmod T = 0$) this process is accurately described by considering that one applies the iterated control $u(t) = \alpha(x(kT), t)$, where $t \in [kT, (k+1)T)$ and $k \in \{\lfloor t_0/T \rfloor, \lfloor t_0/T \rfloor + 1, \dots\}$. When $t_0 \bmod T \neq 0$, however, causality becomes an issue and a technical subtlety concerning the initial conditions arises, namely the initial value $x(\lfloor t_0/T \rfloor)$ is not defined in advance (see Figure 6.2). This can be remedied by adjoining a signal $t \mapsto y(t)$, which coincides with the state $x(kT)$ at the update instants indexed by $k \in \{\lfloor t_0/T \rfloor + 1, \lfloor t_0/T \rfloor + 2, \dots\}$, and then considering the dynamically extended perturbed system

$$\begin{cases} \dot{x} &= b_0(x) + h_0(x, \varepsilon) + \sum_{i=1}^2 \alpha_i(y, t)(b_i(x) + h_i(x, \varepsilon)) \\ \dot{y} &= \sum_{k=\lfloor t_0/T \rfloor + 1}^{\infty} \delta(t - kT)x(kT), \end{cases} \quad (6.13)$$

under the assumption that its initial condition be defined, given any $(x_0, y_0) \in \mathbb{R}^6 \times \mathbb{R}^6$, by setting $(x(t_0), y(t_0))$ equal to (x_0, x_0) if $t \bmod T = 0$, or equal to (x_0, y_0) otherwise.

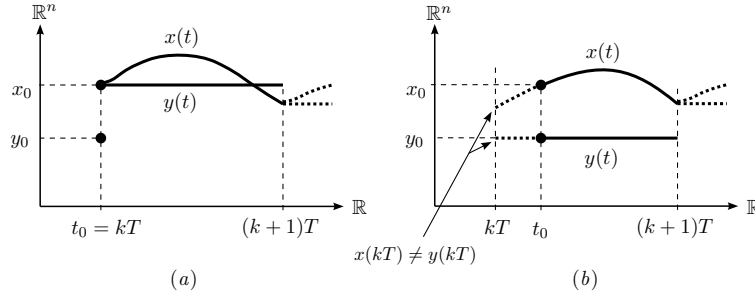


Figure 6.2: Initial conditions for system (6.13). (a) If $t_0 \bmod T = 0$, both $x(\cdot)$ and $y(\cdot)$ are initialized to x_0 . (b) If $t_0 \bmod T \neq 0$, $x(\cdot)$ and $y(\cdot)$ are initialized to x_0 and y_0 , respectively. Note that in the latter case the solutions are in general *not reversible in time*, since extending $x(t)$ and $y(t)$ for $t \in [kT, t_0)$, using the dynamics (6.13), may lead to the condition $x(kT) \neq y(kT)$.

Remark 6.2.1. (i) The meaning of the initial conditions for system (6.13) is illustrated in Figure 6.2. Clearly, the first sample instant after the initial time t_0 occurs at $t = (\lfloor t_0/T \rfloor + 1)T$ or, using the notation in the figure, at $t = (k+1)T$. This explains the initial value for k in the second summation of (6.13). Note also that the trajectories initialized in this way are defined for forward time ($t \geq t_0$), but they may fail to be reversible in time. In other words, when $t_0 \bmod T \neq 0$, the solution $(x(\cdot), y(\cdot))$ may be extended to the interval $[kT, t_0)$ by using the dynamics (6.13), however $x(kT)$ may differ from $y(kT)$. (ii) Up to minor differences in notation, the formulation of the perturbed system as a dynamical extension of the nominal one coincides with the formulation proposed in (Morin and Samson, 1999).

Let us point out that exponential stability of the origin for (6.13) does not imply exponential stability of the origin for $\dot{x} = b_0(x) + h_0^\varepsilon(x) + \sum_{i=1}^2 \alpha(x(kT), t)(b_i(x) + h_i^\varepsilon(x))$. For instance, a solution to the latter system, initialized to $x(t_0) = 0$ when t_0 is not an integer multiple of T , need not be identically zero, so it may fail to satisfy the required inequality

$$\|x(t)\| \leq K \|x(t_0)\| \exp(-\gamma(t - t_0))$$

The problem of robust stabilization may now be formulated as follows.

Problem 6.2.1. (Robust stabilization) Design a control law $\alpha : U \times \mathbb{R} \rightarrow \mathbb{R}^2$ which ensures that, for every disturbance h in a given set $\mathcal{A} \subset \mathcal{D}^3$, there is a constant $\varepsilon_0 > 0$ such that the origin $(x, y) = (0, 0)$ of system (6.13) is locally exponentially stable whenever $\varepsilon \in E$ and $|\varepsilon| \leq \varepsilon_0$.

6.2.2 Design of the periodically updated feedback law

Fix $T > 0$ and set $\omega = 2\pi/T$. Our goal is to design a feedback law $\alpha \in C^0(\mathbb{R}^6 \times \mathbb{R}; \mathbb{R}^2)$, T -periodic in its second argument, such that the solution $x(\cdot)$ to the controlled second-order chained form (SCF)

$$\dot{x} = b_0(x) + \sum_{i=1}^2 \alpha_i(x_0, t) b_i(x), \quad x(0) = x_0 \in \mathbb{R}^6, \quad (6.14)$$

with b_0, b_1, b_2 given in (6.11), satisfies

$$x(T) = Ax_0 + o(\|x_0\|), \quad (6.15)$$

where $A \in \mathbb{R}^{6 \times 6}$ a discrete-time-stable matrix, i.e., a matrix with its spectrum contained in $\{z \in \mathbb{C} : |z| < 1\}$. Motivated by the results of Section 6.1.2, we propose the following controller structure:

$$\alpha_1(x, t) = a_1 x_1 + a_2 x_2 + b \rho(x) \cos(\omega t) \quad (6.16)$$

$$\alpha_2(x, t) = a_3 x_3 + a_4 x_4 - \frac{2\omega^2}{b} \frac{1}{\rho(x)} (a_5 x_5 + a_6 x_6) \cos(\omega t), \quad (6.17)$$

where the vector of control gains $a \in \mathbb{R}^6$ is determined below, $b > 0$, and ρ is given by $\rho(x) = (\sum_{i=1}^6 |x_i|^{r_i})^{\frac{1}{2}}$, with $r = (1, 1, 1, 1, 2, 2)$. In (6.16, 6.17) ρ is a homogeneous norm with respect to a dilation of weight r . In fact, as in the case of the homogeneous feedbacks (6.8), instead of ρ one can also use other continuous, positive-definite functions $\mathbb{R}^6 \rightarrow \mathbb{R}$ that are homogeneous of degree 1 with respect to the dilation. In this thesis, however, no further use is made of this terminology or the associated results, and the interested reader is referred to e.g. (Hermes, 1991; Kawski, 1995) for more detailed discussions on that subject.

The closed-loop system can be explicitly integrated thanks to the simple structure of the second-order chained form and the fact that $u(t) = \alpha(x_0, t)$ is independent of $x(t)$ on the interval $(0, T)$. After some calculations, one verifies the solution $x(\cdot)$ is of the form

$$x(T) = Ax_0 + w(x_0), \quad (6.18)$$

where A is a block-diagonal matrix $A = \text{diag}(A_1, A_2, A_3)$ with blocks defined by

$$A_i = \begin{pmatrix} 1 + \frac{1}{2}T^2 a_{2i-1} & T + \frac{1}{2}T^2 a_{2i} \\ T a_{2i-1} & 1 + T a_{2i} \end{pmatrix}, \quad i = 1, 2, 3. \quad (6.19)$$

The spectrum of A is the union of the spectra of the A_i , each of which can be made equal to $\{k_{i1}, k_{i2}\} \subset \{z \in \mathbb{C} : |z| < 1\}$ —thus making A a discrete-time-stable matrix—by setting

$$a_{2i-1} = \frac{k_{i1} + k_{i2} - k_{i1}k_{i2} - 1}{T^2} \quad \text{and} \quad a_{2i} = \frac{k_{i1} + k_{i2} + k_{i1}k_{i2} - 3}{2T}, \quad i = 1, 2, 3. \quad (6.20)$$

Of course, a_{2i-1} and a_{2i} must be real, for which it suffices to chose k_{i1}, k_{i2} to be complex conjugate. On the other hand, it is readily checked that the function $w = (w_1, \dots, w_6) : \mathbb{R}^6 \rightarrow \mathbb{R}^6$ in (6.18) is given by $w_1 = \dots = w_4 = 0$ and

$$(w_5, w_6)(x_0) = \rho(x_0)L(x_0) + \rho^{-1}(x_0)P(x_0) + Q(x_0),$$

where $L : \mathbb{R}^6 \rightarrow \mathbb{R}^2$ is linear and $P, Q : \mathbb{R}^6 \rightarrow \mathbb{R}^2$ are quadratic. Since $\rho(x_0) = O(\|x_0\|^{\frac{1}{2}})$, it follows that $w(x_0) = O(\|x_0\|^{\frac{3}{2}})$ and hence $w(x_0) = o(\|x_0\|)$, so the solution $x(T)$ has the form (6.15). Since A is discrete-time-stable, there exists a symmetric, positive-definite matrix $P \in \mathbb{R}^{6 \times 6}$ and a real number $\tau \in [0, 1)$ such that $\|Ax_0\|_P \leq \tau \|x_0\|_P$ for every $x_0 \in \mathbb{R}^6$, with $\|x\|_P = \langle x, Px \rangle$ denoting the norm of x induced by P . This means that, locally around the origin, the mapping which assigns $x(T)$ to x_0 is a contraction in the norm $\|\cdot\|_P$.

It is important to remark that the frequency ω of the time-varying terms in the control law (6.16)-(6.17) does not have to be large; indeed it can be selected to be arbitrarily small. This is in contrast with the control law (6.8) that has been presented in (Aneke et al., 2002a) or, more generally, with previous results based on averaging of “highly oscillatory” systems, e.g. (M’Closkey and Murray, 1993; Teel et al., 1992). In these control laws, the frequency $1/\varepsilon$ (of the time-varying part of the controller) have to be chosen sufficiently large in order to be able to guarantee asymptotic stability of the closed-loop system. In practice, however, there is quite some freedom in the choice of the frequency $1/\varepsilon$ and it may still be possible to stabilize the system for low frequencies.

6.2.3 Notational conventions

Let us recall some definitions and properties about local order of mappings, a notion that simplifies the proofs. In this paragraph, n and m represent positive integers, ℓ a nonnegative integer and $\|\cdot\|$ represents Euclidean norm. Consider a neighborhood U of the origin in \mathbb{R}^n . We deal with mappings defined on $U \times \Lambda$, where $\Lambda \subset \mathbb{R}^\ell$, and view the elements of Λ as parameters (e.g. ‘time’ or other parameter). Given a mapping $f : U \times \Lambda \rightarrow \mathbb{R}^m$, we write $f(x, \lambda) = o(\|x\|^k)$ if, for every $\lambda \in \Lambda$,

$$\lim_{x \rightarrow 0} \frac{\|f(x, \lambda)\|}{\|x\|^k} = 0. \quad (6.21)$$

We write $f(x, \lambda) = O(\|x\|^k)$ if for every $\lambda \in \Lambda$ there is a constant $K > 0$ and a neighborhood $U' \subset U$ of the origin such that, for every $x \in U' \setminus \{0\}$,

$$\frac{\|f(x, \lambda)\|}{\|x\|^k} \leq K. \quad (6.22)$$

Consider a mapping $X = (X_1, \dots, X_n) : U \times \Lambda \rightarrow \mathbb{R}^n$ representing a family of *vector fields* $X(\cdot, \lambda) : U \rightarrow \mathbb{R}^n$. We write $X(x, \lambda) = o(\|x\|^k)$ (resp. $X(x, \lambda) = O(\|x\|^k)$) if $X_i(x, \lambda) = o(\|x\|^{k+1})$ (resp. $X_i(x, \lambda) = O(\|x\|^{k+1})$) for $i = 1, \dots, n$. We shall also use the function $\text{Ord} : f \mapsto \text{Ord}(f) \in \mathbb{R} \cup \{+\infty\}$ defined by $\text{Ord}(f) = \sup\{k \in \mathbb{R} : f(x, \lambda) = O(\|x\|^k)\}$.

6.2.4 Stability and robustness analysis

This section presents the main result, which characterizes the stability and robustness properties of the feedback law (6.16,6.17) applied to the second-order chained form. The proof shares the same basic structure as that of Theorem 1 in (Morin and Samson, 1999), and some other technical facts are modifications of the proofs in (Sussmann, 1983) and (Khalil, 1996). For the sake of conciseness, we only prove those claims particular to our solution and explicitly refer the reader to the appropriate references for the details.

Proposition 6.2.1. *The control law α defined in (6.16,6.17) is a local exponential stabilizer for the origin of system (6.13), robust to disturbances in $\mathcal{A} = \{(h_0^\varepsilon, h_1^\varepsilon, h_2^\varepsilon) \in \mathcal{D}^3 : \text{Ord}(h_0^\varepsilon) \geq 1, \text{Ord}(h_0^0) \geq 2 \text{ and } \text{Ord}(h_i^0) \geq 0, i = 1, 2\}$.*

Proof. Let us fix a disturbance $\mathbf{h} \in \mathcal{A}$ defined on an open set $U \times E \subset \mathbb{R}^n \times \mathbb{R}$. It must be shown that there is $\varepsilon_0 > 0$ such that the origin of (6.13) is locally exponentially stable when $\varepsilon \in [-\varepsilon_0, \varepsilon_0] \cap E$. The proof is divided into two main steps corresponding to the following two claims:

Claim 1 For every compact interval $E' \subset E$ there is a compact neighborhood $U' \subset U$ of 0 such that if $x_0 \in U'$ and $\varepsilon \in E'$, the solution $t \mapsto x(t) = \pi(t, 0, x_0, \varepsilon)$ to

$$\dot{x} = b_0(x) + h_0^\varepsilon(x) + \sum_{i=1}^2 \alpha_i(x_0, t)(b_i(x) + h_i^\varepsilon(x)), \quad x(0) = x_0 \quad (6.23)$$

satisfies

$$x(T) = Ax_0 + \lambda(\varepsilon, x_0) + \mu(\varepsilon, x_0) + o(\|x_0\|),$$

where the mappings λ, μ (which need not be uniquely defined) are such that

$$\frac{\|\lambda(\varepsilon, x_0)\|}{\|x_0\|} \rightarrow 0 \quad \text{as } \varepsilon \rightarrow 0, \quad \text{uniformly for } x_0 \in U' \setminus \{0\}, \quad (6.24)$$

$$\frac{\|\mu(\varepsilon, x_0)\|}{\|x_0\|} \rightarrow 0 \quad \text{as } x_0 \rightarrow 0, \quad \text{uniformly for } \varepsilon \in E'. \quad (6.25)$$

Claim 2 (Morin and Samson, 1999, Theorem 1). There exists a nonempty interval $E_0 \subset E$ containing 0 such that, for every $\varepsilon \in E_0$, the origin of system (6.13) is locally exponentially stable.

In (Morin and Samson, 1999, Theorem 1) it has been shown that Claim 1 implies Claim 2. Therefore the proof consists of showing that Claim 1 is valid. In (Lizárraga et al., 2003) it is shown that Claim 1 holds by showing that the system's solution at time T can be represented by means of a Chen-Fliess series expansion. For the details of the proof, we refer to that reference. \square

Remark 6.2.2. (i) In view of the definition of \mathcal{A} , for $\mathbf{h} \in \mathcal{A}$ one can write $h_i(x, \varepsilon) = w_i^\varepsilon(x) + h_i^0(x)$, with $w_i^0(\cdot) = 0$, $h_0^\varepsilon(x) = O(\|x\|^2)$ and $h_j^0(x) = O(\|x\|^0)$, ($i = 1, 2, 3$, $j = 1, 2$). Hence each disturbance vector field can be thought of as consisting of two parts, one containing only “high-order” terms in x and the other one vanishing identically when $\varepsilon = 0$. The terms corresponding to these two parts may have different origins. For instance, $w_i^\varepsilon(x)$ may arise from uncertainty in the knowledge of the physical parameters; if ε is a quantitative measure of the uncertainty, then these terms should vanish when ε equals zero. On the other hand, $h_i^0(x)$ may include high-order terms truncated from a series expansion of the system's nominal model, and these terms do not necessarily vanish when $\varepsilon = 0$. (ii) A measure of the extent to which robustness is ensured by a feedback law α lies in the nature of the set \mathcal{A} . Roughly stated, the larger this set is, the more sources of disturbances α can tolerate. In this respect, the control law in (Aneke et al., 2002a) is *not* robust to disturbances taken from \mathcal{A} , so the origin may be destabilized by the addition of disturbances in \mathcal{A} regardless of how small their magnitude is (i.e., for arbitrarily small $|\varepsilon| > 0$). This lack of robustness, which can be checked by using the results in (Lizárraga et al., 1999), is illustrated through numerical simulation in the Examples section.

In Proposition 6.2.1, the condition that the disturbances belong to \mathcal{A} is *sufficient* but not necessary for stability and robustness. In particular, disturbances in \mathcal{A} satisfy $h_0(x, \varepsilon) = O(\|x\|)$ or, stated otherwise, each component of the drift disturbance satisfies $h_{0,i} = O(\|x\|^2)$. This is somewhat restrictive since in some cases the latter condition is not satisfied and yet the conclusion of the previous proposition seems to hold in simulations. Indeed, a refinement of that result seems plausible, although the proof would require surmounting technical difficulties that we have not been overcome yet. The

presented result might be of interest when addressing the stabilization of systems whose models can be written as a second-order chained form with additional terms. For example, in (Reyhanoglu et al., 1996) the underactuated surface vessel with two independent thrusters was shown to be feedback equivalent to the second-order chained form with an additional term given in (2.8). By viewing these additional terms as disturbances, one might successfully use the control laws (6.16)-(6.17), without modification, to stabilize some of those systems to a point. This has been shown in (Lizárraga et al., 2003) for the underactuated surface vessel. A drawback of the stated condition, however, is that testing it may be difficult in practice.

6.3 Summary

This section was concerned with the feedback stabilization problem of the second-order chained form. The stabilizing controller has been designed by treating the system as two subsystems. By using a high-gain or backstepping result, the both subsystem can be stabilized by a continuous time-varying feedback. This so-called homogeneous feedback stabilizer can be used to globally ρ -exponentially stabilize equilibrium points of the second-order chained form system. To date and to our knowledge, this homogeneous controller is the only one capable of ensuring Lyapunov stability as well as ρ -exponential convergence of the second-order chained form system. Several authors, *cf.* (Imura et al., 1996) and (Astolfi, 1996), have presented discontinuous feedback controllers that achieve exponential convergence towards the origin, but all these controllers fail to guarantee Lyapunov stability of the closed-loop system.

It is known from (Lizárraga et al., 1999) that, homogeneous controllers fail to be robust with respect to modelling errors. Therefore, a periodically updated homogeneous feedback law has been presented that is robust with respect to a certain class of perturbations. These perturbations can be caused by, for example, parameter uncertainties or modelling errors.

At this moment, it is unclear how the results of this chapter can be extended to the feedback stabilization problem of higher-order chained form systems (2.6). In order to apply the same method as presented in Section 6.1.2, a stabilizing function for the virtual input x_3 should be known that stabilizes the $[x_4, \dots, x_{2n}]$ -subsystem. This stabilizing function is, in general, quite difficult to design. In addition, it is not even clear whether the second-order chained form system can be stabilized by smooth or continuous time-varying feedback. It is expected that a combined hybrid/open-loop approach may be more successful in controlling these high-order chained form systems. Nevertheless, such an hybrid/open-loop approach would require the use of a controller to be iterated periodically, which to date is not available. In the following chapter, we will evaluate the presented homogeneous controllers in a simulation environment with the goal of applying them to an experimental set-up.

Computer simulations

In this chapter, we consider an example of an underactuated mechanical system that is subject to a second-order nonholonomic constraint. This example consists of a mechanical system also known as the ‘H-Drive’ servo system, illustrated in Figure 7.1. The H-Drive is an XY-table with three linear motors that has been built by Philips’ Centre for Industrial Technology (CFT) as part of an Advanced Component Mounter (ACM) for pick-and-place operations on Printed Circuit Boards. It consists of two parallel Y-axes that are connected by a beam, the X-axis. The beam, or X-axis, is connected to the Y-axes by two joints that allow rotations in the horizontal plane. Therefore the positions Y_1 and Y_2 along the Y-axes are not necessarily equal, tilting or rotation of the beam is also possible. The position of the beam along the X-axis and the Y-axes is controlled by three linear motors, *i.e.*, Linear Motion Motor Systems (LiMMS). Each linear motor has its own servo system, encoder sensors and is current-controlled.

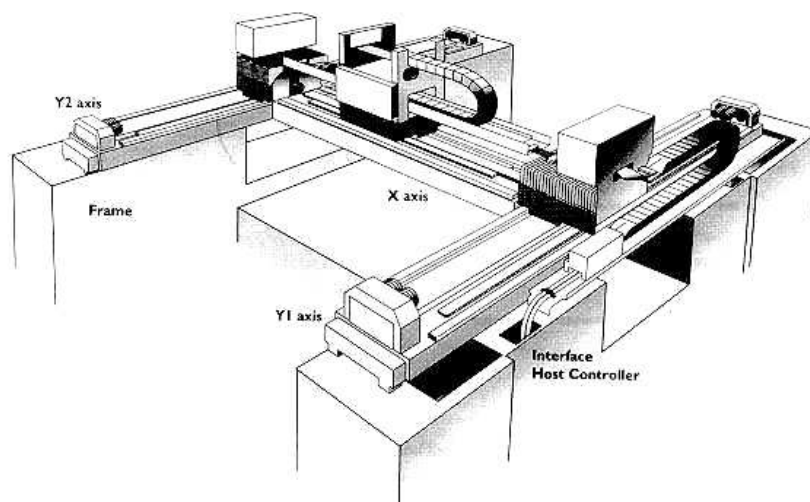


Figure 7.1: The H-Drive servo system.

LiMMS are widely used in high-speed applications and scanning motion systems. A LiMMS is composed of two parts, a number of base-mounted permanent magnets (the stator) and a number of iron-core coils (the translator). The permanent magnets are aligned along the axes and the LiMMS containing the iron-core coils are connected to a guiding rail along the axes using ball bearings. By

applying a three-phase current to the coils, a sequence of repelling and attracting forces can be generated that can be used as a thrust force to move the system. In contrast to traditional electro-motors, *i.e.*, with brushes, LiMMS allow for contactless transfer of electrical to translational power by the Lorentz actuator principle. Therefore, compared to traditional electro-motors, LiMMS have the advantage of less friction, resulting in higher accuracy, high velocity and acceleration; the velocity is mainly limited by the bandwidth of the encoder and the power supply, higher reliability and longer life-time due to reduced wear. A disadvantage of a linear motor is the positional dependency of the thrust force and the cogging forces resulting from the permanent magnets.

In this chapter, it is assumed that an additional rotational link, together with an encoder for measuring the link orientation θ , is attached on top of the LiMMS along the X-axis. In this manner, the link is not actuated directly, but can rotate freely. Using the inputs currents to the X-motor and the Y-motors, we wish to control the longitudinal and transversal position of the rotational link, as well as its orientation.

7.1 The dynamic model

The H-Drive with the additional rotational link, shown in Figure 7.2, is an underactuated mechanical system with three inputs, *i.e.*, the currents i_X , i_{Y1} and i_{Y2} to the motors, and four coordinates, *i.e.*, the positions X, Y1, Y2 and the orientation θ of the rotational link. Denote the mass of the Y motors by m_{Y1} and m_{Y2} respectively, the mass of the X-motor by m_X and the mass and inertia of the rotational link by m_3 and I_3 respectively. The longitudinal forces along the Y-axes are denoted by F_{Y1} and F_{Y2} respectively, and the transversal force along the X-axis by F_X . The distance from the rotational joint at the position $[r_x, r_y]$ to the center of mass of the rotational link is denoted by l and the length of the X-axis beam is denoted by D . The system moves in a horizontal plane and is not influenced by gravity.

By using the Lagrange-Euler formulation it is straight-forward to calculate the dynamic model of the H-Drive. The generalized coordinates are $q = [Y_B, \phi, X, \theta]$, where $Y_B(t)$ denotes the longitudinal position of the center of mass of the beam, $\phi(t)$ denotes the tilt-angle of the beam (see Figure C.1), $X(t)$ the transversal position of the motor along the X-axis. The dynamical model can be written as

$$M(q)\ddot{q} + C(q, \dot{q})\dot{q} = \begin{bmatrix} F \\ 0 \end{bmatrix} \quad (7.1)$$

where the symmetric and positive-definite mass matrix $M(q)$, the matrix representing Coriolis and centrifugal forces $C(q, \dot{q})$ and the input (3×1) -matrix F are given in appendix C.1. By using the coordinate transformation given by the relations

$$Y_B(t) = \frac{Y1(t) + Y2(t)}{2}, \quad \phi(t) = \arcsin\left(\frac{Y1(t) - Y2(t)}{L}\right),$$

this dynamical model can be written in terms of the encoder measurements, *i.e.*, $q = [Y1, Y2, X, \theta]$. Due to the complexity of the resulting equations, this will not be shown here. In fact, we will make an assumption which considerably simplifies the equations of motion of the H-Drive.

As mentioned earlier, the H-Drive is designed to be a servo-system. Therefore, both the Y1- and Y2-axis will be controlled using the servo-controllers given in Appendix C.2. Here, the positions $Y1(t)$ and $Y2(t)$ will be controlled to follow the same reference position. Therefore, the positions $Y1(t)$ and $Y2(t)$ will be approximately equal and the tilt-angle $\phi(t)$ will be small. In fact, the joints that connect the X-beam to the Y-axes only allows a difference of 30 [mm] between the positions of the Y-axes and the length of the X-axis beam is approximately 1 [m]. In this thesis, the nonlinear

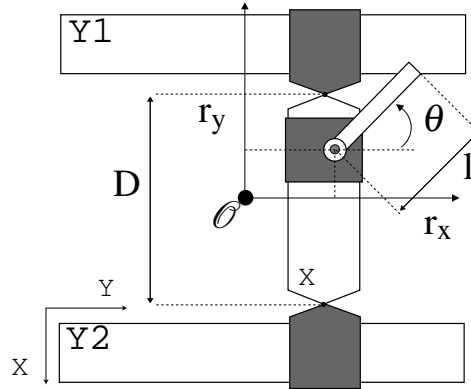


Figure 7.2: The coordinate system of the modified H-drive system with generalized coordinates $[r_x, r_y, \theta]$. The masses along the axes are denoted by m_X , m_{Y1} and m_{Y2} respectively. The mass of the rotational link is denoted by m_3 and its moment of inertia about its axis of rotation by I_3 . The length l denotes the distance between the rotational joint and the center of mass of the link (not shown).

rigid-body tilt-dynamics of the H-Drive are neglected by assuming that the position $Y1(t)$ and $Y2(t)$ are equal, *i.e.*, $Y1(t) = Y2(t) \forall t$. This is illustrated in Figure 7.2, where the underactuated H-Drive manipulator and the coordinate system is shown. By assumption, the origin \mathcal{O} of the global coordinate system is located at $(X, Y) = (-0.3, 0.5)$ (near the center of the H-Drive setup). The generalized coordinates are given by the joint coordinates and orientation of the link, *i.e.*, $q = [r_x, r_y, \theta]$. The joint positions r_x and r_y can be expressed in terms of the encoder measurements $[X, Y1, Y2]$ as follows

$$r_x(t) = \frac{Y1(t) + Y2(t)}{2} - 0.5, \quad r_y(t) = -X(t) - 0.3.$$

The rigid-body dynamics of the Y1- and Y2-motor are assumed to be identical. In practice, this is not true since the masses and electromagnetic properties of two LiMMS motors may vary. Moreover, the LiMMS are influenced by disturbances resulting from cogging forces, reluctance forces and friction. The cogging forces are caused by the attraction between the permanent magnets and the iron cores of the LiMMS. The reluctance forces are caused by a varying self-inductance of the windings in the coils of the translator. The friction is present in the ball bearings between the translator and the guiding rail. If we assume true linear dynamics of the LiMMS, with motor constant k_m , then the dynamic model (after solving for i_{Y1} and i_{Y2}) is given by

$$\begin{aligned} m_{x1}\ddot{r}_x(t) - m_3l\left(\frac{1}{2} - \frac{r_y(t)}{D}\right)\sin(\theta(t))\ddot{\theta}(t) - m_3l\left(\frac{1}{2} - \frac{r_y(t)}{D}\right)\cos(\theta(t))\dot{\theta}(t)^2 &= k_m i_{Y1}(t) \\ m_{x2}\ddot{r}_x(t) - m_3l\left(\frac{1}{2} + \frac{r_y(t)}{D}\right)\sin(\theta(t))\ddot{\theta}(t) - m_3l\left(\frac{1}{2} + \frac{r_y(t)}{D}\right)\cos(\theta(t))\dot{\theta}(t)^2 &= k_m i_{Y2}(t) \\ m_y\ddot{r}_y(t) + m_3l\cos(\theta(t))\ddot{\theta}(t) - m_3l\sin(\theta(t))\dot{\theta}(t)^2 &= -k_m i_X(t) \\ I\ddot{\theta}(t) - m_3l\sin(\theta(t))\ddot{r}_x(t) + m_3l\cos(\theta(t))\ddot{r}_y(t) &= 0 \end{aligned} \quad (7.2)$$

where the masses and inertia are given by

$$\begin{aligned}
 m_{x1} &= m_{Y1} + \frac{m_B}{2} + (m_X + m_3) \left(\frac{1}{2} - \frac{r_y(t)}{D} \right) \\
 m_{x2} &= m_{Y2} + \frac{m_B}{2} + (m_X + m_3) \left(\frac{1}{2} + \frac{r_y(t)}{D} \right) \\
 m_y &= m_X + m_3 \\
 I &= I_3 + m_3 l^2
 \end{aligned} \tag{7.3}$$

Note that a positive current i_X moves the LiMMS along the X-axis in the negative direction of r_y . This is caused by the choice of the coordinate system; the positive y direction along the (r_x, r_y) coordinate system, shown in Figure 7.2, points in the negative y direction of the (X, Y) coordinate system.

From (7.3) it is clear that the dynamics of the Y-motors are influenced by the position of the X-motor. If the X-motor is located close to the Y1-axis, then the effective mass along the Y1-direction becomes larger and higher input-currents will be needed to move the translator. The servo-controllers, used to control the positions of the LiMMS, will be used to compensate this coupling of mass between the X-axis and the Y-axes. Therefore, it is assumed that this coupling of mass can be neglected. By using the average of the Y1- and Y2-dynamics, the dynamical model reduces to

$$\begin{aligned}
 m_x \ddot{r}_x(t) &- \frac{m_3 l}{2} \sin(\theta(t)) \ddot{\theta}(t) - \frac{m_3 l}{2} \cos(\theta(t)) \dot{\theta}(t)^2 = k_m i_Y \\
 m_y \ddot{r}_y(t) &+ m_3 l \cos(\theta(t)) \ddot{\theta}(t) - m_3 l \sin(\theta(t)) \dot{\theta}(t)^2 = -k_m i_X \\
 (I_3 + m_3 l^2) \ddot{\theta}(t) &- m_3 l \sin(\theta(t)) \ddot{r}_x(t) + m_3 l \cos(\theta(t)) \ddot{r}_y(t) = 0
 \end{aligned} \tag{7.4}$$

where i_Y denotes the average of the currents running through the LiMMS of the Y1- and Y2-axis. The masses along the x and y direction reduce to

$$\begin{aligned}
 m_x &= \frac{m_{Y1} + m_{Y2}}{2} + \frac{m_B}{2} + \frac{(m_X + m_3)}{2} \\
 m_y &= m_X + m_3 \\
 I &= I_3 + m_3 l^2
 \end{aligned} \tag{7.5}$$

The model (7.4) represents an underactuated system with three generalized coordinates $[r_x, r_y, \theta]$, denoting the joint position and orientation of the rotational link, and two inputs currents i_X and i_Y to the LiMMS. This model can be transformed into the second-order chained form system, as will be shown in the following section.

7.2 The second-order chained form transformation

In this chapter, the goal is to control the cartesian position $[r_x(t), r_y(t)]$ and the orientation of the rotational link of the underactuated H-Drive manipulator. In order to apply the control methods developed in the Chapter 5 and 6, the dynamic model needs to be transformed into the second-order chained form. In (Imura et al., 1996) a coordinate and feedback transformation was proposed to transform the system (7.4) into the second-order chained form. The coordinate transformation corresponds to the position of the center of percussion (C.P.) of the rotational link. The center of percussion of a link can be interpreted as follows; if one would apply a force perpendicular to the link and at a certain point

below or above the C.P., then a rotation of the link will occur. If however, a force perpendicular to the link is applied exactly at the C.P., then no rotation of the link occurs. The center of percussion can also be characterized as the point that stays at rest when the link is rotated along a circle with a radius equal to the distance between the joint and the C.P. The C.P. is therefore useful in order to generate pure rotational motions of the link, in which the C.P. stays at rest. By performing repeated translational and rotational motions of the link, it is possible to move the unactuated and free rotating link from any initial configuration to any final configuration.

The second-order nonholonomic constraint of the system (7.4) can be written as

$$\lambda \ddot{\theta}(t) - \ddot{r}_x(t) \sin \theta(t) + \ddot{r}_y(t) \cos \theta(t) = 0, \quad (7.6)$$

where

$$\lambda = \frac{I}{m_3 l} \quad (7.7)$$

The parameter λ equals the effective pendulum length of the rotational link, when treated as a rigid-body pendulum suspended from the passive joint. This length also equals the distance from the joint to the so-called 'center of percussion' of the link. The constraint (7.6) was shown to be nonholonomic in (Arai et al., 1998a). The first-order linear approximation of (7.4) is not controllable, since the dynamics are not influenced by gravity. However, it can be shown that a small time local controllability (STLC) property holds (Arai et al., 1998a).

Define the configuration variable $q = [r_x, r_y, \theta]$. In this chapter the coordinate and feedback transformation given in (Imura et al., 1996) will be used to map the equilibrium $(q, \dot{q}) = (0, 0)$ to the origin $(\xi, \dot{\xi}) = (0, 0)$ of the extended chained form. It follows that any equilibrium point, with zero velocity, contained in a certain configuration-space \mathcal{C} , defined hereafter, can be mapped to the origin $\xi = 0$ of the chained form. The feedback transformation $\Omega : (q, \dot{q}, v) \in \mathcal{C} \times \mathbb{R}^3 \times \mathbb{R}^2 \rightarrow \tau \in \mathbb{R}^2$ is given by

$$\begin{bmatrix} i_Y \\ i_X \end{bmatrix} = \frac{1}{k_m} \begin{bmatrix} -\frac{m_3 l}{2} \cos(\theta) \dot{\theta}^2 + \left(m_x - \frac{m_3 l}{2\lambda} \sin^2(\theta) \right) v_x + \left(\frac{m_3 l}{2\lambda} \sin(\theta) \cos(\theta) \right) v_y \\ m_3 l \sin(\theta) \dot{\theta}^2 - \left(\frac{m_3 l}{\lambda} \sin(\theta) \cos(\theta) \right) v_x - \left(m_y - \frac{m_3 l}{\lambda} \cos^2(\theta) \right) v_y \end{bmatrix} \quad (7.8)$$

where v_x and v_y are new inputs. This feedback transformation results in the following partially feedback linearized system:

$$\begin{aligned} \ddot{i}_x &= v_x \\ \ddot{i}_y &= v_y \\ \ddot{\theta} &= \frac{1}{\lambda} (\sin(\theta) v_x - \cos(\theta) v_y). \end{aligned} \quad (7.9)$$

The mapping $\Phi : (q, \dot{q}) \in \mathcal{C} \times \mathbb{R}^3 \rightarrow (\xi, \dot{\xi}) \in \mathbb{R}^6$ follows from the relations

$$\begin{aligned} \xi_1 &= r_x + \lambda (\cos(\theta) - 1), \\ \xi_2 &= \tan(\theta), \\ \xi_3 &= r_y + \lambda \sin(\theta). \end{aligned} \quad (7.10)$$

By taking the new inputs v_x and v_y as follows, the system is transformed into the extended chained form

$$\begin{bmatrix} v_x \\ v_y \end{bmatrix} = \begin{bmatrix} \cos(\theta) & \sin(\theta) \\ \sin(\theta) & -\cos(\theta) \end{bmatrix} \begin{bmatrix} \frac{u_1}{\cos(\theta)} + \lambda \dot{\theta}^2 \\ \lambda (u_2 \cos^2(\theta) - 2\dot{\theta}^2 \tan \theta) \end{bmatrix}. \quad (7.11)$$

The coordinate transformation is only valid for $\theta \in (-\pi/2 + k\pi, \pi/2 + k\pi)$, for $\theta = \pi/2 \pm k\pi, k \in \mathbb{N}$ the coordinate transformation is not well-defined. The configuration-space \mathcal{C} of the configuration variables q is thus given by

$$\mathcal{C} = \{(r_x, r_y, \theta) \in \mathbb{R}^3 \mid \theta \in (-\pi/2 + k\pi, \pi/2 + k\pi), k \in \mathbb{N}\} \quad (7.12)$$

The coordinate transformation (7.10) from local coordinates $(q, \dot{q}) \in \mathcal{C} \times \mathbb{R}^3$ to local coordinates $(\xi, \dot{\xi}) \in \mathbb{R}^3 \times \mathbb{R}^3$ is a diffeomorphism. Together with the feedback transformations (7.8,7.11) the dynamics of the underactuated H-drive manipulator are transformed into the second-order chained form system

$$\begin{aligned} \ddot{\xi}_1 &= u_1 \\ \ddot{\xi}_2 &= u_2 \\ \ddot{\xi}_3 &= \xi_2 u_1. \end{aligned} \quad (7.13)$$

By applying the coordinate transformation it follows that the nonholonomic constraint (7.6) is transformed into the last equation of (7.13). The nonholonomic constraint (7.6) is thus preserved under the coordinate and feedback transformation.

7.2.1 The influence of friction

In this section the influence of friction, present in the LiMMS and the rotational joint of the underactuated link, will be investigated. If friction and cogging forces are included in the model, the transformed system will not be equal to the second-order chained form system. Consider the underactuated system with friction given by

$$\begin{aligned} m_x \ddot{r}_x - \frac{m_3 l}{2} \sin(\theta) \ddot{\theta} - \frac{m_3 l}{2} \cos(\theta) \dot{\theta}^2 &= k_m \dot{r}_y + \tau_{f,Y} \\ m_y \ddot{r}_y + m_3 l \cos(\theta) \ddot{\theta} - m_3 l \sin(\theta) \dot{\theta}^2 &= -k_m \dot{r}_x + \tau_{f,X} \\ I \ddot{\theta} - m_3 l \sin(\theta) \ddot{r}_x + m_3 l \cos(\theta) \ddot{r}_y &= \tau_{f,\theta}, \end{aligned} \quad (7.14)$$

where $\tau_{f,i}, i \in \{X, Y, \theta\}$ denote the friction forces of the LiMMS and the friction torque of the rotational link. By recalculating the transformation, it can be shown that the system (7.14) is transformed into

$$\begin{aligned} \ddot{\xi}_1 &= u_1 - \left(\lambda - \frac{m_3 l}{m_x} \right) \sin(\arctan(\xi_2)) \Delta(\xi, \tau_{f,X}, \tau_{f,Y}, \tau_{f,\theta}) + \frac{\tau_{f,Y}}{m_y} \\ \ddot{\xi}_2 &= u_2 + (1 + \xi_2^2) \Delta(\xi, \tau_{f,X}, \tau_{f,Y}, \tau_{f,\theta}) \\ \ddot{\xi}_3 &= \xi_2 u_1 + \left(\lambda - \frac{m_3 l}{m_y} \right) \cos(\arctan(\xi_2)) \Delta(\xi, \tau_{f,X}, \tau_{f,Y}, \tau_{f,\theta}) + \frac{\tau_{f,X}}{m_x}. \end{aligned} \quad (7.15)$$

where the perturbation Δ of the extended chained form system is given by

$$\Delta(\xi, \tau_{f,X}, \tau_{f,Y}, \tau_{f,\theta}) = \frac{\left(\frac{m_3 l}{m_x} \sin \theta \right) \tau_{f,Y} - \left(\frac{m_3 l}{m_y} \cos \theta \right) \tau_{f,X} + \tau_{f,\theta}}{I - \frac{(m_3 l)^2}{2m_x} \sin^2(\arctan(\xi_2)) - \frac{(m_3 l)^2}{m_y} \cos^2(\arctan(\xi_2))} \quad (7.16)$$

The third equation of (7.15) shows that any residual perturbation in the X-axis, such as friction or cogging forces $\tau_{f,x}$ that are not compensated, will directly act as an additive perturbation in the dynamics of the chained form variable ξ_3 . This makes it even more difficult to control the ξ_3 -dynamics, since the second-order chained form is uncontrollable for $\xi_2 \equiv 0$ or $u_1 \equiv 0$ and, as a result, the perturbations can not be fully compensated. Therefore it is essential to use a low-level servo system to compensate friction, cogging forces and additional perturbations in both the X-axis and Y-axes.

Note that designing the system such that the perturbation $\Delta(\xi, \tau_{f,x}, \tau_{f,y}, \tau_{f,\theta})$ is not present in the first and third equation of (7.15), *i.e.*, $\lambda - \frac{m_3 l}{m_y} = 0$, is not possible. The term $\lambda - \frac{m_3 l}{m_y}$ can be written as

$$\frac{I}{m_3 l} - \frac{m_3 l}{m_y} = \frac{I_3}{m_3 l} + \left(1 - \frac{m_3}{m_y}\right) l.$$

In the case $m_3 < m_y$, considered in this thesis, this term is always positive, and can not be equal to zero. Moreover, if $m_3 > m_y$ and $\lambda - \frac{m_3 l}{m_y} = 0$ holds, then the denominator of the perturbation (7.16) would become zero for small $\xi_2 = 0$ and the perturbation would become infinitely large, *i.e.*, as $\xi_2 \rightarrow 0$ we have that $\Delta \rightarrow \infty$.

As mentioned earlier, the X-axis and the Y-axes are controlled directly by servo controllers. This means that friction and cogging forces that are present in the LiMMS are (partially) compensated for by the servo-loop. Therefore, it is assumed that the friction forces $\tau_{f,x}$ and $\tau_{f,y}$ can be neglected and we focus on the friction torque that is present in the rotational joint of the link. Additionally, the servo controllers (partially) compensate the influence of the link on the dynamics of the LiMMS. Therefore, in this section, only the partially feedback linearized system given by (7.9) is considered and the terms with $m_3 l$ are assumed to be negligible. The transformed mechanical system, *i.e.*, (7.15), then reduces to

$$\begin{aligned}\ddot{\xi}_1 &= u_1 + \Delta_1(\xi_2, \dot{\xi}_2) \\ \ddot{\xi}_2 &= u_2 + \Delta_2(\xi_2, \dot{\xi}_2) \\ \ddot{\xi}_3 &= \xi_2 u_1 + \Delta_3(\xi_2, \dot{\xi}_2),\end{aligned}\tag{7.17}$$

where the perturbation terms are given by,

$$\begin{aligned}\Delta_1 &= -\frac{\xi_2}{\sqrt{1 + \xi_2^2}} \frac{\tau_{f,\theta}(\xi_2, \dot{\xi}_2)}{m_3 l} \\ \Delta_2 &= (1 + \xi_2^2) \frac{\tau_{f,\theta}(\xi_2, \dot{\xi}_2)}{I} \\ \Delta_3 &= \frac{1}{\sqrt{1 + \xi_2^2}} \frac{\tau_{f,\theta}(\xi_2, \dot{\xi}_2)}{m_3 l}.\end{aligned}\tag{7.18}$$

In the previous equation the inverse coordinate transformation, *i.e.*, $\dot{\theta}(t) = \dot{\xi}_2(t)/(1 + \xi_2(t)^2)$, has been used to write the friction term $\tau_{f,\theta}(\dot{\theta})$ in terms of $(\xi_2, \dot{\xi}_2)$ and the terms $\sin(\arctan(\xi_2))$ and $\cos(\arctan(\xi_2))$ have been expressed as $\xi_2/\sqrt{1 + \xi_2^2}$ and $1/\sqrt{1 + \xi_2^2}$ respectively. We conclude that the additive perturbations, such as friction and cogging, present in the rotational joint of the mechanical system result in additive perturbations in the resulting second-order chained form system.

7.3 Friction Compensation

In this section it will be investigated whether the perturbations in the perturbed second-order chained form system can be compensated using the inputs u_1 and u_2 . Note that it makes no difference whether we try to compensate the friction in the original mechanical system or we try to compensate the perturbation terms in the second-order chained form system, as these systems are related through a coordinate and feedback transformation. In section 7.2.1 it was shown that under the influence of friction, the coordinate and feedback transformation of section 7.2 transforms the dynamic model of the underactuated H-Drive system, given by (7.14), into the perturbed second-order chained form system given by (7.17). The resulting perturbation terms Δ_1 and Δ_3 satisfy the relation

$$\Delta_3 + \frac{\Delta_1}{\xi_2} = 0. \quad (7.19)$$

The mechanical system is thus transformed into a system which, in contrast to the second-order chained form system, is not in strict-feedback form. Therefore, the backstepping procedure that has been adopted to design a linear time-varying tracking controller is not valid anymore, and we expect that the tracking-error dynamic will not be \mathcal{K} -exponentially stable. Furthermore, the resulting perturbed second-order chained form system is not homogeneous of degree zero. Therefore, the homogeneity properties that were used to design a continuous time-varying stabilizing controller do not hold anymore, and we expect that the closed-loop system will not be ρ -exponentially stable.

From (7.17) it becomes clear that the perturbation terms Δ_1 and Δ_2 can be compensated directly using the chained inputs u_1 and u_2 , provided that these uncertain perturbation terms are exactly known. By defining $u_1 = \bar{u}_1 - \Delta_1$ and $u_2 = \bar{u}_2 - \Delta_2$, the perturbed chained form system becomes

$$\begin{aligned} \ddot{\xi}_1 &= \bar{u}_1 \\ \ddot{\xi}_2 &= \bar{u}_2 \\ \ddot{\xi}_3 &= \xi_2 \bar{u}_1 + \Delta_3(\xi_2, \dot{\xi}_2) - \xi_2 \Delta_1(\xi_2, \dot{\xi}_2). \end{aligned} \quad (7.20)$$

where the perturbation term is given as

$$\Delta_3(\xi_2, \dot{\xi}_2) - \xi_2 \Delta_1(\xi_2, \dot{\xi}_2) = \sqrt{1 + \xi_2^2} \frac{\tau_{f,\theta}(\xi_2, \dot{\xi}_2)}{m_3 l} \quad (7.21)$$

This shows that compensating the perturbations Δ_1 and Δ_2 actually increases the perturbation in the ξ_3 -dynamics. This is generally not a good idea, since the last equation can not be controlled directly. The ξ_3 -dynamics are controlled using a backstepping procedure in which ξ_2 is a virtual input. This means that the states $(\xi_2, \dot{\xi}_2)$ only converges to zero if the states $(\xi_3, \dot{\xi}_3)$ also converge to zero. Therefore the perturbations acting in the third equation are expected to have a greater influence on the robustness of the closed-loop system, compared to the perturbations acting in the first and second equation. In fact, the effect of the perturbations on stability of the first two equations can be minimized by choosing the gains of the controllers u_1 and u_2 sufficiently high.

At this moment it is not yet clear whether the perturbations in the ξ_3 -dynamics can be compensated using the input u_1 . The compensation of the perturbation Δ_3 is complicated by the fact that the ξ_3 -dynamics can not be controlled using the input u_1 when $\xi_2 \equiv 0$. Also compensating the perturbation Δ_3 using the input u_1 will result in the perturbation term appearing in the ξ_1 -dynamics, which is coupled with the ξ_3 -dynamics. Note that it is not possible to use the state ξ_2 in a backstepping procedure to compensate the perturbation Δ_3 . The perturbation Δ_3 contains non-smooth effects such as friction.

In order to apply a backstepping procedure the virtual input ξ_2 should be at least twice continuously differentiable. This is not the case when using the virtual input ξ_2 to compensate non-smooth effects such as friction. More importantly, however, is the fact that no control input can be applied using the virtual input ξ_2 when $u_1 \equiv 0$. We conclude that due to coupling of the equations, it is not straightforward to compensate the perturbation terms in the second-order chained form system.

Concluding, we can state that using the current coordinate and feedback transformation, it is not clear how to compensate the perturbation Δ_3 by the chained inputs u_1 and u_2 . It is however possible to compensate the effect of the perturbations Δ_1 and Δ_2 . However, through numerical simulation, it can be shown that compensation of these perturbations, generally, reduces control performance because it results in a larger perturbation term in the ξ_3 -dynamics. Therefore, no friction compensation will be used in the simulations.

An important question one might ask is whether it is possible to transform the mechanical system with friction into the second-order chained form. This would require a different coordinate and feedback transformation and, at this moment, it is not clear whether this is possible or not. In certain situations, the friction force can be used in order to control the system. For example, in the case of stabilization, the system can be transferred from one configuration to another by first controlling the link angle to its desired position, and then moving the system very slowly along the x and y direction such that stiction occurs in the rotational joint of the link. The link orientation then stays equal to its desired value, due to the static friction in the joint of the link. It is not clear to what extent the friction torque can be used in order to stabilize the system or perform tracking control. In the situation described above, they can not be used to obtain true stabilization, but can be used for very slow point to point motions. In this thesis, such approaches will not be considered. The focus is on obtaining true asymptotic stabilization or at least a form of practical stability or practical tracking in which the system can be moved arbitrary close to the a desired equilibrium or close to a desired trajectory.

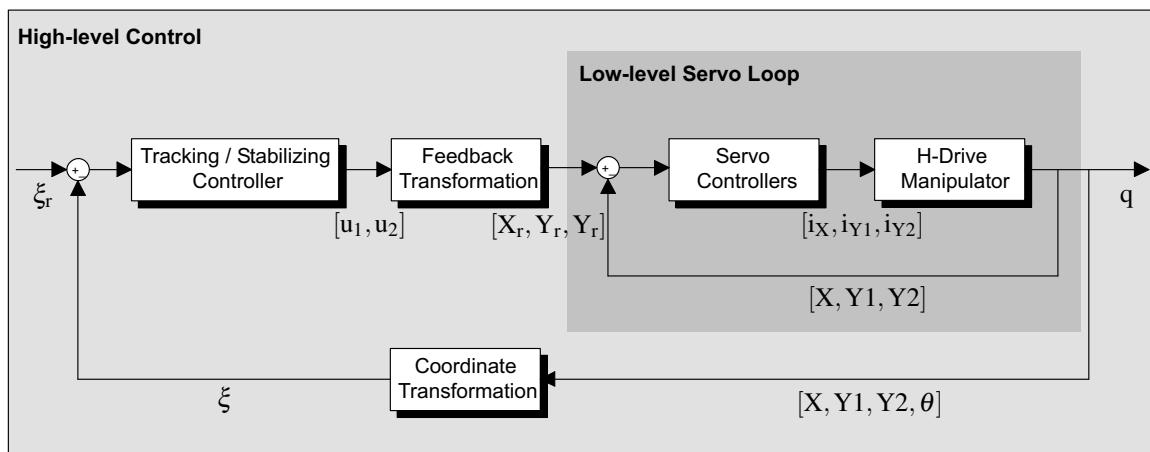


Figure 7.3: The ‘virtual internal model following control’ approach in which the underactuated H-Drive manipulator is controlled by a combination of a high-level controller and a low-level servo-loop. The feedback transformation block includes the double integration that is needed to obtain the reference inputs X_r and Y_r to the servo controllers. The generalized coordinates $q = [r_x, r_y, \theta]$ are thus controlled by two reference inputs X_r and Y_r to the servo-loop, and the system is thus underactuated.

7.4 Tracking Control

In this thesis, the so-called ‘virtual internal model following control’ approach in (Kosuge et al., 1987) is adopted. This means that the X and Y axes are not controlled directly, but by a combination of a high-level controller and a low-level servo-loop depicted in Figure 7.3. The inputs u_1 and u_2 , generated by the tracking and stabilizing control laws of the second-order chained form system, are transformed into desired accelerations for the X and Y axes. These desired accelerations are integrated twice to obtain desired positions X_r and Y_r , which are commanded to the servo controllers for the X and Y -axes. These servo controllers are given in Appendix C.2. Compared to computed-torque methods, the local servo system of the ‘virtual internal model following method’ is able to compensate or suppress unknown disturbances, *e.g.* friction and cogging in the active joints, by the local servo system. Moreover, the servo controllers are used to compensate the distribution of the mass of the X motor along the Y motors.

The performance of the tracking and stabilizing controllers developed in Chapter 5 and Chapter 6 will be tested with and without the influence of friction in the joint of the rotational link. Compared to parameter uncertainties and modelling errors, the frictional perturbation plays a more dominant role and considerably deteriorates the performance of the tracking and stabilizing controllers. The tracking and stabilizing controllers do achieve some degree of robustness with respect to parameter uncertainties, however, the robustness with respect to friction in the joint of the rotational link is marginal. Therefore, no parameter uncertainties will be considered here, but we focus on the effect of a friction torque acting in the joint of the rotational link. This allows us to investigate the robustness properties of the tracking and stabilizing controllers with respect to friction. Since the friction in the actuated X -axis and Y -axes are suppressed by the servo-loop, we shall only consider the friction in the unactuated rotational link. It is assumed that the friction of the rotational link can be modelled by

$$\tau_{f,\theta} = c_s \frac{2}{\pi} \arctan(100 \cdot \dot{\theta}) + c_v \dot{\theta}. \quad (7.22)$$

where c_v and c_s denote the static (Coulomb) and viscous friction coefficients, respectively. The simulations of this chapter are performed using the dynamic model (7.2). The model parameters are chosen such that they approximately match the parameters that have been obtained from the identification procedure in Chapter 8. These model parameters for the dynamic model (7.2), are summarized in Table 7.1. It should be noted that the inertia $I = I_3 + m_3 l^2$ has not been identified, but has been

| parameter | value | unit | parameter | value | unit |
|-----------|--------|-------------------------|-----------|--------|-------------------------|
| m_x/k_m | 0.3994 | [A · s ² /m] | m_y/k_m | 0.1231 | [A · s ² /m] |
| λ | 0.1372 | [m] | D | 0.60 | [m] |
| m_3 | 0.04 | [kg] | l | 0.15 | [m] |
| I | 0.0008 | [kg · m ²] | k_m | 74.4 | [N/A] |
| c_s/I | 0.3 | [1/s ²] | c_v/I | 0.1 | [1/(rad · s)] |

Table 7.1: Simulation parameters H-drive system

approximated using the identified value of λ using the known mass m_3 and length l of the rotational link. The only parameters that need to be identified are the parameters λ , m_x/k_m , m_y/k_m , c_s/I and c_v/I .

In the simulations of this section we want the underactuated H-Drive manipulator to follow a pre-defined path $(q_d, \dot{q}_d) \in \mathcal{C} \times \mathbb{R}^3$. The joint position of the rotational link should follow a trajectory $(r_{xd}(t), r_{yd}(t))$ and the link orientation to follow a trajectory $\theta_d(t)$. This reference trajectory $q = [r_{xd}(t), r_{yd}(t)]$, contained in the configuration-space \mathcal{C} , can be transformed into a reference trajectory ξ_d for the second-order chained form system. A feasible persistently exciting periodic trajectory, with zero initial velocity, for the second-order chained form system is given by

$$\begin{aligned}\xi_{1d}(t) &= r_1 \cos(\omega_1 t), & \xi_{2d}(t) &= r_2 \cos(\omega_2 t), \\ \xi_{3d}(t) &= \frac{r_1 r_2 \omega_1^2}{2(\omega_1 - \omega_2)^2} \cos((\omega_1 - \omega_2)t) + \frac{r_1 r_2 \omega_1^2}{2(\omega_1 + \omega_2)^2} \cos((\omega_1 + \omega_2)t).\end{aligned}\quad (7.23)$$

The corresponding inputs are given by $u_{1d}(t) = -r_1 \omega_1^2 \cos(\omega_1 t)$ and $u_{2d}(t) = -r_2 \omega_2^2 \cos(\omega_2 t)$, with $\omega_1 \neq \omega_2$. If $\omega_1 = \omega_2$, then the solution is not periodic and therefore the case $\omega_1 = \omega_2$ is omitted. This reference trajectory is persistently exciting, and the resulting reference trajectory q_d for the mechanical system (7.4) is given by

$$\begin{aligned}r_{xd}(t) &= r_1 \cos(\omega_1 t) - \lambda (\cos(\arctan(r_2 \cos(\omega_2 t))) - 1), \\ r_{yd}(t) &= \frac{r_1 r_2 \omega_1^2}{2(\omega_1 - \omega_2)^2} \cos((\omega_1 - \omega_2)t) + \frac{r_1 r_2 \omega_1^2}{2(\omega_1 + \omega_2)^2} \cos((\omega_1 + \omega_2)t) - \lambda \sin(\arctan(r_2 \cos(\omega_2 t))), \\ \theta_d(t) &= \arctan(r_2 \cos(\omega_2 t)).\end{aligned}\quad (7.24)$$

This previous equation defines a class of trajectories that depend on the values of the parameters r_1 , r_2 , ω_1 and ω_2 . In the simulations of this chapter, we have selected $r_1 = 0.4$, $r_2 = 0$ and $\omega_1 = 1$ and $\omega_2 = 0$. This means that we try to track a trajectory in which the joint of the rotational link moves along a straight line while the link angle is zero. The resulting trajectory is given by

$$r_{xd}(t) = r_1 \cos(\omega t), \quad r_{yd}(t) = 0, \quad \theta_d(t) = 0. \quad (7.25)$$

We select $d_1 = d_2 = 0$ in the virtual input x_{21} (5.5) and $d_3 = d_4 = 0$ in the controller u_2 (5.7). The linear time-varying tracking controller is then given by

$$\begin{aligned}u_1 &= u_{1d} - k_1(\xi_1 - \xi_{1d}) - k_2(\dot{\xi}_1 - \dot{\xi}_{1d}) \\ u_2 &= u_{2d} - G_3(t)(\xi_2 - \xi_{2d}) - G_4(t)(\dot{\xi}_2 - \dot{\xi}_{2d}) - G_5(t)(\xi_3 - \xi_{3d}) - G_6(t)(\dot{\xi}_3 - \dot{\xi}_{3d}).\end{aligned}\quad (7.26)$$

The time-varying feedback coefficients in (7.26) are given by

$$\begin{aligned}G_3(t) &= k_5 k_6 u_{1d}^4(t) + (k_3 + k_4)(k_5 + k_6) u_{1d}^2(t) + (5k_5 + 3k_6) \dot{u}_{1d}(t) u_{1d}(t) + k_3 k_4 \\ G_4(t) &= (k_5 + k_6) u_{1d}^2(t) + (k_3 + k_4) \\ G_5(t) &= k_5 k_6 k_3 k_4 u_{1d}^3(t) + 2k_5 u_{1d}^{(3)}(t) + (3k_5 k_6 u_{1d}^2(t) + 2k_5(k_3 + k_4)) u_{1d}^{(2)}(t) \\ &\quad + (3k_5 k_6(k_3 + k_4) u_{1d}^2(t) + 2k_5 k_3 k_4) \dot{u}_{1d}(t) + 6k_5 k_6 u_{1d}(t) \dot{u}_{1d}^2(t) \\ G_6(t) &= k_5 k_6(k_3 + k_4) u_{1d}^3(t) + (k_5 + k_6) k_3 k_4 u_{1d}(t) + (5k_5 + k_6) u_{1d}^{(2)}(t) \\ &\quad + (6k_5 k_6 u_{1d}^2(t) + (k_3 + k_4)(3k_5 + k_6)) \dot{u}_{1d}(t),\end{aligned}\quad (7.27)$$

where $u_{1d}^{(k)}(t)$ denotes the k -th derivative of $u_{1d}(t)$. The tuning of the control parameters requires some effort because the parameters have to be chosen such that the closed-loop system is \mathcal{N} -exponentially

stable and, additionally, such that the link angle stays between $-\pi/2$ and $\pi/2$. Otherwise, the coordinate transformation is not well-defined since a singularity occurs at $\theta = \pm\pi/2$. The tuning procedure proceeds as follows. First we determine parameters k_1 and k_2 that achieve good tracking of the ξ_1 -subsystem. It suffices to select k_1 and k_2 such that the characteristic polynomial $s^2 + k_2s + k_1$ is Hurwitz. By choosing these values sufficiently large, we can assure that the perturbation term $\xi_2(u_1 - u_{1d})$ in (5.1) becomes small sufficiently fast. In the next step, we select parameters k_3k_4 and $k_3 + k_4$ that stabilize the tracking-error dynamics of ξ_2 . Since ξ_2 is a virtual input in the backstepping approach that is used to control the ξ_3 -dynamics, the gains (k_3, k_4) should be chosen sufficiently large. Finally, parameters values k_5 and k_6 have to be selected that stabilize the ξ_3 -dynamics. The latter step is the most important one since they determine the convergence of the ξ_3 -dynamics, which can not be controlled directly.

In the simulations, we have chosen the control parameters to be equal to the parameter values that were used in the experimental results of the following chapter. These parameter values are given by

$$k_1 = 4, k_2 = 2\sqrt{2}, k_3k_4 = 40, k_3 + k_4 = 9, k_5 = 5, k_6 = 100.$$

The parameters k_1 and k_2 can be chosen rather small since the perturbation term Δ_1 is small for small values of ξ_2 and the reference value for ξ_2 is zero. The positive control parameters k_3k_4 and $k_3 + k_4$ resulting from the backstepping approach, determine the convergence of the tracking-error dynamics of ξ_2 and these dynamics correspond to the link orientation θ . These parameters are chosen such that the tracking-error dynamics of ξ_2 contain a complex pole pair given by $-4.5 \pm 4.44i$. Since the dynamics of θ may be influenced by friction, which can not be compensated directly, we have chosen k_3k_4 and $k_3 + k_4$ sufficiently large in order to prevent stiction of the link. In the simulations without friction the gain k_3k_4 , typically, has to be chosen larger than 16 and the gain $k_3 + k_4$ larger than 8.

The damping in the ξ_3 -dynamics, *i.e.*, the parameter k_6 , is chosen to be large in order to reduce the magnitude of the excursions that the system makes in the direction of the r_y coordinate. The positive parameters k_5 and k_6 also determine the convergence of the tracking-error dynamics of the chained state ξ_3 and its corresponding mechanical state r_y . These values have been chosen sufficiently large to guarantee convergence of the state ξ_3 . Because the ξ_3 -subsystem is stabilized using a backstepping procedure in which we back-step through the ξ_2 -dynamics, the ξ_2 -dynamics only converge after the tracking-error dynamics of ξ_3 have been stabilized. However, choosing these values too large may result in the link orientation passing through the singularity point $\theta = \pm\pi/2$ of the coordinate and feedback transformation.

The initial condition of the system is chosen to be $[r_x, r_y, \theta] = [0, 0, -20\pi/180]$, *i.e.*, the joint of the rotational link starts in the origin and the orientation of the link is -20 degrees. This corresponds to an initial tracking-error of $\xi(0) - \xi_d(0) = [-0.05, -0.36, -0.01, 0, 0, 0]$ for the chained states. The robustness of the closed-loop system against parameter perturbations will not be tested. Although, the closed-loop system is robust to sufficiently small parameter uncertainties, the system is not robust with respect to perturbations such as friction and cogging. The friction torque, that is present in the rotational joint of the link, has a greater influence on the performance of the system than parameter uncertainties. Therefore, only the robustness with respect to friction in the rotational link will be considered.

As mentioned earlier, the numerical simulations are performed with and without modelling the influence of friction in the rotational joint. This allows us to investigate the robustness properties of the controller. Note that the perturbation Δ_1 and Δ_2 affecting the ξ_1 - and ξ_2 -dynamics, see (7.17), can be suppressed by choosing (k_1, k_2) and (k_3, k_4) sufficiently large. In fact they can even be compensated directly, provided that the friction parameters are known. The parameters (k_5, k_6) should be chosen

sufficiently large such that good convergence of the states ξ_3 is obtained in spite of the perturbation Δ_3 .

7.4.1 Simulation without friction in the rotational link

Consider the situation in which the joint of the rotational link is frictionless. This means that the coordinate- and feedback transformation bring the mechanical system into the extended chained form. The result of tracking the trajectory of a straight line with initial condition $[r_x, r_y, \theta] = [0, 0, -20\pi/180]$ is shown in Figure 7.4. Note that the control currents from the servo-loop are only sent to the H-Drive after 1 second. Disabling the control of the H-Drive before $t = 1$ s allows us to check the initial value of the input currents. These non-zero initial values of the input currents $i_{Y1} - i_{Y1d}$, $i_{Y2} - i_{Y2d}$ together with the non-zero initial values $u_1 - u_{1d}$ and $u_2 - u_{2d}$ are caused by the non-zero initial value $u_{1d}(0)$ of the reference input to the chained form system.

From the simulation it becomes clear that the trajectory is successfully tracked after approximately 10 seconds. The corresponding chained form coordinates and inputs are shown in Figure 7.5. The trajectories of the tracking-error dynamics are asymptotically stable and converge to the origin with an exponential decay rate. Therefore it is concluded that the tracking-error dynamics of the extended chained form system are globally, *i.e.*, on the complete state-space \mathbb{R}^n , \mathcal{H} -exponentially stable. The original mechanical system is only \mathcal{H} -exponentially stable on the subspace \mathcal{C} where the coordinate transformation is well-defined. The simulation result shows the validity of the "virtual internal model control" approach in which the system is not controlled directly but by a combination of a high-level controller and a low-level servo-loop.

7.4.2 Simulation with friction in the rotational link

The performance of the tracking controller is also simulated under the influence of friction in the joint of the rotational link. It is assumed that the friction can be modelled using a simplified model given by (7.22). The friction parameters of the assumed friction characteristic (7.22) are normalized with respect to the inertia I and are given in Table 7.1. The values of the friction coefficients c_s and c_v are in the order of magnitude of the normalized viscous and Coulomb friction coefficients of an H-Drive manipulator available in our lab. The result of tracking the trajectory under the influence of the friction torque is shown in Figure 7.6. The simulation model (7.2) includes the coupling of mass between the X-axis and the Y-axes. However, the influence of this coupling of mass is very small and the difference between the currents to the Y1- and Y2-axis is hardly visible.

The coordinates of the extended chained form system are shown in Figure 7.7. Clearly, the tracking-error dynamics are not \mathcal{H} -exponentially stable, and the trajectory is not perfectly tracked. In fact, after about 10 seconds the system performs a stationary periodic motion around the reference trajectory. This periodic motion is caused by frictional perturbations acting in the perturbed chained form system given by (7.17). The perturbation terms in the ξ_1 - and ξ_2 -dynamics are suppressed by time-invariant parts of the tracking control input u_1 and u_2 . The main difficulty, lies with the perturbation Δ_3 in the ξ_3 -dynamics. Since this perturbation term can not be compensated the performance of the tracking controller is considerably deteriorated. The perturbation Δ_3 prevents the coordinate ξ_3 from converging to zero. Moreover, this perturbation term can not be compensated by the virtual input ξ_2 since the perturbed chained form system is not in strict-feedback form. As a consequence, the virtual input ξ_2 from the backstepping procedure also does not converge to zero and the system performs a periodic motion around the desired reference trajectory.

Approximate cancellation of the perturbation Δ_3 is possible by selecting large values for the gains

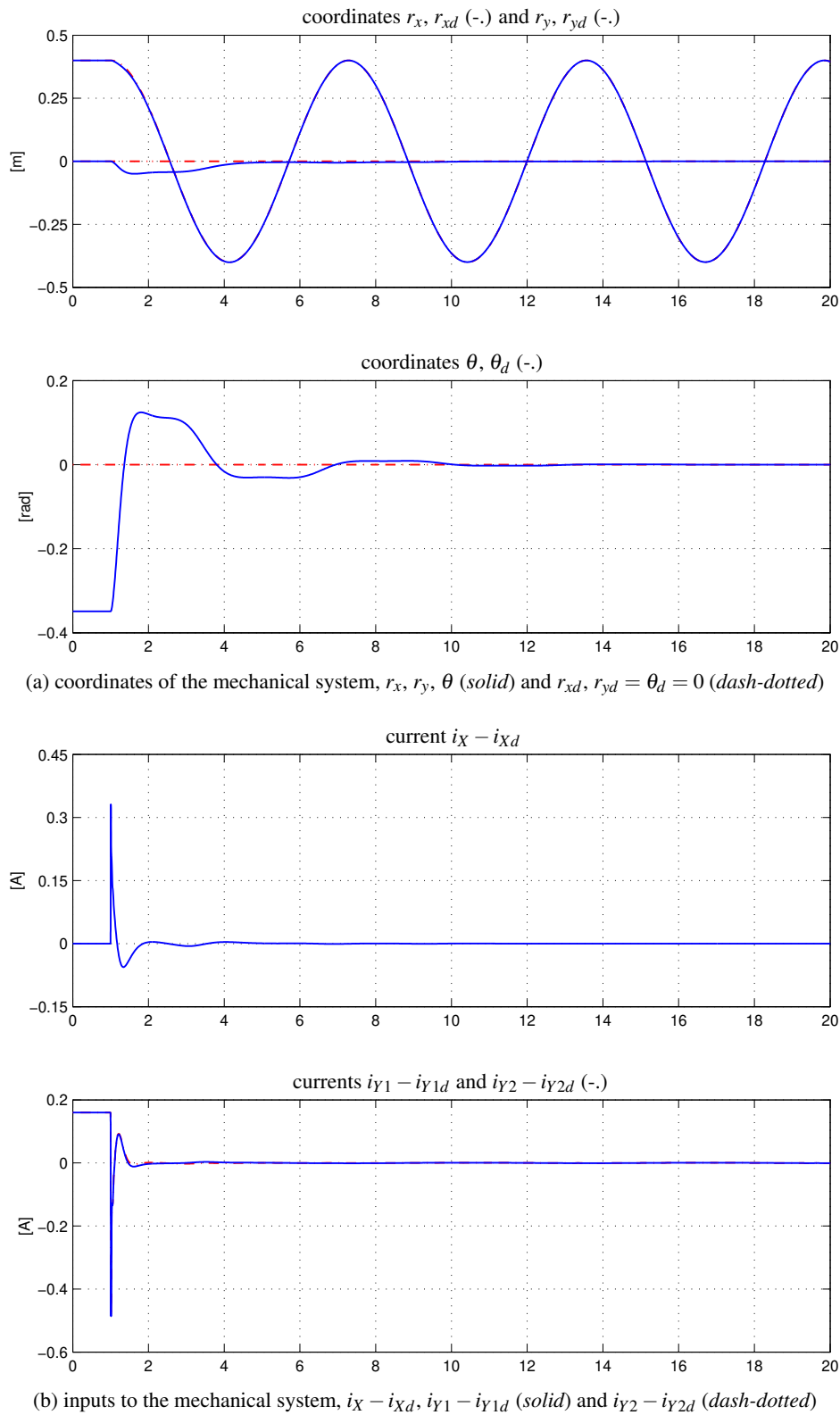


Figure 7.4: Tracking control of the H-drive system without friction; coordinates and inputs of the mechanical system

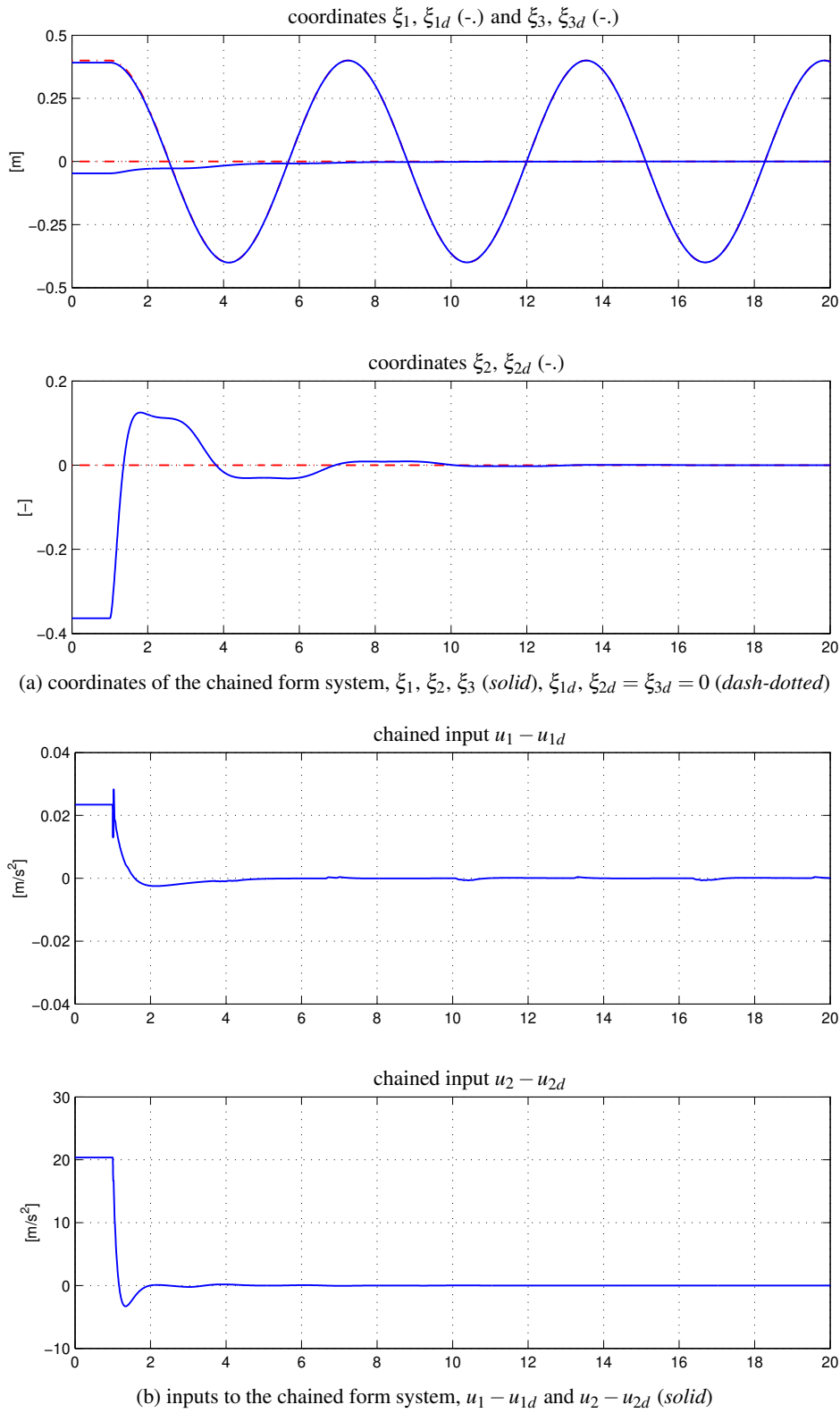


Figure 7.5: Tracking control of the H-drive system without friction; coordinates and inputs of the chained form system

k_5 and k_6 (high gain reduction). The high gains may, however, cause the system to approach the singularity of the coordinate and feedback transformation at $\theta = \pm\pi/2$ and the influence of the gains on the performance of the closed-loop system is not completely understood. In certain cases, increasing the gains k_5 and k_6 results in a smaller tracking error $\xi_3 - \xi_{3d}$ but, in general, this will also result in a larger tracking-error $\xi_2 - \xi_{2d}$. Similarly, increasing the gains k_3k_4 and $k_4 + k_4$ does not improve the performance since the ξ_3 -subsystem is not asymptotically stable anymore. Since the tracking-errors of $\xi_2 - \xi_{2d}$ and $\xi_3 - \xi_{3d}$ are coupled, simply increasing the gains may even result in larger tracking-errors. In other words, due to the backstepping procedure, a trade-off has to be made between the tracking-error in ξ_3 and the tracking-error in ξ_2 . Although the closed-loop system is not \mathcal{K} -exponentially anymore, the tracking-error dynamics are globally uniformly ultimately bounded (UUB), see Chapter 3, meaning that the tracking-errors remain bounded. Note that this UUB property only holds on a subspace \mathcal{C} where the coordinate transformation is well-defined.

The closed-loop system is more susceptible to static friction than to viscous friction in the rotational joint. This can be understood from the fact that the reference trajectory includes a desired value of zero for the orientation θ , and the magnitude of the viscous friction becomes smaller when the system is closer to the desired reference trajectory. The magnitude of the static friction remains the same even when the system is very close to the desired trajectory and only vanishes (in the model) for a zero angular velocity of θ .

7.5 Feedback Stabilization

This section is concerned with the feedback stabilization problem for the underactuated H-drive manipulator. In the simulations we wish to stabilize the joint position to the origin $(r_x, r_y) = (0, 0)$ and the link orientation to $\theta = 0$. The controller is given by

$$u_1 = -k_1 \xi_1 - k_2 \dot{\xi}_1 + h(\xi_1, \dot{\xi}_1, \xi_3, \dot{\xi}_3) \sin(t/\varepsilon) \quad (7.28)$$

$$u_2 = -k_3 k_4 \xi_2 - k_4 \dot{\xi}_2 - k_3 k_4 \frac{2(k_5 \xi_3 + k_6 \dot{\xi}_3)}{h(\xi_1, \dot{\xi}_1, \xi_3, \dot{\xi}_3)} \sin(t/\varepsilon), \quad (7.29)$$

where ξ denotes the state of the second-order chained form and the homogeneous norm $h(\xi_1, \xi_2, \xi_3, \dot{\xi}_3)$ is given by

$$h(\xi_1, \dot{\xi}_1, \xi_3, \dot{\xi}_3) = \sqrt{\xi_1^2 + \dot{\xi}_1^2 + |\xi_3| + |\dot{\xi}_3|}. \quad (7.30)$$

The controller parameters are chosen as

$$k_1 = 4, k_2 = 2\sqrt{2}, k_3 = 15, k_4 = 15, k_5 = 2, k_6 = 2, \varepsilon = 0.25.$$

The parameters k_1 and k_2 are the gains of the stabilizing part of the controller u_1 . These should not be chosen too large, since sufficient excitation of the ξ_1 -dynamics is needed in order to be able to stabilize the ξ_3 -dynamics. The most important parameters are k_3 , k_4 , k_5 and k_6 . The parameters k_3 and k_4 are the gains of the backstepping or high-gain approach, and should be chosen sufficiently large. It is not clear which magnitude is sufficient, however values $k_3 > 10$ and $k_4 > 10$ suffice. The parameters k_3 and k_4 determine the convergence of the link orientation, while k_5 and k_6 determine the convergence of the y -position of the unactuated link. Therefore, choosing k_5 and k_6 large will result in large control efforts u_2 . The frequency $1/\varepsilon$ has to be chosen sufficiently small. In simulation, values of $\varepsilon \leq 0.25$ work fine although the controller gains may be tuned to allow larger values of ε .

As in the case of tracking control, the gain-tuning procedure is complicated by the fact that the system should not only be asymptotically stable, but also the mechanical coordinates should also

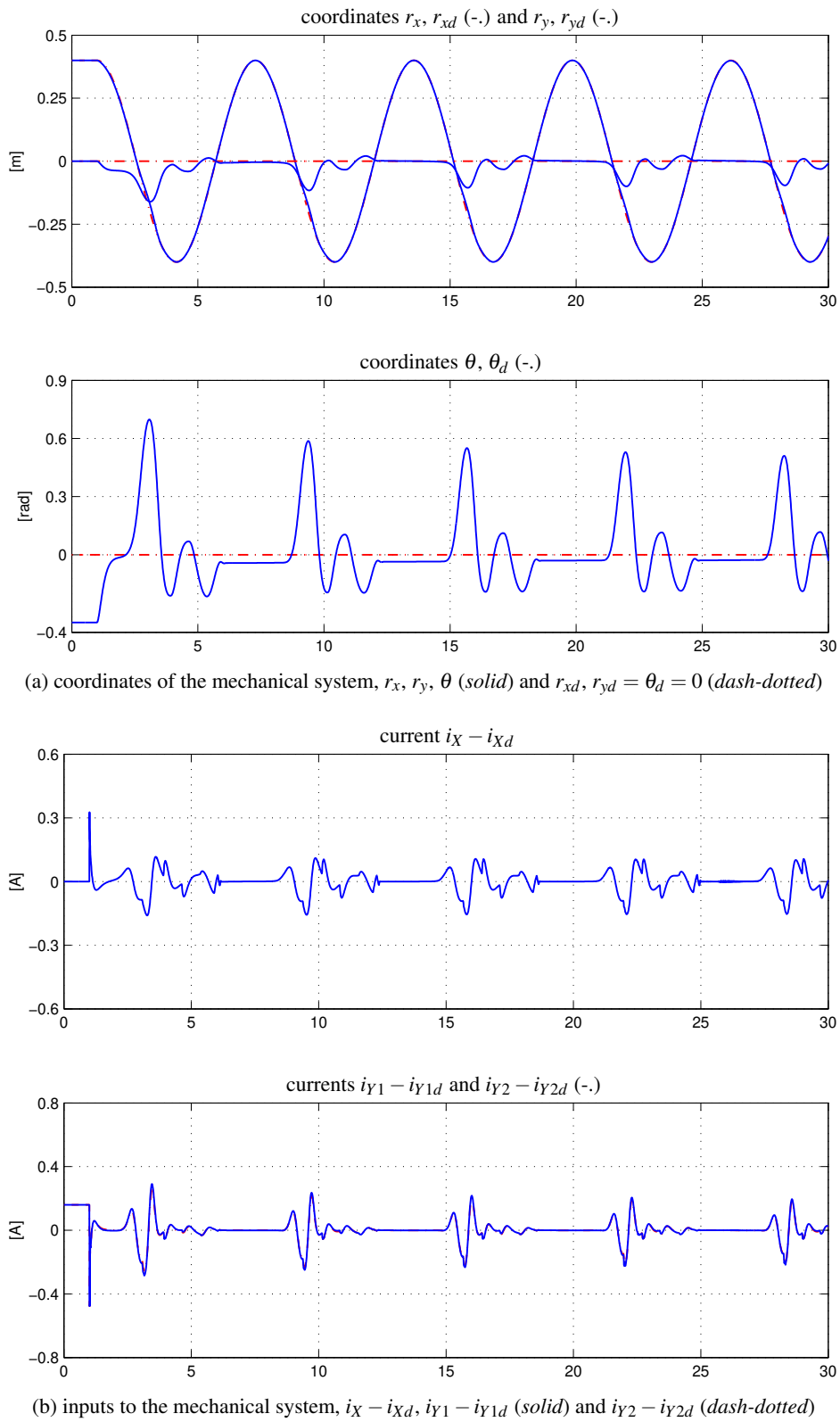
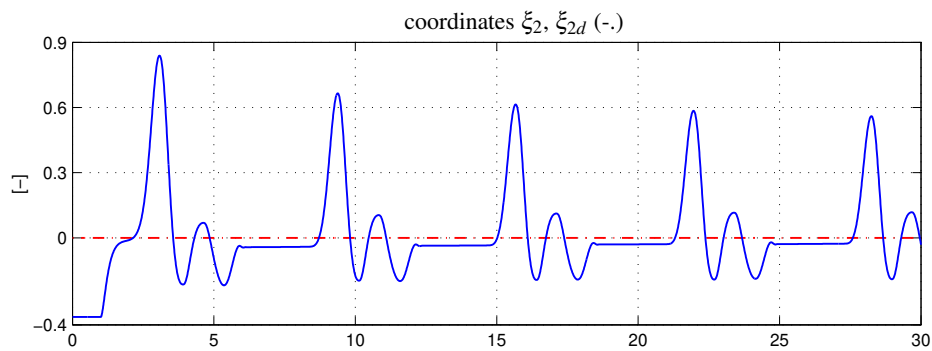
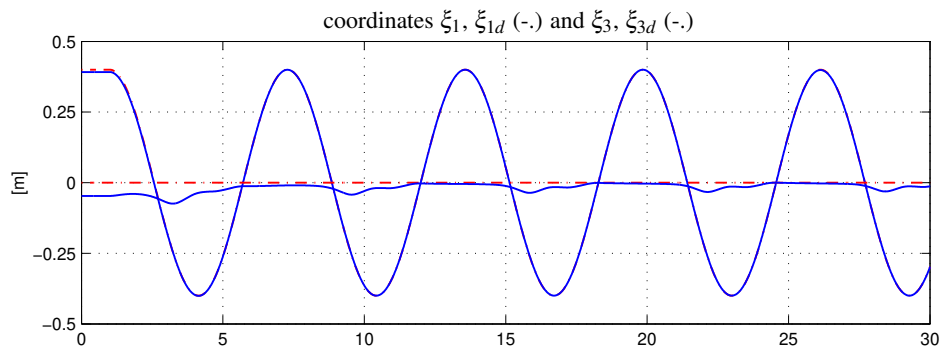
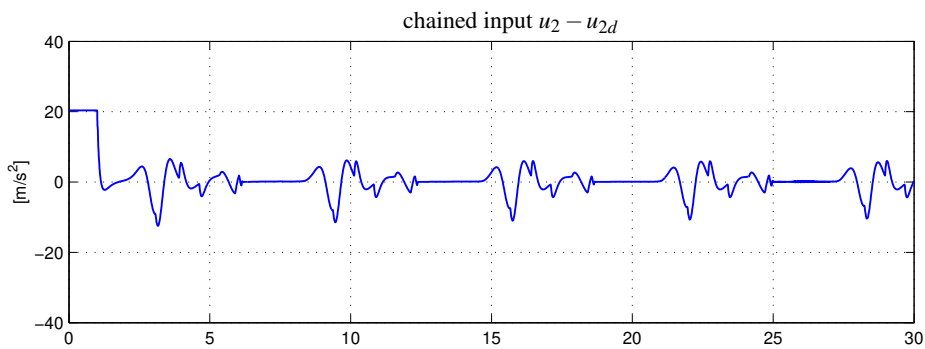
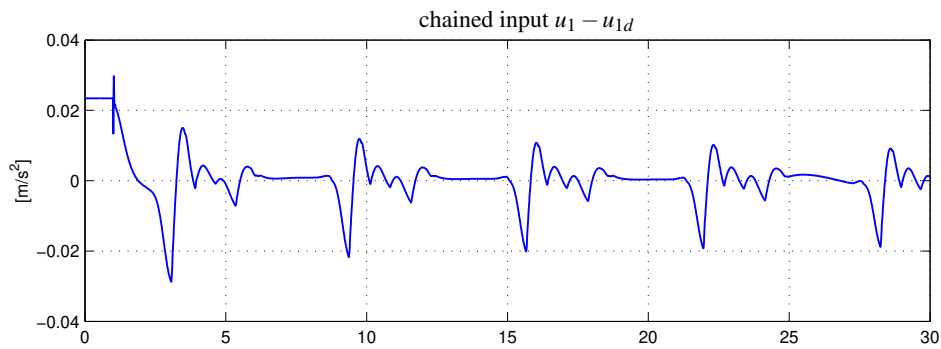


Figure 7.6: Tracking control of the H-drive system with friction; coordinates and inputs of the mechanical system



(a) coordinates of the chained form system, ξ_1, ξ_2, ξ_3 (solid) and $\xi_{1d}, \xi_{2d} = \xi_{3d} = 0$ (dash-dotted)



(b) inputs to the chained form system, $u_1 - u_{1d}$ and $u_2 - u_{2d}$ (solid)

Figure 7.7: Tracking control of the H-drive system with friction; coordinates and inputs of the chained form system

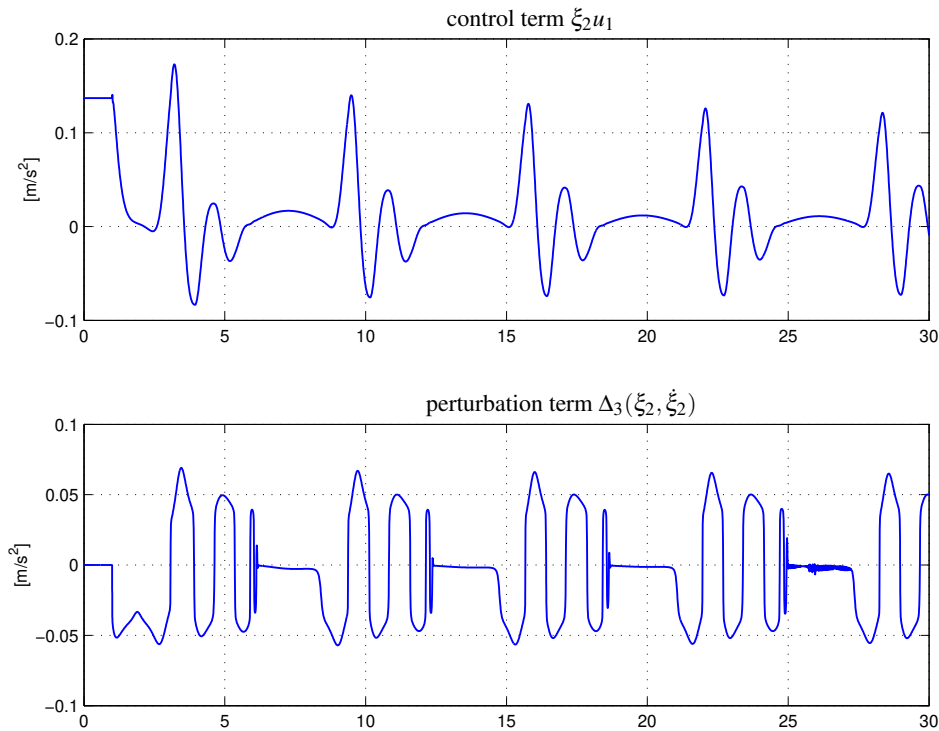


Figure 7.8: Tracking control of the H-drive system with friction; input $\xi_2 u_1$ and the frictional perturbation term $\Delta_3(\xi_2, \dot{\xi}_2)$ of the ξ_3 -dynamics, see (7.18)

remain inside a subspace of \mathbb{R}^n in which the coordinate transformation is valid. This means that choosing the controller gains to high, may result in the system passing through the singular point at $\theta = \pm\pi/2$ of the coordinate and feedback transformation.

7.5.1 Simulation without friction in the rotational link

We start by considering the situation in which the joint of the rotational link is frictionless. This means that coordinate- and feedback transformations bring the mechanical system into the extended chained form. The result of stabilizing the H-drive system with an initial condition given by $[r_x, r_y, \theta] = [0.2, 0.25, -25\pi/180]$ is shown in Figure 7.9. The mechanical system is successfully stabilized to the origin after approximately 40 seconds. The time-span of the plots is constrained to 40 second for clarity of the plots. After 40 seconds, the systems performs a small and damped oscillatory motion around the origin which vanishes asymptotically. Note that the control currents from the servo-loop are only sent to the H-Drive after one period $T = \pi/2$ of the time-varying part of the stabilizing controller. Disabling the control of the H-Drive before $t = \pi/2$ s allows us to check the initial value of the input currents.

The corresponding chained-form coordinates and inputs are shown in Figure 7.10. In Chapter 6 it was shown that the closed-loop system is ρ -exponentially stable with respect to the homogeneous norm

$$\rho(\xi_1, \dot{\xi}_1, \xi_3, \dot{\xi}_3) = \sqrt{\xi_1^2 + \dot{\xi}_1^2 + \xi_2^2 + \dot{\xi}_2^2 + |\xi_3| + |\dot{\xi}_3|}. \quad (7.31)$$

Therefore the homogeneous norm $h(x)$ (7.30), that is used in the controller (7.28), and the homoge-

neous norm $\rho(x)$ given in (7.31) have been shown in Figure 7.11 (a), from which we conclude that the homogeneous controller globally ρ -exponentially stabilizes the second-order chained-form.

Note that the convergence rate of the tracking controller is much faster than the convergence rate of the stabilizing controller. The tracking control problem was solved under the assumption that the trajectories to be tracked are persistently exciting. The designed tracking controller is a linear time-varying feedback controller of which its convergence rate is determined by the persistence of excitation condition. In the stabilization problem also a form of persistence of excitation is needed. After all, the systems considered in this thesis can not be stabilized by any smooth or even continuous time-invariant state-feedback and the system is uncontrollable for $u_1 = 0$. The designed stabilizing controller is a nonlinear controller with a time-varying part of which the amplitude depends on the magnitude of the state. This time-varying part is needed in order to be able to stabilize the system. However, the system becomes less persistently exciting as the system approaches the origin, i.e. the magnitude of the state becomes smaller and therefore also the magnitude of the time-varying part of u_1 . Therefore, it is not surprising that the convergence rate of the linear time-varying tracking controller is better than that of the homogeneous stabilizing controller.

7.5.2 Simulation with friction in the rotational link

If we include friction in the unactuated link, *e.g.* (7.22), the performance of the stabilizing homogeneous controller is considerably deteriorated. As can be seen from Figure 7.12, the closed-loop system is not asymptotically stable. In fact, the system goes into a stable 'limit-cycle' with an amplitude that is determined by the magnitude of the friction.

The corresponding chained coordinates and inputs are shown in Figure 7.13. It is clear that the system is not asymptotically stable. Due to the perturbation $\Delta_3(\xi_2, \dot{\xi}_2)$ the state ξ_3 does not converge to zero, but instead, it performs a periodic motion around zero. Because the time-varying parts of the homogeneous controllers (7.28) depend on the homogeneous norm, this results in the oscillatory behavior shown in the figure. In Figure 7.14, the values of the control term $\xi_2 u_1$ and the perturbation $\Delta_3(\xi_2, \dot{\xi}_2)$ of the ξ_3 -dynamics, *cf.* (7.18), have been plotted. The perturbation term $\Delta_3(\xi_2, \dot{\xi}_2)$ prevents the state ξ_3 from being stabilized to the origin. It should be noted that, similar to the tracking case, the coordinates ξ_2 and ξ_3 are coupled due to the backstepping approach. This means that the amplitude of the resulting "limit-cycle" can not be reduced by simply increasing the gains of the controller. In fact, since the ξ_3 -dynamics are perturbed by $\Delta_3(\xi_2, \dot{\xi}_2)$ there is a error in the stationary value of ξ_3 . By increasing the gains k_5 and k_6 it may be possible to reduce this error, however, only at the cost of increasing the magnitude of the oscillations in the ξ_2 -dynamics.

It is not surprising that the continuous time-varying homogeneous controller does not stabilize the system. Under the influence of friction in the joint of the rotational link, the perturbed second-order chained form is given by (7.17). It is clear that when u_1 and u_2 are of degree one with respect to some dilation, the system will not be homogeneous of degree zero with respect to the dilation with weight $r = (1, 1, 1, 1, 2, 2)$. Moreover, the system is not in strict-feedback form. Therefore, the averaging and backstepping results of Chapter 6 are not valid, and the homogeneous controller may not be a continuous stabilizer for the perturbed extended chained form.

At this point we have not included any simulations with the robust version, *i.e.*, the periodically updated version, of the homogeneous controller. First of all, the robust version is only robust with respect to a class of perturbations that does not include friction. In fact, from Proposition 6.2.1, it is known that the perturbations for which the periodically updates controller is robust, only include drift vector-fields $h_0(x, \varepsilon) = O(\|x\|)$, or in other words, every component of the drift vector-field satisfies $h_{0,i} = O(\|x\|^2)$, which is clearly not the case when including static friction in the model. As expected,

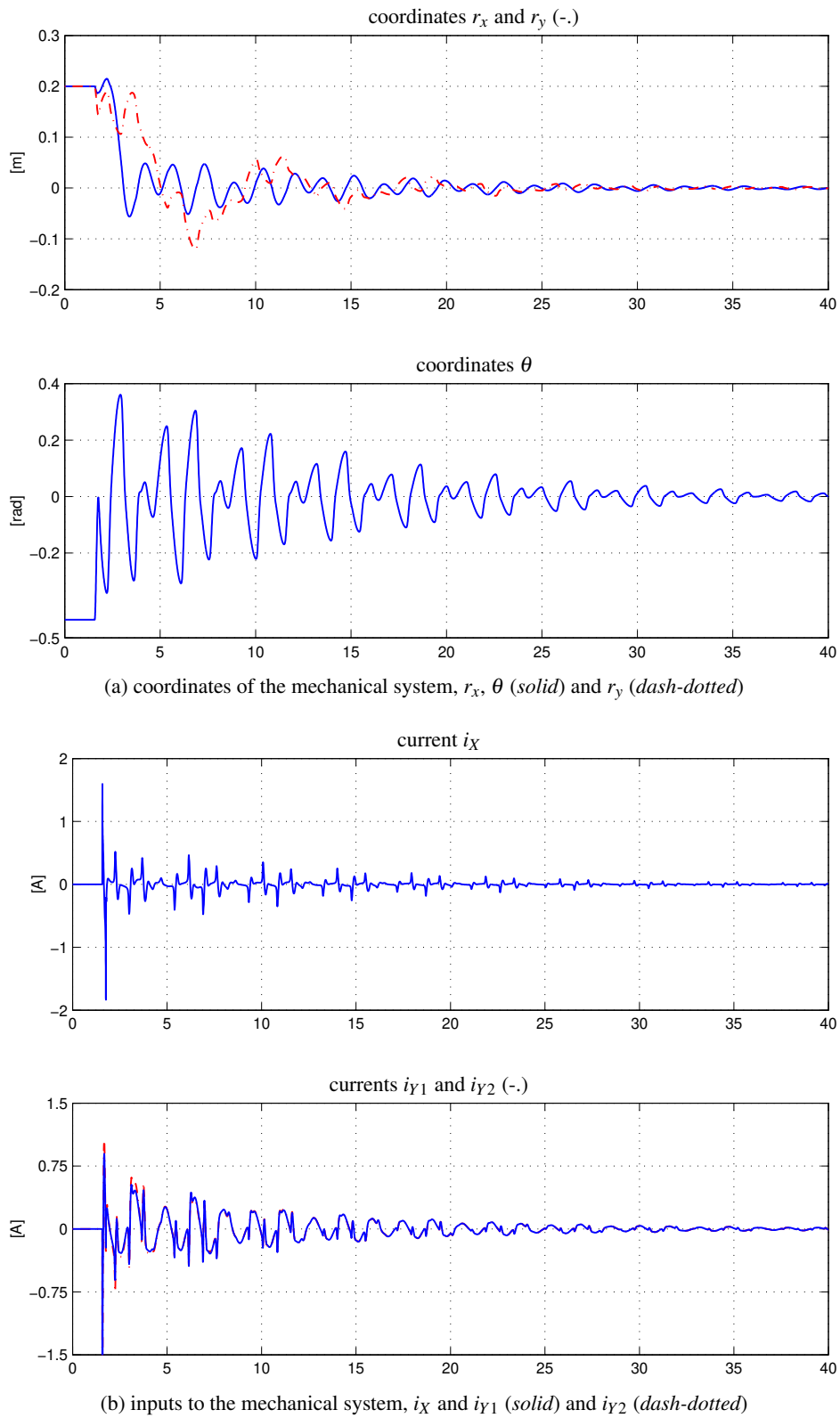


Figure 7.9: Stabilization of the H-drive system without friction; coordinates and inputs of the mechanical system

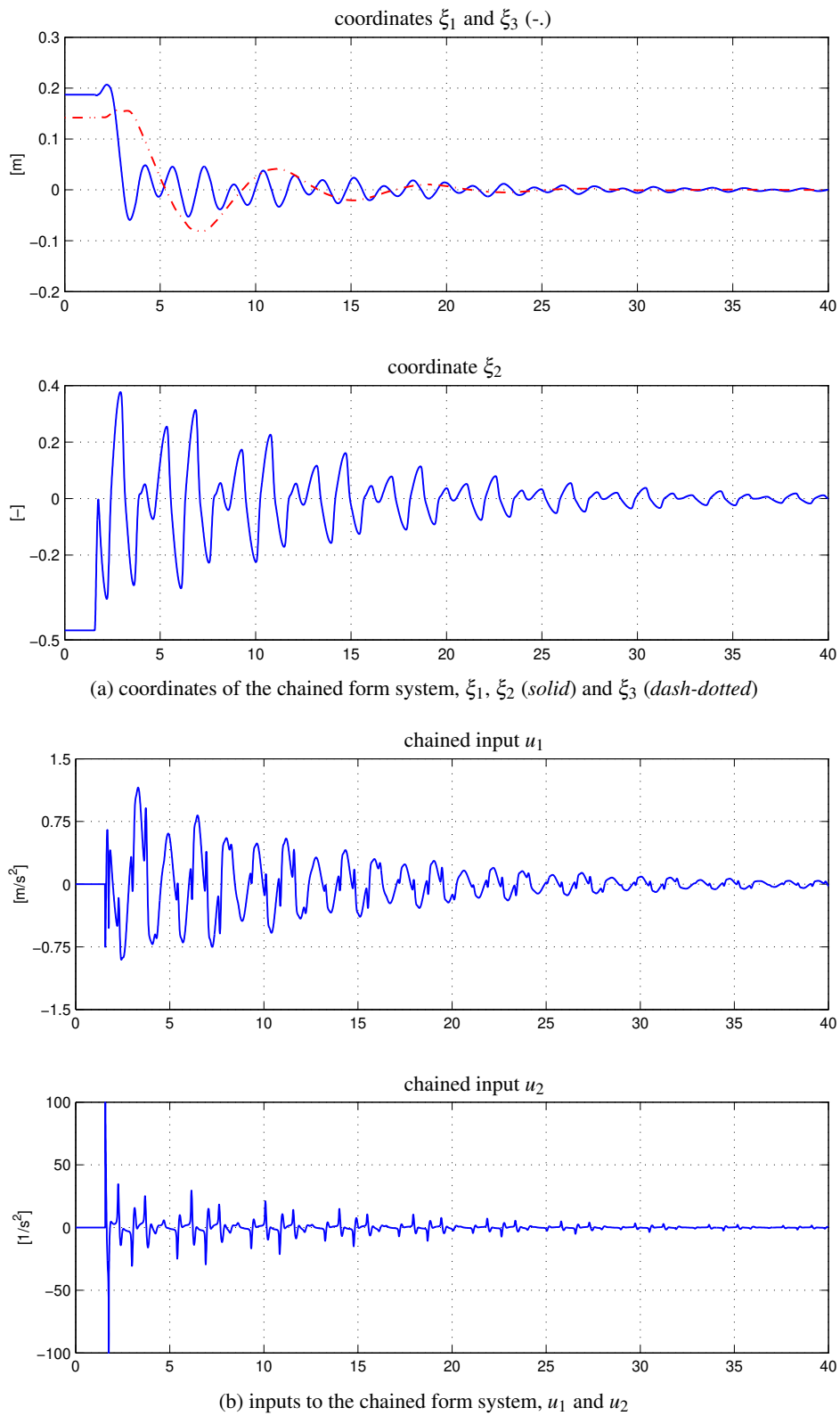


Figure 7.10: Stabilization of the H-drive system without friction; coordinates and inputs of the chained form system

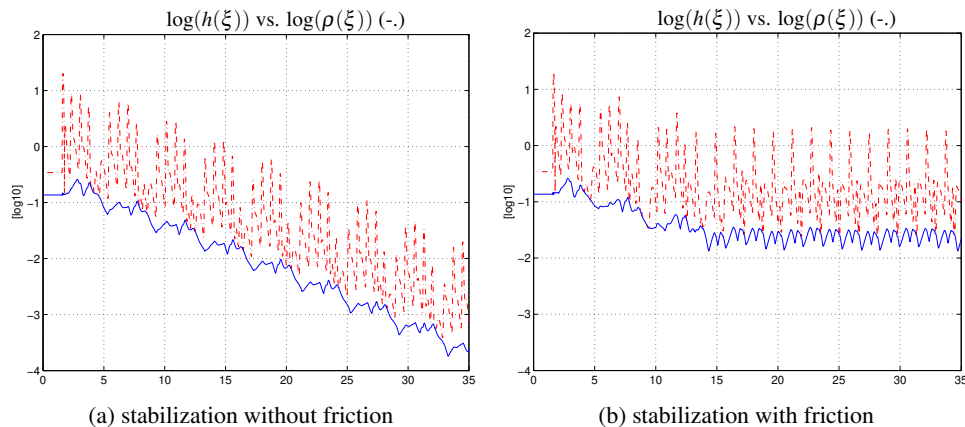


Figure 7.11: Stabilization of the H-drive system without friction (left) and with friction (right); logarithm of the homogeneous norms (7.30) (solid) and (7.31) (dashed)

the simulations with the robust homogeneous controller under the influence of friction did not show any improvement compared to the continuous homogeneous controller. Furthermore, the simulations showed that the convergence rate of the robust homogeneous controller is slightly worse than that of the continuous homogeneous controller.

7.6 Conclusions

We have presented controllers for both tracking and feedback stabilization of a second-order non-holonomic system. This second-order nonholonomic system consists of an underactuated H-drive manipulator. In the simulations, the performance of a linear time-varying tracking controller and a continuous periodic time-varying stabilizing controller has been investigated. The performance was tested with and without modelling friction in the joint of the rotational link.

The tracking controller yields \mathcal{K} -exponential convergence when the, to be tracked, trajectory of the frictionless link satisfies a persistency of excitation condition. If friction in the joint of the rotational link is modelled, the performance of the tracking controller is considerably reduced. In fact, the tracking-error dynamics are not even asymptotically stable, but the tracking errors remain bounded.

The homogeneous time-varying feedback stabilizer achieves ρ -exponentially stability of the closed-loop system without friction. If however, friction is included in the model, the closed-loop dynamics are not even asymptotically stable. The closed-loop system performs a periodic motion around the origin with an amplitude that is determined by the magnitude of the friction. The amplitude of these oscillations around the origin may or may not be reduced by increasing the gains. In some cases, the amplitude can be reduced, but in general, reducing the oscillations in one coordinate increases the oscillations in another coordinate. Moreover, the gains can not be increased too much, since the coordinate transformation is only valid for $\theta \in (-\pi/2, \pi/2)$ and this may lead to a singularity as the link orientation reaches $\theta = \pm\pi/2$.

Concluding, the numerical simulations have shown that in the absence of disturbances and unmodelled dynamics, such as friction or cogging, the controllers achieve the expected performance.

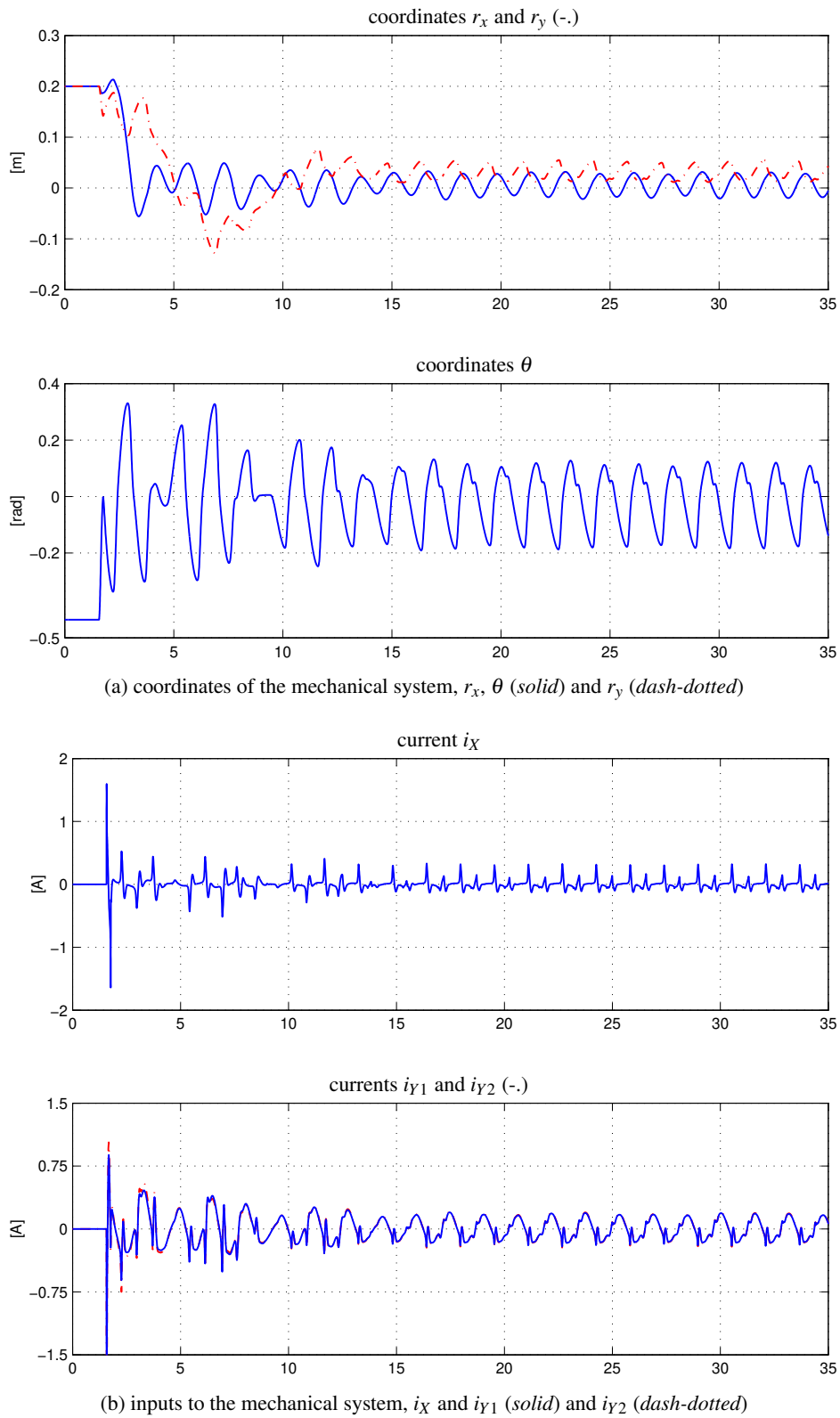


Figure 7.12: Stabilization of the H-drive system with friction; coordinates and inputs of the mechanical system

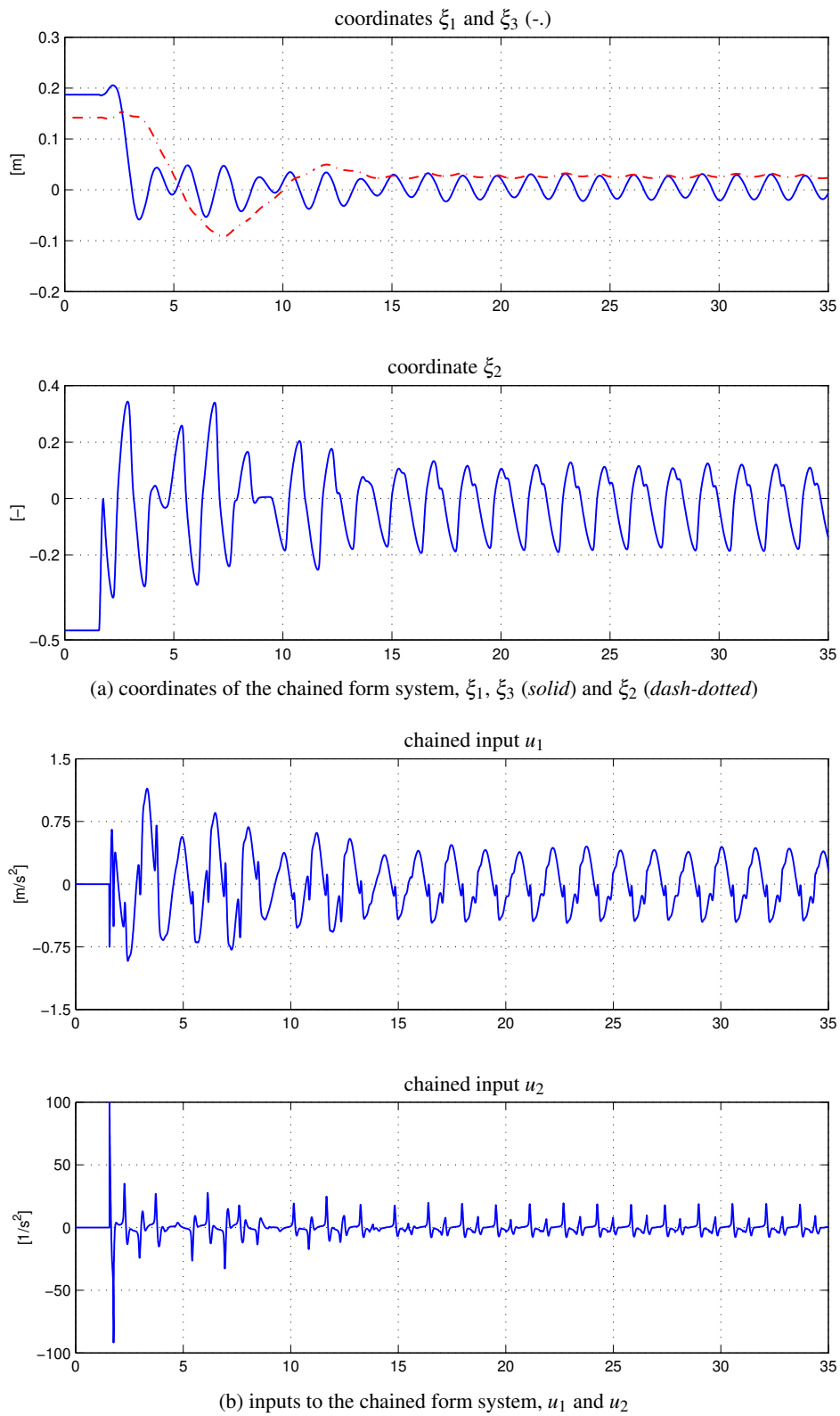


Figure 7.13: Stabilization of the H-drive system with friction; coordinates and inputs of the chained form system

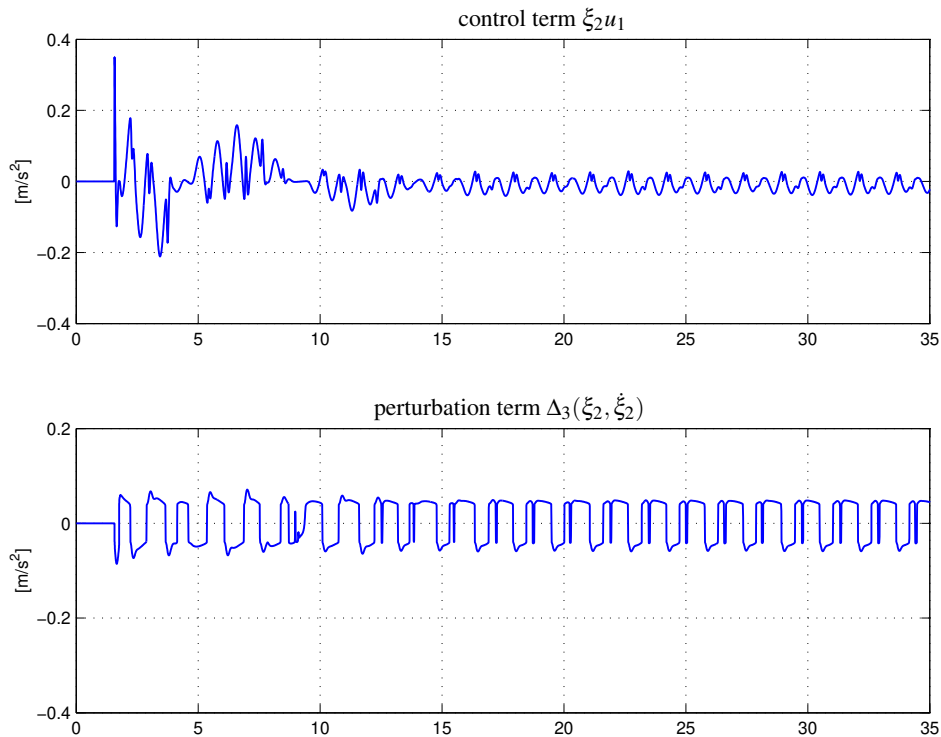


Figure 7.14: Stabilization of the H-drive system with friction; input $\xi_2 u_1$ and the frictional perturbation term $\Delta_3(\xi_2, \dot{\xi}_2)$ of the ξ_3 -dynamics, see (7.18)

However, if friction in the unactuated rotational link is included in the model, the performance is considerably deteriorated. In the case of tracking, the closed-loop dynamics are not globally exponentially stable. Instead, the friction term results in deviations from the desired trajectory. By performing numerical simulations with different friction parameters, it turns out that the closed-loop system is more susceptible to static friction than viscous friction in the rotational link. This is true in both the tracking and stabilization case. Therefore, in an experimental setup, the static friction should be minimized. In the following chapter, the performance of the tracking and stabilizing controllers will be verified by application to a real-life set-up of an underactuated H-Drive manipulator.

Experimental results

In this chapter, experimental results obtained with an underactuated H-Drive manipulator will be presented. The experimental setup consists of an H-Drive servo system that has been built by Philips' Centre for Industrial Technology (CFT) as part of an Advanced Component Mounter (ACM). This H-Drive servo system is now available in the laboratory of the Dynamics and Control Technology Group. The H-Drive servo system is shown in Figure 8.1. In order to obtain an underactuated system that can be used for experimental verification of tracking and stabilizing controllers, an additional rigid rotational link is attached on top of the LiMMS along the X-axis. This underactuated rotational link is shown in Figure 8.2. The angle of the link is measured using an ERO 1324 incremental rotary encoder manufactured by Haidenhain. This encoder outputs an incremental TTL signal and has 5000 linecounts. An additional GEL214-TN004 interpolator, manufactured by Lenord & Bauer, is used with an interpolation factor of 10 to increase the resolution to 50000 counts. The resulting TTL signal is used to obtain a readout in quarters of linecounts, giving the encoder a theoretical resolution of $3.14 \cdot 10^{-5}$ ($2\pi/200000$) radians per count. A dSPACE system in combination with Matlab/Simulink is used as a control system environment. The sampling rate of the system is set to a value of 4 kHz, higher sampling rates resulted in processor overrun errors.



Figure 8.1: The H-drive servo system.

In Figure 8.2 the unactuated rotational link is shown. The rotational link is attached to an aluminium plate that is attached on top of the LiMMS along the X-axis. It should be noted that the joint

connecting the link to the plate is passive, it has neither an actuator nor a brake, and the link rotates freely. The incremental encoder is contained in a cylinder located just below the plate. The link is suspended using a conventional ball-bearing. The size of the bearing was chosen to be as small as possible in order to reduce friction. The plate containing the link together with the ball-bearing and the incremental encoder can be easily removed. The only additional cable that is needed is a cable that transfers the encoder signal to the DSP and also supplies a voltage of 5 [V] from the DSP to the incremental encoder.

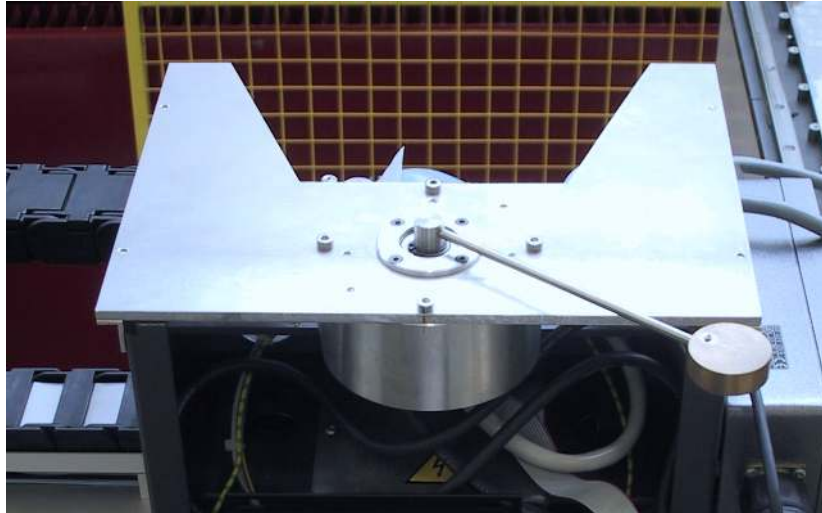


Figure 8.2: The unactuated rotational link.

At the tip of the link, an additional mass has been added to increase the mass m_3 and inertia $I = I_3 + m_3 l^2$ and, as a consequence, reduces the influence of the perturbation Δ_3 in (7.18). In the numerical simulations of the previous chapter it was shown that the r_y coordinate of the link, and its corresponding chained form coordinate ξ_3 , are the most difficult to control. This is caused by a perturbation term acting on the dynamics of the chained form coordinate ξ_3 . As can be seen from (7.18), the influence of the perturbation is reduced by either an increase of the mass m_3 or the length l between the joint and the center of mass (C.M.) of the link. By increasing the length of the link, the distance from the joint to the center of percussion C.P. will also be increased. The coordinate transformation that brings the system into the second-order chained form is based on the fact that a pure rotational motion of the link can be obtained by rotating the joint along a circle of radius λ around the center of percussion. If the distance λ , i.e. the distance from the joint to the C.P., is increased, larger motions of the joint will be needed in order to control the position and orientation of the link. The H-Drive, however, only has a limited workspace in which the X-axis and the Y-axes can move along a distance of approximately 50 and 100 centimeters, respectively. Therefore, in order to prevent too large excursions of the joint position $[r_x, r_y]$ during stabilization or tracking, we have chosen to constrain the length of the link to a rather small value of approximately 15 cm.

As in the previous chapter, the tracking and stabilizing controllers are implemented using a 'virtual internal model following control' approach. In this way, the servo-controllers can be used to compensate the effect of the cogging forces, reluctance forces and friction in the X and Y motors. Moreover, the servo-controllers compensate the distribution of the mass of the X-motor over the Y-motors. The

dynamics of the LiMMS are assumed to be identical, and the Y1- and Y2-axes are therefore controlled by the same servo-controller given in (C.6). These servo-controllers result in position- and acceleration errors smaller than $50 \mu\text{m}$ and 0.15 m/s^2 along the X-axis and Y-axes. In different applications, a servo-accuracy up to approximately $5 \mu\text{m}$ has been shown to be possible. In this thesis, however, no feed-forward loop has been implemented and it is expected that the servo-accuracy can be improved by adding feed-forward to the servo-controllers. In this thesis, no sensitivity analysis has been performed and it is not clear how the accuracy in the servo-loop affects the control of the link angle θ . From simulations that have been performed with friction in the LiMMS and the rotational joint, it follows that the influence of this servo-error along the X and Y axes is negligible compared to the effect of friction in the rotational joint.

The origin \mathcal{O} of the coordinate system is located at $(X, Y) = (-0.3, 0.5)$ (near the center of the H-drive setup) and the displacements r_x and r_y may be written as $r_x = (Y1 + Y2 - 1)/2$, $r_y = -X - 0.3$. The coordinate system of the resulting underactuated manipulator, is shown in Figure 7.2. Because the link is not actuated, but rotates freely, we obtain an underactuated mechanical system with three inputs, *i.e.*, the currents i_X , i_{Y1} and i_{Y2} to the motors, and four generalized coordinates, *i.e.*, the positions X, Y1, Y2 and the orientation θ of the link. Using the inputs currents to the X and Y motors, we wish to control the longitudinal position r_x and transversal position r_y of the rotational link, as well as its orientation θ . As mentioned earlier, the rotational link is connected to the X-motor with a ball-bearing and its dynamics are therefore influenced by friction. The nonholonomic constraint is thus given by

$$\lambda \ddot{\theta}(t) - \ddot{r}_x(t) \sin \theta(t) + \ddot{r}_y(t) \cos \theta(t) = \frac{\tau_{f,\theta}(\dot{\theta})}{m_3 l}, \quad (8.1)$$

where $\lambda = I/(m_3 l)$ equals the effective pendulum length of the rotational link and m_3 denotes the mass of the link and l denotes the distance between the joint and the center of mass of the link. The friction torque acting at the rotational joint is denoted by $\tau_{f,\theta}(\dot{\theta})$. In order to reduce the influence of the friction $\tau_{f,\theta}$, the product $\lambda(m_3 l) = I$ should be large. This justifies the placement of an additional mass at the tip of the link in order to increase the moment of inertia $I = I_3 + m_3 l^2$ about the vertical axis through the joint.

8.1 Parameter identification

Consider the underactuated H-Drive manipulator shown in Figure 7.2. The mass m_3 of the rotational link is much smaller than the masses of the LiMMS. Moreover, the X and Y motors are controlled by a servo-loop and the influence of the dynamics of the rotational link on the dynamics of the X-motor and Y-motors is assumed to be negligible. Therefore it suffices to consider the partially feedback linearized model given by (7.9), *i.e.*,

$$\begin{aligned} \ddot{r}_x &= v_x \\ \ddot{r}_y &= v_y \\ \ddot{\theta} &= \lambda (\sin(\theta)v_x - \cos(\theta)v_y) + \frac{\tau_{f,\theta}}{I}. \end{aligned} \quad (8.2)$$

The inputs v_x and v_y represent the desired accelerations along the r_x - and r_y -direction. These desired accelerations are integrated twice, in order to obtain desired positions for the X and Y motors, and the resulting position error is used as an input to the servo controllers (C.6). Note that the r_x coordinate is controlled by the two LiMMS along the Y-axes, while the r_y coordinate of the joint is controlled by the LiMMS along the X-axis. In the experiments it is thus assumed that the servo controllers compensate

all nonlinearities and perturbations like friction, cogging, reluctance forces and the distribution of the mass along the X-axis over the Y-axes. These servo controllers compensate the friction in the X and Y motors, however, the friction of the rotational link can not be compensated directly. The model to be identified and the corresponding coordinate and feedback transformation, needed to bring the system into the second-order chained form, then only depend on one parameter, *i.e.*, the parameter $\lambda = I/(m_3l)$.

8.1.1 The location of the Center of Percussion

The distance λ between the passive joint and the center of percussion (C.P.) of the free rotating link is the most important parameter in the proposed control design method. The coordinate transformation needed to transform the mechanical coordinates (r_x, r_y, θ) into the chained form coordinates (ξ_1, ξ_2, ξ_3) and to transform the chained form inputs u_1 and u_2 into the desired accelerations v_x and v_y is given in Section 7.2 and only depends on λ . Since λ equals the effective pendulum length of the link when treated as a rigid body pendulum suspended from the passive joint, its value can be obtained from the period T of the pendulum by the relation

$$\lambda = g \left(\frac{T}{2\pi} \right)^2 \quad (8.3)$$

with g denoting the gravitational acceleration. For the experimental underactuated H-Drive manipulator we obtain the parameter values $T = 0.745$ and $\lambda = 0.138$.

8.1.2 Linear least-squares identification

The parameter λ can also be identified by moving the X and Y motors along specified periodic trajectories and recording the angle θ of the link. Suppose that the friction $\tau_{f,\theta}$ can be approximated by a continuous model given by

$$\tau_{f,\theta} = -c_{v\theta} \cdot \dot{\theta} - c_{s\theta} \left(\frac{2}{\pi} \right) \arctan(100 \cdot \dot{\theta}). \quad (8.4)$$

The system is then linear in the parameters $p = [1/\lambda, c_{v\theta}/I, c_{s\theta}/I]^T$. We rewrite the system into the linear form $\ddot{\theta} = A(v_x, v_y, \theta, \dot{\theta})p$ as

$$\ddot{\theta} = \left[(\sin(\theta)v_x - \cos(\theta)v_y) \quad -\dot{\theta} \quad - \left(\frac{2}{\pi} \right) \arctan(100 \cdot \dot{\theta}) \right] p. \quad (8.5)$$

By performing sinusoidal motions $[r_{xd}(t), r_{yd}(t)]$ along the x and y direction and recording the positions r_x and r_y , the accelerations \ddot{r}_x and \ddot{r}_y can be obtained by differentiation. The resolution of the encoders of the LiMMS is sufficient high, and the level of the measurement noise is sufficiently low, to obtain reliable identification results without additional filtering. The acceleration $\ddot{\theta}$ can also be obtained by numerical differentiation, but this amplifies the measurement noise. Therefore, depending on the measurement data, it may be necessary to filter the acceleration signal with, for example, a fourth-order Butterworth filter. This filtering is done in forward and backward direction in order to obtain zero phase distortion.

By recording the link angle θ , differentiating twice and performing additional filtering, we can collect n samples and form a set of linear equations

$$\Phi \cdot p = y, \quad (8.6)$$

with unknown parameter vector $p = [1/\lambda, c_{v\theta}/I, c_{s\theta}/I]^T$ and

$$\Phi = \begin{bmatrix} A(v_x(t_0), v_y(t_0), \theta(t_0)) \\ A(v_x(t_1), v_y(t_1), \theta(t_1)) \\ \vdots \\ A(v_x(t_n), v_y(t_n), \theta(t_n)) \end{bmatrix} \quad y = \begin{bmatrix} \ddot{\theta}(t_0) \\ \ddot{\theta}(t_1) \\ \vdots \\ \ddot{\theta}(t_n) \end{bmatrix}$$

By selecting the sinusoidal trajectory such that the resulting matrix Φ is nonsingular, an estimate of the parameter vector p can be found by using the pseudo-inverse, *i.e.*,

$$p = \Phi^* y \quad (8.7)$$

where

$$\Phi^* = \Phi^T (\Phi \Phi^T)^{-1}.$$

Initially, we performed sinusoidal motions $r_x(t) = -0.3 \cos(\pi t)$ and $r_y(t) = -0.2 \cos(\pi t)$ in the x and y direction respectively. Using this trajectory, we identified the normalized inertia and friction parameters of the link, as well as the normalized parameters in the x and y direction. The obtained parameters are summarized below.

$$\lambda = 0.1364 \text{ [m]}, \quad c_{v\theta}/I = 0.1552 \text{ [1/(rad}\cdot\text{s)]}, \quad c_{s\theta}/I = 1.3185 \text{ [1/s}^2\text{]} \quad (8.8)$$

The viscous friction in the rotational joint is much smaller than the static friction. Assuming a link mass $m_3 = 0.04$ [kg] and a length $l = 0.15$ [m] between the joint and the center of mass of the link, *i.e.*, using the relation $I = (m_3 l) \lambda$, these parameters correspond to a viscous friction torque of about $0.12 \cdot 10^{-3}$ [Nms/rad] and a static friction torque of about $1.0 \cdot 10^{-3}$ [Nm].

Through numerical simulations it follows that the tracking and stabilizing controllers are more susceptible to the static friction torque in the rotational joint than to the viscous friction torque. In some initial tracking and stabilization experiments, it turned out to be very difficult to find control parameters for which the closed-loop system was stable and additionally, for which the system remained inside the workspace of the H-Drive. Therefore we tried to reduce the static friction in the rotational joint by removing all grease from the ball-bearing and replacing it with a different lubricant. This considerably reduced the static and viscous friction in the rotational joint, as will be seen in the sequel.

The link dynamics are not only influenced by friction but also by a gravitational torque resulting from a misalignment of the plane of rotation of the link with the horizontal plane, *i.e.*, the equipotential plane of gravity. The misalignment can be caused by flexibility inside the ball-bearing resulting in a misalignment of the axis of rotation, or from a misalignment of the plate that attaches the link to the LiMMS of the X-axis with the equipotential plane of gravity, see Figure 8.2. These perturbations result in a preference of the rotational link to rotate in the direction of the least potential energy. In the current experiments, this gravitational perturbation is compensated by stiction, resulting from the static friction in the link, and therefore does not influence the existence of equilibria. Additionally, the friction characteristic of the link may not be symmetric, *i.e.*, when rotating in the positive direction the magnitude of the friction torque may be larger than its magnitude when rotating in the negative direction. These perturbations can be understood from the following experiment. By performing a tracking experiment with the initially identified parameters and using the measured data resulted in the parameters given in Table 8.1. For completeness, we have also included the identified parameters m_x and m_y , denoting the effective mass in the direction of r_x and r_y , which have been used in the simulations of the previous chapter. The corresponding condition number and determinant of the information matrix Φ

| parameters | value | unit | parameters | value | unit |
|-----------------|--------|---------------------|-----------------|--------|-------------------|
| m_x/k_m | 0.3263 | $[A \cdot s^2/m]$ | m_y/k_m | 0.1406 | $[A \cdot s^2/m]$ |
| λ | 0.1373 | $[m]$ | I | 0.0008 | $[kg \cdot m^2]$ |
| $c_{v\theta}/I$ | 0.0217 | $[1/(rad \cdot s)]$ | $c_{s\theta}/I$ | 0.3320 | $[1/s^2]$ |

Table 8.1: Parameters of the dynamic model (7.14) of the underactuated H-Drive manipulator

are given by $\text{cond}(\Phi) = 9.62384$ and $\log_{10}(|\Phi|) = 7.7633$. This identification result shows that both the static and viscous friction torques have been considerably reduced by replacing the grease in the ball-bearing by a finer lubricant. The friction is reduced to a viscous friction torque of approximately $1.78 \cdot 10^{-5}$ [Nms/rad] and a static friction torque of approximately $2.73 \cdot 10^{-4}$ [Nm]. The measured and estimated acceleration and the identified friction torque (8.4) together with the residual friction torque given by

$$\ddot{\theta} - \frac{\sin(\theta)\ddot{r}_x - \cos(\theta)\ddot{r}_y}{\lambda_e} \quad (8.9)$$

where λ_e denotes the identified value of λ , are shown in Figure 8.3. It is clear from the figure that

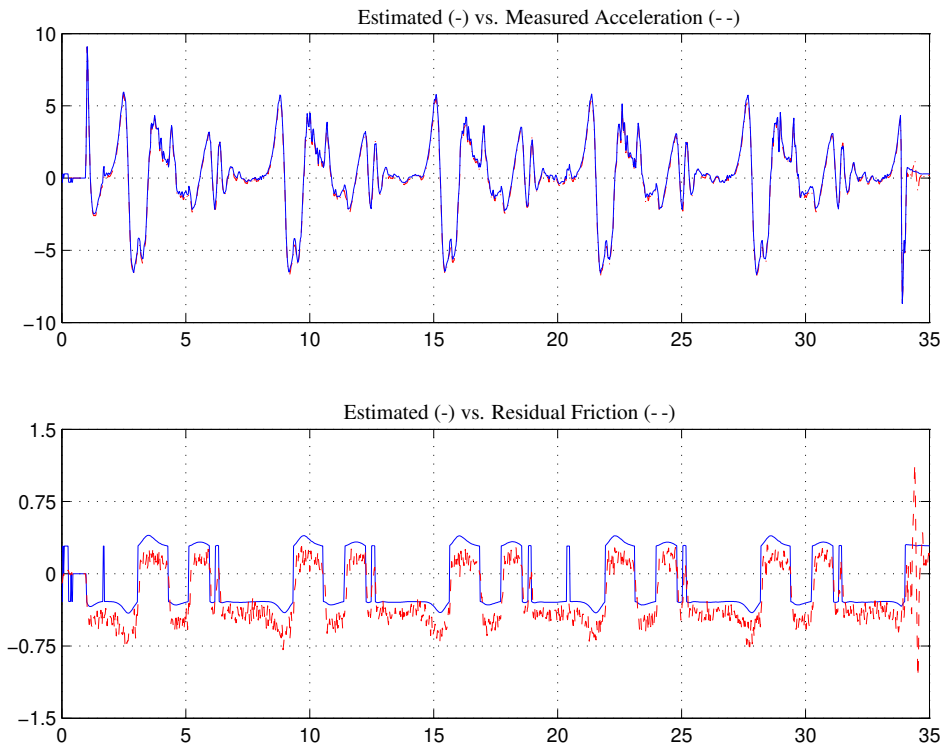


Figure 8.3: Identification of the symmetric friction characteristic (8.4)

an additional negative disturbance torque is present. This disturbance torque has a magnitude of approximately 0.1535 $[1/s^2]$ when normalized with respect to the inertia I or equivalently a magnitude of about $12.64 \cdot 10^{-5}$ [Nm]. It is expected that this identified friction characteristic is caused by a combination of gravitational perturbations, resulting from a misalignment of the plane of rotation of the link with the horizontal plane, and an asymmetric friction characteristic of the rotational joint.

In order to capture the gravitational perturbations it is necessary to identify a nonlinear friction model. Suppose that the plane of rotation of the link is misaligned with the horizontal plane by a rotation angle ϕ_x about the positive x -axis and an angle ϕ_y about the positive y -axis. The additional gravitational torque that is generated can be written as

$$\tau_{z,d} = -m_3gl(\cos(\theta)\sin(\phi_y) - \sin(\theta)\sin(\phi_x)) \quad (8.10)$$

where g denotes the gravitational acceleration. Since ϕ_x and ϕ_y are constants, the least-squares method can be used to identify this gravitational disturbance torque. An Extended Kalman Filter (EKF) can be used to identify the nonlinear friction characteristic of the link, including the Stribeck effect, in combination with the additional gravitational disturbance (8.10). This can be useful when it is possible to compensate the friction and gravitational disturbances in the rotational joint. This may be done by adding a small motor at in rotational joint of the link, that is only used to compensate the effect of perturbations.

Remark 8.1.1. Instead of adding an additional motor at the rotational joint to compensate the frictional and gravitational perturbations, which makes the system fully actuated, it might be possible to compensate the frictional disturbances by using the currents i_x and i_y to the LiMMS. In fact, by transforming the system to the second-order chained form given by (7.17), the perturbations affecting the ξ_1 - and ξ_2 -dynamics can be fully compensated provided that the friction characteristic as well as the gravitational disturbance torque are known. Because the chained states ξ_1 and ξ_2 correspond to the mechanical coordinates r_x and θ , respectively, this means that the perturbations affecting the dynamics of the longitudinal position $r_x(t)$ and the link orientation $\theta(t)$ can be compensated. In view of the results in Section 7.3, it is not yet clear whether the perturbations in the ξ_3 -dynamics or its corresponding transversal position r_y can be compensated using the input currents i_x and i_y to the LiMMS. As the linearization of the second-order chained form system around equilibrium points is not controllable, no compensation is possible at equilibrium points. Therefore, it is expected that compensation of the perturbations is not possible and no identification results that were obtained with an EKF will be presented.

8.2 Experiment with the Tracking Controller

The friction torque and the gravitational disturbance torque, acting in the joint of the rotational link, act as perturbations to the second-order chained form system. Therefore, we do not expect the tracking-error dynamics to be globally \mathcal{K} -exponentially or even asymptotically stable. However, we do expect the system to be uniformly ultimately bounded (UUB), meaning that the system moves along the trajectory with bounded tracking-errors.

In this section, the results of an experiment with the tracking controller is presented. In the experiment, we intend to stabilize the underactuated H-Drive manipulator to a persistently exciting trajectory given by (7.24). The parameters of this trajectory are selected as $r_1 = 0.35$, $r_2 = 0$ and $\omega = 0.5$. The resulting reference trajectory in mechanical coordinate and chained form coordinates is given by

$$\begin{aligned} r_{xd}(t) &= 0.4 \sin(t), & r_{yd}(t) &= 0, & \theta_d(t) &= 0 \\ \xi_{1d}(t) &= 0.4 \sin(t), & \xi_{3d}(t) &= 0, & \xi_{2d}(t) &= 0 \end{aligned} \quad (8.11)$$

The trajectory is thus persistently exciting, *i.e.*, (5.4) holds, and we can apply the tracking controller (7.26) to stabilize the system to the reference trajectory. The equations (8.11) represent a trajectory along the x direction in which the Y motors perform a sinusoidal motion with a frequency of $1/(2\pi)$

Hz while the angle of the link remains equal to zero. This trajectory can be thought of as representing a pendulum on which a varying gravitational field acts, *i.e.*, when the acceleration in the x direction is positive, the system acts as an inverted pendulum and when the acceleration in the x direction is negative, the system acts as a conventional pendulum. The gravitational field is maximal at the end-points of the trajectory and is zero at points where $r_x(t) = 0$.

Initially, it was very hard to find a set of control parameters for which the closed-loop tracking-error dynamics were uniformly ultimately bounded (UUB), see Definition 3.5.1 under the influence of the perturbations and, additionally, would keep the system within the boundary of the workspace. In fact, for some control parameters, the r_y coordinate would become too small and the system would reach the boundary near $r_y = -0.3$. In order to reduce the motion in the y direction, it is necessary to increase the damping in the ξ_3 -dynamics by choosing a large value k_6 . The control parameters are chosen as follows

$$k_1 = 4, k_2 = 2\sqrt{2}, k_3 = 40, k_4 = 9, k_5 = 5, k_6 = 100.$$

Before the start of the experiment, the system is initialized to the equilibrium point given by $[r_x, r_y, \theta] = [0, 0, -0.35]$, *i.e.*, the joint position error is zero and the link has an orientation error of approximately -20 degrees. The experiment is started after the servo-controllers have been enabled at time $t = 1$ [s]. The result of stabilizing the system to this trajectory is shown in Figures 8.4. In this figure, the tracking-error $r_x - r_{xd}$ is small and the difference between r_x and r_{xd} is hardly visible. The tracking-errors $r_y - r_{yd}$ and $\theta - \theta_d$ are larger and do not converge towards zero and thus imply that the tracking-error dynamics are not asymptotically stable. The system performs a periodic motion around the desired trajectory with a maximal deviation of 2.5 and 12 cm in the coordinates r_x and r_y respectively. The maximal deviation in the orientation $\theta(t)$ of the link is approximately 35 degrees. By comparing the experimental results in Figure 8.4 to the simulation results in Figure 7.6 it follows that the experimental result correspond well with the simulation results. The periodic motion due to the perturbations, around the periodic reference trajectory, is qualitatively the same and the maximal deviations are almost equal. The main difference between the experimental results and the simulation is visible in the currents $i_X - i_{X,d}$, $i_Y - i_{Y1,d}$ and $i_Y - i_{Y2,d}$. The currents in the experiment are generally larger and show the influence of un-modelled dynamics such as, cogging and measurement noise.

In Figure 8.5 the chained form coordinates and inputs have been shown. The tracking-errors of the chained coordinates reach their maximal values after the system has passed the point $r_x(t) = 0$ where $u_{1d}(t) = 0$. At this point the persistently exciting signal $u_{1d}(t)$ reaches its zero value and the tracking error of the ξ_3 coordinate increases. This induces an increase of the tracking error of ξ_2 , since the system uses the coordinate ξ_2 , *i.e.*, the virtual input in the backstepping procedure, to reduce the tracking errors in the ξ_3 coordinate. By comparing the experimental results in Figure 8.5 to the simulation results in Figure 7.7 it follows that the experimental results correspond well with the simulation results. The input $u_1 - u_{1d}$ corresponds very well to the simulation results. The main difference is visible in the input $u_2 - u_{2d}$. The input $u_2 - u_{2d}$ is influenced by measurement noise and quantization errors in the measurement of the link-angle θ . Since the damping has been increased by choosing a large value $k_6 = 100$, these measurement noise and quantization errors are amplified. The chained inputs $[u_1, u_2]$ are transformed into desired accelerations and integrated twice. Therefore, this amplification does not cause any problems because the integration step suppresses the high-frequent dynamics that are present in the desired accelerations. In order to improve the visibility of the signals, the inputs $[u_1, u_2]$ in Figure 8.5(b), have been filtered (off-line) using an 8th-order Butterworth filter with a cut-off frequency at 1 [kHz].

As expected from the simulation study, the main difficulty lies with stabilizing the r_y or, equivalently, the ξ_3 coordinates. The system tries to reduce the tracking error in the ξ_3 coordinate by

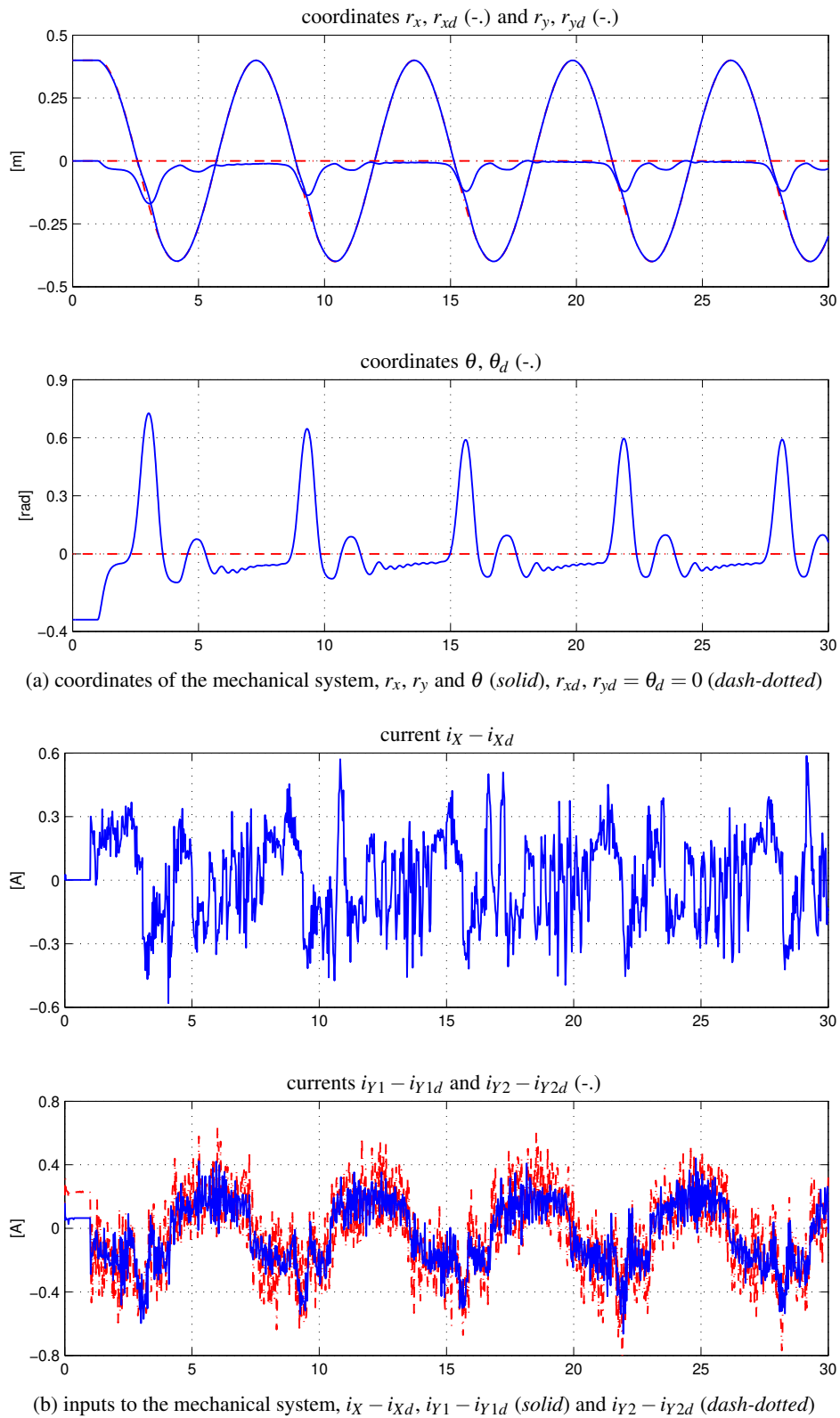


Figure 8.4: Tracking experiment of the underactuated H-Drive manipulator; coordinates and inputs of the mechanical system

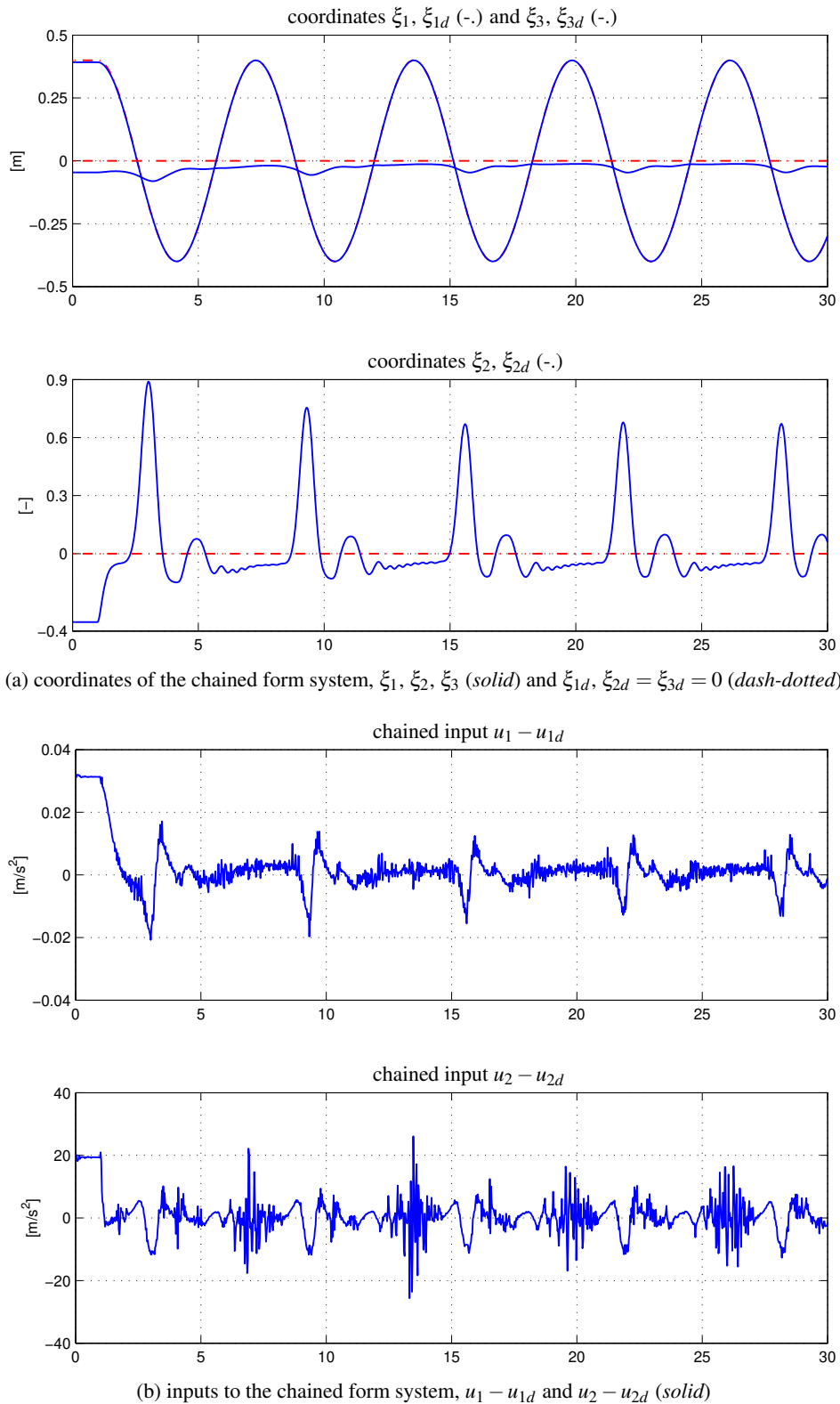


Figure 8.5: Tracking experiment of the underactuated H-Drive manipulator; coordinates and inputs of the chained form system

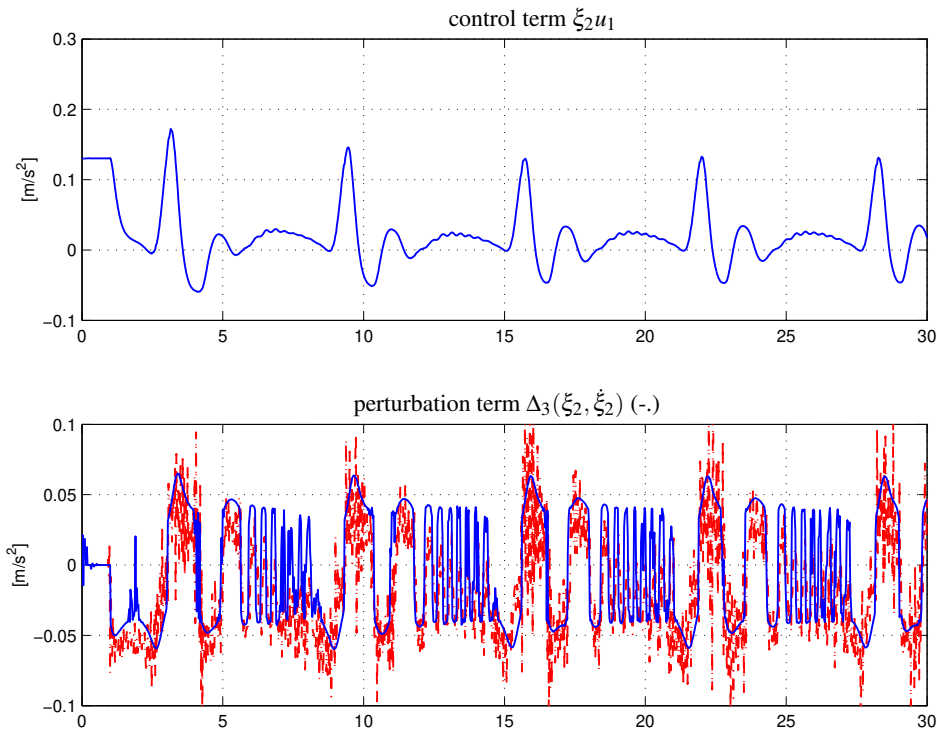


Figure 8.6: Tracking experiment of the underactuated H-Drive manipulator; input $\xi_2 u_1$ and the perturbation $\Delta_3(\xi_2, \dot{\xi}_2)$ (dashed) versus the estimated perturbation $\hat{\Delta}_3(\xi_2, \dot{\xi}_2)$ using the friction characteristic (8.4) with $c_v = 0.1$ and $c_s = 0.3$

performing a periodic motion in which the link orientation $\theta(t)$ acts as a virtual input in the backstepping approach. The perturbation term Δ_3 given in (7.17) prevents the state ξ_3 from converging to the origin. The system thus goes into a stable limit cycle with an amplitude that is determined by the magnitude of the friction. In Figure 8.6, the perturbation term $\Delta_3 = \ddot{\xi}_3 - \xi_2 u_1$ of the perturbed chained form system is shown together with the estimated perturbation $\hat{\Delta}_3$. The estimated perturbation $\hat{\Delta}_3$ is obtained from (7.18) by assuming a continuous symmetric friction characteristic (8.4) with friction parameters given by $c_v = 0.1$ and $c_s = 0.3$. The difference between the actual and estimated value of Δ_3 are caused by a gravitational disturbance torque, measurement noise and the fact that the friction characteristic can not be perfectly modelled by (8.4). To check whether the unactuated link is influenced by a gravitational disturbance torque, the experiment has been repeated with a positive initial angle. If the friction characteristic of the rotational link is symmetric and no gravitational disturbance torque is present, then the response of the system should show a similar behavior, but mirrored with respect to the time-axis. It turns out that if we repeat the experiment with a positive initial angle $\theta(0) = 20$ degrees, then the system still ends up in the lower-half of the workspace ($r_y < 0$), similar to the case with a negative initial angle $\theta(0)$. This is an indication that the link dynamics are influenced by an additional gravitational disturbance torque.

The errors in position and acceleration of the low-level servo-loop are shown in Figure 8.7. The position errors are in the order of magnitude of $50 \text{ } [\mu\text{m}]$ and the acceleration errors are in the order of magnitude of $0.1 \text{ } [\text{m/s}^2]$. These acceleration-errors may be reduced by adding feed-forward or a cogging compensator to the servo-loop. However, based on numerical simulations with comparable

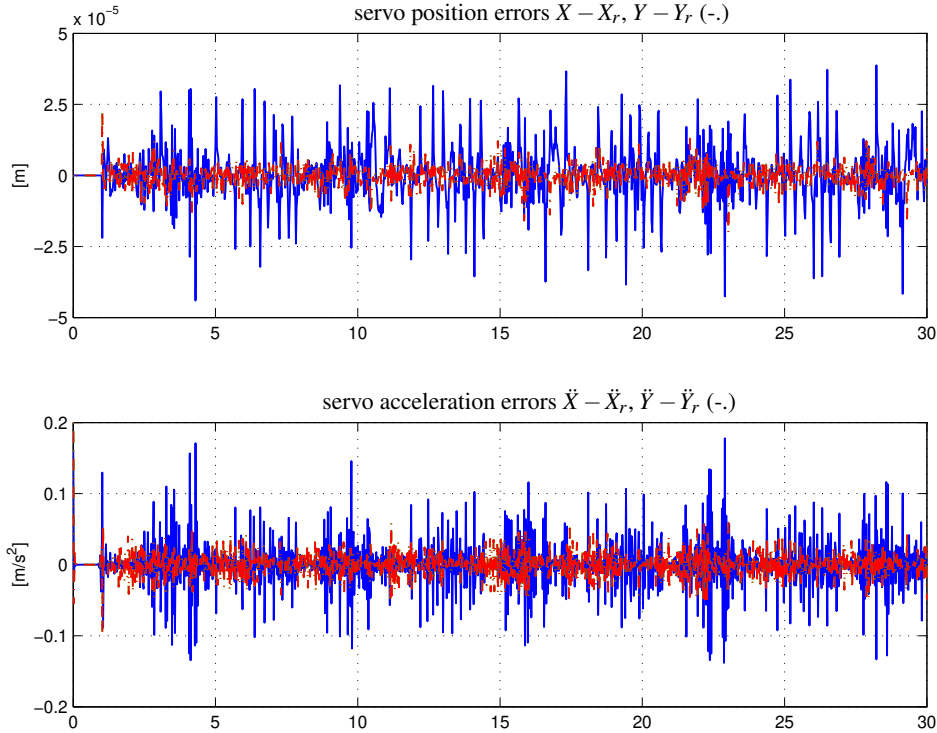


Figure 8.7: Tracking experiment of the underactuated H-Drive manipulator; position and acceleration errors in the servo control loop

acceleration-errors, we do not expect smaller acceleration-errors to improve the control performance.

Remark 8.2.1. An important question that might be asked is how to improve the performance of the controller. First of all, the performance may be improved by additional gain tuning in which the control parameters of the tracking controller, as well as the servo-controllers, are fine-tuned to improve performance by reducing the tracking and/or stabilization errors. By increasing the proportional gain k_5 , it is possible to reduce the tracking error in the transversal position r_y or its corresponding chained state ξ_3 . However, in most cases, this results in larger deviations from zero in the link angle $\theta(t)$ or the chained state ξ_2 . Therefore, the tuning of the controller gains should be a subject of further research. Secondly, the performance may be improved by increasing the product $m_3 l$ by increasing either the mass m_3 or the length l , or both. Since the workspace of the H-Drive is limited we would like to maintain the same length l , and only increase the mass m_3 by adding a larger weight at the tip of the link. A problem which occurs is that this additional weight also increases the effect of gravitational disturbance torques acting in the rotational joint. Finally, the performance of the controller can be improved by reducing the friction and gravitational perturbation torques acting in the rotational joint. This would require the use of either a magnetic bearing or an air-bearing.

8.3 Experiment with the Homogeneous Stabilizing Controller

In the following experiment, we consider the stabilization problem for the underactuated H-Drive manipulator. The system is to be stabilized to the origin $[r_x, r_y, \theta] = [0, 0, 0]$. Since the homoge-

neous stabilizing controller has been designed under the assumption that no perturbations, such as friction and gravitational torques, act on the system, we do not expect the system to be globally ρ -exponentially stable. Instead, we aim at achieving a form of practical stability in which the system stays sufficiently close to the origin. In the simulations, the closed-loop system was shown to exhibit a form of limit-cycling behavior under the influence of friction in the rotational link. In the experiments, besides friction and the fore-mentioned gravitational disturbance torques, we also expect to have perturbations such as measurement noise, quantization errors from the link angle encoder, numerical errors resulting from differentiation and filtering of signals, delays from the dSPACE system including the amplifier and cables and accelerations errors in the servo-loop. It is assumed that friction, cogging and reluctance forces in the LiMMS are completely compensated by the servo-loop. By achieving a form of practical stability, it may be possible to bring the system into a stable motion around the desired equilibrium point.

Before the start of the experiment, the system is initialized to the equilibrium point given by $[r_x, r_y, \theta] = [0.20, 0.20, -0.36]$. This corresponds to an initial joint error of 20 cm in each direction and an initial link orientation error of approximately -20 degrees. The stabilizing homogeneous controller is given by (cf. (7.28)),

$$\begin{aligned} u_1 &= -k_1 \dot{\xi}_1 - k_2 \ddot{\xi}_1 + \sqrt{\dot{\xi}_1^2 + \ddot{\xi}_1^2 + |\dot{\xi}_3| + |\ddot{\xi}_3|} \sin(t/\varepsilon) \\ u_2 &= -k_3 k_4 \dot{\xi}_2 - k_4 \ddot{\xi}_2 - k_3 k_4 \frac{2(k_5 \dot{\xi}_3 + k_6 \ddot{\xi}_3)}{\sqrt{\dot{\xi}_1^2 + \ddot{\xi}_1^2 + |\dot{\xi}_3| + |\ddot{\xi}_3|}} \sin(t/\varepsilon). \end{aligned} \quad (8.12)$$

The control parameters are equal to those in the simulations and given by

$$k_1 = 4, k_2 = 2\sqrt{2}, k_3 = 15, k_4 = 15, k_5 = 2, k_6 = 2, \varepsilon = 0.25.$$

In Figure 8.8 we have shown the result of stabilizing the system with the homogeneous controller. The simulation is only started after one complete period $T = 2\pi\varepsilon$ of the time-varying part of the controllers. At $t = \pi/2$ the servo-controllers are enabled and the system tries to stabilize the system. The coordinate r_x oscillates around the origin with an amplitude of approximately 2.5 cm and the coordinate r_y oscillates around an average value of approximately -3 cm with an amplitude of approximately 2.5 cm. The orientation $\theta(t)$ of the link oscillates around the origin with an amplitude of 11 degrees.

By comparing the experimental results in Figure 8.8 to the simulation results in Figure 7.12 it follows that the experimental results correspond well with the simulation results. The results are qualitatively the same, but the magnitude of the signals are different. Until the time-instant of approximately $t = 12$ [s] the results are similar, but after that time-instant the coordinate r_y becomes negative while it became positive in the simulations. Additionally, the maximal deviation in the link-angle θ is approximately 10 degrees smaller in the positive direction and approximately equal in the negative direction. This is an indication that the system is also influenced by an additional gravitational disturbance torque. After approximately $t = 20$ [s], the system performs a periodic motion around the origin with slightly larger deviations than in the simulation. The currents i_x , i_{y1} and i_{y2} correspond quite well with the qualitative results that were obtained in numerical simulation. The currents are, however, larger than the values in simulation. This is caused by the influence of un-modelled dynamics such as, cogging and measurement noise.

The chained form coordinates and inputs are shown in Figure 8.9. It is clear that the system is neither asymptotically stable, nor ρ -exponentially stable. Instead, the system performs a periodic motion or limit cycle around the origin. At approximately $t = 20$ [s] the coordinate ξ_3 has converged to a nearly constant negative value. In the simulations, the chained coordinate ξ_3 converged to a

nearly constant and positive value. This is an indication that the system is influenced by an additional gravitational torque and the friction characteristic can not be modelled by the simplified characteristic that is used in the simulations. The perturbation Δ_3 can not be compensated and prevents the ξ_3 coordinate from converging to zero. The amplitude of the resulting limit-cycle is determined by the magnitude of the perturbation Δ_3 and the controller gains. Note that the servo controllers do not compensate the perturbations Δ_1 and Δ_2 resulting from the friction in the rotational joint. The perturbations Δ_1 and Δ_2 are only suppressed by the time-invariant part of the stabilizing controllers.

In Figure 8.10 the input $\xi_2 u_1$ is shown and the perturbation Δ_3 has been plotted together with the estimated perturbation $\hat{\Delta}_3$. The estimated perturbation $\hat{\Delta}_3$ is obtained from (7.18) by assuming a continuous symmetric friction characteristic (8.4) with friction parameters given by $c_v = 0.1$ and $c_s = 0.3$. The input $\xi_2 u_1$ tries to increase the value of ξ_3 but does not compensate for the perturbation Δ_3 that prevents convergence of the state ξ_3 to zero. In Figure 8.10 it is clear that the system is influenced by an additional gravitational disturbance torque and, additionally, the friction characteristic may not be symmetric. This gravitational disturbance torque is negative as could be expected from the parameter identification procedure at the beginning of this chapter.

The homogeneous norms $h(x)$ given in (7.30) and $\rho(x)$ given in (7.31) of the second-order chained form system are shown in Figure 8.14(a). The system is clearly not asymptotically stable, however it is uniformly ultimately bounded.

8.4 A heuristic modification of the stabilizing controller

The convergence of the chained coordinate ξ_3 towards the origin can be improved by increasing the gains k_5 and k_6 of the controller. Although the deviation of the coordinate ξ_3 from zero is decreased, the oscillations in the chained coordinate ξ_2 that acts as a virtual input in the backstepping approach, are increased. An additional problem that occurs when increasing the gains k_5 and k_6 is the fact that the quantization errors and measurement noise of the incremental rotary encoder that measures the link angle $\theta(t)$ are amplified. In situations where the homogeneous norm $\sqrt{x_1^2 + x_2^2 + |x_5| + |x_6|}$ becomes small, the gains multiplying ξ_5 and ξ_6 become even larger. These amplified disturbances prevent the system from remaining close to the origin, since they induce high-frequency oscillations in the control inputs u_1 and u_2 , as well the input currents i_X and i_Y . The effect is more noticeable in the currents i_{Y1} and i_{Y2} since, for small angles θ , the dependence of these inputs on the angular velocity $\dot{\theta}$ is larger than in the input i_X , see (7.11). In order to prevent the gains from becoming too large near the origin, we modify the homogeneous stabilizing controller as follows

$$\begin{aligned} u_1 &= -k_1 \xi_1 - k_2 \dot{\xi}_1 + \sqrt{\xi_1^2 + \dot{\xi}_1^2 + |\xi_3| + |\dot{\xi}_3|} \sin(t/\varepsilon) \\ u_2 &= -k_3 k_4 \xi_2 - k_4 \dot{\xi}_2 - k_3 k_4 \frac{2(k_5 \xi_3 + k_6 \dot{\xi}_3)}{\max(M, \sqrt{\xi_1^2 + \dot{\xi}_1^2 + |\xi_3| + |\dot{\xi}_3|})} \sin(t/\varepsilon). \end{aligned} \quad (8.13)$$

The control parameters are selected as

$$k_1 = 4, k_2 = 2\sqrt{2}, k_3 = 15, k_4 = 15, k_5 = 9, k_6 = 6, \varepsilon = 0.25, M = 1,$$

showing that we have increased the gains k_5 and k_6 and lower bounded the denominator in the expression of u_2 . This modification affects the convergence of the controller, in the sense that the proof of asymptotic stability, given in Chapter 6 is not valid anymore. In fact, the closed-loop system is not

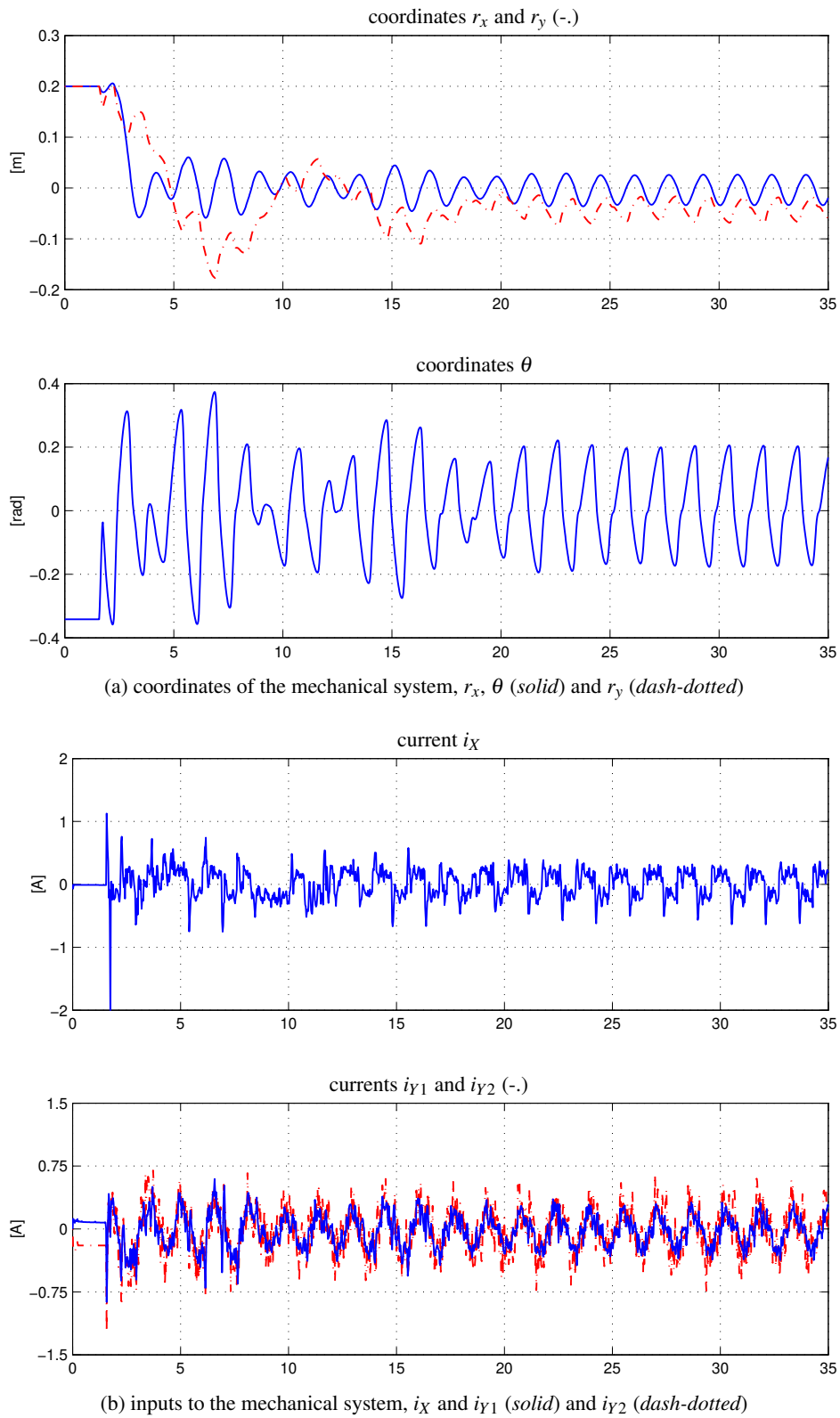


Figure 8.8: Stabilization experiment of the underactuated H-Drive manipulator; coordinates and inputs of the mechanical system

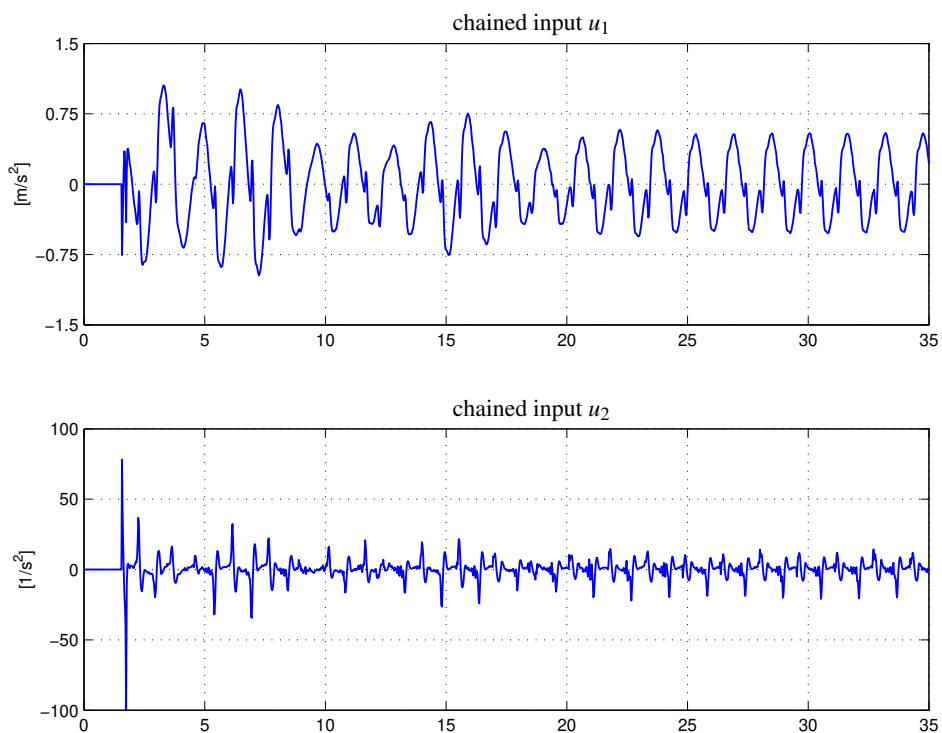
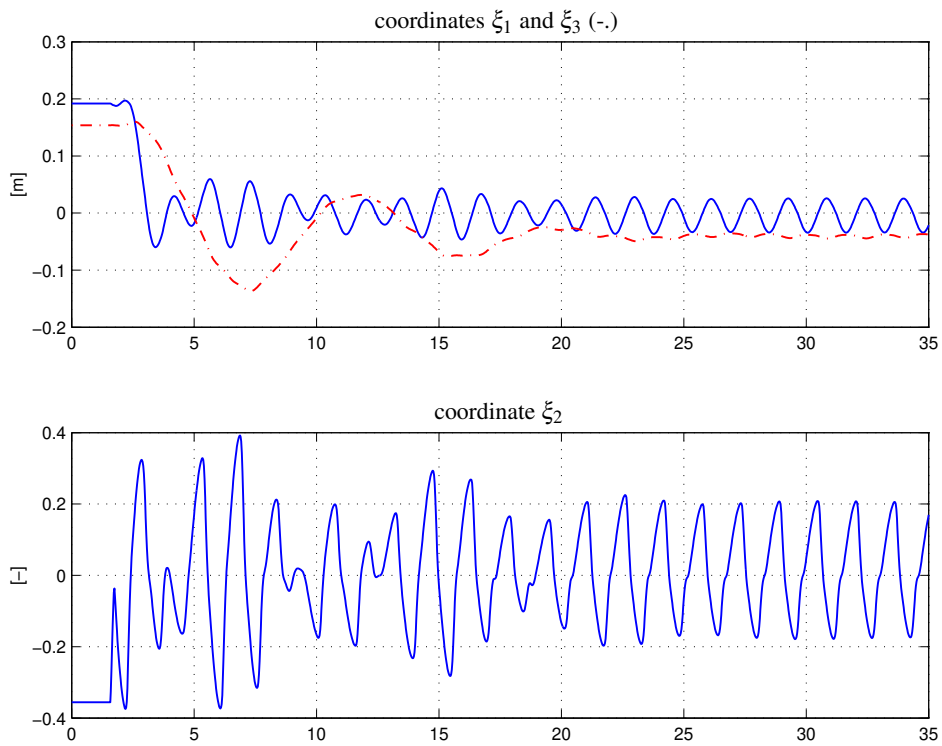


Figure 8.9: Stabilization experiment of the underactuated H-Drive manipulator; coordinates and inputs of the chained form system

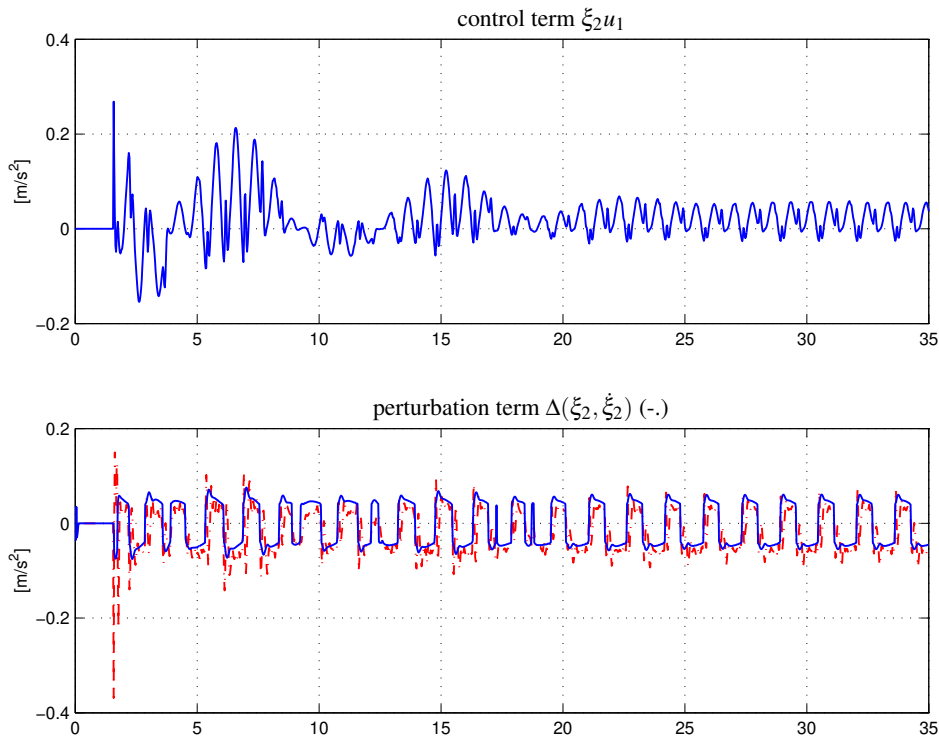


Figure 8.10: Stabilization experiment of the underactuated H-Drive manipulator with the modified controller (8.13); input $\xi_2 u_1$ and the perturbation $\Delta_3(\xi_2, \dot{\xi}_2)$ (dashed) versus the estimated perturbation $\hat{\Delta}_3(\xi_2, \dot{\xi}_2)$ using the friction characteristic (8.4) with $c_v = 0.1$ and $c_s = 0.3$.

homogeneous of degree zero anymore. Using equal control gains, the convergence of the states towards the origin becomes slower when compared to the original controller. In numerical simulations, performed with the modified controllers, the closed-loop system is not asymptotically stable, but only achieves convergence towards a certain ball around the origin. The modified controller, however, has the advantage that additional perturbations such as measurement noise and quantization errors are not, or at least less, amplified.

The performance of the modified controller of (8.13) is shown in Figure 8.11. From the plots it is clear that the system converges faster to the origin due to the increase of the gains k_5 and k_6 ; the system is close to the origin after 10 seconds. At time $t = 15$ s, the system performs a stable limit-cycle with an amplitude that is lower than in the previous experiment. The r_x coordinate oscillates between approximately -0.6 and 2.2 cm, while the r_y coordinate oscillates between approximately 0.5 and 2.5 cm. The maximal deviation of the link orientation $\theta(t)$ is reduced to a value between approximately -7 degrees and 3 degrees. By additional gain-tuning the amplitude of the resulting limit-cycle may be reduced even further, but at this moment no quantitative results are available.

8.5 Extension to practical point-to-point control

As mentioned in the beginning of this chapter, we did not expect to be able to achieve asymptotic stability of the underactuated H-Drive manipulator. Due to the effect of perturbations such as friction and gravitational perturbations, the system can only be brought inside a ball around the origin. The

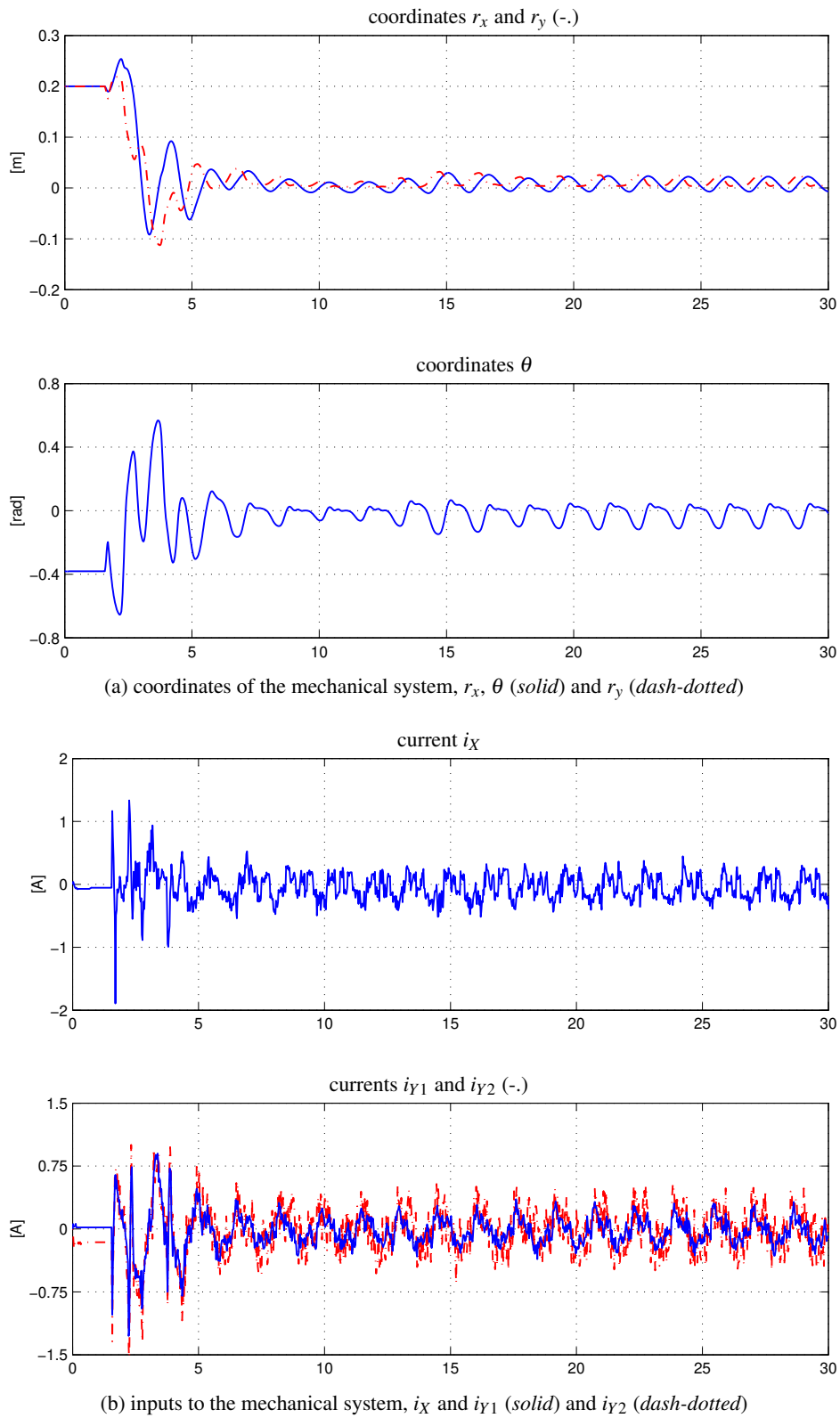


Figure 8.11: Stabilization experiment of the underactuated H-Drive manipulator with the modified controller (8.13); coordinates and inputs of the mechanical system

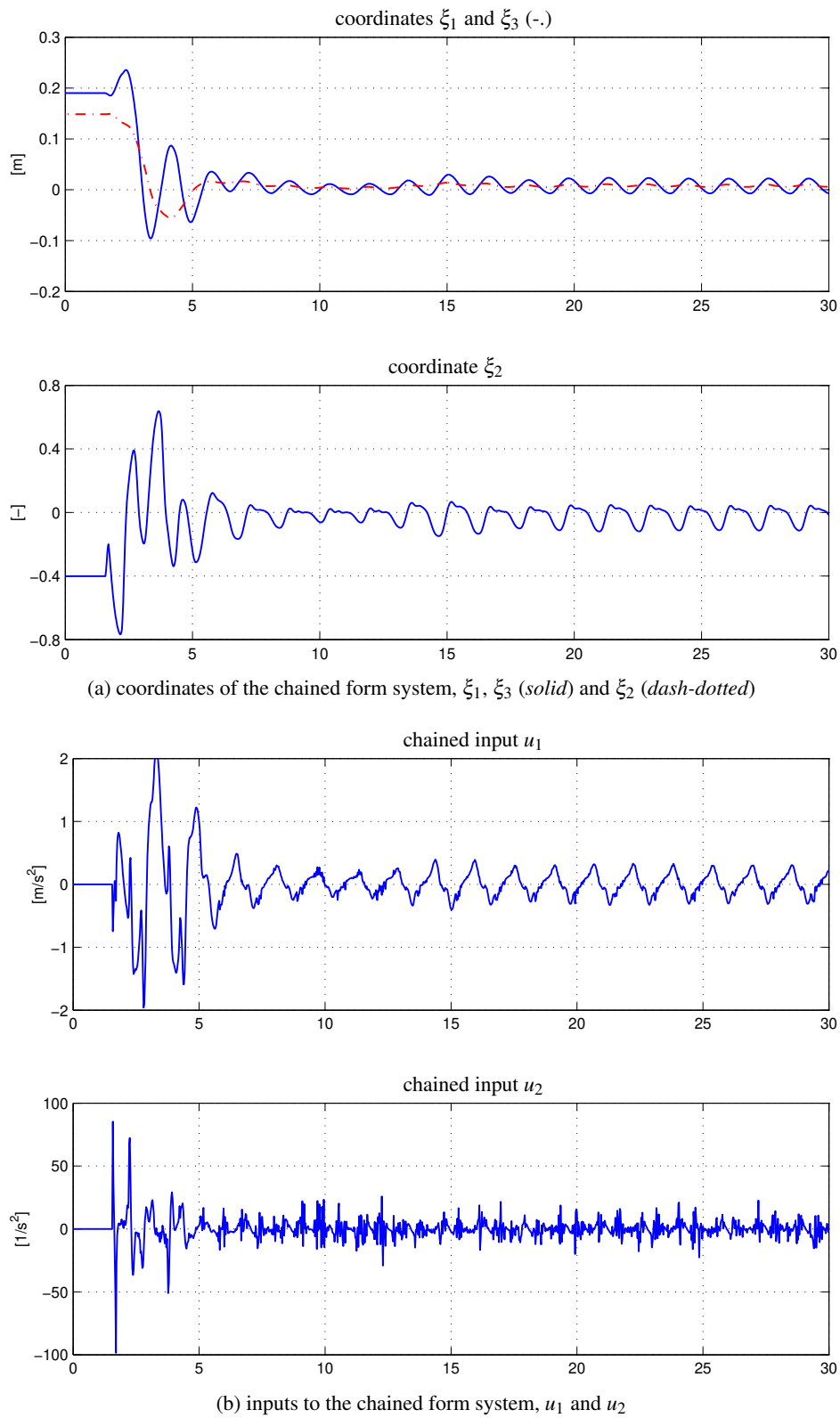


Figure 8.12: Stabilization experiment of the underactuated H-Drive manipulator with the modified controller (8.13); coordinates and inputs of the chained form system

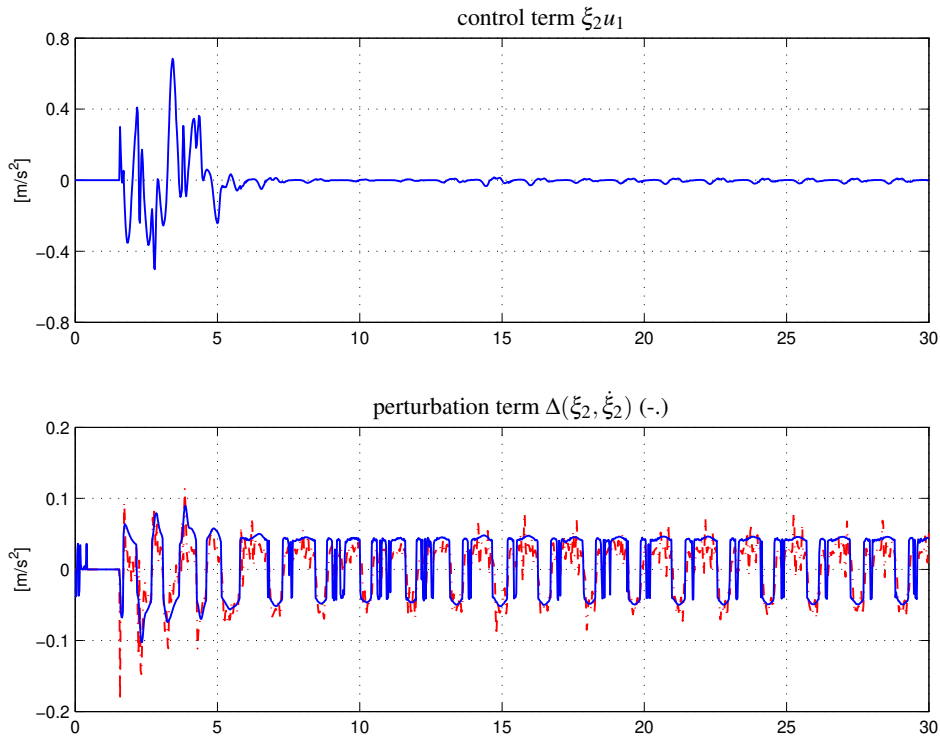
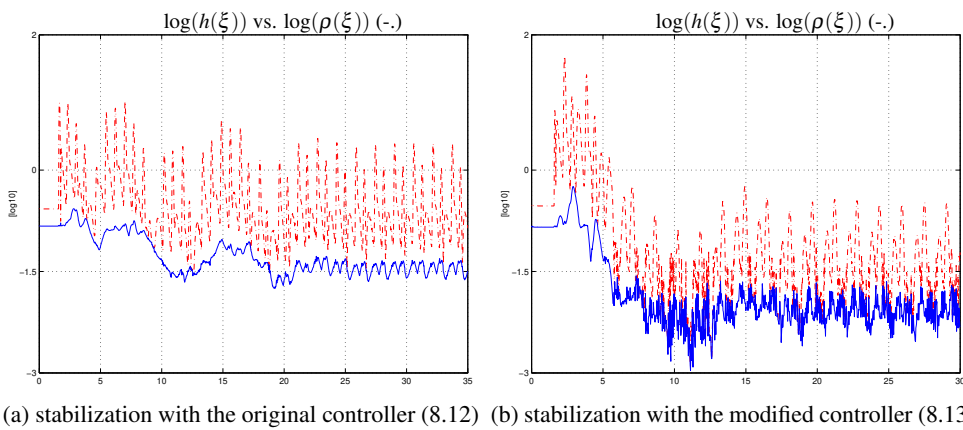


Figure 8.13: Stabilization experiment of the underactuated H-Drive manipulator with the modified controller (8.13); input $\xi_2 u_1$ and the perturbation $\Delta_3(\xi_2, \dot{\xi}_2)$ (dashed) versus the estimated perturbation $\hat{\Delta}_3(\xi_2, \dot{\xi}_2)$ using the friction characteristic (8.4) with $c_v = 0.1$ and $c_s = 0.3$.



(a) stabilization with the original controller (8.12) (b) stabilization with the modified controller (8.13)

Figure 8.14: Stabilization experiment of the underactuated H-Drive manipulator with the modified controller (8.13); logarithm of the homogeneous norms (7.30) (solid) and (7.31) (dashed)

radius of this ball is determined by the magnitude of the perturbations and the gains of the controllers. This means that we have actually achieved a form of practical stability instead of the intended asymptotic stability. In the control community, several definitions of practical stability are available. In this thesis, the notion of practical stability as presented in (de Wit et al., 1994; Pettersen and Nijmeijer, 2000) is considered.

In certain applications, asymptotic stability may not be required or may not be feasible. In these cases, instead of achieving practical stability in which the system oscillates around the origin, it may be desirable to bring the system to a stand-still. This would make it possible to move the system from one configuration to another, whereas the error between the final configuration and the desired configuration are bounded and preferably small. The final configuration error depends on the control gains and perturbations acting on the system. This approach will be illustrated in the following experiment. In this experiment we do not try to achieve practical stability but we try to achieve practical convergence. This means that the system converges towards the desired configuration, and when the error between the actual and desired configuration is small in some sense, the controller is stopped. This means that we only have a form of practical convergence in the sense that the system converges towards the origin, and when it is close enough the controller is switched off and the system reaches an equilibrium state that is close to the origin.

In the following experiments, the modified controller (8.13) is used to bring the system close to the origin. The control parameters are selected as

$$k_1 = 4, k_2 = 2\sqrt{2}, k_3 = 15, k_4 = 15, k_5 = 9, k_6 = 6, \varepsilon = 0.25, M = 1.$$

The system is brought to a stop by setting the desired acceleration, which are integrated twice and fed to the servo-loop, to zero when the following condition is satisfied. By denoting the desired configuration by $[r_{xd}, r_{yd}, \theta_d]$, where in our case $[r_{xd}, r_{yd}, \theta_d] = [0, 0, 0]$, the conditions that have to be satisfied simultaneously are given by

$$\begin{aligned} |r_x - r_{xd}| < 0.01 & \quad |r_y - r_{yd}| < 0.01, & \quad |\theta - \theta_d| < 0.02 \\ |\dot{r}_x - \dot{r}_{xd}| < 0.07 & \quad |\dot{r}_y - \dot{r}_{yd}| < 0.07 & \quad |\dot{\theta} - \dot{\theta}_d| < 0.07. \end{aligned} \quad (8.14)$$

These conditions have been empirically determined by performing subsequent experiments in which the bounds of the conditions are varied. The result of this experiment is shown in Figure 8.15. The figure shows that after approximately $t = 6.5$ s the system has converged to an equilibrium point with a final position error less than 1 cm in the r_x and r_y coordinate, while the error in the orientation angle of the link is less than 0.5 degrees. Note that the servo-loop is still enabled after the condition (8.14) is fulfilled. This is necessary in order to keep the position errors in r_x and r_y small. As can be seen from the control inputs in Figure 8.15, the input currents to the LiMMS do not become equal to zero but instead adopt a constant value that is needed to compensate the cogging effect present between the permanent magnets and the iron-core coils. If the servo-loop is also stopped then the final position errors may be even larger. It should be noted that the dynamics of the link-angle θ are only stable in the sense that small perturbations may drive the angle away from its desired value. If the perturbation causes the conditions (8.14) to be violated, then the stabilizing controller can be enabled again and the system may be brought back to an equilibrium close to the origin. The trajectories in chained form coordinates are shown in Figure 8.16.

8.6 Conclusions

In this chapter several experiments with an underactuated H-Drive manipulator have been presented. As expected from the simulation study, the objective of asymptotic stability could not be reached. It

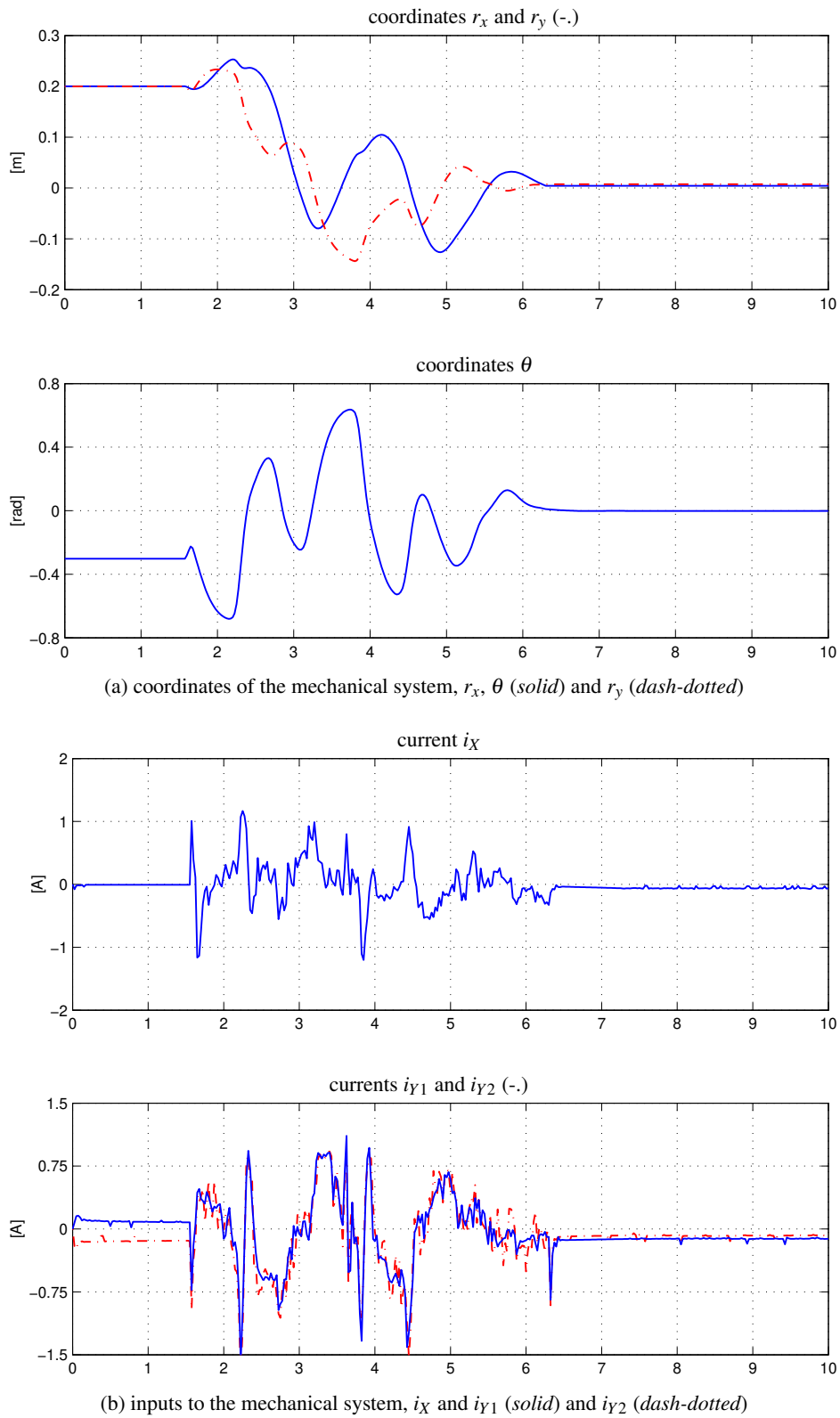


Figure 8.15: Practical point-to-point control of the underactuated H-Drive manipulator; coordinates and inputs of the mechanical system

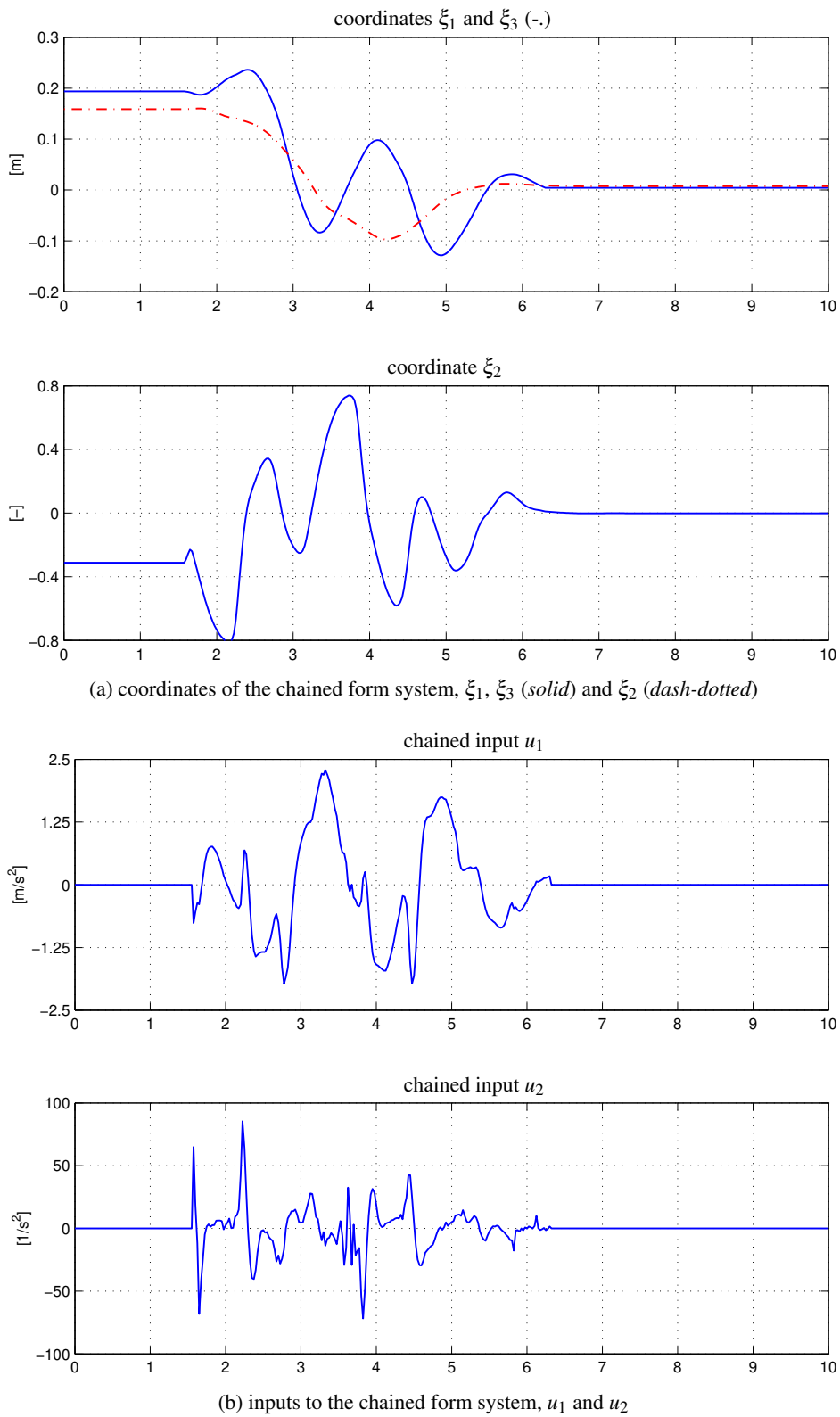


Figure 8.16: Practical point-to-point control of the underactuated H-Drive manipulator; coordinates and inputs of the chained form system

turns out that in both the case of tracking and stabilization, the closed-loop system is not robust with respect to a specific, but relevant, class of perturbations. The perturbations, resulting from friction in the rotational joint and gravitational disturbance torques due to a misalignment of the plane of rotation of the link with the horizontal plane, *i.e.*, the equipotential plane of gravity, measurement noise and cogging forces in the LiMMS, prevent the system from being asymptotically stable. In the case of tracking control, the system performs a periodic motion around the desired reference trajectory. The magnitude of the periodic motion is determined by the magnitude of the perturbations and the controller gains. In the case of stabilization, the system enters a stable limit cycle of which the amplitude is also determined by the magnitude of perturbations and the controller gains. Although the closed-loop system is not asymptotically stable, a form of practical stability has been obtained. This means that the system can be brought inside a ball with a certain distance from the origin, in which the system performs an oscillatory motion. This oscillatory behavior under the influence of perturbations has also been identified in, for example (Pettersen and Nijmeijer, 2000), in which practical stability of an underactuated surface vessel was obtained.

The non-robustness of the controllers was expected since the perturbations result in a second-order chained form system that is not in strict-feedback form and additionally can not be made homogeneous of degree zero by controllers u_1 and u_2 . Therefore, the stability proofs in Chapter 5 and Chapter 6 are not valid anymore. Besides the friction in the rotational joint, the dynamics of the link are influenced by an additional constant gravitational torque. These perturbations considerably deteriorate the performance of the controllers and result in oscillations around the desired equilibrium or trajectory. In the case of stabilization, the system could be controlled to an equilibrium point that is sufficiently close to the origin by extending the stabilizing controller with a discrete event at which the controllers are disabled when the system is sufficiently close to the origin. When the system has converged to a point close to the origin, small perturbations may move the system away from the desired equilibrium point. This behavior can be overcome by re-enabling the controllers when the system moves out of the ball around the origin. The system then tries to bring the system close towards the origin again. This means that a form of practical convergence has been obtained by modifying the stabilizing controller.

The conducted experiments correspond well with the simulation study in the sense that the qualitative and quantitative behavior in the simulations and experiments is similar. From additional simulations that were done, it follows that the closed-loop system is more susceptible to static-friction than to viscous friction torques. This may be understood from the fact that the viscous friction vanishes much faster when approaching the desired equilibrium point and does not have any discontinuities. Therefore, in order to improve the performance of the controllers, the static friction that is present in the rotational joint should be reduced. Furthermore, the influence of the perturbations can be reduced by increasing the mass of the rotational link and the length between its center of mass and the joint. It should be noted that additional gain-tuning may be used to improve the performance even further, however, from our experiences with the experiments the overall improvement is expected to be limited.

Conclusions and Recommendations

In this thesis, the trajectory tracking and feedback stabilization problem for a class of underactuated mechanical systems has been considered. This class consists of underactuated mechanical systems with second-order nonholonomic constraints that can be transformed into the second-order chained form. The control of these systems has proved to be a challenging task since such systems, generally, can not be stabilized by any continuous, static state-feedback. Additionally, the inclusion of a drift-term in the dynamics makes the stabilization and tracking of these systems more difficult. The trajectory tracking problem for second-order nonholonomic mechanical systems is, in general, easier to solve. In fact, linear time-varying controllers can be used to track feasible trajectories. However, additional conditions on the reference trajectory have to be made such that the tracking-error dynamics are asymptotically stable. In general, the trajectories need to satisfy a persistence of excitation condition, meaning that the trajectory is not allowed to converge to a point. Therefore, the tracking and stabilization problems for second-order nonholonomic system require different approaches and have to be considered separately. Examples of such systems are planar underactuated manipulators, including a $PP\bar{R}$ manipulator (Arai et al., 1998a) ($PP\bar{R}$ denotes a manipulator with two prismatic and one revolute joint and the bar above R designates the unactuated or passive joint), a serial-drive $RR\bar{R}$ manipulator (Yoshikawa et al., 2000) and a parallel-drive RRR manipulator with any two joints unactuated, manipulators driven by end-effector forces (Luca et al., 1998), a planar rigid body with an unactuated degree of freedom and underactuated surface vessels (Reyhanoglu et al., 1998, 1999), underactuated underwater vehicles (Egeland et al., 1994), the planar V/STOL aircraft in the absence of gravity (Aneke et al., 2002a) and a hovercraft type vehicle (Tanaka et al., 2000). For these systems, the linearization around any equilibrium point is uncontrollable. In certain cases, when the dynamics of the second-order nonholonomic system is influenced by gravity, the linearization of the system around an equilibrium point is controllable and the system can be stabilized by a continuous or even smooth time-invariant state-feedback. The Acrobot (Spong, 1995) and the V/STOL aircraft (Hauser et al., 1992) are examples of such systems. To date, no conditions are available for testing whether a given underactuated mechanical system can be transformed into the second-order chained form. Nevertheless, finding a coordinate and feedback transformation that brings the system into the second-order chained form really facilitates control design. The transformation into the second-order chained form considerably simplifies the dynamics of the system. Also, it generalizes the design of the controllers in the sense that controllers for the second-order chained-form can be applied to a whole class of second-order nonholonomic systems instead of one specific underactuated mechanical system.

9.1 Conclusions

9.1.1 The control design approach

In Chapter 5, the tracking control problem has been solved by using a combined backstepping and cascade approach. The tracking-error dynamics can be written as a cascade system consisting of a linear time-invariant subsystem and a linear time-varying subsystem. The linear time-invariant part has been stabilized by a linear time-invariant controller, while the time-varying part has been stabilized by using a backstepping procedure in which the link orientation θ acts as a virtual input. This approach results in a linear time-varying controller that globally \mathcal{K} -exponentially stabilizes the tracking-error dynamics. The tracking-error dynamics are only globally \mathcal{K} -exponentially stable if the trajectory to be tracked is persistently exciting, meaning that the trajectory is not allowed to converge to a point. Furthermore, the second-order chained form is globally \mathcal{K} -exponentially; the mechanical system is only globally \mathcal{K} -exponentially on a subspace (or sub-manifold) of \mathbb{R}^n where the coordinate and feedback transformation are well-defined.

To date, most researchers have considered the feedback stabilization problem for the second-order chained form system, and the tracking control problem has received less attention. In certain practical applications, the tracking control problem may be more important than the stabilization problem since it is not only required that the system moves to a different configuration, but the system also has to follow a pre-specified path in order to avoid design constraints or obstacles. The tracking controller has been first presented in (Aneke et al., 2000) and has been published in (Aneke et al., 2003). The designed tracking controller can be seen as an extension of the results in (Jiang and Nijmeijer, 1999) and (Lefeber et al., 2000), in which linear time-varying controllers have been developed for the drift-less chained-form, to tracking control of the second-order chained form with drift. A robustness analysis was performed which allowed us to conclude that the robustness property of the tracking-controller is limited and depends on the trajectory to be tracked; the robustness of the tracking controller depends on the level of the persistency of excitation of the reference acceleration $u_{1d}(t)$. In appendix B the control design approach for the tracking control problem has been extended to the case of higher-dimensional chained form systems. At this moment, to our knowledge, no examples are known of underactuated mechanical systems that can be transformed into a higher-dimensional chained form.

In Chapter 6, the stabilization problem has been solved by using a combined backstepping and averaging approach for homogeneous systems. Instead of using a backstepping approach that requires the construction of a Lyapunov function, a high-gain approach has been adopted. This resulted in a continuous, periodic, time-varying homogeneous stabilizing controller that globally ρ -exponentially stabilizes the closed-loop system. This continuous time-varying homogeneous controller has been first presented in (Aneke et al., 2002b). To date and to our knowledge, this homogeneous controller is the only one capable of ensuring Lyapunov stability as well as exponential convergence, *i.e.*, ρ -exponential stability. It is well-known that homogeneous controllers are not robust with respect to parameter uncertainties. Therefore a periodically updated version of the homogeneous stabilizing controller was presented in which the states of the system are periodically updated at discrete time instants. This controller is robust with respect to a class of additive perturbations that includes perturbations resulting from parameter uncertainties, but excludes non-smooth effects, such as friction, or measurement noise. To our knowledge, the controller of Section 6.2, presented in (Lizárraga et al., 2003), is one of the first capable of achieving robust stabilization of the second-order chained form system.

9.1.2 The simulations and experiments

In Chapter 7 the performance of the controllers has been investigated by performing a simulation study. In these simulations, a servo-system also known as the underactuated H-Drive Manipulator was considered that represents the dynamics of an underactuated PPR̄ manipulator. Instead of controlling the LiMMS (Linear Motion Motor Systems) directly, using the designed tracking and stabilizing controllers, a so-called virtual internal model following control approach was adopted. This means that the chained form inputs (u_1, u_2) are transformed, using the feedback transformation, into desired accelerations of the LiMMS. These desired accelerations are then integrated twice to obtain desired positions that are used in a low-level servo-loop to control the positions of the LiMMS. The objective in the simulations is to control the joint position and orientation of the free rotating link. It turned out that both the tracking controller and the stabilizing controller achieve the objective of asymptotic stability when no perturbations act on the system. If, however, perturbations such as friction are included in the model then the performance is considerably deteriorated and the closed-loop system is not asymptotically stable anymore. Instead, the closed-loop system performs a periodic motion around the desired trajectory or desired equilibrium point. The stabilization and tracking errors are bounded and the magnitude of the oscillations are determined by the magnitude of the perturbations and the magnitude of the controller gains. This means that a form of practical stability has been achieved in which the system can be stabilized into a ball around the reference trajectory or the desired equilibrium point. By modifying the gains, it is possible to influence the magnitude of the oscillations, however, the relation between the control gains and the magnitude of the oscillations is not completely understood.

In Chapter 8 the performance of the tracking and stabilizing controllers have been validated on an experimental underactuated H-Drive Manipulator available in the laboratory of the Dynamics and Control Technology department. This H-Drive manipulator is used as a benchmark set-up for testing tracking or stabilizing controllers for a wide range of underactuated mechanical systems including underactuated ships, underwater vehicles and underactuated three-link manipulators. The friction and cogging forces of the LiMMS were shown to appear as additive perturbations in the second-order chained form. Therefore it is essential to compensate these terms and by using a low-level servo-loop to control the position of the LiMMS, the influence of these friction and cogging forces can be practically eliminated. The main disturbances in the system are the friction and possible gravitational torques in the joint of the rotational link. The experiments confirm the observations that were made during the simulation study, namely that the designed controllers are not robust and the closed-loop system is not asymptotically stable. In both the tracking and stabilization experiments, the closed-loop system exhibited stationary oscillatory behavior similar to the behavior obtained in the numerical simulations. This means that asymptotic convergence towards the desired equilibrium or trajectory can not be achieved with the presented controllers. Although the closed-loop systems are not asymptotically stable, a form of practical stability does hold. This means that the closed-loop system can be driven inside a ball (but not a ball of arbitrary size) around the desired equilibrium or desired trajectory. The experimental results correspond well with the experiments, both qualitatively as quantitatively. The differences between the simulations and experiments are mainly caused by a gravitational disturbance torque and the nonlinear friction characteristic of the link. By using a more sophisticated friction model in conjunction with a model of the gravitational disturbance, the correspondence between the simulations and the experiments can be improved. As mentioned earlier, the periodically updated version of the homogeneous stabilizing controller is not robust with respect to gravitational disturbance torques or non-smooth effects such as friction. Therefore, no simulations or experiments have been conducted using the periodically updated homogeneous controller. For a

comparison of the homogeneous controller and its periodically updated version, the reader is referred to (Lizárraga et al., 2003).

Compensating the perturbations acting on the extended chained form system turns out to be very difficult due to the existence of a second-order nonholonomic constraint and the fact that the link orientation can not be controlled directly. In fact, it is expected that there exist no asymptotically stabilizing controllers for the second-order chained that are robust with respect to vanishing perturbations such as parameter uncertainties as well as non-vanishing perturbations such as friction or gravitational disturbance torques. However, it may be possible to use a modified coordinate and feedback transformation to transform the model of the system including the disturbances, for example friction, into a, possibly different, canonical form. It may even be possible to design controllers that utilize the dissipative nature of the frictional perturbations to stabilize the system to an equilibrium point.

9.1.3 Robustness issues

In many researches dealing with the control of underactuated mechanical systems with second-order nonholonomic constraints the influence of perturbations on the closed-loop dynamics has generally not been taken into account.

In some references dealing with second-order nonholonomic systems such as, for example, underactuated surface vessels, underactuated autonomous underwater vehicles or underactuated robot manipulators, robustness issues have been investigated. However, very few references have considered the design of robust controllers for the second-order chained-form system. To our knowledge, the controller in (Lizárraga et al., 2003) is one of the first capable of achieving robust stabilization of the second-order chained form system. There have been authors who have considered the robust control problem for underactuated manipulators without using a transformation into a canonical form such as the second-order chained form. In (Shin and Lee, 2000) the cartesian coordinates of an experimental underactuated manipulator were controlled by application of robust adaptive control. In (Kim et al., 2001) variable structure based, model reference adaptive control (MRAC) has been used to control a two-link planar underactuated manipulator. The numerical simulations of that reference showed severe chattering which is undesirable in practice. Other references assume the presence of brakes in the passive joints of the manipulator. In (Bergerman and Yangsheng, 1994), for example, a robust variable structure controller (VSC) was developed for controlling the active joints and the brakes of the passive joints.

9.2 Recommendations

In this section recommendations for further research are given. First of all, a short discussion on the use of the second-order chained form in the control design for underactuated mechanical systems will be given. After that, recommendations will be given for the design of robust controllers for the class of second-order nonholonomic systems. Finally, some recommendations for improving the experimental underactuated H-Drive manipulator will be given.

9.2.1 The second-order chained form

In recent years, many underactuated mechanical systems with second-order nonholonomic constraints have been shown to be transformable into the second-order chained form. The transformation into the chained form considerably simplifies the dynamics of the system. The use of the second-order chained form also facilitates control design because tracking or feedback controllers that have been designed

for the second-order chained form can be applied to any system that is transformable into the second-order chained form.

The main difficulty in the current control design approach is the fact that finding a coordinate and feedback transformation that brings the system into the second-order chained form may be difficult or even impossible. In fact, there exists no sufficient conditions that guarantee the existence of a coordinate and feedback transformation that brings a given second-order nonholonomic system to the second-order chained form. Therefore, control design approaches that utilize the second-order chained form are only useful if a coordinate and feedback transformation are known in advance. In the case of mechanical systems with first-order nonholonomic systems, sufficient conditions for converting the system into the first-order chained form are available. In (Murray, 1993) necessary and sufficient conditions have been derived for converting a nonholonomic system into the first-order chained form. In (Murray and Sastry, 1991) a constructive procedure for finding the coordinate and feedback transformation has been presented. One of the results from this work is that all two-input drift-less nonholonomic systems in three and four dimensions can be put in first-order chained form. However, the existence of a drift-term makes the generalization of this result to the case of second-order nonholonomic system very difficult. To our knowledge, no sufficient and necessary conditions have been presented for converting nonholonomic systems into the second-order chained form systems. Therefore, the derivation of these sufficient and necessary conditions is a challenging field of research that requires further investigation.

In certain cases, second-order nonholonomic system can be transformed into the second-order chained form system with some additional terms. By regarding these additional terms as perturbations, it may still be possible to successfully control the system with controllers that were designed for the non-perturbed second-order chained form system. However, in many cases the nonholonomic system is influenced by additional dynamics such as, for example, friction, measurement errors or external disturbances. These additional dynamics result in perturbations of the second-order chained form which considerably deteriorate the performance. Therefore these perturbations are an essential part of the dynamics and can not be neglected. In these situations, it would be interesting to know whether the mechanical system including these disturbances can be transformed into the second-order chained form. This may be checked by using the, to be developed, necessary and sufficient conditions for transformability into the second-order chained form discussed above. If this turns out to be possible, then the controllers for the second-order chained form are still applicable and asymptotic stabilization or tracking is still possible under the influence of the perturbations.

9.2.2 Robust control design

An interesting field for further research is the development of robust stabilizers and tracking controllers for second-order nonholonomic systems. This requires the design of stabilizing or tracking controllers which are robust with respect to a class of perturbations resulting from parameter or modelling errors. Besides parameter or modelling errors, nonholonomic control systems can also be influenced by additional perturbations resulting from non-smooth effects, such as friction, cogging or measurement errors. The design of such controllers turns out to be a very difficult task, due to the existence of the nonholonomic constraint and the fact that the linear approximation around equilibria is generally not controllable. To this date, and to our knowledge, no stabilizers or tracking controllers have been presented that are robust with respect to perturbations that include cogging, measurement errors and non-smooth effects such as friction.

In order to cope with external disturbances such as gravitational effects, the practical stabilization problem should be considered. It is clear that due to the fact that the linearization around equilibrium

points is not controllable, it is impossible to achieve asymptotic stability under the influence of persistent or non-vanishing disturbances. In general, these persistent disturbances will result in instability or give rise to bounded errors. By allowing for controlled oscillations, the system can be stabilized to a ball around the desired equilibrium or reference trajectory. In fact, the results presented in (Do et al., 2002) can be used to extend the results in Chapter 5 to achieve practical stability of the tracking-error dynamics. This means that under additional conditions on the gain, the tracking controllers can be shown to globally exponentially stabilize the system to a ball around the desired trajectory.

Besides the control design methods presented in Chapters 5 and 6, different approaches may be promising in achieving robust controllers for trajectory tracking or feedback stabilization. A few of these approaches are summarized below. In (Luca and Oriolo, 2000) it was shown that a planar underactuated manipulator can be fully feedback linearized and input-output decoupled by means of a nonlinear dynamic feedback, provided that singularity is avoided. The linearizing output is the center of percussion of the link. More recently, the authors of (Ge et al., 2001) derived conditions for 2-input nonholonomic systems with drift to be feedback-linearizable by non-smooth (and eventually discontinuous) coordinate and feedback transformations. In (Mita and Nam, 2001), variable period deadbeat control, in other words multi-rate digital control, was used to stabilize high-order chained form systems. The authors of (Lucibello and Oriolo, 2001) consider a large class of systems, including systems with drift, in the framework of iterative state steering control. Although no algorithm is presented to construct any such controller, it is assumed that a controller is known beforehand, conditions have been pointed out for discrete-time stability and robustness with respect to additive disturbance vector fields.

In view of our experiences with the experiments, it is expected that iterative state steering control is the most promising method for designing robust controllers with respect to a class of perturbations including parameter uncertainties, modelling errors and possibly non-smooth effects such as friction and measurement errors. The combined hybrid/open-loop control approach may be able to cope with a larger class of perturbations than the presented controllers. Although iterative state steering control is not expected to result in controllers that are robust with respect to persistent disturbances, it may result in a high level of robustness by guaranteeing bounded errors for a large class of perturbations.

9.2.3 Improving the experimental set-up

There are three possibilities to improve the experimental performance of the presented controllers under the influence of perturbations. First of all, an improvement can be accomplished by additional gain-tuning of the controllers. The tuning of the gains turned out to be a quite time-consuming task. This is caused by the fact that values for the control parameters have to be found which assure good convergence of the closed-loop system, but also guarantee that the H-Drive stays inside the boundaries of its limited workspace. In Chapter 8 the experimental results correspond well with the numerical simulations. The differences between the experiments and the simulations are mainly caused by the nonlinear friction characteristic of the link, the servo acceleration errors and perturbations such as measurement noise and gravitational disturbance torques. It may be possible to perform the gain-tuning procedure through numerical simulation, provided that a more accurate friction model of the rotational link is available and the gravitational disturbance torque is eliminated or modelled. As it turns out to be very difficult to compensate the perturbations in the second-order chained form system, the overall improvement in performance that can be obtained by additional gain tuning is, however, expected to be limited.

The second possibility for improving the control performance, is reducing the influence of the perturbations by increasing the inertia of the rotational link, as well as its mass and length between

the joint and its center of mass. The main difficulty with this approach is the fact that increasing the length or the mass of the link increases the effect of gravitational perturbations. These gravitational disturbance torques result from a misalignment of the plane of rotation of the link with the horizontal plane, *i.e.*, the equipotential plane of gravity. In the experiments, increasing the mass of the link by a factor 2.5, from $m_3 = 0.04$ to approximately $m_3 = 0.10$ [kg] already results in rotations of the link when no external torque is applied. This indicates that gravitational disturbance torques have to be eliminated before the mass can be increased. This becomes even more critical when reducing the friction level in the rotational joint, since these gravitational disturbance torques may not be cancelled by the static friction torque, and the origin may not be an equilibrium point of the uncontrolled system anymore.

The final possibility for improving the performance is, of course, by reducing the friction in the link. As mentioned earlier, the performance of the tracking and stabilizing controllers is more susceptible to static friction in the joint than to viscous friction. In fact, in simulation, the presented tracking controller still achieves asymptotic stability for a normalized viscous friction coefficient of up to approximately $c_{v,\theta}/I = 7$ [1/(rad · s)]. The closed-loop system, however, does not appear to be asymptotically stable for any value of the normalized static friction coefficient $c_{s,\theta}/I$. Therefore, in order to improve the control performance, it is essential to reduce the magnitude of the static friction in the rotational link. In numerical simulations, reducing the static friction coefficient $c_{s,\theta}/I$ by a factor 10, from its current value 0.3 to 0.03 [1/s²], reduces the maximal error of the joint position to less than 1 [cm] in the longitudinal and transversal direction, while the maximal error in the link orientation is reduced to less than 2.5 degrees. The desired coefficient corresponds to a static friction coefficient of approximately $2.5 \cdot 10^{-5}$ [Nm]. By multiplying the desired coefficient $c_{s,\theta}/I = 0.03$, normalized with respect to the inertia I , with the value $\lambda = 0.1372$ gives us the desired static friction coefficient $c_{s,\theta}/(m_3 l) = 0.4 \cdot 10^{-2}$ [1/s²], normalized with respect to the product $m_3 l$. By further increasing the mass m_3 the maximal deviations from the desired equilibrium or trajectory may be reduced even further.

The most important recommendation for improving the control performance is to reduce the friction by using an air-bearing to suspend the rotational link. This should be done only after the gravitational disturbances have been eliminated. The non-contacting property of an air bearing – air bearings utilize a thin film of pressurized air to provide a friction-less load bearing interface between the surfaces – would practically eliminate all friction in the rotational joint. The friction in the rotational joint can also be reduced by using a magnetic bearing. Although such a bearing is non-contacting and reduces the effect of friction to a minimum, it also introduces drag or cogging forces resulting from eddy-currents generated by the changing magnetic fields.

A stability result for cascaded systems

A.1 A global \mathcal{K} -exponential stability result for non-autonomous cascaded systems

In Chapter 3 we concluded that if in addition to the assumptions in Lemma 3.6.2, the systems Σ_1 and Σ_2 are globally exponentially stable, the cascaded system (3.19) is globally \mathcal{K} -exponentially stable. This result can be strengthened to include the case in which the systems Σ_1 and Σ_2 are globally \mathcal{K} -exponentially stable. In that situation, under some additional assumptions, it can be shown that the cascaded system is also globally \mathcal{K} -exponentially.

First we formulate an additional lemma that will be needed in the proof. This result can be found in Theorem 3.6.10 of (Lakshmikantham and Leela, 1969), and has been used in (Panteley and Loría, 2001).

Lemma A.1.1. *If the system $\dot{x} = f(t, x)$ is GUAS, then for each $\mu > 0$, the system admits a C^1 Lyapunov function $\mathcal{V}(t, z_1)$ such that for all $t \geq t_0$ and for all $x \in \mathbb{R}^n$,*

$$\begin{aligned} (i) \quad & \alpha_1(\|x\|) \leq \mathcal{V}(t, x) \leq \alpha_2(\|x\|), \\ (ii) \quad & \frac{\partial \mathcal{V}}{\partial t} + \frac{\partial \mathcal{V}}{\partial x} f(t, x) \leq -\mu \mathcal{V}(t, x), \end{aligned} \tag{A.1}$$

where α_1 and α_2 are class \mathcal{K}_∞ functions.

The stability result is presented in the following proposition. The proof proceeds along the same lines as the proof given in (Panteley et al., 1998).

Proposition A.1.2. *If in addition to the assumptions in Theorem 3.6.1 both Σ_1 and Σ_2 are globally \mathcal{K} -exponentially stable, and there exist C^1 Lyapunov function $V_1(t, z_1)$ and $V_2(t, z_1)$ satisfying for all $t \geq t_0$ for all $z_1 \in \mathbb{R}^n$,*

$$\begin{aligned} (i) \quad & \alpha_1 \|z_1\|^2 \leq V_1(t, z_1) \leq \alpha_2 \|z_1\|^2, \\ (ii) \quad & \frac{\partial V_1}{\partial t} + \frac{\partial V_1}{\partial z_1} f_1(t, z_1) \leq -\mu V_1(t, z_1), \\ (iii) \quad & \left\| \frac{\partial V_1}{\partial z_1} \right\| \leq \alpha_4 \|z_1\|, \end{aligned} \tag{A.2}$$

with α_1, α_2 and α_4 positive constants, and for all $t \geq t_0$ for all $z_2 \in \mathbb{R}^m$

$$\begin{aligned} (i) \quad & \beta_1 \|z_2\|^2 \leq V_2(t, z_2) \leq \beta_2 \|z_2\|^2, \\ (ii) \quad & \frac{\partial V_2}{\partial t} + \frac{\partial \mathcal{V}}{\partial z_2} f_2(t, z_2) \leq -\mu \mathcal{V}(z_2), \end{aligned} \quad (\text{A.3})$$

with β_1 and β_2 positive constants, respectively, then the cascaded system (3.19) is globally \mathcal{K} -exponentially stable.

Proof. Since the Σ_2 subsystem is globally \mathcal{K} -exponentially stable, it suffices to show the result for $z_1(t)$. Since all conditions of Theorem 3.6.1 are satisfied, the system 3.19 is GUAS and $z = [z_1, z_2]^T$ satisfies

$$\|z(t)\| \leq \beta(\|z(t_0)\|, t - t_0), \quad \forall t \geq t_0 \geq 0,$$

where $\beta(\cdot)$ is a class \mathcal{KL} function. For all initial conditions $\|z(t_0)\| \leq r$ the function $g(t, z_1, z_2)$ can be upper-bounded as $\|g(t, z_1, z_2)\| \leq c_g$, where $c_g = c_g(r) > 0$ is a constant. Consider the subsystem

$$\dot{z}_1 = f_1(t, z_1) + g(t, z_1, z_2)z_2 \quad (\text{A.4})$$

By assumption, the systems $\dot{z}_1 = f_1(t, z_1)$ and $\dot{z}_2 = f_2(t, z_2)$ are globally exponentially stable. By assumption the Lyapunov functions $V_1(t, x)$ satisfies such that

$$\alpha_1 \|z_1\|^2 \leq V_1(t, z_1) \leq \alpha_2 \|z_1\|^2, \quad \dot{V}_1(t, z_1) \leq -V_1(t, z_1), \quad \left\| \frac{\partial V_1}{\partial x} \right\| \leq \alpha_4 \|z_1\|, \quad (\text{A.5})$$

where α_1 and α_4 are positive constants and $\alpha_2(\cdot)$ is a class \mathcal{K}_∞ function. Since the Σ_2 system is also GUAS, it follows from Lemma A.1.1 that there exists Lyapunov function $V_2(t, x)$ such that

$$\beta_1 \|z_2\|^2 \leq V_2(t, z_2) \leq \beta_2 \|z_2\|^2, \quad \dot{V}_2(t, z_2) \leq -V_2(t, z_2), \quad (\text{A.6})$$

Taking the derivative of $V_1(t, x)$ with respect to (A.4), and using (A.5, A.5) we obtain

$$\begin{aligned} \dot{V}_1 & \leq -V_1(t, z_1) + \alpha_4 \|g(t, z_1, z_2)\| \|z_1\| \|z_2\| \leq -\alpha_1 \|z_1\|^2 + \alpha_4 c_g(r) \|z_1\| \|z_2\| \\ & \leq -\frac{\alpha_1}{2} \|z_1\|^2 + \frac{\alpha_4^2 c_g(r)^2}{2\alpha_1} \|z_2\|^2 \leq -\frac{\alpha_1}{2\alpha_2} V_1(t, z_1) + \frac{\alpha_4^2 c_g(r)^2}{2\alpha_1 \beta_2} V_2(t, z_2) \end{aligned} \quad (\text{A.7})$$

Define $\delta_g(r) = \frac{\alpha_4^2 c_g(r)^2}{2\alpha_1 \beta_2}$ and consider the candidate Lyapunov function

$$V(t, z_1, z_2) = V_1(t, z_1) + \Gamma V_2(t, z_2). \quad (\text{A.8})$$

with $\Gamma > 0$ a to be defined positive constant. The derivative of V along the solutions of (3.19) satisfies

$$\dot{V} \leq -\frac{\alpha_1}{2\alpha_2} V_1(t, z_1) + (\delta_g(r) - \Gamma) V_2(t, z_2) \quad (\text{A.9})$$

Suppose that we choose Γ as

$$\Gamma = \frac{2\beta_2}{2\beta_2 - \beta_1} \delta_g(r).$$

A.1 A global \mathcal{H} -exponential stability result for non-autonomous cascaded systems 37

Then we have

$$\dot{V} \leq -\frac{\alpha_1}{2\alpha_2}V_1(t, z_1) - \frac{\beta_1}{2\beta_2}\Gamma V_2(t, z_2) \leq -\gamma V \quad (\text{A.10})$$

where

$$\gamma = \frac{1}{2} \min\left(\frac{\alpha_1}{\alpha_2}, \frac{\beta_1}{\beta_2}\right).$$

Therefore, using the bound $\|z_1\|^2 \leq \frac{V(t, z_1, z_2)}{\alpha_1}$, we obtain

$$\begin{aligned} \|z_1(t, t_0, z_{10}, z_{20})\|^2 &\leq \frac{V(t_0, z_{10}, z_{20})}{\alpha_1} \exp(-\gamma(t - t_0)) \\ &\leq \frac{\alpha_2 \|z_{10}\|^2 + \Gamma \|z_{20}\|^2}{\alpha_1} \exp(-\gamma(t - t_0)) \\ &\leq 2 \frac{\max(\alpha_2, \Gamma)}{\alpha_1} \|z_0\|^2 \exp(-\gamma(t - t_0)) \end{aligned} \quad (\text{A.11})$$

Thus

$$\|z_1(t, t_0, z_{10}, z_{20})\| \leq k(r) \|z_0\| \exp\left(-\frac{\gamma}{2}(t - t_0)\right) \quad (\text{A.12})$$

with

$$k(r) = \sqrt{2 \frac{\max(\alpha_2, \Gamma)}{\alpha_1}}. \quad (\text{A.13})$$

The bound (3.2) is satisfied and we conclude that the system (3.19) is globally \mathcal{H} -exponentially stable. \square

Tracking control of the higher-dimensional chained form

B.1 Cascaded backstepping control

In this thesis, so far, only the second-order chained form (2.7) of dimension $n = 3$ has been considered. This was motivated by the fact that, up to now, no mechanical systems are known that are transformable into a second-order chained form of dimension $n > 3$. In this appendix, the results presented in Chapter 5 will be extended to the case of higher-order second-order chained form systems of the form (2.6). Although, different definitions of the general second-order chained form system may exist, only systems of the form (2.6) will be considered here.

Consider the trajectory tracking problem for the general second-order chained form system (2.6). Define the vector $\xi = (\xi_1, \xi_2, \dots, \xi_n)$. Consider a reference trajectory ξ_d , the tracking error is denoted by $x = [x_{11}, x_{12}, x_{21}, x_{22}, \dots, x_{n1}, x_{n2}]^T$ where

$$x_{i,1} = \xi_i - \xi_{id}, \quad x_{i,2} = \dot{\xi}_i - \dot{\xi}_{id}. \quad (\text{B.1})$$

The tracking dynamics in state-space form can be written as

$$\Delta_1 \begin{cases} \dot{x}_{n,1} = x_{n,2} \\ \dot{x}_{n,2} = x_{n-1,1}u_{1,d} + \xi_{n-1}(u_1 - u_{1,d}) \\ \vdots \\ \dot{x}_{3,1} = x_{3,2} \\ \dot{x}_{3,2} = x_{2,1}u_{1,d} + \xi_2(u_1 - u_{1,d}) \end{cases} \quad \Delta_2 \begin{cases} \dot{x}_{2,1} = x_{2,2} \\ \dot{x}_{2,2} = u_2 - u_{2,d} \end{cases} \quad (\text{B.2})$$

$$\Delta_3 \begin{cases} \dot{x}_{1,1} = x_{1,2} \\ \dot{x}_{1,2} = u_1 - u_{1,d} \end{cases}$$

Suppose that the subsystem Δ_3 has been stabilized to the origin $(x_{1,1}, x_{1,2}) = (0, 0)$ by a controller $u_1(u_{1d}, x_{1,1}, x_{1,2})$. Then $x_{1,2} \equiv 0$ and therefore $u_1 - u_{1,d} \equiv 0$. We design the remaining input u_2 such that the remaining subsystem (Δ_1, Δ_2) is stabilized for $u_1 - u_{1,d} \equiv 0$. In order to make conclusions on the exponential stability of the complete closed-loop system we use Theorem 3.6.1.

Remark B.1.1. In (B.2) the perturbation term $g(t, z_1, z_2)z_2$ depends on the, to be designed, feedback $u_1(t, x)$. When choosing $z_2 = [x_{1,1}, x_{1,2}]$, the perturbation matrix $g(t, z_1, z_2)$ has to be linear with respect to the variable z_1 given by $z_1 = (x_{n,1}, x_{n,2}, \dots, x_{3,1}, x_{3,2})$. This is the case when choosing the feedback u_1 as $u_1 = u_{1d} + k_{1,1}x_{1,1} + k_{1,2}x_{1,2}$.

B.1.1 Stabilization of the (Δ_1, Δ_2) subsystem

Suppose that the Δ_3 subsystem in (B.2) has been stabilized by choosing

$$u_1 = u_{1d} - k_{1,1}x_{1,1} - k_{1,2}x_{1,2}, \quad k_{1,1} > 0, k_{1,2} > 0, \quad (\text{B.3})$$

where the polynomial $p(\lambda) = \lambda^2 + k_1\lambda + k_2$ is Hurwitz. Then $x_{1,1} = x_{1,2} \equiv 0$ and $u_1 - u_{1,d} \equiv 0$ and the time-varying subsystem Δ_1 can be written as

$$\begin{aligned} \dot{x}_{n,1} &= x_{n,2} \\ \dot{x}_{n,2} &= x_{n-1,1}u_{1,d} \\ &\vdots \\ \dot{x}_{3,1} &= x_{3,2} \\ \dot{x}_{3,2} &= x_{2,1}u_{1,d} \\ \dot{x}_{2,1} &= x_{2,2} \\ \dot{x}_{2,2} &= u_2 - u_{2,d} \end{aligned} \quad (\text{B.4})$$

We aim at designing a stabilizing feedback u_2 by applying a backstepping procedure to the system (B.4). This stabilizing feedback is obtained by using a backstepping procedure to design a stabilizing virtual input $x_{2,1}$. Assume that the reference signal $u_{1,d}(t)$ satisfies Assumption 5.1.1. The procedure for obtaining the stabilizing feedback u_2 , consisting of $n - 1$ steps, is given as follows.

step 1 Define $\bar{x}_{n,1} = x_{n,1}$. Consider the first equation $\dot{\bar{x}}_{n,1} = x_{n,2}$ and assume that $x_{n,2}$ is the virtual input. A stabilizing function $x_{n,2} = \alpha_{n,1}(\bar{x}_{n,1})$ for the $\bar{x}_{n,1}$ -subsystem is

$$\alpha_{n,1}(t, x_{n,1}) = -c_{n,1}u_{1,d}(t)^{2d_{n,1}+2}\bar{x}_{n,1},$$

where $c_{n,1} > 0, d_{n,1} \in \mathbb{N}$. Define $\bar{x}_{n,2} = x_{n,2} - \alpha_{n,1}(\bar{x}_{n,1})$ and consider the $\bar{x}_{n,2}$ -subsystem

$$\dot{\bar{x}}_{n,2} = x_{n-1,1}u_{1,d}(t) - \frac{d}{dt}[\alpha_{n,1}(t, \bar{x}_{n,1})].$$

Suppose that $x_{n-1,1}$ is the virtual input. A stabilizing function $x_{n-1,1} = \alpha_{n,2}(t, \bar{x}_{n,1}, \bar{x}_{n,2})$ for the $\bar{x}_{n,2}$ -subsystem is given by

$$\alpha_{n,2}(t, \bar{x}_{n,1}, \bar{x}_{n,2}) = -c_{n,2}u_{1,d}(t)^{2d_{n,2}+1}\bar{x}_{n,2} + \frac{d}{dt}[\alpha_{n,1}(\bar{x}_{n,1})], \quad (\text{B.5})$$

where $c_{n,2} > 0, d_{n,2} \in \mathbb{N}$. Define $\bar{x}_{n-1,1} = x_{n-1,1} - \alpha_{n,2}(t, \bar{x}_{n,1}, \bar{x}_{n,2})$. The $(\bar{x}_{n,1}, \bar{x}_{n,2})$ subsystem is then given by

$$\begin{aligned} \dot{\bar{x}}_{n,1} &= -c_{n,1}u_{1,d}(t)^{2d_{n,1}+2}\bar{x}_{n,1} + \bar{x}_{n,2} \\ \dot{\bar{x}}_{n,2} &= -c_{n,2}u_{1,d}(t)^{2d_{n,2}+2}\bar{x}_{n,2} + u_{1,d}(t)\bar{x}_{n-1,1} \end{aligned}$$

step 2 For notational convenience, define the vector \bar{x} as $\bar{x} = (\bar{x}_{n,1}, \bar{x}_{n,2}, \dots, \bar{x}_{3,1}, \bar{x}_{3,2})^T$. Consider the $\bar{x}_{n-1,1}$ dynamics

$$\dot{\bar{x}}_{n-1,1} = x_{n-1,2} - \frac{d}{dt}[\alpha_{n,2}(t, \bar{x}_{n,1}, \bar{x}_{n,2})].$$

Assume that $x_{n-1,2}$ is the virtual input. A stabilizing function $x_{n-1,2} = \alpha_{n-1,1}(t, \bar{x})$ for the $\bar{x}_{n-1,1}$ -subsystem is

$$\alpha_{n-1,1}(t, \bar{x}) = -c_{n-1,1} u_{1,d}^{2d_{n-1,1}+2} \bar{x}_{n-1,1} + \frac{d}{dt} [\alpha_{n,2}(t, \bar{x}_{n,1}, \bar{x}_{n,2})],$$

where $c_{n-1,1} > 0, d_{n-1,1} \in \mathbb{N}$. Define $\bar{x}_{n-1,2} = x_{n-1,2} - \alpha_{n-1,1}(\bar{x}_{n,1})$ and consider the $\bar{x}_{n-1,2}$ -subsystem

$$\dot{\bar{x}}_{n-1,2} = x_{n-2,1} u_{1,d}(t) - \frac{d}{dt} [\alpha_{n-1,1}(t, \bar{x})].$$

Suppose that $x_{n-2,1}$ is the new virtual input. A stabilizing function $x_{n-2,1} = \alpha_{n-1,2}(t, \bar{x})$ for the $\bar{x}_{n-1,2}$ -subsystem is given by

$$\alpha_{n-1,2}(t, \bar{x}) = -c_{n-1,2} u_{1,d}(t)^{2d_{n-1,2}+1} \bar{x}_{n-1,2} + \frac{\frac{d}{dt} [\alpha_{n-1,1}(t, \bar{x})]}{u_{1,d}(t)}, \quad (\text{B.6})$$

where $c_{n-1,2} > 0, d_{n-1,2} \in \mathbb{N}$. Define $\bar{x}_{n-2,1} = x_{n-2,1} - \alpha_{n-1,2}(t, \bar{x})$. The $(\bar{x}_{n,1}, \bar{x}_{n,2}, \bar{x}_{n-1,1}, \bar{x}_{n-1,2})$ subsystem is then given by

$$\begin{aligned} \dot{\bar{x}}_{n,1} &= -c_{n,1} u_{1,d}(t)^{2d_{n,1}+2} \bar{x}_{n,1} + \bar{x}_{n,2} \\ \dot{\bar{x}}_{n,2} &= -c_{n,2} u_{1,d}(t)^{2d_{n,2}+2} \bar{x}_{n,2} + u_{1,d}(t) \bar{x}_{n-1,1} \\ \dot{\bar{x}}_{n-1,1} &= -c_{n-1,1} u_{1,d}(t)^{2d_{n-1,1}+2} \bar{x}_{n-1,1} + \bar{x}_{n-1,2} \\ \dot{\bar{x}}_{n-1,2} &= -c_{n-1,2} u_{1,d}(t)^{2d_{n-1,2}+2} \bar{x}_{n-1,2} + u_{1,d}(t) \bar{x}_{n-2,1} \end{aligned}$$

step i ($3 \leq i \leq n-2$) Assume that after the $(i-1)$ -th step, we have designed stabilizing functions $\alpha_{n-j+1,1}(t, \bar{x}), \alpha_{n-j+1,2}(t, \bar{x}), (1 \leq j \leq i-1)$ of the form

$$\begin{aligned} \alpha_{n-j+1,1}(t, \bar{x}) &= -c_{n-j+1,1} u_{1,d}^{2d_{n-j+1,1}+2} \bar{x}_{n-j+1,1} + \frac{d}{dt} [\alpha_{n-j+2,2}(t, \bar{x})], \\ \alpha_{n-j+1,2}(t, \bar{x}) &= -c_{n-j+1,2} u_{1,d}(t)^{2d_{n-j+1,2}+1} \bar{x}_{n-j+1,2} + \frac{\frac{d}{dt} [\alpha_{n-j+2,1}(t, \bar{x})]}{u_{1,d}(t)}, \end{aligned} \quad (\text{B.7})$$

where $c_{n-j+1,k} > 0, d_{n-j+1,k} \in \mathbb{N}, k \in \{1, 2\}$, such that the $(\bar{x}_{n,1}, \bar{x}_{n,2}, \dots, \bar{x}_{n-i+2,1}, \bar{x}_{n-i+2,2})$ subsystem with $\bar{x}_{n,1} = x_{n,1}, \bar{x}_{n,2} = x_{n,2} - \alpha_{n,1}(\bar{x}_{n,1})$ and

$$\begin{aligned} \bar{x}_{n-j,1} &= x_{n-j,1} - \alpha_{n-j+1,2}(t, \bar{x}), \quad (1 \leq j \leq i-2) \\ \bar{x}_{n-j,2} &= x_{n-j,2} - \alpha_{n-j+1,1}(t, \bar{x}), \end{aligned}$$

is given by

$$\begin{aligned} \dot{\bar{x}}_{n,1} &= -c_{n,1} u_{1,d}(t)^{2d_{n,1}+2} \bar{x}_{n,1} + \bar{x}_{n,2} \\ \dot{\bar{x}}_{n,2} &= -c_{n,2} u_{1,d}(t)^{2d_{n,2}+2} \bar{x}_{n,2} + u_{1,d}(t) \bar{x}_{n-1,1} \\ &\vdots \\ \dot{\bar{x}}_{n-i+2,1} &= -c_{n-i+2,1} u_{1,d}(t)^{2d_{n-i+2,1}+2} \bar{x}_{n-i+2,1} + \bar{x}_{n-i+2,2} \\ \dot{\bar{x}}_{n-i+2,2} &= -c_{n-i+2,2} u_{1,d}(t)^{2d_{n-i+2,2}+2} \bar{x}_{n-i+2,2} + u_{1,d}(t) \bar{x}_{n-i+1,1} \end{aligned}$$

We wish to prove that the $(\bar{x}_{n,1}, \bar{x}_{n,2}, \dots, \bar{x}_{n-i+1,1}, \bar{x}_{n-i+1,2})$ subsystem has a similar structure. Therefore consider the $\bar{x}_{n-i+1,1}$ subsystem

$$\dot{\bar{x}}_{n-i+1,1} = x_{n-i+1,2} - \frac{d}{dt} [\alpha_{n-i+2,2}(t, \bar{x})].$$

Suppose that $x_{n-i+1,2}$ is a virtual input. A stabilizing function $x_{n-i+1,2} = \alpha_{n-i+1,1}(t, \bar{x})$ for the $\bar{x}_{n-i+1,1}$ -subsystem is

$$\alpha_{n-i+1,1}(t, \bar{x}) = -c_{n-i+1,1} u_{1,d}^{2d_{n-i+1,1}+2} \bar{x}_{n-i+1,1} + \frac{d}{dt} [\alpha_{n-i+2,2}(t, \bar{x})],$$

where $c_{n-i+1,1} > 0, d_{n-i+1,1} \in \mathbb{N}$. Define $\bar{x}_{n-i+1,2} = x_{n-i+1,2} - \alpha_{n-i+1,1}(t, \bar{x})$. The dynamics of $\bar{x}_{n-i+1,2}$ is given by

$$\dot{\bar{x}}_{n-i+1,2} = u_{1,d}(t) x_{n-i,1} - \frac{d}{dt} [\alpha_{n-i+1,1}(t, \bar{x})].$$

Suppose that $x_{n-1,1}$ is a virtual input. A stabilizing function $x_{n-i,1} = \alpha_{n-i+1,2}(t, \bar{x})$ is given by

$$\alpha_{n-i+1,2}(t, \bar{x}) = -c_{n-i+1,1} u_{1,d}(t)^{2d_{n-i+1,1}+1} \bar{x}_{n-i+1,1} + \frac{\frac{d}{dt} [\alpha_{n-i+1,1}(t, \bar{x})]}{u_{1,d}(t)},$$

where $c_{n-i+1,1} > 0, d_{n-i+1,1} \in \mathbb{N}$. Define $\bar{x}_{n-i} = x_{n-i} - \alpha_{n-i+1,2}(t, \bar{x})$. Consider the dynamics of the $(\bar{x}_{n,1}, \bar{x}_{n,2}, \dots, \bar{x}_{n-i+1,1}, \bar{x}_{n-i+1,2})$ subsystem which is given by

$$\begin{aligned} \dot{\bar{x}}_{n,1} &= -c_{n,1} u_{1,d}(t)^{2d_{n,1}+2} \bar{x}_{n,1} + \bar{x}_{n,2} \\ \dot{\bar{x}}_{n,2} &= -c_{n,2} u_{1,d}(t)^{2d_{n,2}+2} \bar{x}_{n,2} + u_{1,d}(t) \bar{x}_{n-1,1} \\ &\vdots \\ \dot{\bar{x}}_{n-i+1,1} &= -c_{n-i+1,1} u_{1,d}(t)^{2d_{n-i+1,1}+2} \bar{x}_{n-i+1,1} + \bar{x}_{n-i+1,2} \\ \dot{\bar{x}}_{n-i+1,2} &= -c_{n-i+1,2} u_{1,d}(t)^{2d_{n-i+1,2}+2} \bar{x}_{n-i+1,2} + u_{1,d}(t) \bar{x}_{n-i,1} \end{aligned}$$

step n-1 After the $n-2$ -th step we have designed stabilizing functions $\alpha_{3,1}(t, \bar{x}), \alpha_{3,2}(t, \bar{x})$ of the form

$$\begin{aligned} \alpha_{3,1}(t, \bar{x}) &= -c_{3,1} u_{1,d}^{2d_{3,1}+2} \bar{x}_{3,1} + \frac{d}{dt} [\alpha_{4,2}(t, \bar{x})], \\ \alpha_{3,2}(t, \bar{x}) &= -c_{3,2} u_{1,d}(t)^{2d_{3,2}+1} \bar{x}_{3,2} + \frac{\frac{d}{dt} [\alpha_{3,1}(t, \bar{x})]}{u_{1,d}(t)}, \end{aligned} \tag{B.8}$$

where $c_{3,1} > 0, d_{3,1} \in \mathbb{N}$ and $c_{3,2} > 0, d_{3,2} \in \mathbb{N}$, such that the $(\bar{x}_{n,1}, \bar{x}_{n,2}, \dots, \bar{x}_{3,1}, \bar{x}_{3,2})$ subsystem with $\bar{x}_{n,1} = x_{n,1}$ and

$$\begin{aligned} \bar{x}_{n-j,1} &= x_{n-j,1} - \alpha_{n-j+1,2}(t, \bar{x}), \quad (1 \leq j \leq n-3) \\ \bar{x}_{n-j,2} &= x_{n-j,2} - \alpha_{n-j,1}(t, \bar{x}), \end{aligned}$$

is given by

$$\begin{aligned} \dot{\bar{x}}_{n,1} &= -c_{n,1} u_{1,d}(t)^{2d_{n,1}+2} \bar{x}_{n,1} + \bar{x}_{n,2} \\ \dot{\bar{x}}_{n,2} &= -c_{n,2} u_{1,d}(t)^{2d_{n,2}+2} \bar{x}_{n,2} + u_{1,d}(t) \bar{x}_{n-1,1} \\ &\vdots \\ \dot{\bar{x}}_{3,1} &= -c_{3,1} u_{1,d}(t)^{2d_{3,1}+2} \bar{x}_{3,1} + \bar{x}_{3,2} \\ \dot{\bar{x}}_{3,2} &= -c_{3,2} u_{1,d}(t)^{2d_{3,2}+2} \bar{x}_{3,2} + u_{1,d}(t) \bar{x}_{2,1}. \end{aligned}$$

Define $\bar{x}_{2,1} = x_{2,1} - \alpha_{3,2}(t, \bar{x})$. Then

$$\dot{\bar{x}}_{2,1} = x_{2,2} - \frac{d}{dt} [\alpha_{3,2}(t, \bar{x})].$$

Suppose that $x_{2,2}$ is a virtual input. A stabilizing function $x_{2,2} = \alpha_{2,1}(t, \bar{x})$ for the $\bar{x}_{2,1}$ -subsystem is

$$\alpha_{2,1}(t, \bar{x}) = -c_{2,1}\bar{x}_{2,1} + \frac{d}{dt} [\alpha_{3,2}(t, \bar{x})],$$

where $c_{2,1} > 0, d_{2,1} \in \mathbb{N}$. Define $\bar{x}_{2,2} = x_{2,2} - \alpha_{2,1}(t, \bar{x})$. The dynamics of $\bar{x}_{2,2}$ is given by

$$\dot{\bar{x}}_{2,2} = u_2 - u_{2,d} - \frac{d}{dt} [\alpha_{2,1}(t, \bar{x})].$$

A stabilizing input is given by

$$u_2 - u_{2,d} = -c_{2,2}\bar{x}_{2,2} + \frac{d}{dt} [\alpha_{2,1}(t, \bar{x})] \quad (\text{B.9})$$

where $c_{2,2} > 0, d_{2,2} \in \mathbb{N}$. Define $\bar{x}_{2,1} = x_{2,1} - \alpha_{2,2}(t, \bar{x})$. The $(\bar{x}_{n,1}, \bar{x}_{n,2}, \dots, \bar{x}_{2,1}, \bar{x}_{2,2})$ subsystem is then given by

$$\begin{aligned} \dot{\bar{x}}_{n,1} &= -c_{n,1}u_{1,d}(t)^{2d_{n,1}+2}\bar{x}_{n,1} + \bar{x}_{n,2} \\ \dot{\bar{x}}_{n,2} &= -c_{n,2}u_{1,d}(t)^{2d_{n,2}+2}\bar{x}_{n,2} + u_{1,d}(t)\bar{x}_{n-1,1} \\ &\vdots \\ \dot{\bar{x}}_{3,1} &= -c_{3,1}u_{1,d}(t)^{2d_{3,1}+2}\bar{x}_{3,1} + \bar{x}_{3,2} \\ \dot{\bar{x}}_{3,2} &= -c_{3,2}u_{1,d}(t)^{2d_{3,2}+2}\bar{x}_{3,2} + u_{1,d}(t)\bar{x}_{2,1} \\ \dot{\bar{x}}_{2,1} &= -c_{2,1}\bar{x}_{2,1} + \bar{x}_{2,2} \\ \dot{\bar{x}}_{2,2} &= -c_{2,2}\bar{x}_{2,2} \end{aligned} \quad (\text{B.10})$$

Remark B.1.2. The stabilizing function $\alpha_{2,1}$ is obtained by differentiating the stabilizing function $\alpha_{3,2}(t, \bar{x})$ two times with respect to time t . The stabilizing function $\alpha_{3,2}(t, \bar{x})$ depends on both $u_{1,d}(t)$ and its higher order derivatives $u_{1,d}^{(k)}(t)$ up to some order k . It is obtained by differentiating each stabilizing function $\alpha_{i,1}(t, \bar{x})$ $2(i-3)+1$ times and each stabilizing function $\alpha_{i,2}(t, \bar{x})$ $2(i-3)$ times. In each step $1 \leq i \leq n-1$ we also divide by $u_{1,d}$. Therefore, the stabilizing function $\alpha_{2,1}$ may not be defined when $u_{1,d}(t) = 0$. By carefully selecting the parameters $d_{i,1}$ and $d_{i,2}$ the stabilizing function $\alpha_{3,2}(t, \bar{x})$ can be made smooth with respect to its argument $u_{1,d}(t)$, *i.e.*, no divisions by $u_{1,d}(t)$ occur. This is possible by choosing $d_{i,1} \geq i-3$ and $d_{i,2} \geq i-3$. Then each stabilizing function $\alpha_{i,1}(t, \bar{x})$ and $\alpha_{i,2}(t, \bar{x})$ can be written as

$$\begin{aligned} \alpha_{i,1}(t, \bar{x}) &= U_{i,1}(\bar{u}_{1,d})\bar{x}_{i,1} + U_{i,2}(\bar{u}_{1,d})\bar{x}_{i,2} + \dots + U_{n,1}(\bar{u}_{1,d})\bar{x}_{n,1} + U_{n,2}(\bar{u}_{1,d})\bar{x}_{n,2} \\ \alpha_{i,2}(t, \bar{x}) &= U_{i,2}(\bar{u}_{1,d})\bar{x}_{i,2} + \dots + U_{n,1}(\bar{u}_{1,d})\bar{x}_{n,1} + U_{n,2}(\bar{u}_{1,d})\bar{x}_{n,2} \end{aligned} \quad (\text{B.11})$$

where $U_{j+1,1}, U_{j+1,2}$ are functions depending on $u_{1,d}(t)$ and its derivatives $\dot{u}_{1,d}^{(k)}(t)$, $k \geq 1$, *i.e.*, $\bar{u}_{1,d} = [u_{1,d}, \dot{u}_{1,d}, \dots, u_{1,d}^{(k)}]^T$. Subsequently $u_2 - u_{2,d}$ becomes equal to linear time-varying feedbacks of the form

$$u_2 - u_{2,d} = k_{2,1}(\bar{u}_{1,d})\bar{x}_{2,1} + k_{2,2}(\bar{u}_{1,d})\bar{x}_{2,2} + \dots + k_{n,1}(\bar{u}_{1,d})\bar{x}_{n,1} + k_{n,2}(\bar{u}_{1,d})\bar{x}_{n,2} \quad (\text{B.12})$$

where $k_{j,1}, k_{j,2}$ are functions depending on $u_{1,d}(t)$ and its derivatives $\dot{u}_{1,d}^{(k)}(t)$, $k \geq 1$.

B.1.2 Stability of the tracking-error dynamics

In this section we show that the complete tracking dynamics are globally exponentially stable. In the previous sections we have stabilized the (Δ_1, Δ_2) -subsystem when $u_1 = u_{1d}$ and the Δ_3 subsystem in (B.2). We can now use Theorem 3.6.1 to investigate the stability properties of the complete system. The result is stated in the following proposition.

Proposition B.1.1. *Suppose that the reference input $u_{1d}(t)$ satisfies Assumption 5.1.1. Consider the system (B.2) in closed-loop with the controller u_2 given by (B.9) and u_1 given by*

$$u_1 = u_{1d} - k_1 x_{11} - k_2 x_{12}, \quad p(s) = s^2 + k_2 s + k_1 \text{ is Hurwitz.} \quad (\text{B.13})$$

Suppose that all parameters d_i are chosen such that $\min_{i=1..n}(d_i) \geq r$ and $d_i \geq i - 3, \forall i$. Moreover, the signals $\xi_2^d(t)$ and the derivative \dot{u}_{1d} in (2.12) are uniformly bounded in t . Then the closed-loop system is globally \mathcal{H} -exponentially stable.

Proof

Define $z_1 = [\bar{x}_{n,1}, \bar{x}_{n,2}, \dots, \bar{x}_{31}, \bar{x}_{32}]^T$ and $z_2 = [\bar{x}_{21}, \bar{x}_{22}, x_{11}, x_{12}]^T$. The system (B.10) can then be written in the form (3.19), $f_1(t, z_1) = A_1(t)z_1, f_2(t, z_2) = A_2 z_2$, as

$$\begin{aligned} \dot{z}_1 &= A_1(t)z_1 + g(t, z_1, z_2)z_2 \\ \dot{z}_2 &= A_2 z_2. \end{aligned}$$

The $(n-2) \times (n-2)$ matrix $A_1(t)$ and the 4×4 matrix A_2 are given by

$$A_1(t) = \begin{bmatrix} -\phi_{n,1}(t) & 1 & 0 & \dots & \dots & \dots & 0 \\ 0 & -\phi_{n,2}(t) & u_{1,d} & 0 & \dots & \dots & 0 \\ \vdots & \ddots & \ddots & \dots & \ddots & & \vdots \\ \vdots & & \ddots & \ddots & \dots & \ddots & \vdots \\ 0 & \dots & \dots & -\phi_{3,1}(t) & 1 & 0 & 0 \\ 0 & \dots & \dots & 0 & -\phi_{3,2}(t) & u_{1,d} & 0 \\ 0 & \dots & \dots & \dots & 0 & -\phi_{3,1}(t) & 1 \\ 0 & \dots & \dots & \dots & 0 & 0 & -\phi_{3,2}(t) \end{bmatrix}$$

$$A_2 = \begin{bmatrix} -c_{2,1} & 1 & 0 & 0 \\ 0 & -c_{2,2} & 0 & 0 \\ 0 & 0 & 0 & 1 \\ 0 & 0 & -k_{1,1} & -k_{1,2} \end{bmatrix}.$$

where $\phi_{j,1}(t) = c_{j,1} u_{1,d}(t)^{2d_{j,1}+2}$ and $\phi_{j,2}(t) = c_{j,2} u_{1,d}(t)^{2d_{j,2}+2}$. The $(2(n-2) \times 4)$ perturbation matrix $g(t, z_1, z_2)$ is given by

$$g(t, z_1, z_2) = - \begin{bmatrix} 0 & 0 & 0 & 0 \\ 0 & 0 & k_1(x_{n-1,1} + \xi_{n-1,d}) & k_2(x_{n-1,1} + \xi_{n-1,d}) \\ \vdots & \vdots & \vdots & \vdots \\ 0 & 0 & 0 & 0 \\ 0 & 0 & k_1(x_{21} + \xi_{2d}) & k_2(x_{21} + \xi_{2d}) \end{bmatrix} + \begin{bmatrix} 0 & 0 & 0 & 0 \\ 0 & 0 & 0 & 0 \\ \vdots & \vdots & \vdots & \vdots \\ 0 & 0 & 0 & 0 \\ u_{1d}(t) & 0 & 0 & 0 \end{bmatrix} \quad (\text{B.14})$$

In order to apply Theorem 3.6.1 we verify the three assumptions.

(1) Consider the Σ_1 subsystem, $\dot{z}_1 = A_1(t)z_1$, given by

$$\begin{aligned}\dot{\bar{x}}_{n,1} &= -c_{n,1}u_{1,d}(t)^{2d_{n,1}+2}\bar{x}_{n,1} + \bar{x}_{n,2} \\ \dot{\bar{x}}_{n,2} &= -c_{n,2}u_{1,d}(t)^{2d_{n,2}+2}\bar{x}_{n,2} + u_{1,d}(t)\bar{x}_{n-1,1} \\ &\vdots \\ \dot{\bar{x}}_{3,1} &= -c_{3,1}u_{1,d}(t)^{2d_{3,1}+2}\bar{x}_{3,1} + \bar{x}_{3,2} \\ \dot{\bar{x}}_{3,2} &= -c_{3,2}u_{1,d}(t)^{2d_{3,2}+2}\bar{x}_{3,2}\end{aligned}$$

By recursively applying Theorem 3.6.1 it will be shown that the system is GUAS. Because the system is linear time-variant, we conclude GES, *cf.* Theorem 6.13 in (Rugh, 1996). Consider the $(\bar{x}_{3,1}, \bar{x}_{3,2}, \bar{x}_{4,1}, \bar{x}_{4,2})$ subsystem.

$$\begin{aligned}\dot{\bar{x}}_{4,1} &= -c_{4,1}u_{1,d}(t)^{2d_{4,1}+2}\bar{x}_{n,1} + \bar{x}_{4,2} \\ \dot{\bar{x}}_{4,2} &= -c_{4,2}u_{1,d}(t)^{2d_{4,2}+2}\bar{x}_{n,2} + u_{1,d}(t)\bar{x}_{3,1} \\ &\vdots \\ \dot{\bar{x}}_{3,1} &= -c_{3,1}u_{1,d}(t)^{2d_{3,1}+2}\bar{x}_{3,1} + \bar{x}_{3,2} \\ \dot{\bar{x}}_{3,2} &= -c_{3,2}u_{1,d}(t)^{2d_{3,2}+2}\bar{x}_{3,2}\end{aligned}$$

Suppose that $y_1 = (\bar{x}_{4,1}, \bar{x}_{4,2})$ and $y_2 = (\bar{x}_{3,1}, \bar{x}_{3,2})$ and that the perturbation term is

$$g(t, y_1, y_2) = \begin{bmatrix} 0 & 0 \\ u_{1,d}(t) & 0 \end{bmatrix}$$

By Assumption 5.1.1 and Proposition 5.1.2 the Γ_1 subsystem

$$\begin{aligned}\dot{\bar{x}}_{4,1} &= -c_{4,1}u_{1,d}(t)^{2d_{4,1}+2}\bar{x}_{n,1} + \bar{x}_{4,2} \\ \dot{\bar{x}}_{4,2} &= -c_{4,2}u_{1,d}(t)^{2d_{4,2}+2}\bar{x}_{n,2}\end{aligned}$$

is GES and assumption (1) in Theorem 3.6.1 is satisfied. By Assumption 5.1.1 the signal $u_{1,d}(t)$ is necessarily bounded, and the interconnection term $g(t, z_1, z_2)$ satisfies $\|g(t, y_1, y_2)\| \leq \|u_{1,d}(t)\| \leq M$ and assumption (2) in Theorem 3.6.1 is satisfied. Because the Γ_2 subsystem, *i.e.*, $(\bar{x}_{3,1}, \bar{x}_{3,2})$ subsystem is GES assumption (3) in Theorem 3.6.1 also satisfied and we conclude that the $(\bar{x}_{3,1}, \bar{x}_{3,2}, \bar{x}_{4,1}, \bar{x}_{4,2})$ subsystem is GES. Continuing in this manner it can be shown that the complete $(\bar{x}_{3,1}, \bar{x}_{3,2}, \dots, \bar{x}_{n,1}, \bar{x}_{n,2})$ subsystem is GES. This done by induction:

Suppose that the $(\bar{x}_{3,1}, \bar{x}_{3,2}, \dots, \bar{x}_{j,1}, \bar{x}_{j,2})$, $(4 \leq j \leq n)$ subsystem is GES. It remains to be shown that the $(\bar{x}_{3,1}, \bar{x}_{3,2}, \dots, \bar{x}_{j+1,1}, \bar{x}_{j+1,2})$ subsystem is GES. The $(\bar{x}_{3,1}, \bar{x}_{3,2}, \dots, \bar{x}_{j+1,1}, \bar{x}_{j+1,2})$ subsystem can be written in the form (3.19) with the Γ_1 subsystem given by

$$\begin{aligned}\dot{\bar{x}}_{j+1,1} &= -c_{j+1,1}u_{1,d}(t)^{2d_{j+1,1}+2}\bar{x}_{j+1,1} + \bar{x}_{j+1,2} \\ \dot{\bar{x}}_{j+1,2} &= -c_{j+1,2}u_{1,d}(t)^{2d_{j+1,2}+2}\bar{x}_{j+1,2}\end{aligned}$$

which is GES by Assumption 5.1.1 and Proposition 5.1.2. The Γ_2 subsystem given by the $(\bar{x}_{3,1}, \bar{x}_{3,2}, \dots, \bar{x}_{j,1}, \bar{x}_{j,2})$, $(4 \leq j \leq n)$ subsystem which is GES. The perturbation term is given by the $(2 \times 2(j-3))$ matrix

$$g(t, y_1, y_2) = \begin{bmatrix} 0 & 0 & \dots & 0 \\ u_{1,d}(t) & 0 & \dots & 0 \end{bmatrix}$$

and satisfies $\|g(t, y_1, y_2)\| \leq \|u_{1,d}(t)\| \leq M$. By Theorem 3.6.1, the $(\bar{x}_{3,1}, \bar{x}_{3,2}, \dots, \bar{x}_{j+1,1}, \bar{x}_{j+1,2})$ subsystem is GES. By converse Lyapunov theory, *i.e.*, Theorem 3.12 in (Khalil, 1996), a suitable Lyapunov function $V(t, z_1)$ for the Σ_1 subsystem is guaranteed to exist when the matrix $A_1(t)$ is uniformly bounded in t . By assumption the reference input $u_{1,d}$ is uniformly bounded and therefore also the time-varying matrix $A_1(t)$, which gives the desired result.

(2) The $(2(n-2) \times 4)$ matrix $g(t, z_1, z_2)$ is given by

$$g(t, z_1, z_2) = - \begin{bmatrix} 0 & 0 & 0 & 0 \\ 0 & 0 & k_1(x_{n-1,1} + \xi_{n-1,d}) & k_2(x_{n-1,1} + \xi_{n-1,d}) \\ \vdots & \vdots & \vdots & \vdots \\ 0 & 0 & 0 & 0 \\ 0 & 0 & k_1(x_{21} + \xi_{2d}) & k_2(x_{21} + \xi_{2d}) \end{bmatrix} + \begin{bmatrix} 0 & 0 & 0 & 0 \\ 0 & 0 & 0 & 0 \\ \vdots & \vdots & \vdots & \vdots \\ 0 & 0 & 0 & 0 \\ u_{1,d}(t) & 0 & 0 & 0 \end{bmatrix}$$

and can be written as

$$g(t, z_1, z_2) = - \sum_{j=2}^{n-1} (x_{j,1} + \xi_{n-1,d}) E_{2(n-j),3..4}^k + u_{1,d}(t) E_{1,1} \quad (\text{B.15})$$

where $E_{1,1}$ is a $(2(n-2) \times 4)$ matrix with the $(1, 1)$ -th entry $E[1, 1] = 1$ and all remaining entries $E[k, l] = 0, k \neq 1, \wedge l \neq 1$. $E_{i,3..4}$ is a $(2(n-2) \times 4)$ matrix with the $(i, 3)$ -th entry and $(i, 4)$ -th entry $E[i, j] = 1, j = 3, 4$ and all remaining entries $E[k, l] = 0, k \neq i, \wedge l \neq 3, 4$. Then $g(t, z_1, z_2)$ satisfies

$$\begin{aligned} \|g(t, z_1, z_2)\| &\leq - \sum_{j=2}^{n-1} (|x_{j,1}| + |\xi_{j,d}|) \|E_{2(j-1)-1,3..4}^k\| + |u_{1,d}(t)| \|E_{1,1}\| \\ &\leq -K_1 \sum_{j=2}^{n-1} |x_{j,1}| + (K_1 M_d + M K_2) \end{aligned} \quad (\text{B.16})$$

where we used the fact that $\|u_{1,d}(t)\| \leq M$ and $\|\xi_{j,d}\| \leq \|\xi_d\| \leq M_d$ and K_1 and K_2 denote the norms of the matrices upper-bounds on the matrices $E_{1,1}$ and $E_{i,3..4}$. We can write for $(2 \leq j \leq n-1)$

$$|x_{j,1}| = |\bar{x}_{j,1} + \alpha_{j+1,2}(t, \bar{x})| \leq |\bar{x}_{j,1}| + |\alpha_{j+1,2}(t, \bar{x})| \quad (\text{B.17})$$

where $\alpha_{n,1}(t, \bar{x}) = -c_{n,1} u_{1,d}^{2d_{n,1}+2} \bar{x}_{n,1}$ and for $(2 \leq j \leq n-2)$

$$\begin{aligned} \alpha_{j+1,1}(t, \bar{x}) &= -c_{j+1,1} u_{1,d}^{2d_{j+1,1}+2} \bar{x}_{j+1,1} + \frac{d}{dt} [\alpha_{j+2,2}(t, \bar{x})], \\ \alpha_{j+1,2}(t, \bar{x}) &= -c_{j+1,2} u_{1,d}(t)^{2d_{j+1,2}+1} \bar{x}_{j+1,2} + \frac{d}{dt} [\alpha_{j+1,1}(t, \bar{x})], \end{aligned} \quad (\text{B.18})$$

with $c_{j+1,1}, c_{j+1,2} > 0$ and $d_{j+1,1}, d_{j+1,2} \in \mathbb{N}$. All stabilizing functions, see Remark B.1.2, can be written as

$$\alpha_{j+1,2}(t, \bar{x}) = U_{j+1,1}(\bar{u}_{1,d}) \bar{x}_{j+1,1} + U_{j+1,2}(\bar{u}_{1,d}) \bar{x}_{j+1,2} + \dots + U_{n,1}(\bar{u}_{1,d}) \bar{x}_{n,1} + U_{n,2}(\bar{u}_{1,d}) \bar{x}_{n,2}$$

for all $(2 \leq j \leq n-1)$ and where $U_{j+1,1}, U_{j+1,2}$ are functions depending on $u_{1,d}(t)$ and its derivatives $\dot{u}_{1,d}^{(k)}(t), k \geq 1$, i.e., $\bar{u}_{1,d} = [u_{1,d}, \dot{u}_{1,d}, \dots, u_{1,d}^{(k)}]^T$. The signal $u_{1,d}(t)$ and its derivatives $\dot{u}_{1,d}^{(k)}(t), k \geq 1$ are bounded. Therefore we conclude that

$$\alpha_{j,2}(t, \bar{x}) \leq \bar{U}_{n,1}|\bar{x}_{n,1}| + \bar{U}_{n,2}|\bar{x}_{n,2}| + \dots + \bar{U}_{j,1}|\bar{x}_{j,1}| + \bar{U}_{j,2}|\bar{x}_{j,2}| \quad (\text{B.19})$$

where $U_{j,1}$ and $U_{j,2}, j \in 2, \dots, n-1$ are constants depending on the bounds $|u_{1,d}(t)| \leq M$ and $|u_{1,d}^{(k)}(t)| \leq Md$.

- (3) The characteristic polynomial of the Σ_2 subsystem is given by $\chi(s) = (s+c_1)(s+c_2)p(s)$ where $p(s)$ is given in (5.15). Because the polynomial $p(s)$ is Hurwitz and the c_i 's are positive, the Σ_2 subsystem is GES. The existence of a class \mathcal{K} function $\zeta(\cdot)$ satisfying condition (3.23) follows directly from the GES of the Σ_2 subsystem.

By Theorem 3.6.1 and Lemma 3.6.2 we conclude \mathcal{K} -exponentially stability of the complete closed loop system. □

Summarizing, we have exponentially stabilized the (Δ_1, Δ_2) and Δ_3 subsystems separately. We then conclude by Theorem 3.6.1 and Lemma 3.6.2 that the combined system is \mathcal{K} -exponentially stable when the reference input $u_{1,d}$ satisfies Assumption 5.1.1 and its derivatives $u_{1,d}^{(k)}$ are uniformly bounded over t .

B.2 Robustness considerations

In this section we investigate the robustness properties of the closed-loop system. Uniform exponential stability is a desirable property because it implies exponential stability with respect to bounded vanishing perturbations and uniformly bounded solutions with respect to bounded non-vanishing perturbations. In this section we will show that the closed-loop system (Σ_1, Σ_2) are uniformly exponentially stable and determine (conservative) bounds, on the perturbation, for which the closed-loop system is robust in some sense.

In order to show that the closed-loop system Σ_1 is exponentially stable, we need the following lemma. It gives a result for asymptotic stability of a scalar perturbed system.

Lemma B.2.1 (Lemma 1 in (Sørdalen and Egeland, 1995)). *Consider the nonlinear, one-dimensional, time-varying system*

$$\dot{x} = -a(x,t)x + d(x,t) \quad t \geq t_0, x(t_0) \in \mathbb{R} \quad (\text{B.20})$$

under the following assumptions:

- *There exists a solution $x(t)$ for any $x(t_0)$ and any $t \geq t_0$; when $a(x,t)$ and $d(x,t)$ are continuous in x and t , there exists at least one solution.*
- *$a(x,t)$ has the property that for all solutions $x(t)$, there exists positive constants λ and P such that*

$$-P_1 + \lambda_1(t-t_0) \leq \int_{t_0}^t a(x(\tau), \tau) d\tau \leq P_2 + \lambda_2(t-t_0), \quad \forall t \geq t_0, \forall t_0 \geq 0. \quad (\text{B.21})$$

- The signal $d(x, t)$ is bounded for any $t \geq t_0$ and any $x(t)$ by

$$|d(x(t), t)| \leq D \exp(-\gamma(t - t_0)) \quad (\text{B.22})$$

for some positive constants D and γ .

Then

$$\forall \varepsilon > 0, \quad |x(t)| \leq c(|x(t_0)| + D) \exp(-(\alpha - \varepsilon)(t - t_0)) \quad (\text{B.23})$$

where $\alpha = \min(\lambda_1, \gamma) > 0$ and $c = \max(\exp(P_1), \exp(P_1)/\varepsilon)$.

The previous lemma shows that a solution $x(t)$ of (B.20) converges exponentially to zero if $a(x, t)$ and $d(x, t)$ satisfy conditions (B.21) and (B.22) respectively.

Consider the closed-loop Σ_1 subsystem, $\dot{z}_1 = A_1(t)z_1$, given by

$$\begin{aligned} \dot{\bar{x}}_{n,1} &= -c_{n,1}u_{1,d}(t)^{2d_{n,1}+2}\bar{x}_{n,1} + \bar{x}_{n,2} \\ \dot{\bar{x}}_{n,2} &= -c_{n,2}u_{1,d}(t)^{2d_{n,2}+2}\bar{x}_{n,2} + u_{1,d}(t)\bar{x}_{n-1,1} \\ &\vdots \\ \dot{\bar{x}}_{3,1} &= -c_{3,1}u_{1,d}(t)^{2d_{3,1}+2}\bar{x}_{3,1} + \bar{x}_{3,2} \\ \dot{\bar{x}}_{3,2} &= -c_{3,2}u_{1,d}(t)^{2d_{3,2}+2}\bar{x}_{3,2} \end{aligned} \quad (\text{B.24})$$

By Proposition 5.1.2, the $(\bar{x}_{3,1}, \bar{x}_{3,2})$ subsystem is exponentially stable, i.e.,

$$|\bar{x}_{3,2}| \leq \varphi_{3,2}|x_{3,2}(t_0)| \exp(-\gamma_{3,2}(t - t_0))$$

Using Lemma(B.2.1) we obtain

$$|\bar{x}_{3,1}| \leq D_{3,1} \exp(-\lambda_{3,1})(t - t_0)$$

where $\lambda_{3,1} = \min(\gamma_{3,1}, \gamma_{3,2}) - \varepsilon_{3,1}$ and $D_{3,1} = \varphi_{3,1}(|x_{3,1}(t_0)| + \frac{\varphi_{3,2}|x_{3,2}(t_0)|}{\varepsilon_{3,1}})$. Since $u_{1,d}(t)$ is bounded, i.e., $u_{1,d}(t) < M, \forall t$, we obtain in a similar way that

$$|\bar{x}_{4,2}| \leq D_{4,2} \exp(-\lambda_{4,2})(t - t_0)$$

with $\lambda_{4,2} = \min(\gamma_{4,2}, \lambda_{3,1}) - \varepsilon_{4,2}$ and $D_{4,2} = \varphi_{4,2}(|x_{4,2}(t_0)| + M \frac{D_{3,1}}{\varepsilon_{4,2}})$. Then

$$|\bar{x}_{4,1}| \leq D_{4,1} \exp(-(\lambda_{4,1})(t - t_0))$$

with $\lambda_{4,1} = \min(\gamma_{4,1}, \lambda_{4,2}) - \varepsilon_{4,1}$ and $D_{4,1} = \varphi_{4,1}(|x_{4,1}(t_0)| + \frac{D_{4,2}}{\varepsilon_{4,1}})$. Continuing in this manner, we obtain for $3 \leq k \leq n$

$$\begin{aligned} |\bar{x}_{k,1}| &\leq D_{k,1} \exp(-(\lambda_{k,1})(t - t_0)) \\ |\bar{x}_{k,2}| &\leq D_{k,2} \exp(-(\lambda_{k,2})(t - t_0)) \end{aligned}$$

where $\gamma_{k,1} = \varepsilon_1 c_{k,1}$, $\gamma_{k,2} = \varepsilon_1 c_{k,2}$ and $\varphi_{k,1} = \exp(-c_{k,1} \delta \varepsilon_1)$, $\varphi_{k,2} = \exp(-c_{k,2} \delta \varepsilon_1)$ and

$$\begin{aligned} \lambda_{k,1} &= \min(\gamma_{k,1}, \lambda_{k,2}) - \varepsilon_{k,1}, \quad \lambda_{k,2} = \min(\gamma_{k,2}, \lambda_{k-1,1}) - \varepsilon_{k,2} \\ D_{k,1} &= \varphi_{k,1}(|x_{k,1}(t_0)| + \frac{D_{k,2}}{\varepsilon_{k,1}}), \quad D_{k,2} = \varphi_{k,2}(|x_{k,2}(t_0)| + \frac{MD_{k-1,1}}{\varepsilon_{k,2}}). \end{aligned}$$

The parameters $\lambda_{3,1}$, $\lambda_{3,2}$, $D_{3,1}$ and $D_{3,2}$ in the previous equation are given by $\lambda_{3,1} = \min(\gamma_{3,1}, \gamma_{3,2}) - \varepsilon_{3,1}$, $\lambda_{3,2} = \gamma_{3,2}$, $D_{3,1} = \varphi_{3,1}(|x_{3,1}(t_0)| + \frac{\varphi_{3,2}|x_{3,2}(t_0)|}{\varepsilon_{3,1}})$ and $D_{3,2} = \varphi_{3,2}(|x_{3,2}(t_0)|)$. Further substitution gives, for $4 \leq k \leq n$

$$\begin{aligned} \lambda_{k,1} &= \min(\gamma_{k,1} - \varepsilon_{k,1}, \gamma_{k,2} - \varepsilon_{k,1} - \varepsilon_{k,2}, \lambda_{k-1,1} - \varepsilon_{k,1} - \varepsilon_{k,2}) \\ \lambda_{k,2} &= \min(\gamma_{k,1} - \varepsilon_{k,2}, \gamma_{k-1,1} - \varepsilon_{k-1,1} - \varepsilon_{k,2}, \lambda_{k-1,2} - \varepsilon_{k-1,1} - \varepsilon_{k,2}) \\ D_{k,1} &= \varphi_{k,1}|x_{k,1}(t_0)| + \frac{\varphi_{k,1}\varphi_{k,2}}{\varepsilon_{k,1}}|x_{k,2}(t_0)| + \frac{\varphi_{k,1}\varphi_{k,2}}{\varepsilon_{k,1}\varepsilon_{k,2}}MD_{k-1,1}, \\ D_{k,2} &= \varphi_{k,2}|x_{k,2}(t_0)| + \frac{\varphi_{k,2}\varphi_{k-1,1}}{\varepsilon_{k,2}}M|x_{k-1,1}(t_0)| + \frac{\varphi_{k,2}\varphi_{k-1,1}}{\varepsilon_{k,2}\varepsilon_{k-1,1}}MD_{k-1,2}. \end{aligned}$$

$$|\bar{x}_{k,1}| \leq D_{k,1} \exp(-\lambda_{n,1}(t - t_0))$$

$$|\bar{x}_{k,2}| \leq D_{k,2} \exp(-\lambda_{n,2}(t - t_0))$$

Since

$$\begin{aligned} D_{k,1} &= \sum_{j=0}^{k-3} \alpha_{k-j,1}^k |x_{k-j,1}(t_0)| + \frac{\varphi_{k-j,2}}{\varepsilon_{k-j,1}} \alpha_{k-j,1}^k |x_{k-j,2}(t_0)| \\ &= \alpha_{k,1}^k |x_{k,1}(t_0)| + \frac{\varphi_{k,2}}{\varepsilon_{k,1}} \alpha_{k,1}^k |x_{k,2}(t_0)| + \sum_{j=1}^{k-3} \alpha_{k-j,1}^k |x_{k-j,1}(t_0)| + \frac{\varphi_{k-j,2}}{\varepsilon_{k-j,1}} \alpha_{k-j,1}^k |x_{k-j,2}(t_0)| \\ D_{k,2} &= \beta_{k,2}^k |x_{k,2}(t_0)| + \sum_{j=1}^{k-3} \beta_{k-j,1}^k |x_{k-j,1}(t_0)| + \frac{\varphi_{k-j,2}}{\varepsilon_{k-j,1}} \beta_{k-j,1}^k |x_{k-j,2}(t_0)|, \end{aligned}$$

where we defined

$$\begin{aligned} \alpha_{k,1}^k &= \varphi_{k,1}, \quad \alpha_{k-j,1}^k = \left(\prod_{i=0}^{j-1} \frac{\varphi_{k-i,1}\varphi_{k-i,2}M}{\varepsilon_{k-i,1}\varepsilon_{k-i,2}} \right) \varphi_{k-j,1}, \quad j \geq 1, \\ \beta_{k,2}^k &= \varphi_{k,2}, \quad \beta_{k-j,1}^k = \left(\prod_{i=0}^{j-2} \frac{\varphi_{k-i,2}\varphi_{k-i-1,1}M}{\varepsilon_{k-i,2}\varepsilon_{k-i-1,1}} \right) \frac{\varphi_{k-j+1,2}\varphi_{k-j,1}M}{\varepsilon_{k-j+1,2}}, \quad j \geq 1, \end{aligned}$$

where we defined $\prod_{i=0}^k = 1$ for $k < 0$ such that $\beta_{k-1,1}^k = \frac{\varphi_{k,2}\varphi_{k-1,1}M}{\varepsilon_{k,2}}$. Moreover, it holds that

$$\alpha_{k-j,1}^k = \frac{\varphi_{k,1}}{\varepsilon_{k,1}} \left(\prod_{i=0}^{j-1} \frac{\varphi_{k-i,2}\varphi_{k-i-1,1}M}{\varepsilon_{k-i,2}\varepsilon_{k-i-1,1}} \right) \frac{\varphi_{k-j+1,2}\varphi_{k-j,1}M}{\varepsilon_{k-j+1,2}} = \frac{\varphi_{k,1}}{\varepsilon_{k,1}} \beta_{k-j,1}^k, \quad j \geq 1,$$

and therefore for $k \geq 3$ we have

$$\begin{aligned} D_{k,1} &= \varphi_{k,1}|x_{k,1}(t_0)| + \frac{\varphi_{k,2}\varphi_{k,1}}{\varepsilon_{k,1}}|x_{k,2}(t_0)| + \frac{\varphi_{k,1}}{\varepsilon_{k,1}} \sum_{j=1}^{k-3} \beta_{k-j,1}^k \left(|x_{k-j,1}(t_0)| + \frac{\varphi_{k-j,2}}{\varepsilon_{k-j,1}}|x_{k-j,2}(t_0)| \right) \\ D_{k,2} &= \varphi_{k,2}|x_{k,2}(t_0)| + \sum_{j=1}^{k-3} \beta_{k-j,1}^k \left(|x_{k-j,1}(t_0)| + \frac{\varphi_{k-j,2}}{\varepsilon_{k-j,1}}|x_{k-j,2}(t_0)| \right), \end{aligned}$$

Consider the upper-triangular $2(n-2) \times 2(n-2)$ matrix D given by

$$\begin{aligned} D_{2k+1,2k+1} &= \varphi_{n-k,1}, \quad D_{2k+1,2j+1} = \frac{\varphi_{n-k,1}}{\varepsilon_{n-k,1}} \beta_{n-j,1}^{n-k}, \quad j > k \\ D_{2k+2,2k+2} &= \varphi_{n-k,2}, \quad D_{2k+2,2j+2} = \frac{\varphi_{n-k,1}\varphi_{n-k-1,2}}{\varepsilon_{n-k,1}\varepsilon_{n-k-1,2}} \beta_{n-j,1}^{n-k}, \quad j > k, \end{aligned} \tag{B.25}$$

$0 \leq k \leq n-3$. The matrix D has the following structure

$$\begin{aligned}
 D &= \begin{bmatrix} \varphi_{n,1} & \frac{\varphi_{n,1}\varphi_{n,2}}{\varepsilon_{n,1}} & * & \dots & \dots & \dots & * \\ 0 & \varphi_{n,2} & \frac{\varphi_{n,2}\varphi_{n-1,1}}{\varepsilon_{n,1}}M & * & \dots & \dots & * \\ \vdots & \ddots & \ddots & \dots & \ddots & & \vdots \\ \vdots & & \ddots & \ddots & \dots & \ddots & \vdots \\ 0 & \dots & \dots & \varphi_{4,1} & \frac{\varphi_{4,1}\varphi_{4,2}}{\varepsilon_{4,1}} & \frac{\varphi_{4,1}\varphi_{4,2}\varphi_{3,1}}{\varepsilon_{4,1}\varepsilon_{4,2}}M & \frac{\varphi_{4,1}\varphi_{4,2}\varphi_{3,1}\varphi_{3,2}}{\varepsilon_{4,1}\varepsilon_{4,2}\varepsilon_{3,1}}M \\ 0 & \dots & \dots & 0 & \varphi_{4,2} & \frac{\varphi_{4,2}\varphi_{3,1}}{\varepsilon_{4,2}}M & \frac{\varphi_{4,2}\varphi_{3,1}\varphi_{3,2}}{\varepsilon_{4,2}\varepsilon_{3,1}}M \\ 0 & \dots & \dots & \dots & 0 & \varphi_{3,1} & \frac{\varphi_{3,1}\varphi_{3,2}}{\varepsilon_{3,1}} \\ 0 & \dots & \dots & \dots & 0 & 0 & \varphi_{3,2} \end{bmatrix} \\
 &= \begin{bmatrix} \varphi_{n,1} & \frac{\varphi_{n,1}\varphi_{n,2}}{\varepsilon_{n,1}} & \frac{\varphi_{n,1}}{\varepsilon_{n,1}}\beta_{n-1,1} & \frac{\varphi_{n,1}\varphi_{n-1,2}}{\varepsilon_{n,1}\varepsilon_{n-1,2}}\beta_{n-1,1} & \dots & \dots & \frac{\varphi_{n,1}}{\varepsilon_{n,1}}\beta_{3,1} & \frac{\varphi_{n,1}\varphi_{3,2}}{\varepsilon_{n,1}\varepsilon_{3,2}}\beta_{3,1}^n \\ 0 & \varphi_{n,2} & \beta_{n-1,1} & \frac{\varphi_{n-1,2}}{\varepsilon_{n-1,1}}\beta_{n-1,1} & \dots & \dots & \beta_{3,1} & \frac{\varphi_{n-1,2}}{\varepsilon_{n-1,1}}\beta_{3,1}^n \\ \vdots & \ddots & \ddots & \dots & \dots & \ddots & \vdots & \vdots \\ \vdots & & \ddots & \ddots & \dots & \dots & \ddots & \vdots \\ 0 & \dots & \dots & \dots & \varphi_{4,1} & \frac{\varphi_{4,1}\varphi_{4,2}}{\varepsilon_{4,1}} & \frac{\varphi_{4,1}}{\varepsilon_{4,1}}\beta_{3,1}^4 & \frac{\varphi_{4,1}\varphi_{3,2}}{\varepsilon_{4,1}\varepsilon_{3,1}}\beta_{3,1}^4 \\ 0 & \dots & \dots & \dots & 0 & \varphi_{4,2} & \beta_{3,1}^4 & \frac{\varphi_{3,2}}{\varepsilon_{3,1}}\beta_{3,1}^4 \\ 0 & \dots & \dots & \dots & \dots & 0 & \varphi_{3,1} & \frac{\varphi_{3,1}\varphi_{3,2}}{\varepsilon_{3,1}} \\ 0 & \dots & \dots & \dots & \dots & 0 & 0 & \varphi_{3,2} \end{bmatrix}
 \end{aligned}$$

Since $z_1(t) = [\bar{x}_{n,1}, \bar{x}_{n,2}, \dots, \bar{x}_{3,1}, \bar{x}_{3,2}]^T$, we can write

$$|z_1(t)| \leq D|z_1(t_0)| \exp(-\lambda(t-t_0)),$$

where $\gamma = \min(\gamma_{n,1}, \gamma_{n,2})$ and therefore

$$\|z_1(t)\| \leq \|D\| \|z_1(t_0)\| \exp(-\lambda(t-t_0)).$$

By Remark 3.4.1, a Lyapunov function $V_1(t, z_1) = z_1^T P(t) z_1$ for the Σ_1 subsystem is given by (3.11), i.e.,

$$P(t) = \int_t^\infty \phi^T(\tau, t) \phi(\tau, t) d\tau \quad (\text{B.26})$$

where $\phi(t, t_0)$ denotes the unknown transition matrix of the system. Along solutions of the Σ_2 subsystem the Lyapunov function $V_1(t, z_1)$ satisfies

$$\begin{aligned}
 \frac{1}{2L} \|z_1\|^2 &\leq V_1(z_1) \leq \frac{\|D\|^2}{2\lambda} \|z_1\|^2 \\
 \dot{V}_2(z_1) &\leq -\|z_1\|^2 \\
 \frac{\partial V}{\partial z_1} &\leq \frac{\|D\|^2}{\lambda} \|z_1\|
 \end{aligned} \quad (\text{B.27})$$

The closed-loop (Σ_2) subsystem is given by

$$\dot{z}_2 = \begin{bmatrix} -c_{2,1} & 1 & 0 & 0 \\ 0 & -c_{2,2} & 0 & 0 \\ 0 & 0 & 0 & 1 \\ 0 & 0 & -k_{1,1} & -k_{1,2} \end{bmatrix} z_2. \quad (\text{B.28})$$

By solving (3.10) for $Q(t) = I$ and $\dot{P}(t) = 0$, a time-invariant Lyapunov function $V_2(x) = x^T P x$ is obtained that is given by

$$P = 1/2 \begin{bmatrix} \frac{1}{c_{21}} & \frac{1}{c_{21}(c_{22} + c_{21})} & 0 & 0 \\ \frac{1}{c_{21}(c_{22} + c_{21})} & \frac{c_{21}c_{22} + c_{21}^2 + 1}{c_{21}c_{22}(c_{22} + c_{21})} & 0 & 0 \\ 0 & 0 & \frac{k_{12}^2 + k_{11}^2 + k_{11}}{k_{11}k_{12}} & \frac{1}{k_{11} + 1} \\ 0 & 0 & \frac{1}{k_{11}} & \frac{1}{k_{11}k_{12}} \end{bmatrix}.$$

The Lyapunov function V_2 satisfies

$$\begin{aligned} \lambda_{\min}(P)\|z_2\|^2 &\leq V_2(z_2) \leq \lambda_{\max}(P)\|z_2\|^2 \\ \dot{V}_2(z_2) &\leq -\|z_2\|^2 \\ \frac{\partial V}{\partial z_2} &\leq 2\lambda_{\max}(P)\|z_2\| \end{aligned} \quad (\text{B.29})$$

Now consider the Lyapunov function $V(t, z) = V_1(t, z_1) + V_2(z_2)$. Then the Lyapunov function V satisfies

$$\begin{aligned} \min\left(\frac{1}{2L}, \lambda_{\min}(P)\right)\|z\|^2 &\leq V_2(z) \leq \max\left(\frac{\|D\|^2}{2\lambda}, \lambda_{\max}(P)\right)\|z\|^2 \\ \dot{V}_2(z) &\leq -\|z\|^2 \\ \frac{\partial V}{\partial z} &\leq \max\left(\frac{\|D\|^2}{\lambda}, 2\lambda_{\max}(P)\right)\|z\| \end{aligned} \quad (\text{B.30})$$

By Theorem 3.5.1 we conclude that the closed-loop system (Σ_1, Σ_2) is robust with respect to vanishing perturbations, *i.e.*, $\delta(t, z_1) = 0$ for $x = 0$, satisfying

$$\|\delta(t, x)\| < \frac{1}{\max\left(\frac{\|D\|^2}{\lambda}, 2\lambda_{\max}(P)\right)}, \quad \forall z \in \mathbb{R}^n \quad (\text{B.31})$$

By Theorem 3.5.2 we conclude that solutions of the system are globally ultimately bounded for non-vanishing perturbations, *i.e.*, $\delta(t, x) \neq 0$ for $x = 0$, satisfying

$$\|\delta(t, x)\| < \frac{1}{\max\left(\frac{\|D\|^2}{\lambda}, 2\lambda_{\max}(P)\right)} \sqrt{\frac{\min\left(\frac{1}{2L}, \lambda_{\min}(P)\right)}{\max\left(\frac{\|D\|^2}{2\lambda}, \lambda_{\max}(P)\right)}} \theta r, \quad \forall \|z\| < r, z \in \mathbb{R}^n. \quad (\text{B.32})$$

The underactuated H-Drive manipulator

C.1 Dynamic model of the underactuated H-Drive Manipulator

In this appendix, a dynamic model for the underactuated H-Drive Manipulator will be derived. This dynamic model is used as a starting point for a simplified dynamic model presented in Chapter 7.

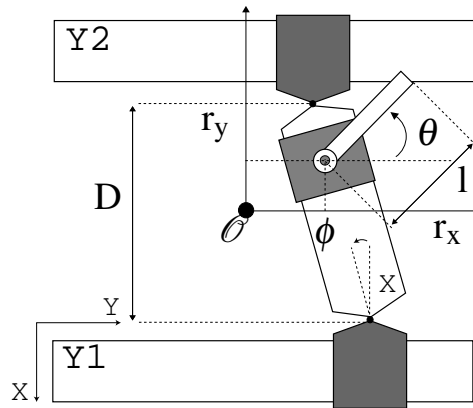


Figure C.1: The coordinate system of the modified H-drive system with generalized coordinates $[r_x, r_y, \phi, \theta]$. The masses along the axes are denoted by m_X , m_{Y1} and m_{Y2} respectively. The mass of the rotational link is denoted by m_3 and its moment of inertia about its axis of rotation by I_3 . The length l denotes the distance between the rotational joint and the center of mass of the link (not shown).

The coordinate system of the underactuated H-Drive Manipulator is illustrated in Figure C.1. Denote the mass of the Y motors by m_{Y1} and m_{Y2} respectively, the mass of the x motor by m_X , the mass and inertia of the beam by m_B and I_B and the mass and inertia of the rotational link by m_3 and I_3 respectively. The longitudinal forces from the Y axes are denoted by F_{Y1} and F_{Y2} respectively, while the transversal force from the X axis is denoted by F_X . The distance from the rotational joint at the position $[r_x(t), r_y(t)]$ to the center of mass of the rotational link is denoted by the length l and the length of the X -axis beam is denoted by D . The system moves in a horizontal plane and is not influenced by gravity. The generalized coordinates are given by $q = [Y_B(t), \phi(t), X(t), \theta(t)]$, where $Y_B(t)$ denotes the position along the Y axis of the center of mass of the beam, $\phi(t)$ the tilt-angle, $X(t)$ the position of the X motor along the X axis and $\theta(t)$ the orientation of the rotational link.

Assume that the center of mass of the X axis beam moves along a straight line through the origin \mathcal{O} in the direction of the Y axis. The position vectors, in (X, Y) coordinates, from the origin \mathcal{O} to the center of mass of the rigid bodies are given by

$$\begin{aligned} r_{B(t)} &= [0, Y_B(t)], \\ r_{Y1}(t) &= [(D/2) \cos(\phi(t)), Y_B(t) + (D/2) \sin(\phi(t))], \\ r_{Y2}(t) &= [-(D/2) \cos(\phi(t)), Y_B(t) - (D/2) \sin(\phi(t))], \\ r_{X(t)} &= [(X(t) + D/2) \cos(\phi(t)), Y_B(t) + (X(t) + D/2) \sin(\phi(t))], \\ r_{link} &= [(X(t) + D/2) \cos(\phi(t)) - l \sin(\theta(t)), Y_B(t) + (X(t) + D/2) \sin(\phi(t)) + l \cos(\theta(t))]. \end{aligned}$$

Note that the position $X(t)$ along the X axis is given by $X \in [-0.613, 0.059]$. By assumption, the center of mass of the beam is located at the position $X(t) = -D/2$, where the length D of the beam is approximately equal to 0.6 m. The kinetic energy of the system is

$$T = 1/2 (m_B \dot{r}_B^2 + m_{Y1} \dot{r}_{Y1}^2 + m_{Y2} \dot{r}_{Y2}^2 + m_X \dot{r}_X^2 + I_B \dot{\phi}^2 + m_3 \dot{r}_3^2 + I_3 \dot{r}_{link}^2). \quad (C.1)$$

Using the Euler-Lagrange formulation, *i.e.*,

$$\frac{d}{dt} \left(\frac{\partial T}{\partial \dot{q}_i} \right) - \frac{\partial T}{\partial q_i} = F_i, \quad i = \{1, \dots, 4\},$$

the dynamic model of the underactuated H-Drive Manipulator can be written in the form

$$M(q)\ddot{q} + C(q, \dot{q})\dot{q} = \begin{bmatrix} F \\ 0 \end{bmatrix}. \quad (C.2)$$

The (4×4) symmetric and positive-definite mass matrix $M(q)$ is given by

$$\begin{aligned} M_{[1,1]} &= m_{Y1} + m_{Y2} + m_X + m_B + m_3, \\ M_{[1,2]} &= ((X(t) + D/2)(m_X + m_3) + (D/2)(m_{Y1} - m_{Y2})) \cos(\phi(t)), \\ M_{[1,3]} &= (m_X + m_3) \sin(\phi(t)), \\ M_{[1,4]} &= -m_3 l \sin(\theta(t)), \\ M_{[2,2]} &= I_B + (m_X + m_3)(X(t) + D/2)^2 + (D/2)^2(m_{Y1} + m_{Y2}), \\ M_{[2,3]} &= 0, \\ M_{[2,4]} &= -m_3 l (X(t) + D/2) \sin(\theta(t) - \phi(t)), \\ M_{[3,3]} &= m_X + m_3, \\ M_{[3,4]} &= -m_3 L \cos(\theta(t) - \phi(t)), \\ M_{[4,4]} &= I_3 + m_3 l^2. \end{aligned} \quad (C.3)$$

The (4×4) matrix representing Coriolis and centrifugal forces $C(q, \dot{q})$ is given by

$$\begin{aligned}
C_{[1,1]} &= C_{[2,1]} = C_{[3,1]} = C_{[3,3]} = C_{[4,1]} = C_{[4,4]} = 0, \\
C_{[1,2]} &= (m_X + m_3) \cos(\phi(t)) \frac{dX(t)}{dt} - ((m_X + m_3)(X(t) + D/2) + (D/2)(m_{Y1} - m_{Y2})) \sin(\phi(t)) \frac{d\phi(t)}{dt}, \\
C_{[1,3]} &= (m_X + m_3) \cos(\phi(t)) \frac{d\phi(t)}{dt}, \\
C_{[1,4]} &= -m_3 l \cos(\theta(t)) \frac{d\theta(t)}{dt}, \\
C_{[2,2]} &= (m_X + m_3)(X(t) + D/2) \frac{dX(t)}{dt}, \\
C_{[2,3]} &= (m_X + m_3)(X(t) + D/2) \frac{d\phi(t)}{dt}, \\
C_{[2,4]} &= -m_3 l (X(t) + D/2) \cos(\theta(t) - \phi(t)) \frac{d\theta(t)}{dt}, \\
C_{[3,2]} &= -(m_X + m_3)(X(t) + D/2) \frac{d\phi(t)}{dt}, \\
C_{[3,4]} &= m_3 l (\sin(\theta(t) - \phi(t)) \frac{d\theta(t)}{dt}), \\
C_{[4,2]} &= m_3 l (X(t) + D/2) \cos(\theta(t) - \phi(t)) \frac{d\phi(t)}{dt} - m_3 l \sin(\theta(t) - \phi(t)) \frac{dX(t)}{dt}, \\
C_{[4,3]} &= -m_3 l \sin(\theta(t) - \phi(t)) \frac{dX(t)}{dt}.
\end{aligned} \tag{C.4}$$

The matrices M and C satisfy the property that $\dot{M} - 2C$ is skew-symmetric. The (4×1) input matrix F is given by

$$\begin{aligned}
F_{[1,1]} &= F_{Y1} + F_{Y2}, \\
F_{[2,1]} &= (D/2)(F_{Y1} - F_{Y2}) \cos(\phi(t)), \\
F_{[3,1]} &= F_X, \\
F_{[4,1]} &= 0.
\end{aligned} \tag{C.5}$$

C.2 The servo controllers

Suppose that two controller $u_1 = \alpha_1(\xi, t)$ and $u_2 = \alpha_2(\xi, t)$ have been designed for the second-order chained form (7.13). Using relation (7.11) these inputs can be transformed into desired accelerations v_x and v_y for the X - and Y -axes, *cf.* (7.9). In order to compensate for the friction and cogging forces in the X and Y -axes, these desired accelerations are integrated twice to obtain desired positions r_{xd} and r_{yd} for the position of the unactuated joint. These desired positions are then commanded to servo controllers for the X and Y -axes. This approach, depicted in Figure 7.3, can be identified as 'virtual internal model following control' (Kosuge et al., 1987), in which a local servo system is used to control the system. The desired positions of the servo system are obtained by integrating the desired accelerations which are commanded from a top-level controller.

In (van der Voort, 2002) the frequency responses of the X and Y axes have been measured. In order to reduce the effect of static friction and cogging, the motors are translated along a trajectory

with a constant speed of $0.02 \text{ [m/s}^2\text{]}$ and covers about 0.1 [m] . During this motion a band-limited white-noise signal generated at 5 [kHz] , *i.e.*, the sampling-rate of the system, with a power-intensity of 10^{-5} [Nm/s] is injected at the input of the PID controller. As mentioned earlier, the dynamics of the Y -axes are influenced by the position along the X axis. Therefore, the frequency responses have been measured for different positions along the X -axis. This makes it possible to develop a Linear Parameter-Varying (LPV) model which incorporates the coupling of the X - and Y -dynamics. In this thesis, however, it is assumed that the X - and Y -axes are decoupled, and PID controllers are used to control the X and Y axes independently.

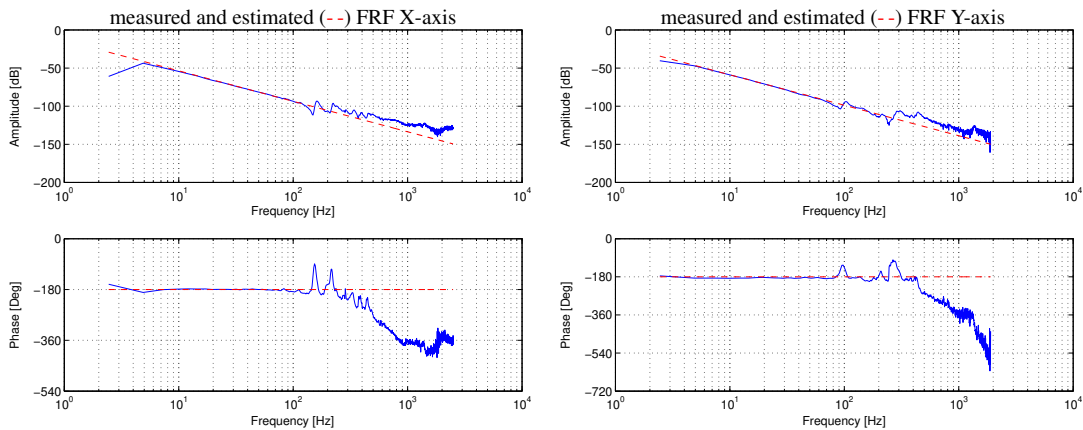


Figure C.2: Frequency responses function (FRF) of the X - (left) and $Y1$ -axis (right) of the H-drive system

The frequency response of the X -axis with the Y -axis located at $Y = 0.5 \text{ [m]}$ and the frequency response of the $Y1$ axis with the X -axis located at $X = 0.3 \text{ [m]}$ are shown in Figure (C.2). For frequencies below 100 [Hz] , the system behaves like a double integrator, *i.e.*, the magnitude shows a slope of -40 [dB/decade] and a phase around -180 degrees. By fitting the frequency response for these lower frequencies with a double integrator, we conclude that the lumped masses are given by $m_X/k_m = 0.12066$ and $m_Y1/k_m = 0.21914 \text{ [A} \cdot \text{s}^2/\text{m]}$. In (Hendriks, 2000) the motor constant of the LiMMS was calculated and given by $k_m = 74.4 \text{ [N/A]}$, thus these lumped masses correspond to masses $m_x = 8.98 \text{ [kg]}$ and $m_y = 16.30 \text{ [kg]}$, respectively.

The frequency response of the X -axis shows that there are resonance frequencies at $149, 161, 210$ and 223 [Hz] . The frequency response of the Y -axis shows resonance frequencies at $93, 102, 246$ and 300 [Hz] . As mentioned earlier, the dynamics of the Y axes are influenced by the dynamics of the X -axes. In fact, in (van der Voort, 2002) frequency responses of the Y axes have been measured with the X axis located at different positions. In that reference it is shown that besides the resonance frequency at 102 [Hz] , a second resonance frequency occurs at 135 [Hz] . The damping of this eigenfrequency is highly position dependent, *i.e.*, it is well damped when the mass of the X motor is located far away from the Y axis and poorly damped when the mass of the X motor is located near to the Y axis.

In (van der Voort, 2002), the position dependency of the dynamics of the Y axis has been captured by developing a Linear Parameter Varying (LPV) model, in which the position of the X axis acts as the varying parameter. In this manner it is possible to design H_∞ controllers and LPV controllers that compensate the position dependency of the resonance frequency at 135 [Hz] . It turns out, however, that the H_∞ controllers are only locally stable, *i.e.*, when one of the controllers is used for the whole

operating range of the H-Drive, then instability may occur. It is however possible to design PID controllers that guarantee stability over the whole operating range. Therefore, we assume that the dynamics of the X and Y axes are decoupled and design PID controllers for the X and Y axes which are globally asymptotically stable. These controllers are of the type PI Lead/Lag in series with a second-order low-pass with a cut-off frequency at 300 Hz, and are given by

$$C_{servo,X} = \frac{0.6755s^2 + 106.1s + 4000}{4.4806 \cdot 10^{-9}s^3 + 1.6892 \cdot 10^{-5}s^2 + 1.5920 \cdot 10^{-2}s} \quad (C.6)$$

$$C_{servo,Y} = \frac{1.182s^2 + 185.7s + 7000}{4.4806 \cdot 10^{-9}s^3 + 1.6892 \cdot 10^{-5}s^2 + 1.5920 \cdot 10^{-2}s}$$

Since the LiMMS motors for the X and Y -axes are of the same type, it is assumed that all three motors have similar dynamics. The structure of the controllers therefore only differ in gains, since the mass in the direction of the Y -axes is larger than in the X -direction. We aim at compensating the resonance frequencies by adding notches to these PID controllers. The bode diagrams of the resulting PID controllers are shown in Figure C.3. The frequency response of the resulting open-loop transfer

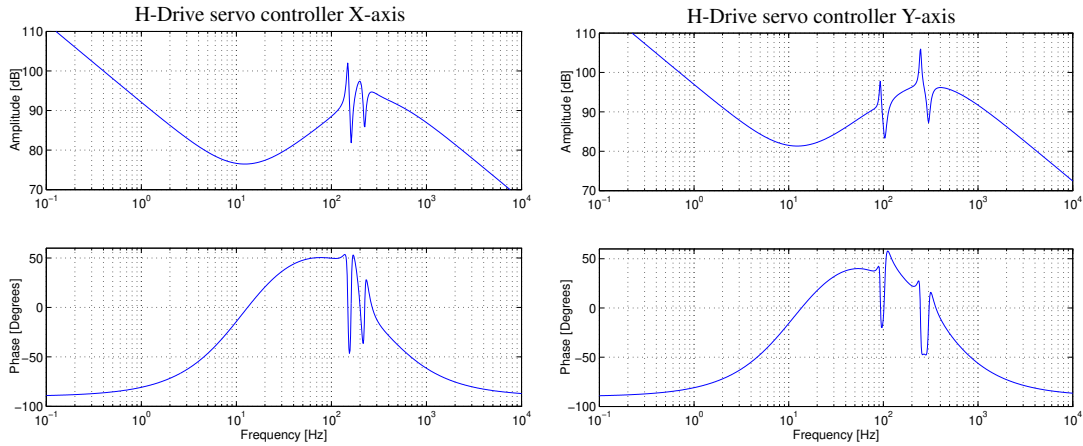


Figure C.3: Bode diagram of the servo controller for the X - (left) and Y -axes (right)

is shown in Figure C.4. The X -axis has a bandwidth of around 60 [Hz] with a phase-margin of 50 degrees and a gain-margin of 18 [dB]. The Y -axis has a bandwidth of around 52 Hz and a phase-margin of 35 degrees and a gain-margin of 16 [dB]. Using the frequency responses of the Y axis measured at different positions of the X axis, see (van der Voort, 2002), it can be verified that the closed-loop systems are asymptotically stable over the whole operating range.

C.3 Motion Planning

In Chapter 4 a number of trajectory generation methods have been presented for the second-order chained form. In Section 7.2, it was shown that the underactuated H-Drive Manipulator is transformable into the second-order chained form. In this section, the trajectory generation methods will be illustrated by application to the underactuated H-Drive Manipulator. Because these methods are used to generate point-to-point motions, the resulting trajectories are not persistently exciting. Therefore, the trajectory generation methods have not been used to generate reference trajectories for the

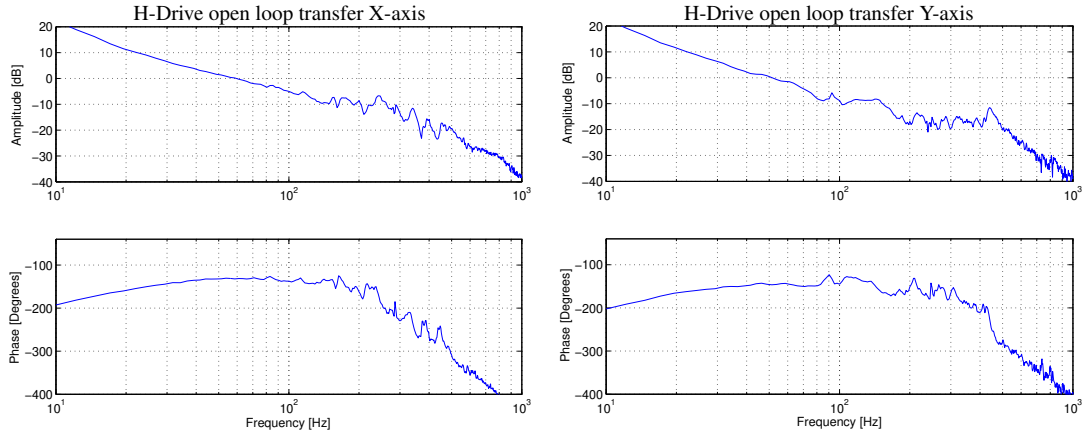


Figure C.4: Frequency response of the open-loop system of the X- (left) and Y-axes (right)

tracking problem, presented in Chapter 7 and 8. The flatness-based approach, presented in Section 4.4, can not be used to generate trajectories that pass through singularities of the endogenous transformation and the solution (4.16) of the point-to-point steering method, presented in Section 4.5, can not be used to generate trajectories when the desired final value of the state ξ_1 is equal to its initial value, *i.e.*, $\xi_{10} = \xi_{1T}$. Therefore, the focus will be on the variational method and the sub-optimal method, presented in Section 4.6 and 4.7 respectively, and the flatness-based method and the solution (4.16) will not be considered here.

Consider the problem of moving the rotational link from an initial zero-velocity configuration q_A to a desired final zero-velocity configuration q_B . By transforming these configurations to the second-order chained form, we obtain an initial zero-velocity position ξ_A and a desired final zero-velocity position ξ_B for the second-order chained form. Here, we consider the motion planning problem for the configurations given by

$$\begin{aligned} q_A &= [0, -0.3, 0], & q_B &= [0, 0.3, 0], \\ \xi_A &= [0, 0, -0.3], & \xi_B &= [0, 0, 0.3]. \end{aligned} \quad (\text{C.7})$$

This trajectory can be interpreted as the equivalent of a parallel parking motion, often encountered in mobile robotics, for an underactuated PPR manipulator. This desired motion of the rotational link is interesting because, due to the nonholonomic constraint, it is difficult to control the ξ_3 coordinate of the system. Moreover, the trajectory passes through the singularities encountered in the flatness-based approach and the solution (4.16) of the point-to-point steering problem.

The variational method and the sub-optimal methods will be compared on the basis of computational effort, control effort and the length of the trajectory. These measures will be evaluated for the chained form coordinates as well as the original mechanical coordinates. Note that the coordinate transformation into the second-order chained form is only defined for link angles in the set $\{\theta(t) \mid |\theta(t)| < \pi/2\}$. In this thesis, a 'virtual internal model following control' approach has been adopted to control the underactuated H-Drive Manipulator. Therefore, the desired input currents to the LiMMS will not be generated, but instead the coordinate transformation is used to transform the desired inputs $[u_1, u_2]$ into desired accelerations $[v_x, v_y]$ of the LiMMS along the x - and y -direction. In order to compare the variational and the sub-optimal methods, we also define the following measures:

- the computational effort in seconds of computing time is denoted by the measure \mathcal{T} .

- the control effort \mathcal{U} in terms of the inputs of the second-order chained form and the control effort \mathcal{V} in terms of the accelerations of the underactuated H-Drive manipulator:

$$\begin{aligned}\mathcal{U} &= \int_0^T (u_1(t)^2 + u_2(t)^2) dt \\ \mathcal{V} &= \int_0^T (v_x(t)^2 + v_y(t)^2) dt\end{aligned}\tag{C.8}$$

- the length \mathcal{L} of the trajectory in terms of the chained form states and the length \mathcal{D} in terms of the mechanical states of the underactuated H-Drive manipulator::

$$\begin{aligned}\mathcal{L} &= \int_0^T (\dot{\xi}_1(t)^2 + \dot{\xi}_2(t)^2 + \dot{\xi}_3(t)^2) dt \\ \mathcal{D} &= \int_0^T (\dot{r}_x(t)^2 + \dot{r}_y(t)^2 + \dot{\theta}(t)^2) dt\end{aligned}\tag{C.9}$$

In the variational method the motion planning problem is formulated as a set of nonlinear equalities given by (4.18). The basis functions are chosen as a finite number of harmonic functions, *i.e.*,

$$h(t) = [1 \quad \sin(\omega t) \quad \cos(\omega t) \quad \sin(2\omega t) \quad \cos(2\omega t) \quad \sin(3\omega t) \quad \cos(3\omega t)]\tag{C.10}$$

A SQP method available through the 'fmincon' procedure in the Matlab Optimization Toolbox has been used to solve the resulting nonlinear optimization problem. In the sub-optimal method (FDM), the optimal control problem has been formulated by a boundary value problem (BVP) given by (4.27). In order to solve this BVP the Finite Differences Method (FDM) is applied with a uniform mesh of 200 points to approximate the solution. In both methods, the desired final configuration is reached after one second, *i.e.*, $T = 1$ [s]. The initial conditions in both methods are chosen as a set of randomly generated numbers.

Remark C.3.1. Suppose that a trajectory $\xi(t)$ connecting the points ξ_A and ξ_B is available on the time-interval $t \in [0, T]$. Consider the 'stretched' trajectory $\bar{\xi}(t) = \xi(t/\alpha)$ defined on the time-interval $t \in [0, \alpha T]$. The corresponding inputs are given (by differentiation) as $\bar{u}(t) = u(t/\alpha)/\alpha^2$. The cost-criterion J for the stretched trajectory is given as

$$J = \int_0^{\alpha T} (\bar{u}_1(t)^2 + \bar{u}_2(t)^2) dt = (1/\alpha^4) \int_0^{\alpha T} (u_1(t/\alpha)^2 + u_2(t/\alpha)^2) dt = (1/\alpha^3) \int_0^T (u_1(t)^2 + u_2(t)^2) dt.$$

The stretched trajectory thus remains optimal for the cost-criterion $J = \int_0^T (u_1(t)^2 + u_2(t)^2) dt$. In fact, this property holds for any quadratic cost-criterion

$$J = \int_0^T \xi(t)^T Q \xi(t) + u(t)^T R u(t) dt$$

where $\xi(t) = [\xi_1(t), \dot{\xi}_1(t), \dots, \xi_6(t), \dot{\xi}_6(t)]$, $u(t) = [u_1(t), u_2(t)]$ and Q and R are constant positive-definite symmetric matrices.

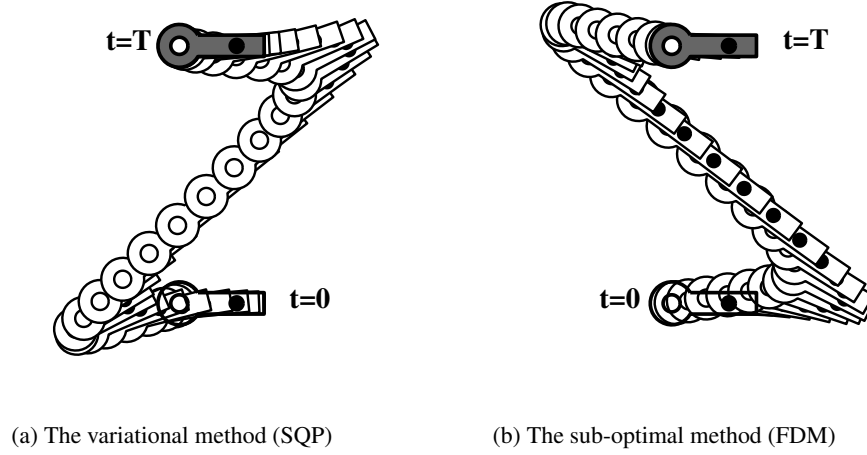


Figure C.5: Stroboscopic visualization of the motion planning solutions; the black dot (•) denotes the position of the center of percussion at a distance of 13 [cm] from the joint.

The solution of the variational method (SQP) to the motion planning problem is shown in Figure C.6 and the solution of the sub-optimal method (FDM) is shown in Figure C.7. In order to transform the chained form states and inputs to the mechanical states and accelerations the parameter value $\lambda = 0.13$ [m] has been used. This value is in the order of magnitude of the value of λ in Table 8.1. In Figure C.5 a stroboscopic visualization of the solutions is given, by assuming a link length of 0.1725 [m].

| method | \mathcal{T} [s] | \mathcal{L} [m] | \mathcal{U} [m/s] | \mathcal{D} [m, rad] | \mathcal{V} [m/s] |
|-------------|-------------------|-------------------|---------------------|------------------------|---------------------|
| variational | 17.14 | 5.76 | 273.85 | 4.93 | 175.66 |
| sub-optimal | 45.97 | 5.23 | 244.13 | 4.59 | 151.03 |

Table C.1: Measures of the motion planning methods

The corresponding measures have been summarized in Table C.1. The variational method does not guarantee a solution, *i.e.*, in some cases the design variables may not converge to a solution. In addition, the variational method only generates a feasible trajectory connecting the points ξ_A and ξ_B and is not uniquely defined, *i.e.*, more than one solution may exist. In fact, when using a different initial condition for the same motion planning problem, a second solution can be found that resembles the trajectory from the sub-optimal method.

The sub-optimal method only generates sub-optimal solutions in the sense that only a local minimum to the optimal control problem can be found, since the Hamiltonian of the optimal control problem is non-convex. This means that there may exist multiple solutions or local minima to the optimal control problem. If a different initial condition is chosen then the FDM may converge to a different local minimum. For the current motion planning problem, however, different initial conditions did not result in different trajectories and the calculated solution may be a global minimum. If the Hamiltonian of the optimal control problem is convex, then the FDM converges to a global

minimum and an optimal solution has been found.

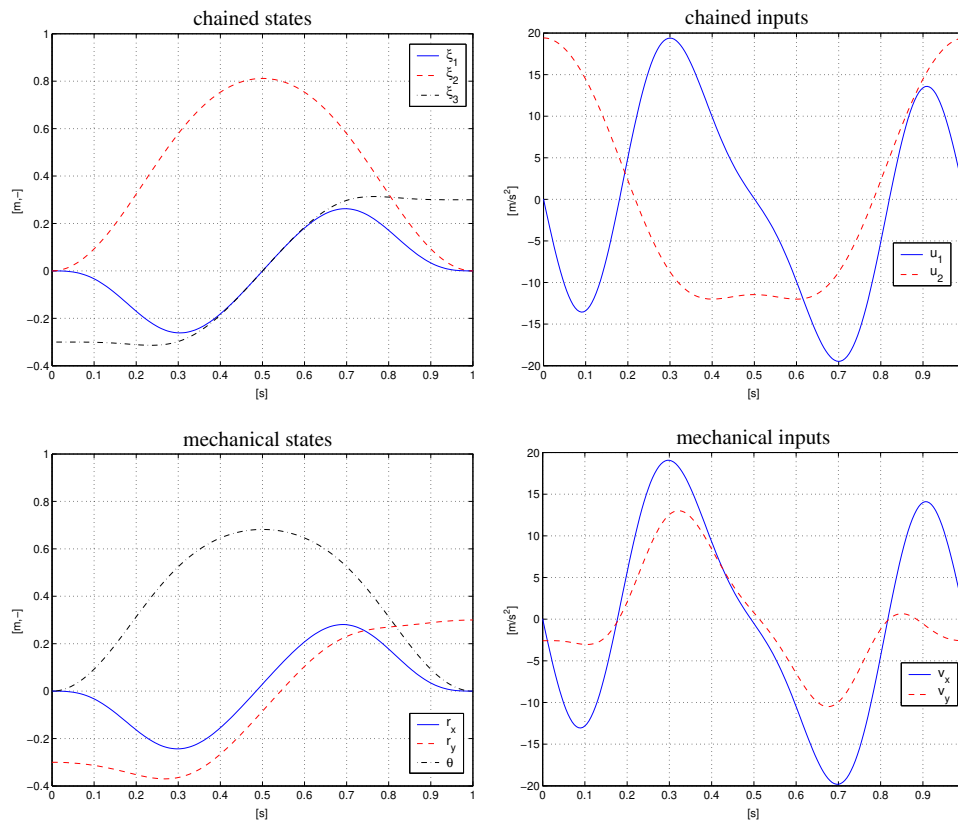


Figure C.6: The solution of the variational method (SQP) to the motion planning problem (C.7); r_x, ξ_1, u_1 (solid), r_y, ξ_2, u_2 (dashed) and θ, ξ_3 (dash-dotted).

As expected the sub-optimal methods generates a trajectory that is closer to the optimal solution, *i.e.*, the measure \mathcal{U} is smaller, than the variational method. The required computational effort is however larger. It should be noted that both methods can be used to solve the motion planning problem in terms of the dynamics of the mechanical system without using a transformation into the second-order chained form. In certain cases, the resulting trajectories will look completely different from the trajectories that are based on the second-order chained form. The main advantage of using the second-order chained form is that it considerably reduces the computational time needed to solve the motion planning problem. Furthermore, the presented trajectory generation methods may be generalized to include obstacle avoidance, see (Verhoeven, 2002) for more information.

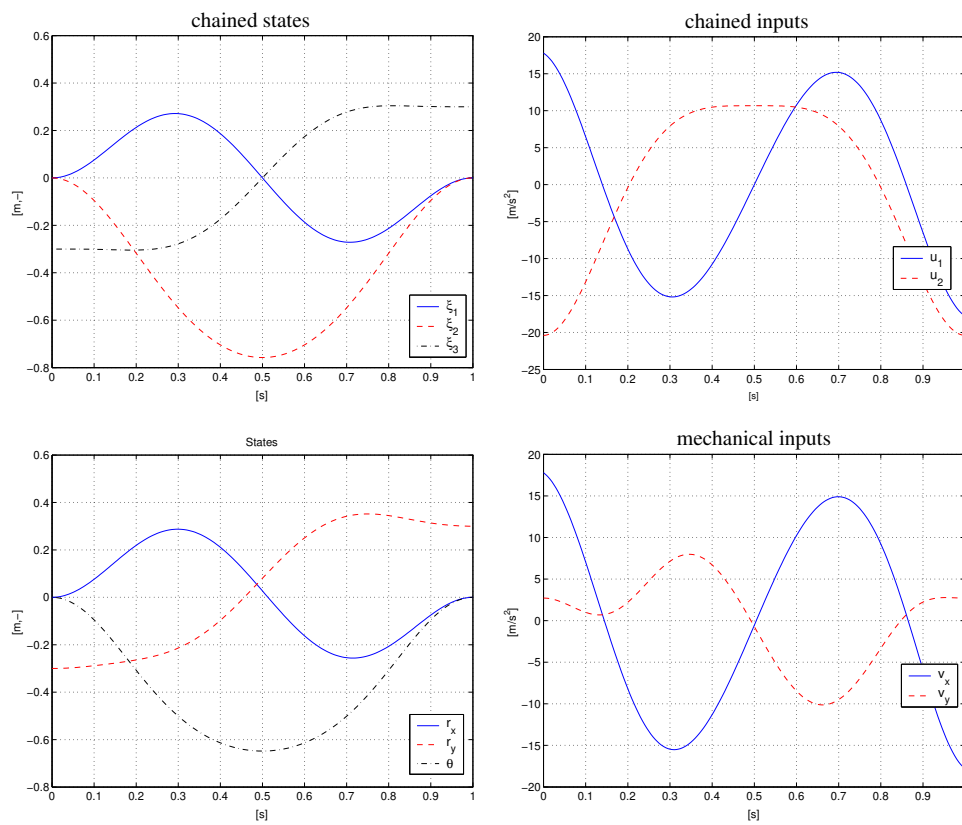


Figure C.7: The solution of the sub-optimal method (FDM) to the motion planning problem (C.7); r_x, ξ_1, u_1 (solid), r_y, ξ_2, u_2 (dashed) and θ, ξ_3 (dash-dotted).

Bibliography

- Aneke, N. P. I., Lizárraga, D. A., and Nijmeijer, H. (2002a). Homogeneous stabilization of the extended chained form system. In *Proceedings of the IFAC World Congress*. Barcelona, Spain. Paper no. T-Tu-A08-1 (cd-rom).
- Aneke, N. P. I., Lizárraga, D. A., Nijmeijer, H., and de Jager, A. G. (2002b). Homogeneous stabilization of an underactuated manipulator. In *Proceedings of the Mechatronics 2002 Conference*. University of Twente, Enschede, The Netherlands, pp. 848–857.
- Aneke, N. P. I., Nijmeijer, H., and de Jager, A. G. (2000). Trajectory tracking by cascaded backstepping control for a second-order nonholonomic mechanical system. In A. Isidori, F. Lamnabhi-Lagarrigue, and W. Respondek (eds.), *Nonlinear Control in the Year 2000*, Springer: Paris, volume 258 of *Lecture Notes in Control and Information Sciences*. pp. 35–49.
- Aneke, N. P. I., Nijmeijer, H., and de Jager, A. G. (2003). Tracking control of second-order chained form systems by cascaded backstepping control. *International Journal of Robust and Nonlinear Control*, **13**, 95–115. Published online: 30 September 2002.
- Arai, H., Tanie, K., and Shiroma, N. (1998a). Nonholonomic control of a three-dof planar underactuated manipulator. *IEEE Transactions on Robotics and Automation*, **14**, 681–695.
- Arai, H., Tanie, K., and Shiroma, N. (1998b). Time-scaling control of an underactuated manipulator. In *Proceedings of the IEEE International Conference on Robotics and Automation*. pp. 2619–2626.
- Ascher, U. M., Mattheij, R. M. M., and Russel, R. D. (1988). *Numerical solution of boundary value problems for ordinary differential equations*. Prentice Hall.
- Astolfi, A. (1996). Discontinuous control of nonholonomic systems. *Systems and Control Letters*, **27**, 37–45.
- Bergerman, M. and Yangsheng, X. (1994). Robust control of underactuated manipulators: analysis and implementation. In *Proceedings of the IEEE International Conference on Systems, Man and Cybernetics*. volume 1, pp. 925–930.
- Bertsekas, D. P. (1995). *Nonlinear Programming*. Athena Scientific.
- Brockett, R. W. (1983). Asymptotic stability and feedback stabilization. In R. W. Brockett, R. S. Milman, and H. J. Sussmann (eds.), *Differential Geometric Control Theory*, Birkhauser, Boston. pp. 181–191.
- Coron, J.-M. (1995). On the stabilization in finite time of locally controllable systems by means of continuous time-varying feedback law. *SIAM Journal on Control and Optimization*, **33**(3), 804–833.
- Coron, J.-M. and Rosier, L. (1994). A relation between continuous time-varying and discontinuous feedback stabilization. *Journal of Mathematical Systems, Estimation and Control*, **4**(1), 67–84.

- de Wit, C. C., Berghuis, H., and Nijmeijer, H. (1994). Practical stabilization of nonlinear systems in chained form. In *Proceedings of the 33rd IEEE Conference on Decision and Control*. volume 4, pp. 3475–3480.
- Do, K. D., Jiang, Z. P., and Pan, J. (2002). Robust global stabilization of underactuated ships on a linear course. In *Proceedings of the American Control Conference*. volume 1, pp. 304–309.
- Egeland, O. and Berglund, E. (1994). Control of an underwater vehicle with nonholonomic acceleration constraints. In *Proceedings of the IFAC Conference on Robot Control*. Capri, Italy, pp. 845–850.
- Egeland, O., Berglund, E., and Sjørdalen, O. J. (1994). Exponential stabilization of a nonholonomic underwater vehicle with constant desired configuration. In *Proceedings IEEE International Conference on Robotics and Automation*. San Diego CA, U.S., volume 1, pp. 20–25.
- Fletcher, R. (1980). *Practical Methods of Optimization*, volume Vol. 1 Unconstrained Optimization and Vol 2. Constrained Optimization. John Wiley & Sons Ltd.
- Fliess, M., Lévine, J., Martin, P., and Rouchon, P. (1994). Nonlinear control and lie-bäcklund transformations: Towards a new differential geometric standpoint. In *Proceedings of the 33rd Conference on Decision and Control*. Lake Buena Vista, FL, volume 1, pp. 339–344.
- Fliess, M., Lévine, J., Martin, P., and Rouchon, P. (1995). Flatness and defect of non-linear systems: Introductory theory and examples. *International Journal of Control*, **61**(6), 1327–1361.
- Ge, S. S., Sun, Z., Lee, T. H., and Spong, M. W. (2001). Feedback linearization and stabilization of second-order non-holonomic systems. *International Journal of Control*, **74**(14), 1383–1392.
- Gill, P. E., Murray, W., and Wright, M. H. (1981). *Practical Optimization*. Academic Press, London.
- Hauser, J., Sastry, S., and Meyer, G. (1992). Nonlinear control design for slightly non-minimum phase systems: application to V/STOL aircraft. *Automatica*, **28**(4).
- Hendriks, S. G. M. (2000). *Iterative Learning Control on the H-Drive*. Master's thesis, Eindhoven University of Technology. DCT 2000.37.
- Hermes, H. (1991). Nilpotent and high-order approximations of vector fields systems. *SIAM Review*, **33**, 238–264.
- Imura, J., Kobayashi, K., and Yoshikawa, T. (1996). Nonholonomic control of a 3 link planar manipulator with a free joint. In *Proceedings of the 35th IEEE Conference on Decision and Control*. Kobe, Japan, volume 2, pp. 1435–1436.
- Iwamura, M., Yamamoto, M., and Mohri, A. (2000). Near-optimal motion planning for nonholonomic systems using time-axis transformation and gradient method. In *Proceedings of the IEEE Conference on Robotics and Automation*. volume 2, pp. 1811–1816.
- Jiang, Z. P. and Nijmeijer, H. (1999). A recursive technique for tracking control of nonholonomic systems in chained form. *IEEE Transactions on Automatic Control*, **44**, 265–279.
- Kawski, M. (1995). Geometric homogeneity and stabilization. In *Proceedings of the IFAC Nonlinear Control Systems Design Symposium (NOLCOS)*. Tahoe City, California, volume 1, pp. 164–169.
- Khalil, H. K. (1996). *Nonlinear systems*. Prentice Hall, Upper Saddle River, New York, second edition.
- Kim, M.-S., Oh, S.-K., Shin, J.-H., and Lee, J.-J. (2001). Robust model reference adaptive control of underactuated robot manipulators. In *Proceedings of the IEEE International Symposium on Industrial Electronics*. volume 3, pp. 1579–1584.

- Kobayashi, K. (1999). *Controllability Analysis and Control Design of Nonholonomic Systems*. Ph.D. thesis, Department of Mechanical Engineering, Kyoto University, Japan.
- Kolmanovsky, I. and McClamroch, N. H. (1995). Developments in nonholonomic control problems. *IEEE Control Systems Magazine*, **15**, 20–36.
- Kosuge, K., Furuta, K., and Yokoyama, T. (1987). Virtual internal model following control of robot arms. In *Proceedings of the IEEE International Conference on Robotics and Automation*. pp. 1549–1554.
- Laiou, M.-C. and Astolfi, A. (1999). Quasi-smooth control of chained systems. In *Proceedings of the American Control Conference*. San Diego, California, pp. 3940–3944.
- Lakshmikantham, V. and Leela, S. (1969). *Differential and Integral Inequalities: Theory and Applications*, volume 1. Academic Press, New York.
- Lee, E. B. and Markus, L. (1967). *Foundations of optimal control theory*. John Wiley & Sons Ltd.
- Lefeber, E. (2000). *Tracking Control of Nonlinear Mechanical Systems*. Ph.D. thesis, Universiteit Twente, Enschede.
- Lefeber, E., Robertsson, A., and Nijmeijer, H. (1999). Linear controllers for tracking chained-form systems. In D. Aeyels, F. Lamnabhi-Lagarrigue, and A. J. van der Schaft (eds.), *Stability and Stabilization of Nonlinear Systems*, Springer Verlag, volume 246 of *Lecture Notes in Control and Information Sciences*. pp. 183–199.
- Lefeber, E., Robertsson, A., and Nijmeijer, H. (2000). Linear controllers for exponential tracking of systems in chained-form. *International Journal of Robust and Nonlinear Control*, 243–263.
- Lewis, F. L. and Syrmos, V. L. (1995). *Optimal Control*. John Wiley & Sons Ltd.
- Li, Z. and Canny, J. F. (eds.) (1993). *Nonholonomic Motion Planning*. Kluwer.
- Lizárraga, D., Aneke, N. P. I., and Nijmeijer, H. (2003). Robust point-stabilization of underactuated mechanical systems via the extended chained form. *Submitted to: SIAM Journal of Control and Optimization*, -(-), -.
- Lizárraga, D. A., Morin, P., and Samson, C. (1999). Non-robustness of continuous homogeneous stabilizers for affine control systems. In *Proceedings of the IEEE Conference on Decision and Control (CDC)*. Phoenix, Arizona, volume 1, pp. 855–860.
- Luca, A. D., Mattone, R., and Oriolo, G. (1998). Steering a class of redundant mechanisms through end-effector generalized forces. *IEEE Transactions on Robotics and Automation*, **14**, 329–333.
- Luca, A. D. and Oriolo, G. (2000). Motion planning and trajectory control of an underactuated three-link robot via dynamic feedback linearization. In *Proceedings of the 2000 IEEE International Conference on Robotics & Automation*. San Francisco, CA, pp. 2789–2795.
- Lucibello, P. and Oriolo, G. (2001). Robust stabilization via iterative state steering with an application to chained-form systems. *Automatica*, **37**(1), 71–79.
- Lynch, K. M., Shiroma, N., Arai, H., and Tanie, K. (1998). Motion planning for a 3-dof robot with a passive joint. In *Proceedings of the IEEE International Conference on Robotics and Automation*. volume 2, pp. 927–932.
- McClamroch, N. H., Kolmanovsky, I., Cho, S., and Reyhanoglu, M. (1998). Control problems for planar motion of a rigid body with an unactuated internal degree of freedom. In *Proceedings of the American Control Conference*. Philadelphia, USA, volume 1, pp. 229–233.

- M'Closkey, R. and Morin, P. (1998). Time-varying homogeneous feedback: design tools for exponential stabilization of systems with drift. *International Journal of Control*, **71**(5), 837–869.
- M'Closkey, R. T. and Murray, R. M. (1993). Nonholonomic systems and exponential convergence: some analysis tools. In *Proceedings of the 32nd IEEE Conference on Decision and Control*. CDC, San Antonio, Texas, pp. 943–948.
- Mita, T. and Nam, T. K. (2001). Control of underactuated manipulators using variable period dead-beat control. In *Proceedings of the IEEE International Conference on Robotics and Automation*. volume 3, pp. 2735–2740.
- Morin, P. and Samson, C. (1997). Time-varying exponential stabilization of a rigid spacecraft with two control torques. *IEEE Transactions on Automatic Control*, **42**(4), 943–948.
- Morin, P. and Samson, C. (1999). Exponential stabilization of nonlinear driftless systems with robustness to unmodeled dynamics. *Control, Optimization and Calculus of Variations (COCV)*, **4**, 1–35.
- Murray, R. M. (1993). Control of nonholonomic systems using chained forms. *Fields Institute Communications*, **1**, 219–245.
- Murray, R. M., Li, Z., and Sastry, S. S. (1994). *A Mathematical introduction to Robotic Manipulation*. CRC Press.
- Murray, R. M. and Sastry, S. S. (1991). Steering nonholonomic systems in chained forms. In *Proceedings of the 30th IEEE Conference on Decision and Control*. CDC, Brighton, England, pp. 1121–1126.
- Murray, R. M. and Sastry, S. S. (1993). Nonholonomic motion planning: Steering using sinusoids. *IEEE Transactions on Automatic Control*, **38**(5), 700–716.
- Neimark, Y. and Fufaev, N. A. (1972). *Dynamics of Nonholonomic Systems*, volume 33. American Mathematic Society Translations.
- Nijmeijer, H. and van der Schaft, A. J. (1990). *Nonlinear Dynamical Control Systems*. Springer: New York.
- Oriolo, G. and Nakamura, Y. (1991). Control of mechanical systems with second-order nonholonomic constraints: Underactuated manipulators. In *Proceedings of the 30th Conference on Decision and Control*. CDC, Brighton, England, pp. 2398–2403.
- Panteley, E., Lefeber, E., Loría, A., and Nijmeijer, H. (1998). Exponential tracking control of a mobile car using a cascade approach. In *Proceedings of the IFAC Workshop on Motion Control*. Grenoble, pp. 221–226.
- Panteley, E. and Loría, A. (1998). On global uniform asymptotic stability of nonlinear time-varying systems in cascade. *Systems and Control Letters*, **33**(2), 131–138.
- Panteley, E. and Loría, A. (2001). Growth rate conditions for uniform asymptotic stability of cascaded time-varying systems. *Automatica*, **37**, 453–460.
- Pettersen, K. Y. (1996). *Exponential Stabilization of Underactuated Vehicles*. Ph.D. thesis, Norwegian University of Science and Technology, Department of Engineering Cybernetics.
- Pettersen, K. Y. and Nijmeijer, H. (1998). Tracking control of an underactuated surface vessel. In *Proceedings IEEE Conference of Decision and Control*. Florida, U.S., volume 4, pp. 4561–4566.
- Pettersen, K. Y. and Nijmeijer, H. (2000). Semi-global practical stabilization and disturbance adaptation for an underactuated ship. In *Proceedings of the 39th IEEE Conference on Decision and Control*. Sydney, Australia, volume 3, pp. 2144–2149.

- Pomet, J.-B. and Samson, C. (1994). Exponential stabilization of nonholonomic systems in power form. In *IFAC Symp. on Robust Control Design*. pp. 447–452.
- Rathinam, M. and Murray, R. M. (1998). Configuration flatness of lagrangian systems underactuated by one control. *SIAM Journal on Control and Optimization*, **36**(1), 164–179.
- Reyhanoglu, M., Cho, S., McClamroch, N. H., and Kolmanovsky, I. V. (1998). Discontinuous feedback control of a planar rigid body with an unactuated degree of freedom. In *Proceedings of the 37th Conference on Decision and Control*. volume 1, pp. 433–438.
- Reyhanoglu, M., van der Schaft, A. J., McClamroch, N. H., and Kolmanovsky, I. (1996). Nonlinear control of a class of underactuated systems. In *Proceedings of the 35th Conference on Decision and Control*. Kobe, Japan, pp. 1682–1687.
- Reyhanoglu, M., van der Schaft, A. J., McClamroch, N. H., and Kolmanovsky, I. (1999). Dynamics and control of a class of underactuated mechanical systems. In *IEEE Transactions on Automatic Control*. volume 44, pp. 1663–1671.
- Rugh, W. J. (1996). *Linear System Theory*. Prentice-Hall, 2nd edition.
- Shin, J.-H. and Lee, J.-L. (2000). Experimental verification for robust adaptive control of an underactuated robot manipulator with second-order nonholonomic constraints. In *Proceedings of the International Conference on Intelligent Robots and Systems*. volume 2, pp. 1534–1558.
- Sørdalen, O. J. and Egeland, O. (1993). Exponential stabilization of chained nonholonomic systems. In *Proceedings of the European Control Conference 1993*. Groningen, The Netherlands, pp. 1438–1443.
- Sørdalen, O. J. and Egeland, O. (1995). Exponential stabilization of nonholonomic chained systems. *IEEE Transactions on Automatic Control*, **40**(1), 35–49.
- Spong, M. W. (1995). The swingup control problem for the Acrobot. *IEEE Control Systems Magazine*, **15**(1), 49–55.
- Sussmann, H. J. (1979). Subanalytic sets and feedback control. *Journal of Differential Equations*, **31**, 31–52.
- Sussmann, H. J. (1983). Lie brackets and local controllability: a sufficient condition for scalar-input systems. *SIAM Journal on Control and Optimization*, **21**, 686–713.
- Sussmann, H. J. (1987). A general theorem on local controllability. *SIAM Journal on Control and Optimization*, **25**(1), 158–194.
- Tanaka, K., Iwasaki, M., and Wang, H. O. (2000). Stable switching fuzzy control and its application to a hovercraft type vehicle. In *Proceedings of the 9th IEEE International Conference on Fuzzy Systems*. pp. 804–809.
- Teel, A. R., Murray, R. M., and Walsh, G. (1992). Nonholonomic control systems: From steering to stabilization with sinusoids. In *Proceedings of the IEEE Conference on Decision and Control (CDC)*. Tucson, USA, volume 2, pp. 1603–1609.
- van der Voort, A.-J. (2002). *LPV Control Based on a Pick and Place Unit*. Master’s thesis, Eindhoven University of Technology. DCT 2002.31.
- Verhoeven, R. (2002). *Motion planning for underactuated manipulators*. Master’s thesis, Eindhoven University of Technology, Eindhoven, The Netherlands. DCT 2000.47.
- Walsh, G., Tilbury, D., Sastry, S., Murray, R., and Laumond, J.-P. (1994). Stabilization of trajectories for systems with nonholonomic constraints. *IEEE Transactions on Automatic Control*, **39**(1), 216–222.

-
- Yoshikawa, T., Kobayashi, K., and Watanabe, T. (2000). Design of desirable trajectory with convergent control for 3-d.o.f manipulator with a nonholonomic constraint. In *Proceedings of the 2000 IEEE International Conference on Robotics & Automation*. San Fransisco, CA, volume 2, pp. 1805–1810.
- Zabczyk, J. (1989). Some comments on stabilizability. *Applied Mathematics and Optimization*, **19**, 1–9.

Summary

Underactuated mechanical systems, or system having more degrees of freedom than actuators, are abundant in real-life. Examples of such systems include, but are not limited to, road vehicles such as cars and trucks, mobile robots, underactuated robot manipulators, surface vessels, underwater vehicles, helicopters and spacecraft. In certain cases, these underactuated mechanical systems are subject to second-order nonholonomic constraints. A second-order nonholonomic constraint is known as an acceleration constraint which is non-integrable, which means that the constraint can not be written as the time-derivative of some function of the generalized coordinates and velocities. Therefore, the second-order nonholonomic constraint can not be eliminated by integration and this constraint forms an essential part of the dynamics.

The interest for underactuated mechanical systems with second-order nonholonomic constraints can be motivated by the fact that, in general, the stabilization problem can not be solved by smooth (or even continuous) time-invariant state feedbacks. Typically, a first indication for this obstruction follows from the fact that the linearization around equilibrium points is not controllable. The control of this class of underactuated mechanical system is thus a challenging problem for which many open problems exist. To date, many researches have only considered the stabilization problem and the tracking control problem has received less attention. However, in practice, the tracking control problem is more important than the stabilization problem because one does not only want the system to move from one point to another, but the system should also move along a specified path. This specified path may be necessary in order to avoid obstacles or to satisfy requirements which are imposed on the motion of the system. The tracking control problem can be solved by imposing additional requirements on the trajectory to be tracked. In general, the reference trajectory has to satisfy a so-called persistence of excitation condition, meaning that the reference trajectory is not allowed to converge to a point. This means that the tracking and stabilization problems require different approaches and have to be treated separately.

In this thesis, the tracking and stabilization problem are considered for a class of underactuated mechanical systems. This class consists of second-order nonholonomic mechanical systems that can be transformed into a canonical form, called the second-order chained form, by a suitable coordinate- and feedback transformation. The second-order chained form facilitates controller design for second-order nonholonomic systems because the dynamics of the system are considerably simplified and provides the possibility to design controllers for a whole class of second-order nonholonomic systems instead of a specific mechanical system. The tracking control problem for the second-order chained form, in which the controlled system should move along a specified reference trajectory, can be solved by application of a combined cascade and backstepping approach, provided that the trajectory to be tracked does not converge to a point. This approach results in a linear time-varying controller that stabilizes the second-order chained form system to the desired trajectory with exponential convergence. In addition to the tracking control problem, also some methods for generating state-to-state

trajectories are presented which additionally give an explicit way of showing controllability for such underactuated mechanical systems. These methods allow the generation of feasible trajectories that connect an initial state and a desired final state and which are optimal in some sense, *i.e.*, by formulating the trajectory generation as an optimal control problem the resulting trajectory is a local minimum of a certain cost-criterion.

The stabilization problem for the second-order chained form, in which the system should be stabilized to a desired equilibrium point, can also be solved by application of a combined averaging and backstepping approach for homogeneous systems.

It is well-known that the stability analysis of nonlinear time-varying systems can be quite involved and, in general, is very hard to solve. If the nonlinear time-varying system is homogeneous, the theory of homogeneous systems can be used, under additional requirements, to investigate its stability properties. A homogeneous system is associated with a corresponding homogeneous norm. In addition, a homogeneous system, under certain conditions, shares the same properties as a linear system in the sense that asymptotic stability implies exponential stability and local stability implies global stability. The combined averaging and backstepping approach results in a continuous homogeneous controller that stabilizes the system to a desired equilibrium point. To date and to our knowledge, this homogeneous controller is the only one capable of ensuring Lyapunov stability as well as exponential convergence of the second-order chained form system with respect to the corresponding homogeneous norm. It is well-known that homogeneous controllers are not robust with respect to parameter uncertainties. Therefore a periodically updated version of the homogeneous stabilizing controller has been given in which the states of the system are periodically updated at discrete time instants. This controller is robust with respect to a class of additive perturbations that includes perturbations resulting from certain parameter uncertainties, but excludes non-smooth effects, such as friction, or measurement noise.

In order to successfully apply the controllers, they should first be tested in experiments with real-life second-order nonholonomic systems. The developed tracking and stabilizing controllers have been validated on an experimental set-up that consists of an underactuated H-Drive manipulator. This experimental set-up has the same dynamics as a planar horizontal underactuated PPR manipulator, or in other words a manipulator with two prismatic and one unactuated rotational joint. This experimental setup can be used as a benchmark set-up for controllers of second-order nonholonomic systems. In the experiments the goal is to use the two control inputs to control the two planar positions as well as the orientation of the link. The experimental results correspond to the simulation results and show the validity of the control design approaches in the sense that the system can be controlled to a region around the desired trajectory or equilibrium. Due to disturbances, mainly resulting from friction in the rotational link, measurement noise and gravitational disturbances, the closed-loop system is not asymptotically stable, but instead, oscillates around the desired trajectory or equilibrium. The size of the region around the desired trajectory or equilibrium, to which the system is controlled, depends on the magnitude of the disturbances. This shows the need for controllers that are robust with respect to perturbations, including non-smooth effects such as friction, or controllers which include disturbance adaptation or compensation.

In most research dealing with the control of underactuated mechanical systems with second-order nonholonomic constraints the influence of perturbations on the closed-loop dynamics has generally not been taken into account. Nevertheless, the experimental results show that underactuated mechanical systems are more susceptible to perturbations than fully actuated mechanical systems. This is caused by the fact that no actuator is available to directly compensate (part of) the perturbations acting on the un-actuated degree of freedom. Therefore, the development of robust controllers for underactuated mechanical systems is an important issue that should be a subject of further research.

Samenvatting

Ondergeactueerde systemen, of systemen met meer vrijheidsgraden dan actuatoren, zijn veel voorkomende mechanische systemen. Voorbeelden van dergelijke ondergeactueerde systemen zijn onder andere wegvoertuigen zoals auto's en vrachtwagens, mobiele robots, ondergeactueerde robot manipulators, schepen, onderwatervoertuigen, helicopters en ruimtevaartuigen. In bepaalde gevallen, zijn deze systemen onderhevig aan tweede-orde niet-holonome beperkingen. Een tweede-orde niet-holonome beperking is een versnellings-beperking die niet-integreerbaar is, oftewel de beperking kan niet geschreven worden als een functie van de gegeneralizeerde coördinaten en snelheden. Daardoor is de tweede-orde beperking niet elimineerbaar door middel van integratie en vormt de constraint dus een essentieel onderdeel van de dynamica van het systeem.

De interesse in deze specifieke klasse van ondergeactueerde mechanische systemen kenmerkt zich door het feit dat, over het algemeen, deze systemen niet gestabiliseerd kunnen worden door middel van een gladde (of zelfs continue) tijd-invariante toestandsterugkoppeling. Een eerste indicatie hiervoor is het feit dat de linearisatie rond een evenwichtspunt niet regelbaar is. Het regelen van deze klasse van ondergeactueerde systemen is een uitdagend onderzoeksgebied waarin vele open problemen bestaan. Tot op heden is in veel onderzoek alleen het stabilisatieprobleem beschouwd en heeft het volgprobleem minder aandacht gekregen. Dit terwijl, in de praktijk, het volgprobleem belangrijker is dan het stabilisatieprobleem omdat het systeem niet alleen van punt naar punt gebracht moet worden, maar vaak ook een bepaald pad moet volgen. Dit is met name van belang wanneer het systeem obstakels moet vermijden of wanneer er bepaalde voorwaarden worden gesteld aan de beweging van het systeem. Het volgprobleem voor deze klasse van systemen kan opgelost worden wanneer bepaalde restricties worden gesteld aan het te volgen traject. Over het algemeen wordt verondersteld dat het systeem aan een bepaalde persistente excitatie conditie voldoet, hetgeen inhoudt dat het referentietraject niet naar een punt convergeert. Dit betekent dat het volg- en stabilisatieprobleem verschillende benaderingen vereisen en afzonderlijk beschouwd moeten worden.

In dit proefschrift, beschouwen we het volg- en stabilisatieprobleem voor een klasse van ondergeactueerde mechanische systemen. Deze klasse bestaat uit tweede-orde niet-holonome mechanische systemen die getransformeerd kunnen worden naar een kanonieke vorm, beter bekend als de tweede-orde "chained form", door middel van een geschikte coördinaten- en ingangstransformatie. Het volg- of tracking probleem, waarin het systeem langs een bepaald referentie traject geregeld moet worden, kan opgelost worden door toepassing van een gecombineerde cascade en 'backstepping' methode onder de voorwaarde dat de te volgen trajectorie niet naar een punt convergeert. De resulterende regelaar is een lineaire tijd-variante toestands-terugkoppeling die het systeem naar de te volgen trajectorie brengt met exponentiele convergentie. Naast het tracking probleem worden ook een aantal methoden gepresenteerd voor het genereren van een trajectorie die twee toestanden van de tweede-orde "chained form" verbindt, waarmee dus op een expliciete manier de regelbaarheid van dergelijke ondergeactueerde systemen wordt aangetoond. Met deze methoden is het mogelijk om een trajectorie

te vinden die een begintoestand en een gewenste eindtoestand van het systeem verbindt en daarnaast optimaal is in een bepaalde zin; *i.e.*, door het trajectoriegeneratieprobleem als een optimaal besturingsprobleem te formuleren is de trajectorie een lokaal minimum van een bepaald kostencriterium.

Het stabilisatieprobleem kan ook opgelost worden door een gecombineerde middelings en ‘backstepping’ methode voor homogene systemen. Homogeniteit is een eigenschap die gebruikt kan worden voor stabiliteitsanalyse van tijdsafhankelijke niet-lineaire systemen. Het is algemeen bekend dat de stabiliteitsanalyse van tijdsafhankelijke systemen vaak erg complex en moeilijk oplosbaar is. Als het systeem homogeen is, kan door gebruik te maken van de homogeniteit, onder aanvullende voorwaarden, toch een stabiliteitsanalyse uitgevoerd worden. Een homogeen systeem wordt geassocieerd met een bijbehorende homogene norm. Daarnaast bezit een homogeen systeem onder bepaalde voorwaarden dezelfde eigenschappen als een lineair systeem, in de zin dat asymptotische stabiliteit ook exponentieel stabiel impliceert en lokale stabiliteit ook globale stabiliteit. De gecombineerde middelings en ‘backstepping’ methode resulteert in een homogene regelaar die in staat is elk gewenst evenwichtspunt van de tweede-orde “chained form” te stabilizeren. Tot op heden en voor zover bekend, is deze homogene regelaar de enige die naast Lyapunov stabiliteit ook exponentiële convergentie met betrekking tot de bijbehorende homogene norm kan garanderen. Het is algemeen bekend dat homogene regelaars niet robuust zijn met betrekking tot verstoringen die veroorzaakt worden door, bijvoorbeeld, parameteronzekerheden. Daarom wordt ook een periodiek aangepaste versie van de regelaar gepresenteerd waarbij de toestanden periodiek worden aangepast op discrete tijdstippen. Deze regelaar is robuust met betrekking tot een bepaalde klasse van additieve verstoringen, waaronder verstoringen veroorzaakt door bepaalde parameteronzekerheden vallen, maar geen niet-gladde effecten, zoals wrijving, en meetrui.

Om de ontwikkelde regelstrategieën in de praktijk te kunnen toepassen dienen ze eerst getest te worden. De ontwikkelde tracking en stabiliserende regelaars zijn toegepast op een experimentele opstelling bestaande uit een ondergeactueerde H-brug manipulator. De dynamica van de experimentele opstelling is vergelijkbaar met de dynamica van een planair horizontale en ondergeactueerde PPR manipulator, of met andere woorden een manipulator met twee prismatische joints en een ongeactueerde roterende joint in het horizontaal platte vlak. Deze experimentele opstelling kan gebruikt worden voor validatie van regelaars voor tweede-orde niet-holonome systemen. In de experimenten wordt getracht, door middel van de twee ingangen op het systeem, zowel de twee planaire posities als de oriëntatie van de roterende link te regelen. De experimentele resultaten komen goed overeen met de simulaties en tonen de geldigheid van de gekozen aanpak in de zin dat het systeem geregeld kan worden naar een gebied rond de gewenste trajectorie of het gewenste evenwichtspunt. Ten gevolge van verstoringen in het systeem, zoals met name de wrijving in het scharnier van de roterende link, de meetrui en een verstoringskoppel ten gevolge van de zwaartekracht, is het geregelde systeem niet asymptotisch stabiel maar oscilleert rond de gewenste trajectorie of het gewenste evenwichtspunt. De grootte van het gebied waarin deze oscillaties plaatsvinden hangt af van de grootte van de perturbaties. Hierdoor is er behoefte aan regelaars die robuust zijn met betrekking tot verstoringen, waaronder niet-gladde effecten zoals wrijving, of regelaars die een bepaalde vorm van verstorings-adaptatie of -compensatie bevatten.

In veel onderzoek naar het regelen van tweede-orde niet-holonome systemen wordt de invloed van verstoringen of perturbaties niet in beschouwing genomen. Echter, uit de experimenten blijkt dat ondergeactueerde systemen gevoeliger zijn voor verstoringen dan volledig geactueerde systemen omdat er geen actuator beschikbaar is waarmee de perturbaties, werkend op de niet-geactueerde vrijheidsgraad, (gedeeltelijk) gecompenseerd kunnen worden. Hierdoor is de ontwikkeling van robuuste regelaars voor ondergeactueerde mechanische systemen een belangrijk onderzoeksgebied dat een onderwerp voor verder onderzoek zou moeten zijn.

Acknowledgements

First of all, I would like to thank my promotor Henk Nijmeijer and my co-promotor Bram de Jager for their support and their contribution to the work presented in this thesis. I also thank my promotor Maarten Steinbuch, Arjan van de Schaft and Carsten Scherer for their useful comments that helped me to improve the contents of this thesis. I am grateful to David Lizarraga for his support and the interesting and clarifying conversations we had on the control of underactuated mechanical systems. In addition, I want to mention Jan Kok and René van de Molengraft for their support during the first phases of my Ph.D. project.

I want to thank my colleagues of the Mechanical Engineering Department for the good atmosphere and the pleasant time during my stay at the Dynamics and Control Group. In particular I thank Frank Willems, Olaf van de Sluis, Erwin Meinders, Frank Swartjes, Alejandro Rodriguez-Angeles, Ron Hensen, Rogier Hesselting, Alex Serrarens, Bas Vroemen, Sascha Pogromsky, Nathan van de Wouw and Inés López. I also thank Dragan Kostic and Wilbert Dijkhof who both helped me with filming the experiments. I thank the students Roel Verhoeven, Tim Klaassen and Ilona Soons for their valuable work. I thank Toon van Gils and Karel Koekkoek from the laboratory for their help with the experimental set-up. I am grateful to my younger brother Igwe who helped me to make the cd-rom accompanying this thesis.

Finally, I thank my girlfriend Claudia who has always supported and encouraged me to complete this work. Without you things would have been a lot more difficult and less enjoyable. I also thank our parents and our family for their support and their interest in my work.

Edo Aneke, February 2003

Curriculum Vitae

- 1975** Born in Delft, The Netherlands.
- 1986-1989** HAVO, Christelijk Lyceum Delft, The Netherlands.
1989-1991 Atheneum-B, Christelijk Lyceum Delft.
- 1991-1992** Atheneum-B, Wessel Gansfort College, Groningen, The Netherlands.
- 1992-1998** M.Sc. Applied Mathematics, University of Twente,
Faculty of Mathematical Sciences, Enschede, The Netherlands.
- M.Sc. project: Application of disturbance decoupling to active car steering,
German Aerospace Center (DLR), Institute of Robotics and Mechatronics,
Oberpfaffenhofen, Germany.
- 1998-2003** Ph.D. Mechanical Engineering, Eindhoven University of Technology,
Department of Mechanical Engineering, Eindhoven, The Netherlands.
- Ph.D. project: Control of underactuated mechanical systems, Dynamics and
Control Group.
- 2003** Research Engineer, Ford Motor Company, Ford Research Center Aachen
(FFA), Vehicle Electronics & Controls Group, Aachen, Germany.

Propositions

accompanying the thesis

Control of Underactuated Mechanical Systems

1. Although the yaw dynamics of a car can not be decoupled from disturbance torques by means of a static or dynamic state feedback, it is possible when using state-derivative information in the feedback loop.
In: Application of nonlinear disturbance decoupling to active car steering, N. Aneke, J. Ackermann, T. Buente, H. Nijmeijer, *Proceedings of the European Control Conference*, Karlsruhe, Germany, 1999.
2. The second-order chained form for second-order nonholonomic systems plays the same role as the chained form system for first-order nonholonomic systems, in the sense that the transformation into chained form facilitates control design by simplifying the system dynamics. This thesis: Chapter 1.
3. The tracking control problem for the second-order chained form can be solved by linear time-varying feedback, provided that the reference trajectory does not converge to a point. Therefore, the tracking problem and the stabilization problem require different approaches and have to be treated separately. This thesis: Chapter 5.
4. The feedback stabilization problem for the second-order chained form can not be solved by any smooth or continuous time-invariant feedback. It can be solved when considering continuous periodic time-varying feedback. This thesis: Chapter 6.
5. In order to cope with non-vanishing external perturbations, such as friction and possible gravitational effects, the practical stabilization problem for underactuated mechanical systems could be considered instead of the asymptotic stabilization problem. This thesis: Chapter 9.
6. Engineering is making a flawed early version and then refining to make it right.
In: T. DeMarco, *Structured analysis and systems specification*, Yourdon Press, 1979.
7. When somebody says that something can't be done, he or she is usually wrong.
In: S. Maguire: *Debugging the Development Process*, Microsoft Press, 1994.
8. Failure is the opportunity to begin again more intelligently.
By: Henry Ford, 1863 - 1947.
9. Engineering is sometimes like applying a sticker: if there's a bubble and you try to get rid of it, it always appears elsewhere.
10. Do not be afraid to try new things. Remember, the Ark of Noah was built by amateurs; the Titanic by professionals.

Edo Aneke.

Eindhoven, 11th March 2003.